Investigation of differences in cortical activation during wrist flexion and extension performed under real, passive and motor imagined paradigms.

A Thesis Presented
By
Stefan Stoeckigt
To
The Faculty of Health Sciences

Dissertation submitted to the University of Cape Town In Partial Fulfilment of the requirements for the degree of
Master of Science in Medicine
In
Biomedical Engineering

Keywords: EEG, MRCP, Phase Synchrony, PLV, ERD/ERS

DECLARATION

I, Stefan Stoeckigt, declare that this dissertation is my own, unaided work, unless otherwise acknowledged. It is being submitted for the degree of Master of Science of Biomedical Engineering at the University of Cape Town (UCT). It has not been submitted before for any degree or examination at any other university.

Signature: Signed by candidate ……..

Date: …15/11/2015……..

ACKNOWLEDGEMENT

There are several people that I owe my gratitude to, that helped me through the process of this research. Firstly, I would like to thank my wife, Sureka Stoeckigt and my family for their encouragements and support through my dissertation. I would like to thank my supervisor, Dr. Lester John (University of Cape Town), Dr. Thomas Franz and Dr. Tania Douglas for all the help and guidance, and Nikhil Divekar for the design of the electromyography (EMG) system.

This dissertation would not be possible without the financial support of the University of Cape Town, as well as the National Research Foundation (NRF) of South Africa. This dissertation was made possible with the assistance from the University of Cape Town in terms of the use of the necessary equipment. I would also like to thank C. Harris (University of Cape Town, Department of Human Biology) for assistance in the construction of the equipment used for this dissertation.

ABSTRACT

The neuromuscular control comparison between flexion and extension of the upper extremities has been conducted in a number of studies. It has been speculated that differences in the corticospinal pathway between flexion and extension may play a role in the cortical difference detected between flexion and extension, resulting in higher cortical activation for extension. However, it is still unclear as to what roles these pathways play, and to what degree other factors (muscle force activation, sensory feedback, frequency of movement, structural and/or functional differences) might influence the cortical activation in the brain. It has been speculated that the difference in cortical muscular pathways is due to flexion movements being used more often in day to day activities, therefore requiring less cortical activation for that movement. Through the investigation of the cortical differences present during different movement types, a deeper understanding into the differences between flexion and extension may be obtained. No previous study has compared the cortical differences between flexion and extension of the upper extremities during different movement types.

In this study, an offline investigation is conducted between wrist flexion and extension, during real, passive and motor imaginary movement with the help of a servo controlled hand device. Simultaneous recording of EEG, EMG and wrist dynamics (velocity, angle, strain) were made on fifteen healthy right handed subjects performing 60 randomized repartitions of right wrist flexion and extension, for kinaesthetic motor imaginary, passively moved, and voluntary real active movements. Real movements were conducted at 10% relative subject maximum voluntary contraction (MVC). A servo controlled hand device was used to regulate dynamic force applied for real movements, and provide motion during passive movements. The use of different movement types with the aid of a servo controlled hand device, may give a deeper understanding into the effects of muscle force activation, rate of movement and corticospinal pathway on flexion and extension.
In order to investigate the cortical differences between flexion and extension, subjects perceived difficulty, movement dynamics, movement related cortical potential (MRCP), event related desynchronization and synchronization (ERD/ERS), and phase locking value (PLV) were measured. Each measurement examines a different aspect of the cortical activation present in the brain, during the different movement types.

Although relative muscle force activation between wrist real flexion and extension was similar, the motor cortex activation during extension was higher than during flexion, by MRCP and mu-band ERD, with subjects also perceiving real wrist extension to be more difficult to perform. Passive movements found higher motor cortex activation for flexion (MRCP, beta-band ERD), however higher somatosensory cortical activation was present during extension, by mu-band ERS and PLV. Motor imagined wrist flexion showed higher cortical activation during wrist flexion, by MRCP and beta-band ERD. Although numerous variables were tested (each in difference frequency bands), with some being significant and others being non-significant, overall it can be suggested that there was higher cortical activation for extension. The higher cortical activation during wrist extension movements may be due to corticospinal and somatosensory motor control pathways to motor neuron and from sensory neuron pools for extensor/flexor muscle and muscle spindle of the upper extremities. This investigation contributes to the current literature relating to cortical differences between flexion and extension of the upper extremities, by including the real, passive and motor imaginary differences between flexion and extension.

TABLE OF CONTENTS

Page

LIST OF TABLES

LIST OF FIGURES

GLOSSARY OF TERMS AND ABBREVIATIONS

Index Term	*Description*
AAR	Automatic artefact removal
Alpha	Neural oscillations in the 8-12Hz frequency range, associated with wakeful relaxation.
BCI	Brain Computer Interface
Beta	Frequency band of brain rhythms occurring between 8-12Hz
bPLV	bi Phase Locking Value
BSS	Blind source separation
CAR	Common Average Referencing
CM1	contralateral primary motor cortex
CNS	Central Nervous System
Contralateral	Corresponding part to opposite side of the body
CSD	Current Source Density
CSF	Cerebral Spinal Fluid
CSF	Cerebrospinal Fluid
DC	Direct Current
Delta	Neural oscillations in the 0-4Hz frequency range, associated with the deepest stages of sleep.
DOF	Degree of Freedom
ECoG	Electrocorticography
EEG	Electroencephalography
EMG	Electromyogram
EOG	Electrooculography
ERD	Event Related Desynchronization
ERP	Event Related Potential
ERS	Event Related Synchronization
Gamma	Neural oscillations in the 25-100Hz range, which may be associated with conscious perception.
HEOG	Horizontal Electrooculography
IC's	Independent Components
ICA	Independent Component Analysis
M1	Primary Motor cortex/area
Motor Imaginary	Mental process of imagination of performing a particular movement.
MRCP	Movement Related Cortical Potential
Mu	Frequency band of brain rhythms occurring between 8-12Hz
MVC	Maximum Voluntary Contraction
P.V	Cauchy principle value
PCA	Principle component analysis
PID	Proportional Integral Derivative
PLV	Phase Locking Value
PMA	Premotor cortex/area
Pronation	Rotation of hand so that the palm faces downwards
Proprioception	Sensory information of how the body is position.

PWM	Pulse Width Modulation
RIWE	Right Imaginary Wrist Extension
RIWF	Right Imaginary Wrist Flexion
ROM	Range of Motion
RPWE	Right Passive Wrist Extension
RPWF	Right Passive Wrist Flexion
RRWE	Right Real Wrist Extension
RRWF	Right Real Wrist Flexion
SL	Surface Laplacian
SMA	Supplementary Motor cortex/area
SNR	Signal to Noise Ratio
Supination	Rotation of hand so that the palm faces upwards
Theta	Neural oscillation in the 4-6Hz.
VEOG	Vertical Electrooculography

1. Introduction

When comparing the neurological differences between flexion and extension, there are a number of unknowns. Increasingly more evidence indicates that there are neuromuscular control system differences between extension and flexion movements of the upper extremities (Palmer & Ashby, 1992; Raptis, Burtet, Forget, & Feldman, 2010; Yue et al., 2000). These neuromuscular differences represent structural and possible functional differences in the control systems and cortical muscular pathways. Previous research suggests that higher cortical activation was observed during extension, due to these cortical muscular control systems (Yue et al., 2000). However movements were often poorly calibrated with little regard to the movement differences that may occur.

Yue et al. (2000) reported that there were differences in cortical activation (measured by MRCP and fMRI) between flexion and extension. It is known that wrist flexion and extension muscle forces are different. In addition, it is known that cortical activation (as measured by ERD/ERS) varies with percentage maximum voluntary contraction (MVC) (Alegre et al., 2002). Even though Yue et al. has accounted for the difference in muscle force activation, they did not account for the differences between subject relative muscle force activation and the effects of gravity. Therefore, it is unknown whether Yue's results are simply because of the flexion and extension muscle force differences. In addition to force difference, it is unknown whether afferent pathways vary with flexion and extension, and the role that corticospinal projection plays. Since Yue's et al. (2000) experiment with real movements inherently include the effect of these afferent pathways and the effect of passive returning movement, this could be an additional reason to explain the observed cortical differences detected between flexion and extension. Since motor systems inherently include sensory inputs to execute and plan the movements, the effect of these sensory input on the cortical activation is still unclear. Furthermore, it was also speculated by Yue that wrist flexion is used more often in day to day activities, which could result in differences in the cortospinal pathways. This frequency of use has been shown by Seitz et al. (1990) to decrease the cortical activation of that particular motor task.

Similar neurological differences to Yue's findings have been observed in patients with brain injuries to their motor function, with joints often in the flexed position, which supports the known fact that flexor muscles of the upper extremities are more facilitated or less inhibited by the corticospinal and other cortical and subcortical motor-control systems (Yue et al., 2000). It has also been observed in patients with Parkinson disease, that there is a greater impairment in extension movements as compared to flexion movements (Robichaud, Pfann, Comella, Brandabur, & Corcos, 2004). Furthermore, amongst these patients it is more difficult for them to relearn movements involving extension as compared to flexion (Yue et al., 2000).

The rate and the force of the movement have a direct relationship to the brain volume activation; motor cortex neurons related to wrist extension discharge at a higher rate than those relating to wrist flexion for each unit of force increment (Dai, Liu, Saghal, Brown, & Yue, 2001). For an increase in muscle force output there has been shown to be an increase in brain activation (Dai et al., 2001), and an increase in beta rhythms de-synchronisation (Stancak, Riml, & Pfurtscheller, 1997). An increase in the rate at which the movement is performed, results in an increase in the movement related cortical potential (MRCP) rate of change (Gu, Dremstrup, & Farina, 2009; Vlodek Siemionow & Yue, 2000). These differences could result in different levels of MRCP and Event Related de-synchronization

(ERS/ERD) values when comparing wrist extension and flexion, causing higher amplitude levels in the motor cortex and supplementary motor areas (SMA) of the brain for extension (A. Vuckovic & Sepulveda, 2008; Yue et al., 2000). This makes it difficult to accurately isolate what is causing these neurological differences, and whether the increase in cortical activation is due to an increase in force required to perform wrist extension, or as a result of differences in cortical muscular pathways.

Many of the differences detected between flexion and extension could be based on brain volume activation changes in the brain's volume. It has been shown that ERD/ERS is a useful method for discriminating between different movement types (A. Vuckovic & Sepulveda, 2008). This method looks at the power changes in a particular frequency band, which can indicate differences between motor movements. The main disadvantage of using power and amplitude changes to discriminate between flexion and extension is that so many other factors can influence them, such as the rate of movement, the power of the movement and the type of movement (Siemionow & Yue, 2000), making it difficult to accurately discriminate between the different movement types, if the source of the power change is not known.

Coherence between two signals has been used to classify the difference between extension and flexion (Williams, Soteropoulos, & Baker, 2009). One of the main disadvantages of this method is that it is still sensitive to amplitude change, which in turn will make it sensitive to the power changes in the brain. Even though it shows the coupling between two signals, this coupling can still be as a result of a power change in the two sources. Phase Locking Value (PLV) is a novel technique that looks at phase synchronization between two signals. The main advantage of PLV over coherence is that PLV is insensitive to the amplitude change, and only looks at the phase changes between two signals (Wei, Wang, Gao, & Gao, 2007). This makes PLV ideal for analysing the differences between flexion and extension.

Movement types, such as passive and motor imaginary may affect the cortical activation effect, caused by the differences in muscle force activation, rate of movement and corticospinal pathway between flexion and extension. These movements could also be influenced by differences in corticospinal and/or other pathways projected to the motor-neuron pools of flexor and extensor muscles of the upper extremities, with passive movements only getting affected by reflex and sensory corticospinal pathways. Many studies have shown the effects of active movements and motor imagery on the brain activity. However, less attention has been given to passive movements. Vuckovic *et al*. (2008) conducted an experiment where ERDS was used to visually analyse imaginary and real wrist movement differences between flexion, extension, pronation and supination. The real movements were conducted without regard to the difference in muscle activation that may occur between different movement types. Current available research suggest that it is unknown whether the previously mentioned differences in cortical brain activity between flexion and extension movements are still present during passive movements or even motor imaginary movements. By comparing the differences between flexion and extension during active movements, passive movements and motor imaginary movements using MRCP, ERS/ERD and PLV analysis, the underlining cause for the differences between real (active) wrist flexion and extension may be discovered.

In order to reduce the complexity of inferring the origins of the cortical differences observed between flexion and extension, three movement type are examined as demonstrated in Figure 1-2. Imaginary movements (dark green & red) cortical activation should predominantly be as a result of neurological difference, with minimal affect from corticospinal pathways and sensory feedback. Passive movements (grey & blue) should include neurological and sensory pathways (proprioception). Real movements (purple and light green) should be a combination of movement related, corticospinal pathways and sensory input, including efferent and afferent pathways.

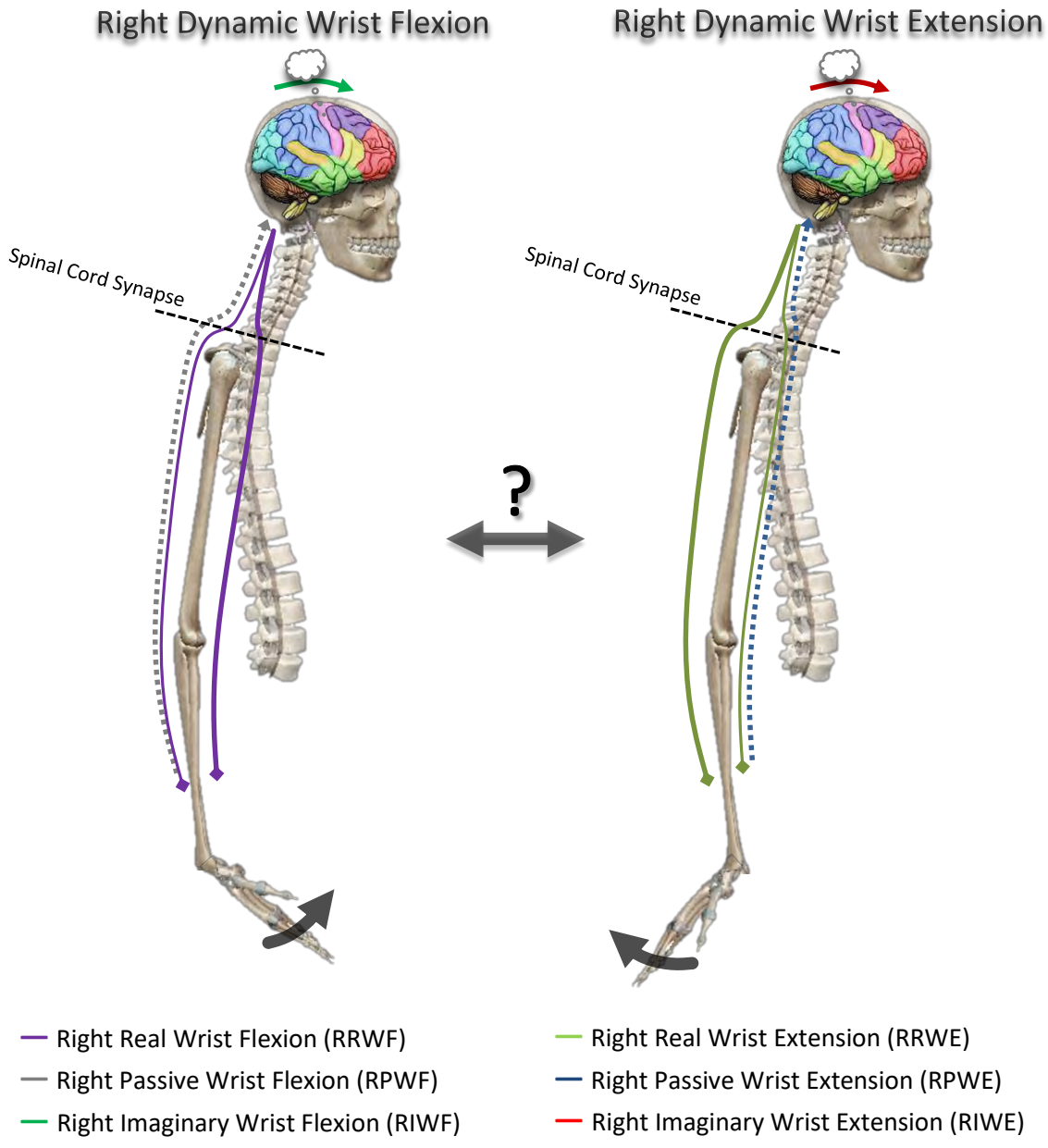

Figure 1-1: Dotted line (▪▪▪), sensory feedback pathways. Solid line (—), muscle control pathways. Illustration of the different sensory feedback and muscle control pathways using during wrist flexion and extension (Kandel, Jessel, & Schwartz, 2000).

1.1 Current Investigation

1.1.1 Rationale

Although there have been studies showing the cortical activation differences in the brain between flexion and extension, it is still unknown whether the observed differences are as a result of differences in muscle force activation, frequency of movement, corticospinal pathways and/or structural and possible functional differences in the brain. Through the analysis of the cortical differences present during wrist flexion and extension of different movement types, a deeper understanding of these differences may be obtained, where each different movement type looks at a particular aspect which could contribute to the cortical differences. To the best of my knowledge no previous study has simultaneously compared the cortical differences between flexion and extension of the upper extremities during different movement types, with the cortical comparison between passive flexion and extension has not been previously explored.

1.1.2 Aim

The aim of this study is to investigate the corticospinal and neurological differences between flexion and extension of the upper extremities, through investigation of real (active), passive (active) and motor imaginary movements.

1.1.3 Objectives

In order to achieve the proposed aim, perceived difficulty, movement dynamics, MRCP, ERDS and PLV were measured and compared between flexion and extension, through the following movement type investigations:

- The cortical differences between real (active) right wrist flexion and extension, applied at the same relative level of muscle force activation, in relation to 10% MVC to investigate the effect of relative muscle force activation.
- A comparison of the level of cortical differences between passive (active) right wrist flexion and extension, to investigate cortical effect of somatosensory (afferent) pathways.
- The differences between motor imaginary right wrist flexion and extension, to investigate the effect of frequency of movement on cortical activation, with minimal influence from corticospinal (efferent) and somatosensory (afferent) pathways.

1.1.4 Hypothesis

It is hypothesised that the difference in cortical activation differences in the brain between wrist flexion and extension, will result in higher cortical activation for wrist extension, whiles still accounting for the cortical effects due to differences in muscle force activation and sensory feedback. This would confirm the previous results by Yue et al. (Yue et al., 2000), which suggested that there are differences in the corticospinal and subcortical motor control system between flexion and extension of the upper extremities. However, it must be noted that the effects of relative muscle force activation and sensory feedback were not accounted for in Yue's study.

1.1.5 Significance of the study

The cortical activation comparison in the brain between wrist flexion and extension for different movement types may provide insight into the functional and cortical differences reported between flexion and extension of the upper extremities, and the contribution of corticospinal and subcortical networks. The understanding into the neurological differences relating to movements and their corticospinal pathways could help improve the rehabilitation process in patients suffering from brain injuries.

1.1.6 Scope and limitations

This dissertation is limited to the study of the right wrist in 15 right handed human subjects, using EEG neuroimaging. Only neurologically normal healthy subjects are used during the study. Three movement types are examined: motor imaginary, passive movements and real (active) voluntary movements.

Real wrist movements are applied to a resistive force against motion, of 10 % related to the maximum muscle force output. This study is limited to only one output force during real movements. Passive movements are limited to one rate of motion and applied to the maximum angle for both movements. Imaginary movements are limited to kinaesthetic motor imagery and not visual-motor imagery, as the former yields better cortical activation (see section 3.4.1).

All analyses are limited to the comparison between wrist flexion and extension for imaginary passive and real movements. MRCP analysis is limited to the Theta and Beta bands, whilst ERDS analysis is conducted around the peak frequencies in the Mu, low beta, mid-range beta and high beta rhythms only. PLV analysis is limited to the 5-40Hz range and is only calculated between the SMA and remaining electrode (see section 4.2.4.3).

1.1.7 Summary of methodology

The comparison of cortical activation in the human brain during flexion and extension for different wrist movements (real, passive, imagined), in fifteen right handed subjects is conducted with the help of a servo controlled hand device (see appendix C.1), which is designed for the purpose of this study. The cortical activation of the brain is recorded with the aid of a 128 channel EEG system, and used to investigate the MRCP, ERD/ERS and PLV for each movement type (see Figure 1-2).

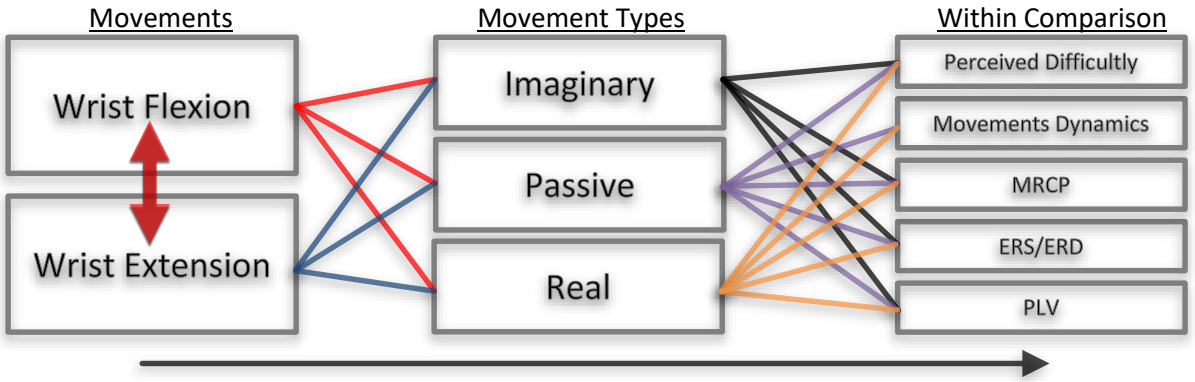

Figure 1-2: Approach to studying the differences between wrist flexion and extension, down to the movement type and analysis techniques.

This dissertation addresses the above mentioned shortfalls, through the analysis of subject perceived movements difficulty, wrist movement dynamics (wrist Angle, Strain and Velocity), movements related cortical potential (MRCP), event related de/synchronization (ERS/ERD) and phase locking value (PLV) through the within comparison of wrist flexion and extension during imaginary, passive and real movements (Figure 1-2). In order for the necessary experiments to be conducted, the design of a suitable experimental paradigm (see section 4.1.1) is necessary to analyse the differences between wrist flexion and extension, for real, passive and imaginary movements. This is entailed in the design of a hand device (see section 4.1.2) that is required during passive and active wrist movements, which regulates the force applied during real movements, and provides motion during passive movements.

1.2 Overview

This introduction gives a brief background and literature review on research into wrist movements using EEG. This is followed by a detailed study into neurological differences between wrist flexion an extension for different movement types. The remaining chapters are broken down as follows:

Chapter 2 gives the background into the structure of the human brain, including commonly used analytical techniques, such as MRCP, ERDS and PLV analysis.

Chapter 3 contains the literature review discussing previous research into the different movement types (real, passive and imaginary) and cortical features associated with those movements (wrist flexion and extension).

Chapter 4 gives the methodology used in the investigation of the differences between wrist flexion and extension movements, including the analytical procedure and experimental setup. A total of 15 right handed neurological normal subjects were used during the study.

Chapter 5 presents the results for the MRCP, ERDS and PLV analysis, comparing wrist flexion and extension for the different motor movement types. This section also includes the force, angle and rate of motion results for the different movement types.

Chapter 6 contains the discussion of the results presented in chapter 5, including possible future work which may be undertaken.

Chapter 7 presents the conclusion on the study, into the cortical differences detected between wrist flexion and extension.

The appendices give more information on the subjects; including age, experimental order, MVC values and subject frequencies of interest used in the ERS/ERD analysis. The appendices also include the detailed design of the hand device required in the experiments and results for proven techniques, including MRCP, ERS/ERD and PLV analysis and artefact correction results.

2. Background

There are many different neuroimaging modalities that can be used to analyse cortical activation in the brain. Electroencephalography (EEG) and electrocorticography (ECoG) are two electrophysiological methods that measure the direct electrical activity from the brain. Metabolic methods like functional magnetic resonance imaging (fMRI), use magnetic fields to detect the changes in the local cerebral blood flow/activation and oxygenation levels during neural activation. Nuclear imaging techniques, such as Positron Emission Tomography (PET) rely on gamma rays emitted from a positron-emitting radionuclide tracer, to image the activation in the brain. Despite the good spatial resolution of fMRI and PET, determining the time sequence of activation is limited. Even though EEG has poor spatial resolution compared to ECoG, PET and fMRI, it is by far the most widely used recording modality, due to its non-invasive manner, easy electrode placement and high temporal resolution (Nicolas-Alonso & Gomez-Gil, 2012). Although all these neuroimaging methods have been used in the study of cortical activation in the brain, this dissertation will focus on EEG (see section 2.1.2), due to its portability, relative inexpensiveness and high temporal resolution, which makes it ideal for the study of movement related cortical activation.

This section will present appropriate background information to form the basis of this study. Section 2.1 discusses the structure of the brain relating to motor movements, followed by a description of electrocephalography (EEG) and various EEG filtering methods in Section 2.1.3. Section 2.2 describes various types of analytical techniques used in the study of EEG and its relation to the detection and comparison of the differences between wrist flexion and extension movements.

2.1 Introduction into neurophysiology

The study of the underlying anatomical structure of the human brain can help in determining the neurological differences that may occur between various types of movements of the wrist. This section will start off with a brief introduction into the anatomical structure, followed by an introduction into EEG and its data analysis methods (see Figure 2-1).

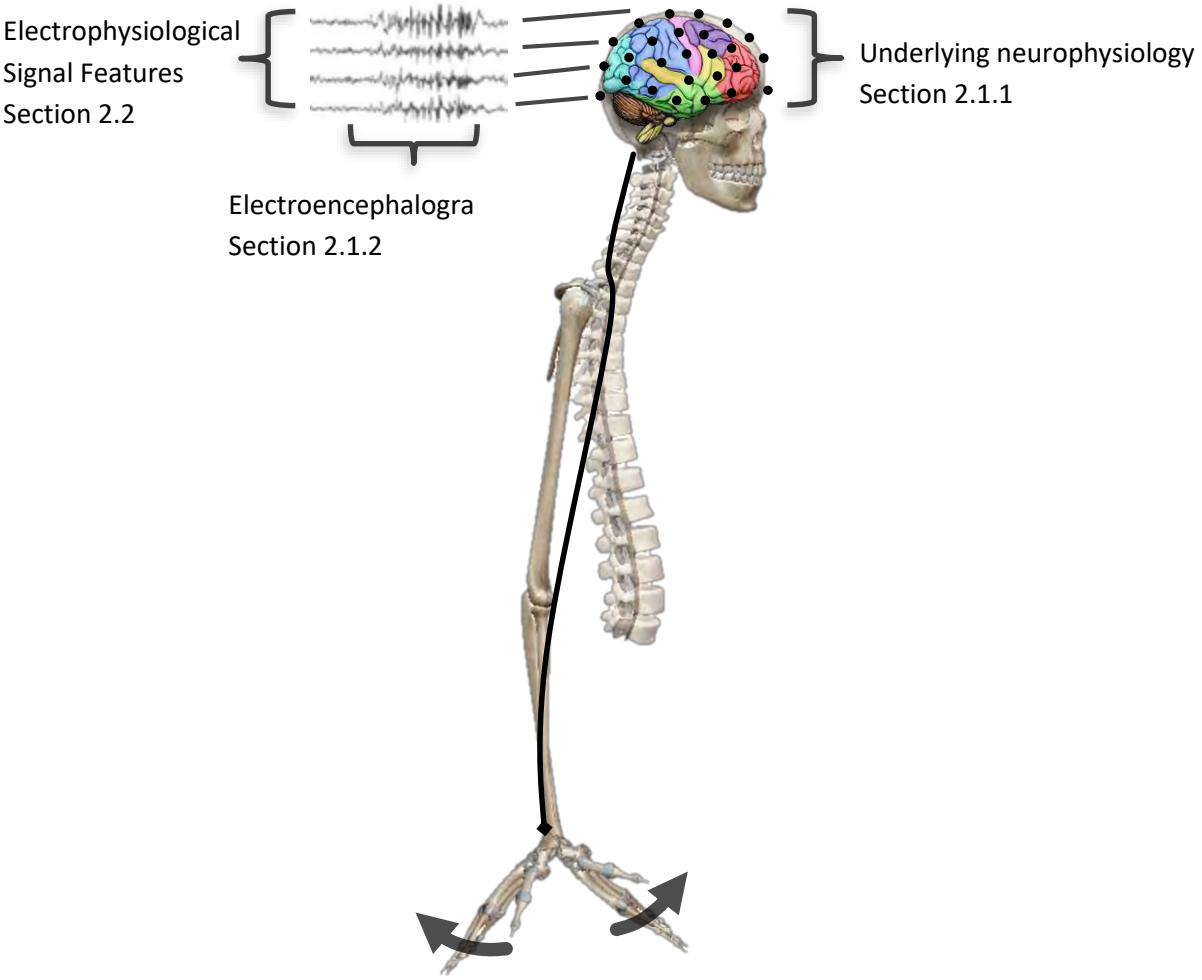

Figure 2-1: Breakdown of background chapter, into the electrophysiological, electroencephalogram and underlying neurophysiology.

2.1.1 Underlying neurophysiology

The cerebral cortex is responsible for almost all of the body's control and information processing centres. It is divided by sulcus into four major lobes; frontal, parietal, occipital and temporal. The frontal lobe is responsible for recognizing future consequences based on the result of current actions, identifying similarities between different events, and choosing between actions. The main functions of the parietal lobe, are the integration of sensory information from different parts of the body. The occipital lobe is responsible for visual processing, and the temporal lobe is responsible for auditory processing (Kandel et al., 2000). The regions of the cerebral cortex involved in movements and control are located in the frontal lobe (motor systems) and the parietal lobe (sensory systems).

The cerebral cortex motor area (located in the parietal lobe) is subdivided into two main areas; the primary motor area (M1) and several premotor areas. Two main premotor areas include the premotor area (PMA) and the supplementary motor area (SMA). Populations of neurons are projected from the different motor areas to the brain stem and spinal cord, which control muscle and joint movements. These motor areas all play different roles in movement control, with the primary motor cortex being the most important area responsible for motor control.

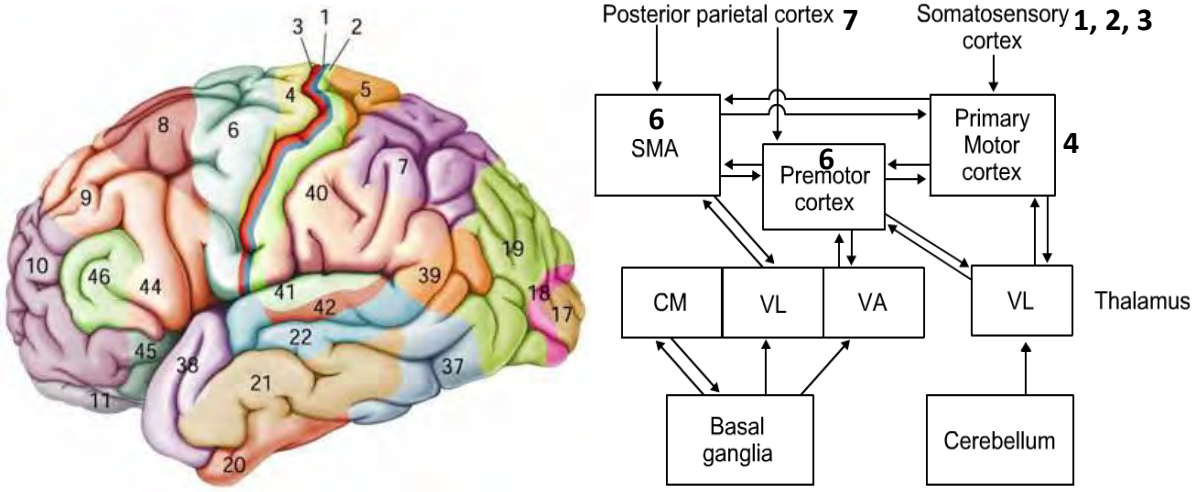

Figure 2-2: (Left) Lateral view of the cerebral hemispheres with functional division of the cerebral cortex, dividing the brain up into main areas of interest. Brodmann's areas associated to the; primary somatosensory cortex (1-3), primary motor cortex (4), Premotor area (6), primary visual cortex (17), secondary visual cortex (19), posterior parietal cortex (7), prefrontal Cortex (9), and anterior prefrontal cortex (10) (Drouin & Tassin, 2002). (Right) Illustration of major connection between different areas of the brain (including the relative Brodmann areas) involved in motor control (Byrne, J. H. and Dafny, 1997).

The primary motor cortex is located in the precentral gyrus at the posterior border of the frontal lobe, which controls simple features of movements. This area receives somatotopically organized inputs from two different sources; the primary somatosensory cortex and posterior parietal (area 5, Figure 2-2). These areas are primarily involved in stimuli and sensory modalities for motor planning. The primary motor cortex is specially divided into different areas that are associated with the control of different body parts. These different areas are somatotopically represented in a distorted image of the human body known as Homunculus (Figure 2-3), in which each body part is associated an area relative to its corresponding neural connections in the brain. The different control areas are orderly arranged along the gyrus, with the face, digits, hand, arm, trunk, leg, and foot. Tasks that require the greatest precision and finest motor control, like fingers, hand and face movements, require a larger number of neural connections and hence a larger area of the primary motor cortex (Kandel et al., 2000). It is clear from Figure 2-3 that cortical areas responsible for hand, wrist and finger control, are very close to each other, with wrist movements such as flexion and extension occupying the same area. EEG electrodes associated with the primary motor cortex according to the international 10-20 montage are; Cz, C1, C2, C3, C4, C5 and C6.

The premotor cortex lies in the frontal lobe and extends anterior to the precentral gyrus on the lateral and medial surface of the cortex, as shown in Figure 2-2. This area plays an important role in sensory guidance, planning and execution of movements. Unlike the primary motor cortex which only controls simple movements, the premotor cortex evokes more complicated movements of multiple muscles and joints (Kandel et al., 2000). The premotor cortex has dense connections between its own areas and also receives major inputs from the prefrontal cortex (area 5, 7 and 46, Figure 2-2), of which each area projects to a different area in the premotor area (PMA). Stimulation of the PMA represents more natural coordinated hand shaping or reaching movements. Most of the premotor areas are projected to the primary motor cortex, although some are projected to the spinal cord and overlap with the primary motor cortex. This suggests that the premotor neurons can control motor movements

independently from the primary motor cortex. EEG electrodes associated with the premotor cortex according to the international 10-20 montage are; FC1, FC2, FC4, FC5 and FC6.

The supplementary motor area (SMA) is part of the sensorimotor cerebral cortex, located in front of the primary motor cortex on the medial face of the frontal hemisphere (Figure 2-2), Brodmann area 6 in the premotor cortex. The SMA plays an important role in the planning of motor movement, bimanual control, movement preparation, and is involved in the performance and imagination of more complex tasks. This includes the learning of a sequence of movements and in the automatic performance of a sequence of movements from memory. The SMA is made up of two distinct parts, the SMA proper (or: caudal SMA) and pre-SMA (or: rostral SMA). The pre-SMA is primarily involved in the learning of a new sequence of movements, with more neuron activation for new sequences compared ones that have already been learned.

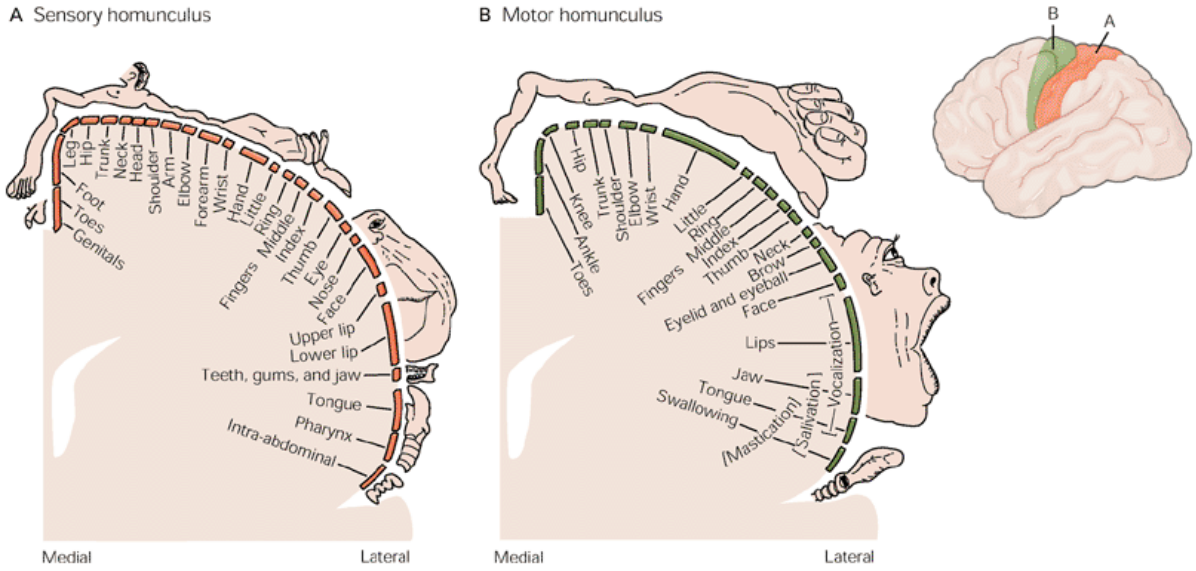

Figure 2-3: The somatotopical arrangement of the primary motor cortex (right) and Somatosensory Cortex (left). The size and position of a particular body part in the Homunculus is an estimated of the size of the area in the cortex associated with sensory feedback or control of that body part (Kandel et al., 2000).

The somatosensory cortex (sensory cortex), primary motor cortex, supplementary motor cortex (SMA) and premotor cortex are all required for control, preparation and sensation of movements, whether they are voluntary, passive or imaginary movements. Through afferent and efferent cortical spinal pathway by the motor and sensory cortex (see Figure 2-3) and major connection between different cortical area (Figure 2-2-right) movement control is possible.

Areas of interest involved in voluntary, imaginary and automated movements of the wrist, include region of primary motor cortex and primary sensory cortex. The SMA and PMA will also be considered, as these areas are the source of movements and control information.

In order to get a better understanding of the neural activity during the different types of movements, the exact time course of the neural information conveyed between difference brain regions must be determined. There are many different techniques that can be used to record neural signals, but only a few will offer the precise timing required for the neural communications.

2.1.2 Electroencephalography

Neuroimaging techniques can be divided into two main categories; structural or functional neuroimaging. Structural neuroimaging provides an anatomical representation of different regions of the brain and is communally used in the diagnosis of tumours or brain injuries. Functional neuroimaging provides a way to visualize how information is processed in different parts of the brain. Many functional brain imaging techniques measure the metabolism and blood flow in the brain. Although this method can produce excellent spatial resolution images of the brain, it fails to extract the necessary temporal resolution of neural communication which is limited by hemodynamic response. Methods that record the electrical and magnetic fields caused by the simultaneous activation of a population of nerve cells, such as EEG, can offer a more precise timing of neural activity down to the millisecond scale. (Nicolas-Alonso & Gomez-Gil, 2012).

EEG is a non-invasive measurement of the electrical activity of a combination of different processes in the brain, which is recorded on the scalp. Specifically, it involves the recording of brain signals that are emitted from the head measurements of the electrical potential difference across the scalp, which arises from current flow within the head and the brain. Therefore, it is used to denote electrical neural activity of the brain. The human brain consists of approximately 100 billion central neurons that are activated during different neural processors. Due to the large number of neural processors and the limited number of EEG measurement sites, each EEG electrode is considerably mixed with information sources from all over the brain. Electrical potentials generated by a single neuron are too small to be detected by EEG on the scalp. These sources picked are as a result of dipole summation of postsynaptic potentials of pyramidal cells in the cerebral cortex and hippocampus. Dipoles in the brain are caused by intracellular ions move through and out the neuron, creating a source of opposite charge. These charged dipoles conduct through the brain until they reach the scalp, where EEG signal detects the charge of the end of the dipole that is closest to the scalp. Volume conduction causes the dipole signals to spread out laterally when it reaches high electrical impedance of the scalp and skull which results in the spatial blurring of the neural signals. Hence, scalp distribution can be distorted and does not accurately reflect the exact location of neural sources (Thatcher, Biver, & North, 2004). The high scalp and skin impedance result in a very small EEG signal (uV range). This makes it difficult to measure and easily susceptible to noise and artefacts from muscle movements, eye movements and blinks. The result of a low signal to noise ratio (SNR) for EEG and the variability of neural signals with regard to time and subjects add to the difficulty in extracting patterns associated with movements.

The first human EEG recording was reported in 1929 by German psychiatrist, Hans Berger. The recording was performed using a one-channel bipolar method for duration of one to three minutes. Berger was the first to describe the different wave rhythms which were present in the brain and reported that the alpha rhythms (Berger's wave) are one of the major components in the EEG signal. Berger was also one of the first to use analytical methods to analysing EEG signals, by applying Fourier analysis to an EEG sequences (Brazier, 1963). Since then, many different methods of analysing EEG has been developed in order to get a better understanding of how the brain works. This has been done over a broad spectrum, from using EEG for the analysis in full term and premature new-borns, to the investigations of evoked potentials (EP) as a method for monitoring mental illnesses. One of the earliest pioneers of EEG, Napolean Cybulski, made an observation of the appearance of fast EEG

rhythms in a dog, caused by peripheral electrical stimulation (Edwards, 2007). Based on the work of Napolean Cybulski, Kaufman expressed that EEG could be used in the study of epileptic attacks, but it wasn't until Fischer and Lowenbach that the first epileptic EEG studies on human where conducted demonstrating epileptic spikes. Although EEG had the potential to become a valuable clinical diagnostic tool, it was W. Gray Walter that first used EEG in the clinical diagnostic of brain abnormalities. Since then EEG has been mainly used in the investigate brain functions and neurological disorders. In recent years there has been a growth in new EEG analytical methods in order to extract more complex signals.

2.1.2.1 EEG Rhythms

EEG is generally described in terms of its frequency bands. There are five dominant EEG brain rhythms which are distinguished by their different frequency ranges. The amplitudes and frequency characteristics of the brain rhythms are known to vary from one human to another. Changes in brain rhythms can also be contributed to the mental state, (for example wakefulness) and the age of the human. These five frequency bands are name delta (δ), theta (θ), alpha (α), beta (β), and gamma (γ) (Figure 2-4) with delta starting at 0.5 Hz to high gamma waveforms in excess of 100Hz, of which alpha and beta rhythms are associated to real and imagery motor movements (Sanei & Chambers, 2007).

- Delta and Theta rhythms are very low frequencies waveforms in the 0.5 – 8Hz range. In adults they often indicate deep sleep or drowsiness. The Delta band lies below 4Hz and the Theta band lies within 4 to 8Hz. The presences of Theta waves have been associated with cognitive processing and concentration. Due to the low frequency of the delta and theta waveform it is easily confused with artefact signals generated by head movements and by muscle contraction of the neck and jaw (Nicolas-Alonso & Gomez-Gil, 2012).
- Alpha waves are one of the most prominent rhythms in the brain, and are often presents when the brain is alert but unfocused, indicating a relaxed awareness. The alpha waves lie within the frequency range of 8-13Hz and originate in the posterior part of the head, usually found around the occipital region of the brain. In most subjects there is an increase in alpha rhythms in the occipital region when they are relaxed or close their eyes. Alpha rhythms are often used to indicate some kinds of sleep and reversible coma. There are Alpha wave variants called mu (μ), generated in the motor cortex. The mu amplitude is strongest when no movement is performed and is reduced in the corresponding motor area by a movement. The intention to perform a movement and imagining a movement can result in the decrease in alpha waves over the corresponding area in the motor cortex (Wolpaw, Birbaumer, McFarland, Pfurtscheller, & Vaughan, 2002).
- Beta waves are in the 14-26 Hz range and are often referred to as the waking rhythm. They indicate that the brain is actively thinking and focusing on the outside world. Similarly to mu rhythms, beta band oscillations occur over the motor cortex, predominantly in the sensorimotor cortex in humans. The beta waves in the motor cortex are associated with muscle contractions for isotonic movement, and have been shown to increase when movements have been resisted or voluntarily suppressed. Sensory feedback in static motor control is represented by bursts of beta activity which reduces when the movement changes. The de-synchronization/suppression of beta waves occur prior and during the change in movements and can be blocked by motor activity or tactile stimulation during real movements or motor imaginary (Baker, 2007).

- Rhythms above the Beta range are commonly referred to as gamma waves with frequencies in excess of 25Hz. Gamma waves are very hard to detect due to their rare occurrence and low amplitudes. The detection of these rhythms usually indicates or confirms certain brain diseases. Phase-locking gamma oscillations have been proven to be a good indication for the differentiation between fast and slow motor responses (Fründ, Busch, Schadow, Körner, & Herrmann, 2007) and is a good indication of event-related synchronization (ERS – see section 2.2.2) of the brain.

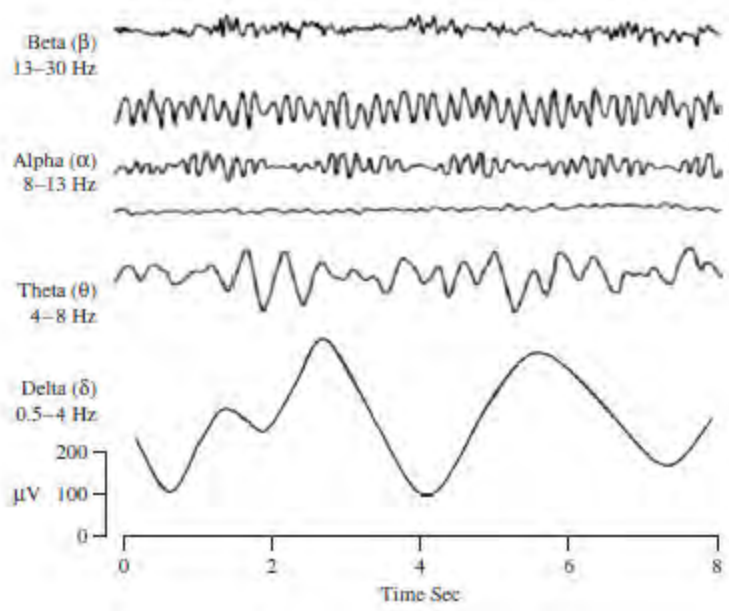

Figure 2-4: Normal brain frequencies, for Beta, Alpha, Theta and Delta rhythms (Sanei & Chambers, 2007).

2.1.3 Established techniques in electroencephalography data analysis

There are a number of methods used to improve pattern detection in EEG signals. Surface Laplacian helps with improving the spatial resolution of the raw EEG, while independent component analysis performs a statistical separation of underlying features contained within the EEG data.

2.1.4 Spatial Filters

EEG signals are known to have high temporal resolution, but suffer from poor spatial resolution. These signals are derived from ionic currents which originate from the cerebral tissue, and are transformed into electrical current, and picked up by EEG electrodes on the surface of the scalp. As a result of the low skull conductivity compared to the cerebral spinal fluid (CSF), ionic currents originating from the cortex collide more with tissue molecules causing greater deviation from their trajectories. The ion deviation causes the scalp potential to be blurred considerably compared to that of the cortex. In order to improve the SNR in EEG signals caused by spatial blurring, spatial filters can be used. Commonly used spatial filters include surface Laplacian, spline interpolation and circular Laplacian.

Scalp surface Laplacian (SL) is an alternative way of viewing EEG data. The scalp EEG signals can be improved by transforming the signals into measures of electrical current source density (CSD) and reducing the effect of skull conductivity. By applying surface Laplacian to the scalp potential data, a higher spatial resolution can be obtained reducing the spatial blur of the recorded EEG signals (Geodesics, Note, Ferree, & Srinivasan, 2000). This means that EEG patterns from localised cortical

sources can be better detected with EEG signals which has been transformed with surface Laplacian, compared to that of the raw, unprocessed data. For most brain computer interface (BCI) applications surface Laplacian is applied to the raw EEG data to improve its spatial resolution (Babiloni, 2001).

The scalp surface Laplacian, current source density transformation is represented in Eq 2.1 and Eq 2.2. The Laplacian represents the double derivative of the flux, $\Delta^2\emptyset$ and $\frac{\Delta J}{\sigma}$ is the net current through the scalp, where σ is the scalp conductivity (flow of electrons) and ΔJ, represent the change in electrical current density on the surface of the scalp.

$$\boldsymbol{L(x,y,z) = \frac{\partial^2\emptyset}{\partial^2 z} + \frac{\partial^2\emptyset}{\partial^2 x} + \frac{\partial^2\emptyset}{\partial^2 y} = \frac{\Delta J}{\sigma}} \qquad \textbf{Eq 2.1}$$

By reducing the net current through the scalp to zero, the radial (flux) electrical current, $\frac{\partial^2\emptyset}{\partial^2 z}$ through the scalp is extracted, reducing the spatial blur (Eq 2.2).

$$\boldsymbol{\frac{\partial^2\emptyset}{\partial^2 z} = -\left(\frac{\partial^2\emptyset}{\partial^2 x} + \frac{\partial^2\emptyset}{\partial^2 y}\right)} \qquad \textbf{Eq 2.2}$$

Spline interpolation (Ferree & Ph, 1996) is a global technique for calculating the scalp SL, that was used previously in geophysics (Wahba & Wendelberger, 1980) but has been adapted to EEG. This method is based on global averaging rather than local, which only looks at neighbouring electrodes. The SL has been used in many EEG applications to improve the detection the EEG pattern. The main disadvantage of accurate SL estimates for EEG application is that it requires a large number of electrodes for local estimation methods (Ferree & Ph, 1996). However, a recent study concluded that the accuracy of the SL is not highly dependent on the number of electrodes used (Babiloni, 2001). In this study the SL of a high and low (one-third the electrodes) resolution system was classified for imaginary hand movements. It was concluded that the accuracy of the SL was not dependent on the resolution of the EEG system. The low resolution SL was shown to convey the same information as the high resolution SL. The low resolution system with only 9 electrodes had an average mental pattern recognition level of 81% compared to that of 82% for the 26 electrode SL, producing the same performance level for both full and low resolution SL data (Babiloni, 2001).

The circular Laplacian method was introduced by Song *et al.* (2006) as an alternative to spline interpolation. This method is based on the Hjorth's (1975) methods, but instead using just the 4 neighbouring electrodes to calculate the electrode potentials, the circular Laplacian method uses the interpolation and integration from a circle of variable radii around the desired electrode to predict the electrodes potentials. This method was proven to be 5% more accurate than the Hjorth's method. Through the variation of the radii of the circles on which the interpolation and integration is applied, various frequencies can be filtered out, and it act like a bandpass filter (Song & Epps, 2006). The radius of the circular Laplacian must be selected carefully for the EEG study as small Laplacian method have higher spatial filtering frequency and can weakens the mu-rhythm activities (Zhou, Wan, Ming, & Qi, 2010).

2.1.5 Independent Component Analysis

In the biomedical field, Independent Component Analysis (ICA) is a relatively new technique of signal processing and data analysis. ICA is a blind source separation technique that attempts to separate the problem of which sensor signals, of unknown mixtures and unknown source signal, is in which position. ICA is used to separate statistically independent sources from a set of linear mixed signals (Hyvärinen & Oja, 2000; James & Hesse, 2005).

The following gives the properties of ICA (Hyvärinen & Oja, 2000):

- ICA will only separate linearly mixed sources
- Changing the order in which points are plotted has no effect on the outcome of the algorithm, as ICA only deals with clouds of points.
- Even when the sources are not independent, ICA finds a space where there are maximum independents.
- Changing the channel order (for instance swapping electrode locations in EEG) also has no effect on the outcome of the algorithm. When ICA is applied to EEG there is no information about the location of the electrodes within the ICA algorithm.
- Perfectly Gaussian sources cannot be separated, as ICA separates sources by maximizing their non-Gaussianity.

The ICA Model (Eq 2.3) recovers a finite number of signals sources, s, by using a blind source separation method which calculates an unknown, unmixed matrix, A, and multiplying its inverse with the known signals, x. The weighting matrix, W, is equal to the inverted A matrix and represents the weighting of each independent component (IC) for each EEG signal (Hyvärinen & Oja, 2000).

$$\boldsymbol{x = As} \quad \boldsymbol{or} \quad \boldsymbol{x = \sum_{i=1}^{n} a_i s_i} \qquad \textbf{Eq 2.3}$$

$$\boldsymbol{\therefore s = Wx} \qquad \textbf{Eq 2.4}$$

The ICA Model is represented in Figure 2-5, with X being the linear combination of the independent components and represents the EEG signal sources. S is the independent components that are mixed into the sensors signals X. The Mixing Matrix, A, represents the degree to which each of the independent Components contributes to the mixed sensors X and the unmixing matrix, W, represents the weighting functions of each independent component in each sensor X (James & Hesse, 2005).

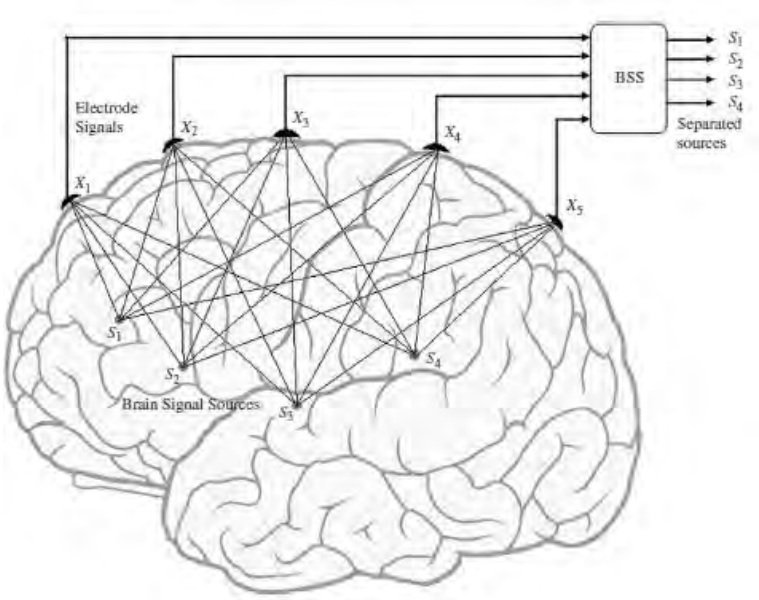

Figure 2-5: ICA model diagram, where X is the measurement of the EEG sensors, S represent the linear missed independent source. ICA produces the unmixing matrix W, that unmixed the mixed in depended component x(t), to give an estimate of the independent sources $\widehat{S}$ (James & Hesse, 2005; Sanei & Chambers, 2007)**.**

This method has been extended to EEG, to help filter out noise that is contained in the raw EEG signals (Jung T. et al., 2000) obtained from the scalp, which have a high signal to noise ratio (SNR), making it very difficult to extract brain rhythms. The EEG signals contain artefacts which include eye movement, motion artefact and electrical noise. ICA is used to separate the EEG signals into it independent components which will isolate the artefacts from the brain rhythms.

2.2 Electrophysiological Signal Features

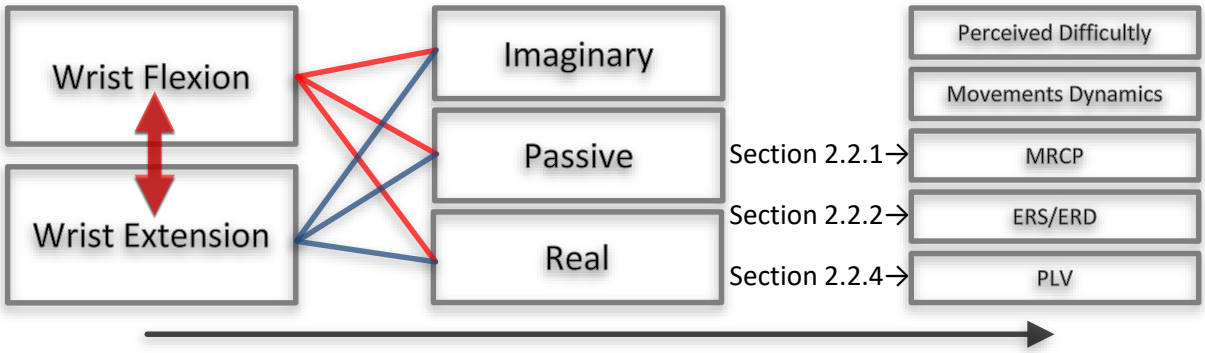

Figure 2-6: Diagram illustrating the different analysis techniques; MRCP - movement related cortical activation, ERDS – Event related de/synchronization, PLV – Phase locking value.

2.2.1 Movement Related Cortical Potential

Movement related cortical potential (MRCP) is an electrophysiological feature associated with movements, emanating from the motor cortex. MRCP are slow changing cortical potentials that occur at frequencies below 3Hz. According to Shibasaki *et al. (2006),* MCRP's can divided into 8 components, four each before and after the movement onset. Pre-movements components illustrated in Figure 2-7, include Bereitschaftpotential (BP), Negative Slope (NS'), P-50, N-10. Post-movements components include N+50, P+90, N+160 and P+300 (Hiroshi Shibasaki & Hallett, 2006). Similarly to

event related potential (ERP), MRCP are calculated by taking the additive average of the trials around the onset of movement (refer to Eq 2.5). The main difference between ERP and MRCP is the frequency band in which they are present.

$$\boldsymbol{MRCP(j) = \frac{1}{N}\sum_{i=1}^{i=N} x(i,j)} \qquad \textbf{Eq 2.5}$$

The Bereitschaftpotential (BP) refers to the pre-motor event-related negativity of the MRCP that occurs approximately 2s before the onset of movement (Hiroshi Shibasaki & Hallett, 2006) and is associated with planning and execution. They are extremely small compared to normal brain rhythms (hundred times small than alpha rhythms), and only become apparent when averaging to the onset of movements. The Pre-movement component (P+90) is predominant over the parietal region and contralateral hemisphere with the N+50 and P+90 peaks being related to kinaesthetic feedback (H Shibasaki, Barrett, Halliday, & Halliday, 1980).

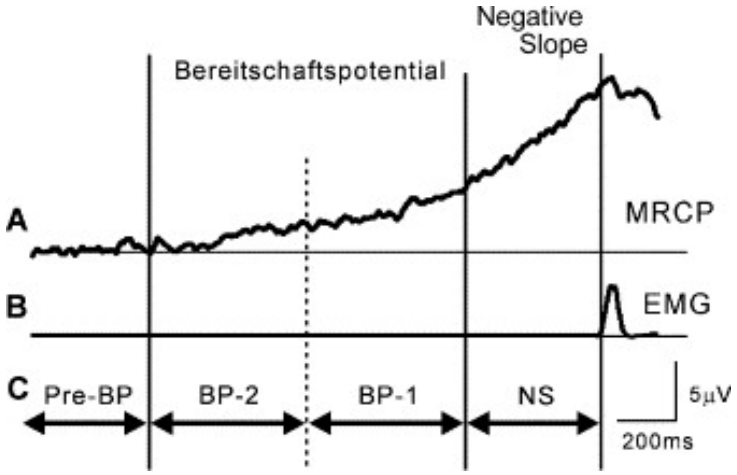

Figure 2-7: Typical MRCP waveform showing the pre-movement components. A) Movements Related Coritical Potential, B) rectified EMG activity, C) Pre-movement components. (Wasaka, Nakata, Kida, & Kakigi, 2005)

The BPs are divided into two time regions, the early pre-movement negativity (early BP) and the late pre-movement negativity (late BP), the latter having an increased gradient just before the movement onset. The early BP starts about 2 seconds before the onset of movement and is thought to represent a general preparation for the planned movement. Early BP might also be site-specific within the SMA and lateral premotor cortex, starting off in the pre-SMA and SMA proper and thereafter moving to the PMA with maximum activation in the centre-parietal midline. The late BP starts about 0.5 seconds before movement onset and is site-specific to the movement being performed, occurring in the precise somatotopic area corresponding to the contralateral M1 and lateral PMA associated to that movement. The late BP is maximal over the contralateral central (C1 or C2 of the International 10-20 System) is responsible for the hand movements. The negative slope (NS) occurs after the early BP and can be distinguished based on the sudden increase in the gradient of the slope.

Table 2-1: Effects of different factors on early and late BP in Movement related Cortical Potentials (Hiroshi Shibasaki & Hallett, 2006)**.**

Factors	Early BP	Late BP
Level of intention	Larger	
Preparatory state	Earlier onset	
Movement selection	Larger	No effect
Learning	Larger during learning	
Praxis movement	Start parietally	
Force	Larger	
Speed	Later onset	
Precision	No effect	Larger
Discreteness	No effect	Larger
Complexity	No effect	Larger
Mirror movement	No change	Involved

The magnitude and time course of the BP for self-paced condition can be influenced by various characteristics such as pace of movement repetition, force exerted, speed, precision, learning, level of intension, movement selection and complexity of movement (Table 2-1). In experiments where subjects were required to repeat the same movements once every 5s or longer, the BP will start much earlier, compared to natural movements, as the subject has time to prepare for the movement (Hiroshi Shibasaki & Hallett, 2006). It is also believed that BP may reflect an intention to act in stroke patients preforming motor execution imagination (Niazi et al., 2011). Slobounov *et al* (2004), found that with an increase in the perceived effort of a movement there is an increase in the BP amplitude for the last 100ms segment (Semyon Slobounov, Hallett, & Newell, 2004). Since perceived effort is commonly associated with a stronger exerted force, intension and motivation, the effect of these factors cannot be clearly distinguished from each other. Increasing the applied force results in a proportional increase in the amplitude of MRCP's, whilst the speed of a movement affects both the time and magnitude, with faster movements resulting in increasing magnitude and a delay in the beginning of the BP (Siemionow, Yue, Ranganathan, Liu, & Sahgal, 2000).

2.2.2 Event-related desynchronization and synchronization

Event-related potentials (ERP), such as evoked potentials and slow negative potentials shift, represent the phase-locked responses of cortical neurons. Event-related desynchronization and synchronization (ERD/ERS) can reflect both phased and non-phased locked changes in activity of local interaction, between neurons and interneurons that control the frequency components. ERP are mostly affected by afferent activation (Median Nerve Stimulation) while ERD/ERS are affected by changes between neurons that modulate the frequency of the cortical signals. This makes ERD/ERS calculations frequency band specific. Since the frequency bands are inversely proportional to their output power, ERD in the alpha band have higher amplitudes than ERD in the beta bands.

Event-related desynchronization (ERD) describes the short lasting event-related localized amplitude attenuation of EEG-rhythms within a given frequency band, while event-related synchronization (ERS) describes the short-lasting event-related localized enhancement of these rhythms. This may be considered as a change in the synchrony of the localized neuronal populations resulting in an increase or decrease of synchronicity between localized rhythms (Pfurtscheller & Lopes Da Silva, 1999). Any kind of external stimulation (notably sensory stimuli) or internal voluntary movements can give rise to spontaneous frequency band specific EEG changes of amplitudes.

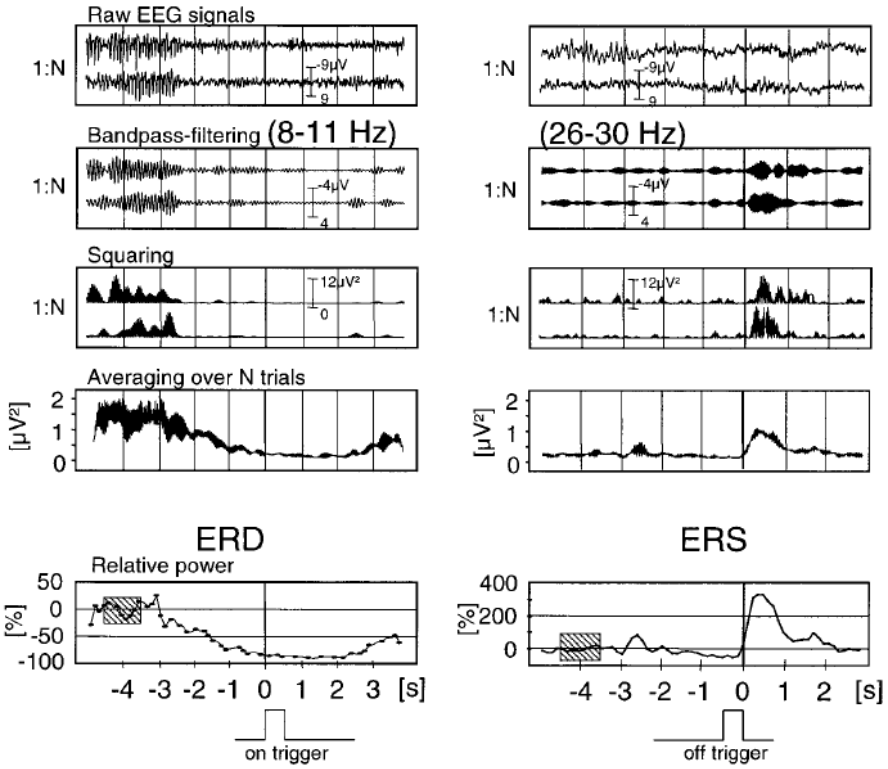

Figure 2-8: Graphical illustration of the method for calculating ERD and ERS (Pfurtscheller & Lopes Da Silva, 1999)

Various methods are used to quantify ERD/ERS. The most common methods are; band power, task-related power, and event-related spectral perturbation. Two basic methods are generally used in the calculation of the event-related power, the classical ERD instantaneous band power method and the inter-trial variance method, as shown by Eq 2.6 and Eq 2.7 respectively.

$$\bar{P}_{(j)} = \frac{1}{N}\sum_{i=1}^{N} x^2_{f(i,j)} \qquad \textbf{Eq 2.6}$$

$$IV_{(j)} = \frac{1}{N-1}\sum_{i=1}^{i=N}\left\{x_{f(i,j)} - \bar{x}_{f(j)}\right\}^2 \qquad \textbf{Eq 2.7}$$

For the equation illustrated above, each trial is band pass filtered around a particular frequency denoted by $x_{f(i,j)}$, for *j* samples at the *ith* trial. For the classical band power method, the event related data is first band passed, and then the samples are squared and averaged over all trials. For the power method, the power changes are calculated with both phase locking (e.g. evoked potentials) and non-phase locking components in a frequency band for signal x. The intertribal variance methods only calculate the non-phase locking components in the signal, by subtracting the filtered event related component ($\bar{x}_{f(j)}$) from the original filtered signal ($x_{f(i,j)}$). The ERS/ERD are defined as a percentage change of power ($A_{(j)}$) increasing or decreasing at each sample point related to an average power in a time window (R).

The ERD calculation for each sample, j, is given in Eq 2.8, where $A_{(j)}$ refers to either the instantaneous power ($\bar{P}_{(j)}$) or the inter-trial variance ($IV_{(j)}$) with the inter-trial variance (R) being an

average reference period in $\boldsymbol{A_{(j)}}$ (Kalcher & Pfurtscheller, 1995). The ERD/ERS calculation method is illustrated in Figure 2-8.

$$\boldsymbol{ERD/ERS_j = \frac{A_{(j)} - R}{R} \times 100\%} \qquad \textbf{Eq 2.8}$$

Real or imagined movement of the arms or feet induces Mu and Beta ERD in the motor cortex associated to those movements. The ERD starts about 2s prior to the onset of movement. This means that it is related not only to the actual execution of motion but also in planning, preparation and judgement of the movement to be carried out. Beta ERD are much more somatotopically focal than Mu ERD. Also, pre-movement Mu ERD are independent of movement speed, duration and type of movement i.e. finger, thumb and hand movement all result in very similar Mu ERD patterns in the same cortical region. Beta ERD for hand motion has been found to be slightly more anterior than Mu ERD (Neuper, W??rtz, & Pfurtscheller, 2006), although the force exerted and rate of the movement will affect the post movements ERD (Doležal, Šťastný, & Sovka, 2006). For instance, an increase in the rate or the force of a movement results in an increase in post-movements ERD. ERS generally occurs in areas of the cortex that are inhibited or inactive. Such areas are not related to the action that is being performed. It has been shown by Neuper et al. (2006) that visual stimulation results in ERD in the occipital region (active region) and ERS in the central region (non-related region). Similarly, during voluntary hand movements ERD can be detected in the central region (active region) and ERS in the occipital region (non-related region). This same phenomenon also applies when comparing the same type of modality e.g. motion. When comparing hand and foot motion, hand motion results in hand area (active) ERD and foot (inactive) area ERS while foot motion results in hand (active) area ERS and foot (inactive) area ERD (Neuper et al., 2006).

2.2.3 Event-Related Spectral Perturbation (ERSP)

Event-Related Spectral Perturbation (ERSP) represents a time frequency decomposition of the EEG data, which characterises changes in the spectral content (Delorme & Scott Makeig, 2004), making it a useful tool for analysing brain oscillatory activity in EEG data (J. Liou et al., 2009). ERSP measures mean event-related brain dynamics changes of the EEG power spectrum at a channel (Delorme & Scott Makeig, 2004) and reveals an aspect which is not contained in the ERP average. ERSP can be viewed as a generalization of ERD as it reveals more information of the brain dynamics than narrow band ERD, because the spectral changes normally involve more than one frequency.

To calculate ERSP (Eq 2.9) the average of the power spectrum, $F_k(f,t)$ over a sliding window needs to be computed for n trials at frequency, f, and time, t. The spectral estimate is calculated using sinusoidal wavelet (short-time DFT) transform, as it has been shown to obtain better frequency resolution at higher frequencies as compared to other approaches (Delorme & Makeig, 2004).

$$\boldsymbol{ERSP(f,t) = \frac{1}{n}\sum_{k=1}^{n} |F_k(f,t)|^2} \qquad \textbf{Eq 2.9}$$

ERSP has been used in many EEG applications; ranging from studying the concomitant dynamics of components during learning u-rhythm regulations (Delorme & Scott Makeig, 2003), to extracting EEG frequencies responsible for auditory evoked stimulation.

2.2.4 Phase synchronization

Most electrophysiological signal features are based on the behaviour of separate signals without regard to the information between the different brain regions and the coupling information between EEG signals. However, many brain regions are dependent on different functional areas that are widely distributed throughout the brain (Felix Darvas, Miller, Rao, & Ojemann, 2009). The communication between the different brain areas exhibits coupling phenomena in the brain signals. This brain coupling can be detected with phase synchronization and gives new insight into the working of the brain and new methods for feature extraction (Wei et al., 2007). *"The impetus to investigate phase relations of electrophysiological brain signals, such as the scalp-recorded electroencephalogram (EEG), is based on the fact that such a measure reflects the cooperative interactions between anatomically disparate neural populations."* (Brunner, Scherer, Graimann, Supp, & Pfurtscheller, 2006).

Linear and non-linear methods can be used in the calculation of signal coupling in the brain. Linear coupling includes; cross-correlation for the time domain and coherence for the frequency domain, while non-linear methods include; nonlinear regression coefficients for amplitude coupling and phase locking value (PLV) for phase coupling. Due to the non-linear behaviour of the human brain during cognitive task, nonlinear methods such as PLV can give a deeper insight into the computation basis for human cognition and control (Wei et al., 2007).

2.2.4.1 Phase locking Value

Phase locking is a time domain synchronization measurement of frequency. Phase synchronization is a measurement that shows whether the phase shift between any two signals is close to a constant over a specified time interval. Mean spectral coherence is an alternate method that can be used to solve for phase synchronization. However, coherence is affected by both amplitude and phase effects, while PLV characterizes the nonlinear coupling of phase (Wei et al., 2007). A 2004 study on phase synchronization concluded that PLV in general yields a better result as compared to coherence. It was stated that synchronization is more restricted than coherence due to the fact that an increase in coherence does not necessarily imply an increase synchronization (Gysels & Celka, 2004).

Phase Lock Value (PLV) is sensitive to coupling of the same phase and same frequency in two signals. For discrete signals the Phase lock value is calculated as follows:

$$\boldsymbol{PLV(f,t)} = \left| \frac{\mathbf{1}}{\boldsymbol{N_{trial}}} \sum_{\boldsymbol{trial}=\mathbf{1}}^{\boldsymbol{N_{trial}}} \boldsymbol{e}^{j(\Delta \boldsymbol{\phi}^{\boldsymbol{trial}}(\boldsymbol{f},\boldsymbol{t}))} \right| \qquad \textbf{Eq 2.10}$$

In Eq 2.10, N_{trial} is the number of trials required to calculate the PLV over, and $\Delta\emptyset(f,t)$ represents the phase difference between the two EEG electrodes. PLV's are then normalized, where zero indicates no phase coupling and one indicates perfect phase coupling between two EEG electrode signal in a particular frequencies band (Gysels & Celka, 2004).

$$\Delta\emptyset(\boldsymbol{f},\boldsymbol{t}) = \emptyset_{\boldsymbol{x}}^{\boldsymbol{trial}}(\boldsymbol{f},\boldsymbol{t}) - \emptyset_{\boldsymbol{y}}^{\boldsymbol{trial}}(\boldsymbol{f},\boldsymbol{t}) \qquad \textbf{Eq 2.11}$$

The instantaneous phase, $\emptyset_s^{trial}(f,t)$ is calculated in Eq 2.12, where $s(t)$ is the EEG trial data and $\tilde{s}(t)$ is the Hilbert transform of the EEG trial data.

$$\emptyset_s^{trial}(f,t) = arctan\left(\frac{\tilde{s}(t)}{s(t)}\right) \quad \textbf{Eq 2.12}$$

To calculate the PLV (PLV) the instantaneous phase of each signal needs to be estimated by using the Hilbert transform (Wei et al., 2007), or by convolving it with a Gabor wavelet (Felix Darvas et al., 2009). The Gabor and Hilbert methods have been shown to produce basically the same results (Quyen et al., 2001). The main difference is that the Hilbert transform requires the data to be filtered prior to calculating the phase synchrony. With the Gabor method, the wavelet is designed around the frequency of interest. The most commonly used method for calculating the phase synchrony is the Hilbert transforms due to its quick computation time. (Pereda, Quiroga, & Bhattacharya, 2005).

The Hilbert transform $\tilde{s}(t)$ is given by:

$$\tilde{s}(t) = \frac{1}{\pi} p.v. \int_{-\infty}^{+\infty} \frac{s(\tau)}{t-\tau}\, d\tau \quad \textbf{Eq 2.13}$$

with p.v representing the Cauchy principal value.

Phase synchrony has been shown to be a robust method for differentiating motor imagery states (Wang et al., 2006). In a recent study that looked at the amplitude and phase coupling relationship between imaginary motor movements, a classification accuracy of 84.4% to 90.6% was obtained for left hand and right hand movements respectively (Wei et al., 2007).

3. Literature Review

Literature discussing relevant flexion and extension studies will be presented in section 3. An overview of the current literature relating to the investigation is represented in section 3.1. Studies related to the differences between flexion and extension are discussed in section 3.2 and section 3.3, followed by the investigated movement types in section 3.4.

3.1 Overview of current literature

The neuromuscular differences between flexion and extension of the upper extremities could be attributable to cortical muscular pathways and/or due to structural and possible functional differences in the brain. Consideration must be given to the effect that each movement type will have on the cortical activation of the brain, and the electrophysiological features that might be associated with them. Through the review of wrist flexion or extension during real (active) voluntary movements, passively induced movements and motor imaginary movements, the underlining source of the cortical activation present during the movements may be obtained.

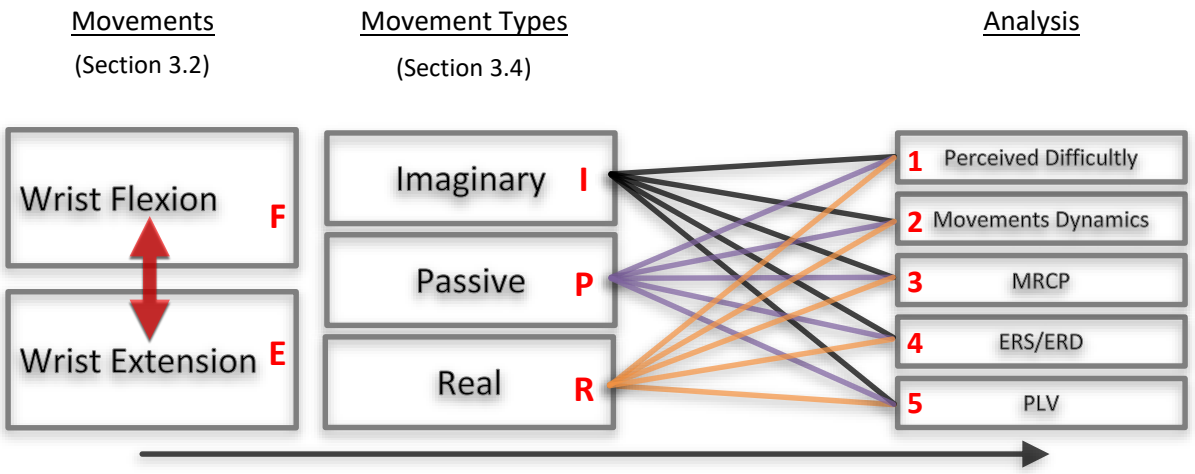

Figure 3-1: Literature review overview diagram illustrating the relation between the different movement analysis. Refer to Table 3-1 for literature studies corresponding to the red letters and numbers.

Table 3-1: Overview of relevant literature for the study between flexion and extension for imaginary, passive and real movements (Refer to the above Figure 3-1 for index numbers). Underlined regions indicated areas of interest for the investigation in to the differences between flexion and extension of the upper extremities.

Index Figure 3-1	Author	Comment/Review
F&E-R-3	Yue *et al. (2000)*	There exists higher brain volume activation during thumb extension compared to flexion movements, with an increase in the MCRP levels for thumb extension. These differences may be as a result of different corticospinal and/or other pathway projected to the motoneuron pools of flexor and extensor muscles of the upper extremities.

E-R-3	(Gu et al., 2009)	Two movements types where preformed, wrist extension and rotation at two different speeds, fast and slow. It was shown that the average rebound rate of the MRCP was greater for the faster imagined movements compared to the slower ones, but was not dependent on the movement type.
R-2&4	(Siemionow & Yue, 2000)	For an increase in the rate of rising force applied there was a strong correlation with the magnitude of the MRCP in the sensorimotor cortex and SMA. For an increase in force there was an equal increase in the magnitude of MRCP levels.
F&E-R-2	(Delp, Grierson, & Buchanan, 1996)	Peak voluntary flexion force ranged from 5.2Nm to 18.7Nm, with the average peaking at 40° flexion while peak voluntary yextension force ranged 3.4Nm to 9,4Nm. The average extension force were relatively constant from 30° flexion to 70° extension. Passive force for flexion and extension remained near zero but increased at the end of the range of motion, with the average passive flexion force of 05.Nm at 90° flexion and 1.2Nm at 90° extension.
E-P-4	(Alegre et al., 2002)	Passive movements consisted of brisk wrist extensions were compared to ballistic movements of six healthy volunteers. A beta band desynchronisation was observed after the beginning of the wrist extension movements, followed by beta synchronization. A similar observation was observed during ballistic movements, but without pre-movements components.
E&F-P-4	(Müller et al., 2003)	The study consisted of event-related beta EEG changes during wrist movements (extension/flexion) that were stimulated by functional electrical stimulation (FES), and compared to active and passive hand movements. A prominent ERD is found immediately after the induced FES, followed by a beta ERS similar to that in active and passive wrist movements. It was shown that for stimulated movements no ERD is detected prior to movement onset. However, it was concluded that afferent inputs from joint, tendon and muscle receptors to the primary somatosensory area could account for the post-movements beta ERS as seen in other studies.
E-R-2	(Stancak et al., 1997)	Four levels of external load (0g, 30g, 80g and 130g) were applied to the right index finger while brisk voluntary extension was performed. Prior to movement, desynchronisation of the contralateral sensorimotor areas, were higher for loads of 80g and 130g compared to no load. The largest load resulted in the longest mu-rhythm desynchronisation in both hemispheres after the

		movement onset, and longest beta-synchronisation post movement compared to no load. This shows that movement related desynchronisation and synchronisation are influenced by external load opposition finger movements.
F&E-I-4	(A. Vuckovic & Sepulveda, 2008)	Three seconds sustained imaginary and real right hand movements were performed, on which the energy density maps were calculated over a fixed 240ms, 2Hz time frequency window. The movements preformed are right wrist flexion/extension and pronation/supination. Electrode Cp3 showed the largest differences in the higher alpha and the beta bands for both real and imaginary movements.
E&F-I-4	(Stancák, 2000)	This paper investigated brisk right index figure movements preforming extension-flexion and flexion–extension. It was observed that finger extension and flexion movements induce unequal B synchronization over the contralateral primary motor areas.
P-4	(Müller-Putz et al., 2007)	This study compared ERD/ERS patterns between paraplegic patients and healthy subjects preforming active and passive foot movements. There are midcentral-focused beta ERD/ERS patterns during passive, active and imaginary foot movements in the healthy subject, but in the paraplegic patients a diffuse and broad distribution ERD/ERS patterns during attempted foot movements, with no significant ERD/ERS patterns during passive foot movements were noticed.
I&P&R-4	(Formaggio et al., 2013)	Passive movement of the right hand showed a desynchronisation over C3 and C4, with significant alpha and beta band differences over the contralateral SMA (C3). Motor Imaginary right hand movements resulted in ERD over the contralateral SM1, alpha range ERD over C3 and beta range ERD over P3, Pz.
I-5	(Spiegler, Graimann, & Pfurtscheller, 2004; Wang, Hong, Gao, & Gao, 2006)	Right hand movements resulted in an increase in the phase locking between the SMA and left M1 area, while left hand movements resulted an increase in phase locking between the SMA and right M1 area.

Table 3-1 displays a general overview of the current literature, the investigation between flexion and extension of different movement types and analytical techniques, as shown in Figure 3-1. It can be noted that there are very few studies that focus on the differences between flexion and extension for different movement types, and these comparisons are primarily limited to ERDS and MRCP movement analysis (see section 2.2). As far as it is known, no previous studies that have compared the phase synchrony between cortical areas for wrist flexion and extension, due to the difficulty involved in distinguishing between movements of the same limb. Furthermore, although previous studies have looked at the differences between passive and real movements, they have not focused on the inherent differences between passive flexion and extension.

3.2 Functional differences between wrist flexion and extension

The functional differences between wrist flexion and extension differences are reported in the literature review. A brief overview of the anatomical and physical differences of the wrist is given in the subsections below.

3.2.1 Anatomical movement differences between wrist flexion and extension

There are a number of anatomical differences between wrist flexion and extension, predominately in the six superficial muscle groups associated with the wrist movements (see Figure 3-2, top anterior forearm and the bottom posterior forearm). The muscle groups associated with wrist extension: are *extensor carpi radialis longus*, *extensor carpi radialis brevis*, *extensor carpi ulnaris* and those associated with wrist flexion are: f*lexor carpi radialis*, *palmaris longus* and *flexor carpi Ulnaris*. Other muscles that are not specific to the wrist movements but that have been understood to contribute to the forces produced during movement include, but are not limited to, *extensor digitorum*, *flexor digitorum superficilis* and *flexor digitorum profundus* (Martini et al., 2014; Netter, 2003).

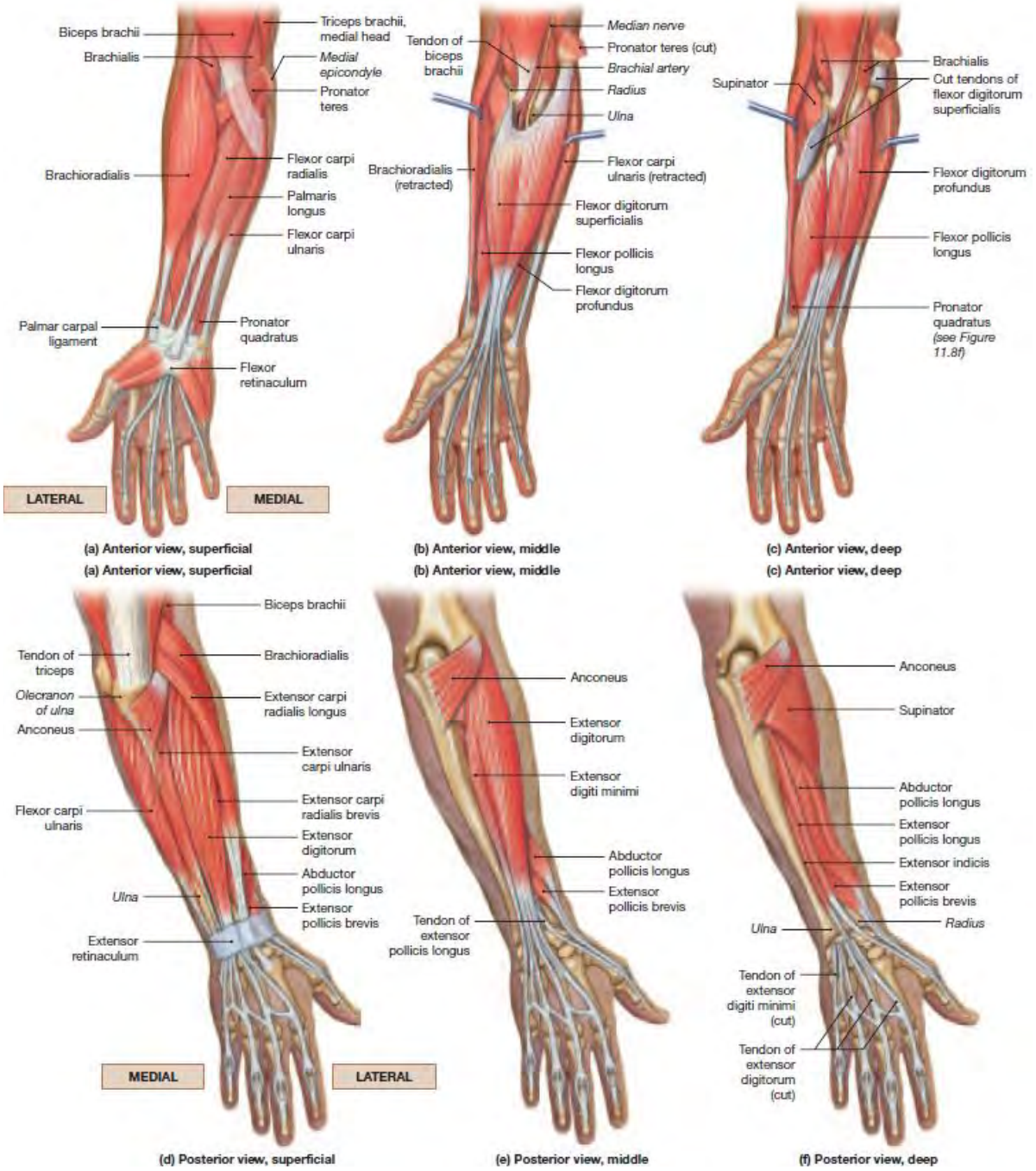

Figure 3-2 Anterior forearm (top) and Posterior forearm (bottom) muscles groups required for wrist flexion and extension (Martini et al., 2014).

3.2.2 Physical movement differences between flexion and extension

The physical movement (Movement Dynamics) differences between wrist flexion and extension, can be seen in range of motions and the maximum output forces of each movement. Figure 3-3 (left) shows the average maximum isometric force for wrist flexion and extension at different wrist angles. The peak real wrist flexion moments ranged from 5.2Nm to 18.7Nm, with the average peaking at 40° flexion. The peak real wrist extension force ranged from 3.4Nm to 9,4Nm, remaining relatively constant from 30° flexion to 70° extension. During passive wrist flexion and extension (Figure 3-3, right) the peak force remained near zero, but increased at the end of the range of motion, with an

average passive wrist moment of 0.5Nm, at 90° flexion and 1.2Nm, at 90° extension (Delp et al., 1996).

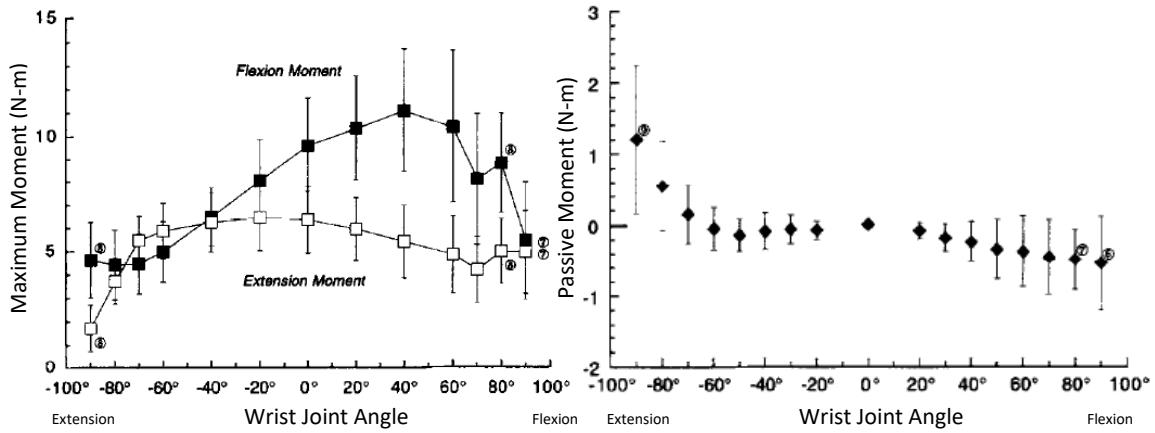

Figure 3-3: Average maximum isometric moments of wrist flexion and extension related to the flexion-extension angle (left).Passive flexion and extension moments verse flexion and extension angles (right). Error bars indicated the 95% confidence interval (Delp et al., 1996)**.**

For finger flexion-extension and extension-flexion movements, similar differences exist to those observed in wrist flexion and extension. The maximum voluntary output force of finger flexion is considerably higher than that of extension. This is supported by an increase in peak burst EMG for finger flexion, in both flexion-extension and extension-flexion movements. Movement and EMG burst duration is highest for extension-flexion movements in both the contraction and return phase (Aleksandra Vuckovic & Sepulveda, 2008a). During passive movements, the tendon force in an extended wrist is two to three times greater than in a wrist flexed, regardless of number of digits moved. In a passive extended wrist the tendon tension lies at 940g ± 143g, while in a passive flexed wrist yields a tendon tension of 76g ± 37g (Lieber, Amiel, Kaufman, Whitney, & Gelberman, 1996). There is also a difference in the normal range of motion (ROM) between wrist flexion and extension, with a wrist extension ROM ranging at 0-70° and wrist flexion ROM at 0-90° (Lowe, 2006).

3.2.3 Effects of fatigue

Both amplitude and frequency factor show EMG time domain changes due to muscle fatigue, thereby decreasing the ability of muscles to create force. Edward et al. (1996) showed that muscle fatigue appears to affect the dynamic stability of the movement, whilst Granacher et al. (2010) reported a decrease in the velocity and stride length. Muscle fatigue can also alter the latency and magnitude of the reflex response, which can result in an increase in the movement relaxation response (Behrens, Mau-Moeller, Wassermann, & Bruhn, 2013; Descarreaux, Lafond, Jeffrey-Gauthier, Centomo, & Cantin, 2008). The cortical changes caused by muscle fatigue are not under voluntary control, and usually occur much slower compared to voluntary changes (Klimesch, 1999).

As mentioned above investigation involving voluntary active or static muscle contraction, may be affected by fatigue if they are conduction over an extended period with extensive muscle force activation. Therefore, it is important to ensure that the experiment is designed in such a manner that these effects can be averted.

3.3 Neurophysiological movement differences

3.3.1 Flexion and Extension

Previously researched neurological features, such as Movement Related Cortical Potential (MRCP) have been used in the differentiation of flexion and extension movements. However, Palmer and Ashby (1992) have shown differences in neural descending projection to the motor neuron pool associated with flexor and extensor muscle groups. Yue et al. *(2000)* showed that during active thumb flexion and extension, higher brain volume activation occurs during thumb extension. It was speculated that this difference in brain volume activation could be due to differences in corticospinal pathway projections to the motoneuron pools. Flexor muscles of the upper extremities are more facilitated or less inhibited by the corticospinal and other cortical and subcortical motor-control systems, while extensor muscles are less facilitated by these systems. Therefore, higher level of brain activation may be needed to activate the extensor muscles. This could account for the differences in MRCP between thumb extension and flexion, with higher movement related amplitude level in the motor cortex and SMA for thumb Extension (Yue et al., 2000).

Another study of right index finger brisk extension-flexion and flexion-extension movements by Stancák (2000) observed post movement beta synchronisation following movement onset. During the extension-flexion movements, a higher post movement beta synchronisation amplitude was present, with more widespread activation over the contralateral M1 areas. The difference could be due to more complex neurological networks required for finger extension movements (Stancák, 2000). Similarly Aleksandra *et al*. (2008) examined the cortical differences in real and imaginary movements for wrist flexion, extension, pronation and supination. Classification rates of 80% true positive were achieved for imaginary wrist flexion movements, when comparing to wrist extension. For real movements higher classification rates were achieved for any combination of movements (Aleksandra Vuckovic & Sepulveda, 2008a). However, Stancák et al. (2000) and Aleksandra *et al.* (2008) gave little regard to the effect that difference in movement force may have on the cortical activation in the brain. Refer to section 3.4.3.3 for the effect of muscle force activtion on cortical activation for volutary movement.

3.3.2 Active and Passive

Previous research has shown that the brain activation associated with active and passive movements are clearly different, mainly in the motor areas of the brain. Weiller *et al.* (1996) recorded the cerebral blood flow (rCBF) during right elbow active and passive movements using Positron Emission Tomography (PET). The movement consisted of one complete motion of flexion and extension at a frequency of two seconds. Both active and passive movements resulted in cortical activations in the contralateral sensorimotor cortex, supplementary motor area (SMA), and the bilaterally inferior parietal lobe. Additional active movement activations occurred in the cingulate gyrus and in the basal ganglia. Activations of the contralateral sensorimotor cortex resulted in almost identical magnitude, extent and location for both active and passive movements. (Weiller et al., 1996). Mima *et al*. (1999) conducted a similar PET experiment, in which the differences between active and passive finger movement were analysed. Similar cortical activation was present in the sensorimotor areas during passive and active motor tasks. Active finger movements resulted in cortical activation in the contralateral primary sensorimotor cortex, premotor cortex, supplementary motor cortex, bilateral

secondary somatosensory area and basal ganglia, whilst passive finger movement activation occurred in the contralateral primary and secondary somatosensory areas (Mima et al., 1999).

Alegre *et al.* (2002) studied the beta band changes between passive and ballistic wrist extension movements by comparing the pre-movements period. In Figure 3-4 the ERD at the beginning of the movements were followed by an increase ERS. Similar post movement ERD/ERS patterns occurred during both movements. However no pre-movement passive components were present (Alegre et al., 2002).

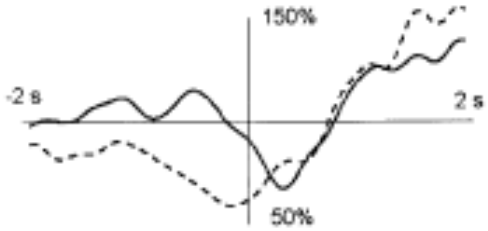

Figure 3-4: Beta band (15-25Hz) ERD and ERS, comparing passive (- - -) and Ballistics (----) movements (Alegre et al., 2002)

3.3.2.1 Movement Training

Lotze *et al.* (2003) used fMRI to record cortical activation during active and passive consecutive wrist flexion-extension movements to observe the effects of training on the improvements of motor performance. The implementation of a torque motor was used so that the amplitude and duration ranges of the passive movements would be similar to the active movements. A higher level of cortical activation was present during active movements than during passive movements in the contralateral primary motor cortex (cM1) before training. This increase in cortical activation could account for the significantly better performance observed during active training compared to passive training (Lotze et al., 2003). Thickbroom *et al.* (2003) also observed an overall increase in cortical activation in voluntary movements, with lower passive movements activation occurring over the SMA, SM1 area (Thickbroom et al., 2003).

3.3.3 Somatosensory system

The somatosensory system is responsible for receiving, interpreting and passing on relevant sensory information to areas of the brain that assimilate and respond to the sensation about the length, degree of stretch tension, muscle contraction, pain, temperature, pressure and joint position. The nervous system has a greater number of sensory fibre pathways than motor fibres (Kandel et al., 2000). The nervous system receives sensory information through different pathways, each responsible for different groups of sensation involving; touch, pain and temperature (Spinothalamic tract), and proprioception (medial lemniscus tract, refer to section 3.3.4.2).

All movements of the body cause a stimulation of sensory receptors, which activate neurons in the brain through afferent sensory pathways. These sensory input to the brain can directly or indirectly, via the somatosensory cortex, affect the cortical activation of different areas of the brain. Seki and Fetz (2012), studied the manner by which afferent signals during movements are processed by the CNS, through the investigation of the sensory evoked potential in the spinal cord, somatosensory and motor cortex, and premotor cortex in monkeys. It was shown that afferent inputs are suppressed, in

the spinal cord, somatosensory, motor and premotor cortex during active limb movements. However, during movement preparation suppression only occurred in the motor cortex (Seki & Fetz, 2012). Nashmi et al. (1994), conducted a ERD/ERS study to determine the motor activities that are associated with an increase in beta band activity in the sensorimotor area. Movement preparation, instead of the motor activity itself, was found to increase beta activity in the sensorimotor area of the brain (Nashmi et al., 1994).

Movement related beta band studies have shown ERD occurring shortly before and during the movement, with a burst of beta ERS occurring in a one second period after the movement onset (refer to section 2.2.2). This post movement beta ERS has been reported after voluntary hand movements, passive movements and imaginary movements. Muller-Putz *et al.* (Müller-Putz et al., 2007) studied the event related beta change that occurrs during active and passive attempted foot movements. Mid central beta ERD/ERS patterns were present during passive, active and imagined movements in healthy subjects. It has been concluded that the beta ERS oscillations after the foot movements could be the result of afferent inputs to the cortical representation areas in the brain (Müller-Putz et al., 2007). Beta ERS after voluntary movements has also been thought to reflect termination of motor commands. Cassim *et al.* (2000) conducted a study where active movements were compared with passive movements, and passive movements after deafferentation by ischaemic nerve blockers. Post movement beta band ERS was present in both active and passive movements. However the ERS was not present in passive movements that had nerve blockers. The post-movement ERS may also reflect movements related to somatosensory processing, and not only as a result of termination of motor commands (Cassim et al., 2001). Similarly, post movement beta ERS were observed during the illusion of movements. Keinrath *et al.* (2006) conducted an experiment where active, passive and the illusion of movements were compared. The beta band power activation for active movements was significantly higher compared to passive and illusion movments. All the movment types resulted in similar short lasting, post-movment beta ERS over the motor areas, suggesting that somatic perception of limbs movments plays a role in the somatosensory system and the primary motor cortex. (Keinrath, Wriessnegger, M??ller-Putz, & Pfurtscheller, 2006).

3.3.4 Corticospinal and Somatosensory pathways

The cortical difference detected between flexion and extension in section 3.3.1, could be due to a number of areas involved in movement control. This includes the primary motor cortex, sensory motor cortex and its associated pathways involved in muscle control and sensory feedback (refer to section 3.3.3). The corticospinal pathway and sensory pathways are repersented in Figure 3-5, and subsection 3.3.4.1 and 3.3.4.2.

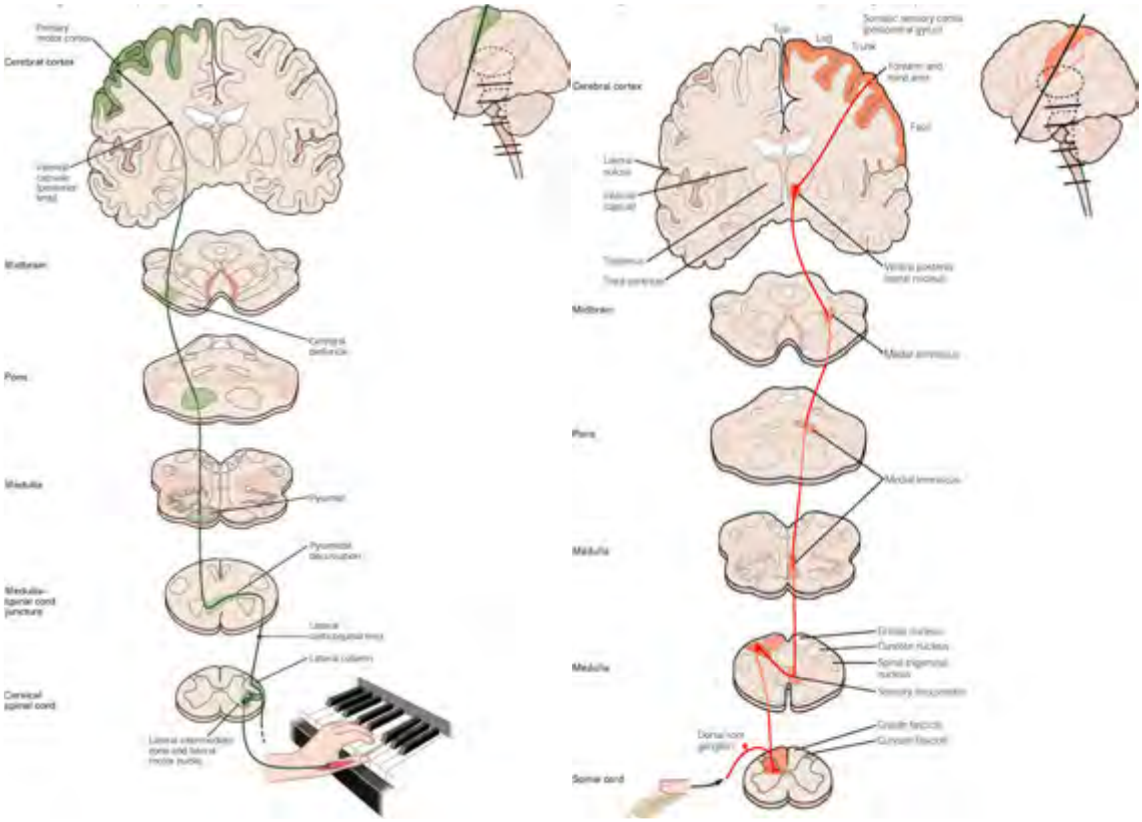

Figure 3-5: (Left) A representation of the corticospinal pathways involved in movement control. (Right) A representation of the sensory pathways involved in fine touch and proprioception (Kandel et al., 2000).

3.3.4.1 Corticospinal Pathways

The corticospinal track is the pathways that conveys axial and limb motor control, through which the brain can control the movement of muscle, as shown in Figure 3-5 (left). The corticospinal pathway arises from the primary motor cortex (precentral gyrus) neurons, of which one will innovate the axial muscle and the other, the limb muscle. They exit the cortex through the internal capsule and into the continue brain stem, where the limb fibers decussate (cross over) in the medulla of the brain stem. After the brain stem the fibers run down the corticospinal tracks, and when at their required target levels, the limb fibers and axial fibers (through decussation) connect to a synapse in the spinal cords' grey matter neurons (lower motor neurons). The neurons then project to the limb and axial muscles (Kandel et al., 2000). Differences in corticospinal pathways could affect the cortical activation required to perform a particular movement, as concluded by Yue et al. (2000). Refer to section 3.4.3.2 for the involvement of corticospinal pathways on active voluntary movements.

3.3.4.2 Medial Lemniscus Pathways

The Dorsal column medial lemniscus is one of the major afferent pathways, conveying fine touch and sensory information of how the body is positioned (proprioception) from the upper and lower limb, as shown in Figure 3-5 (right). This sensory information is conveyed through the spinal cord via the dorsal root ganglion neurons situated outside the spinal cord. These neurons project from the body to the spinal cord through the gracile and cuneate fasciculus via the medial lemniscus. From the spinal cord the pathway ascends into the brain stem where they decussate, and travels through to the primary sensory cortex of the brain associate sensory representation area (Kandel et al., 2000). Refer

to section 3.4.2.1 for more information on the involvement of afferent pathways in passive movements.

3.4 Movement Types and Neurophysiological features

3.4.1 Imaginary Movements

Motor imaginary movements can be defined as the mental simulation or execution of a given movement through the process of mental rehearsal, without any overt movement. Motor imaginary of a corresponding real movement can produce a similar premotor cortical activation to that which would be produced if the movement was real, as shown in the below studies.

Pfurtscheller *et al*. (2006) used mu rhythm ERD/ERS to classify different imagined motor tasks. During the planning or execution of motor tasks, motor rhythms were suppressed resulting in mu ERD in the relative motor cortex location. This was tested to see if these phenomena could be used as features to classify four motor imaginary tasks: right hand, left hand, tongue and feet motion. Hand movement imagination, resulted in a suppressed mu rhythm (ERD) of the hand area, while imagination of foot or tongue movement resulted in enhanced mu rhythm (ERS) of the same hand area (Figure 3-6). The enhanced mu rhythm resulted in narrow band frequency components at 12 Hz ± 1.0, while suppressed mu rhythm resulted in broader band frequencies at 10.9 Hz ± 0.9 (Pfurtscheller, Brunner, & Lopes da Silva, 2006).

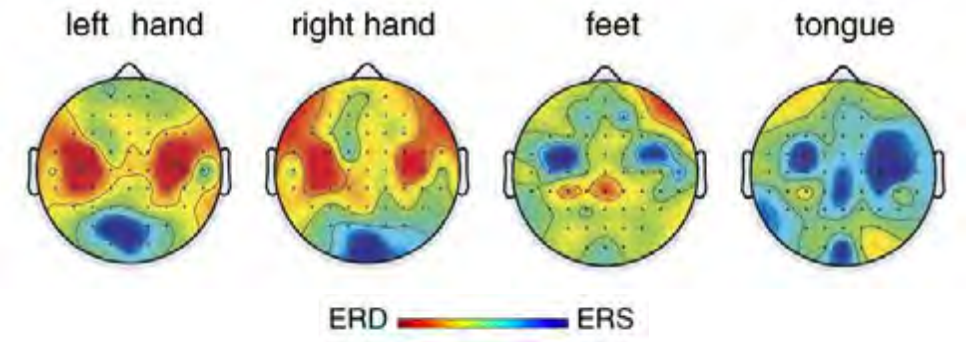

Figure 3-6: Single subject ERD/ERS topographical maps of the upper alpha band (10-12Hz) for 4 motor imaginary tasks; left hand, right hand, feet and tongue (Pfurtscheller, Brunner, & Lopes da Silva, 2006)**.**

Pfurtscheller *et al*. (2005) also investigated post-movement Beta ERS related to four motor imagery tasks: right hand motion, left hand motion, feet and tongue motion. Most of the subjects exhibited Beta ERS at the vertex after feet motor imaginary movements. Only a small number of subjects exhibited Beta ERS at the vertex after hand motor imaginary movements, with more subjects exhibiting Beta ERS at the contra-lateral hand area. None of the subjects showed Beta ERS after tongue imaginary movements. These motor imaginary features could be used along with mu rhythm ERD/ERS to increase classification accuracies in BCI applications (Pfurtscheller, Neuper, Brunner, & Lopes Da Silva, 2005).

3.4.1.1 Motor imagined movement types

There are two types of motor imaginary movements that can be performed, kinaesthetic motor imagery or visual-motor imagery. The main difference between the two is the way in which the movements are imagined. For kinaesthetic motor imagery, movements are imagined as a first person process (imagine self-performed action with interior view), whilst for visual-motor imagery the

movements are imagined in the third person process (imagine performing action with exterior view .i.e 'mental video'). For both kinaesthetic and visual-motor imagery there is a desynchronisation (ERD) in the lower alpha and beta band components. The main difference between the two kinds of imaginary movements is that desynchronisation patterns for kinaesthetic imagery is followed by a beta band synchronisation (beta ERS) in the sensorimotor area. Figure 3-7 shows the topographical differences between kinaesthetic and visual-motor imagery, with the recognition of visual-motor imagery barely above random, whilst the classification rate for kinaesthetic motor imagery in the left central derivation is much higher compared to right central and occipital sites. Neuper *et al.* (2005) showed that for single trial motor imagery, classification rates of 67% can be obtained for kinaesthetic motor imaginary movements, compared to 56% classification accuracy for visual-motor imaginary movements (Neuper et al., 2005).

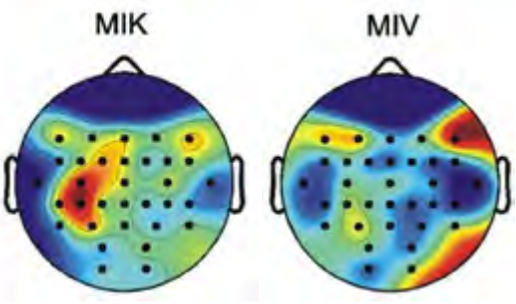

Figure 3-7: ERD/ERS topographical plot of kinaesthetic motor imagery (MIK) and visual-motor imagery (MIV) showing the differences in synchronization and desynchronization patterns between the two types of motor imagery. The recognition of MIV is barely above random, whilst MIK left central derivation is clearly higher compared to right central and occitipal sites (Neuper et al., 2005)**.**

3.4.1.2 Rate of movement

Müller-Putz *et al*. (2010) used post-movment beta rebound (ERS) during executed brisk feet movements in order to train a classifier to identify brisk foot motor imaginary movements. The difference between the movement types was that the motor imaginary beta rebound amplitudes were smaller than those of the executed movements (Müller-Putz, Kaiser, Solis-Escalante, & Pfurtscheller, 2010). An experiment was also conducted by Gu *et al*. (2009), that studied motor imaginary movements. In this experiment, subjects were instructed to imagine wrist motor movements at either a slow or fast rate. It was shown that the average rebound rate of the MRCP was greater for the faster imagined movements compared to the slower ones (Gu et al., 2009).

The mental rehearsal and visual imagery in planning a movement, activates similar patterns in the premotor and posterior parietal cortical regions to those that take place during real movements (Kandel et al., 2000). During motor imaginary movements the speed at which the movement is imagined affects the time delay of the peak negativity in the MRCP's (Gu et al., 2009). There is a shorter time delay during fast movement imagination compared to slow movement imagination. Recently, Ying *et al.* (2009) used speed of movement to differentiate between imagined wrist extension and wrist rotation. Each movement was imagined at a slow and fast pace. MRCP peak negativity and rate of rebound, as well as ERD/ERS power were used as features to differentiate each movement task from each other. Discrimination between the speeds of movements resulted in a higher classification rate than the classification of different movement types of the same joint (Gu et al., 2009).

3.4.1.3 Motor Imagined Phase locking

Phase synchronization is another method that is used in the classification of motor imaginary movements. Unlike ERD/ERS and MRCP, which only look at the feature extracted from the dynamic behaviours of separate signals, phase synchrony uses the coupling information between signals. Wang *et al*. (2006), used phase locking value (PLV) in the single trial study of left/right hand motor imagery movements, through the analysis of the phase synchrony that can occur between the supplementary motor area (SMA) and primary motor areas (M1). Right hand movements resulted in an increase in the phase locking between the SMA and left M1 area, while left hand movements resulted an increase in phase locking between the SMA and right M1 area (Wang et al., 2006). Similar phase locking effects were observed when comparing left and right motor imaginary movements, for a combination of foot and hand imagined movements. However, when comparing the phase synchrony between the left and right M1 areas, no significant differences were observed between left and right motor imaginary movements (Wei et al., 2007; Zhou et al., 2010).

Although it has been shown that motor imagery can be classified using ERD/ERS and PLV, it is difficult to differentiate between antagonistic movements of the same joint or same limb. This makes it difficult to distinguish between wrist flexion and wrist extension, and movement of the wrist verse movement of fingers of the same hand, as these actions produce very similar patterns of ERD/ERS in similar cortical areas.

3.4.2 Passive Movements

It has also been suggested that the magnitude of recovery can be predicted by looking at the cortical activation after passive movements (Alary et al., 1998) and that passive movements may lead to improvements in motor performance (Lotze et al., 2003). One of the main cortical differences between real (active/volutary) and passive movements is the absence of pre-movement patterns. Post movement patterns are still present, with beta ERD decrease starting after the passive movement onset (Alegre et al., 2002; Müller-Putz et al., 2007).

3.4.2.1 Involvement Reflex in afferent and efferent pathways

In early studies, reflex was primarily viewed an automatic stereotyped movements, contained entirely within the spinal cord, in response to sensory stimuli from muscles, joints and skin. However, it is now known that reflex response can be conditioned to adapt to a particular task through higher cortical activation. Conditioning a reflex can be induced in response to a stimulus that is not directly related to the reflex stimulus itself. Reflex also plays an important role in modulating motor output movement through stretch reflex that acts to resist the lengthening of a muscle. When a voluntary movement is performed, its function is not as a discrete reflex, but as a closed feedback loop to keep the muscle length as close as possible to the desired value. When a muscle is stretched there is an increase in the spindle discharge which results in a shortening of the muscle. This shortening of the muscle decreases the spindle discharge resulting in a reduction in muscle contractions and the lengthening of the muscle. This constant adjustment is a result of the stretch reflex feedback loop function, which acts continuously in order to keep the muscle at a desired length. The feedback loop also allows for efficient adjustments of weight bearing muscles responding to a change in load at the level of the spinal cord, without having to rely on cortical processors (Angelaki & Bergman, 2010). This feedback loop is illustrated in Figure 3-8, where the agonist and antagonist muscle spindles are used in the spinal cord to control and provide feedback to the muscles during movements. Muscle

control and spindle stimulation are conveyed to the brain through the descending (corticospinal pathways) and ascending projections.

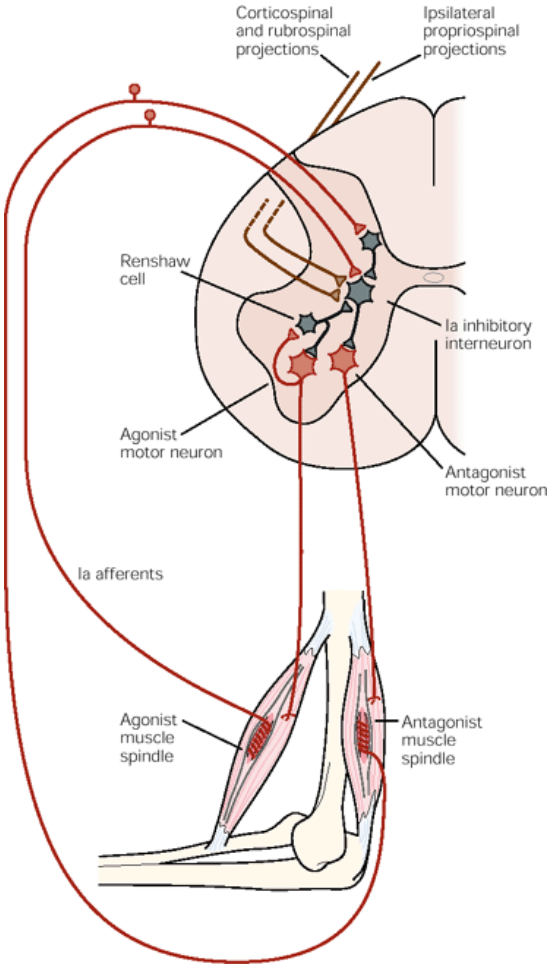

Figure 3-8: The feedback loop responsible for muscle control and reflex (Kandel et al., 2000)**.**

The primary somatosensory cortex is located in the parietal lobe, caudal to the central sulcus on the postcentral gyrus. Its primary purpose is to guide directed movement through the regulation of movements with sensory information. The somatosensory inputs also play an important role in reflex. The simplest controls of the primary motor cortex are those that are affected by sensory stimuli. This is due to the strong sensory inputs that the motor cortical neurons receive from the muscle spindles and joints. Sensory inputs also play a very important role in muscle and movement control, with rapid motor adjustments mediated by pathways in which somatosensory inputs reach the primary motor cortex through projection from the primary sensory cortex. Without somatosensory inputs the ability to perform gross movements tends to be imprecise, with fine movement control becoming impossible. Alegre *et al. (2002)* suggested that afferent proprioceptor inputs (reafference for joint, tendons and muscle receptors) during voluntary movements may affect the later part of the beta ERD (Alegre et al., 2002). Pfurtshellar *et al*. (2001) speculated that the ERDS observed is more related to the attention of the incoming stimulus.

Investigations involving passive movements inherently include the effect of reflex and somatosensory input in the brain. Therefore, cortical activation present during passive movements could be due to a number of factors including reflex and somatosensory pathways, resulting in activation of the primary motor cortex via the somatosensory inputs.

3.4.3 Voluntary Real (Active) Movements

Voluntary movements are the organization of selected joint and body segments, required to perform a particular task. There are several features that can cause neural organization in the premotor areas for motor preparation. Firstly, if a subject internally initiates a sequence of movements, this involves primary and supplementary motor areas. Secondly, movements are triggered by an external sensory event, involving the lateral premotor areas. Thirdly, mental rehearsal and visual imagery to plan a movement activates the same patterns in the premotor and posterior parietal cortical areas as those that occur during real movements. Finally, the more a particular movement is learnt, its performance increases to the point where is starts to become automatic, resulting in changes in the premotor area activation during the movements (Kandel et al., 2000).

3.4.3.1 Frequency of Movements

Voluntary movements are different from reflex and passive movements in that they are an organization of actions around a purposeful goal. This means that a selection of joints and muscle will move to achieve a particular task with increasingly more effectiveness as the voluntary movements are experienced and learnt. The increase in occurrence of a particular movement, can cause a decrease in the neural response due to the learning capacity of the brain through repeated exposure of identical stimuli in the brain (C. Büchel, J.T. Coull, 1999), which has been shown by Seitz et al. (1990) to decrease the cortical activation of that particular motor task. It has also been established that wrist flexion is more frequently used in comparison to wrist extension (Divekar & John, 2013; Yue et al., 2000), indicating that the central nervous system (CNS) adapts more easily to a repeated motor task, making them more automatic with less cortical activation.

3.4.3.2 Involvement of Corticospinal pathways

The areas in the primary motor cortex associated with a particular muscle group influence the activation of those muscle via the corticospinal tracts of the spinal cord, through projections directly from the motor neurons in the brain. The corticospinal tracts from the motor cortex consist of millions of axons that project through the subcortical white matter, making monosynaptic connections with motor neurons, and influencing other motor regions of the brain, including the cerebellum and basal ganglia. The corticospinal tracts are modulated by both sensory and motor information (see Figure 3-9, green/purple tracts), including tactile, visual and proprioceptive information, making voluntary movements accurate and precisely timed (Kandel et al., 2000). Motor neurons in the brain can be influenced by corticospinal pathways being facilitated by the reflex loop (refer to section 3.4.2.1) inside the spine (Raptis et al., 2010). Most neurons in the primary motor cortex become active only shortly before and during the movement. The intent to perform a movement also affects the firing pattern, with the patterns of neurons altering shortly before the movement takes place. The firing of neurons in the primary motor cortex is affected by the direction and amplitude of the muscle force of a movement, and not by the displacement of the movement itself. Trans-cranial magnetic stimulation studies have also shown that motoneurons in the primary motor cortex are facilitated by the corticospinal pathway prior to the muscle activation and are also modulated during the muscle activation (Raptis et al., 2010; Schneider, Lavoie, Barbeau, & Capaday, 2004).

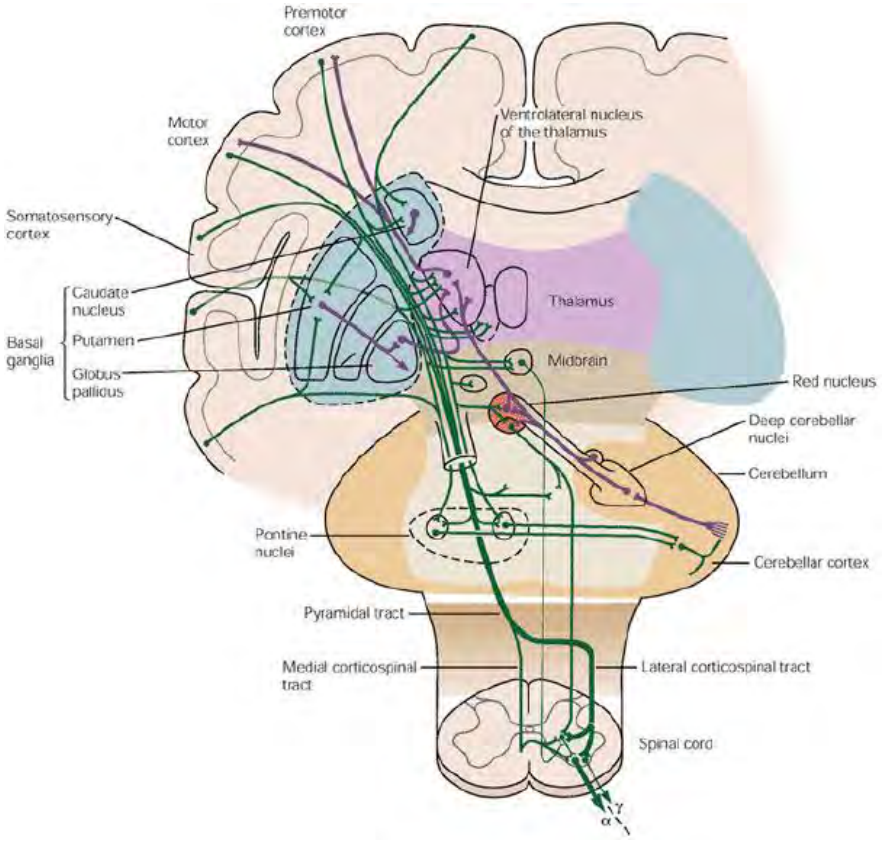

Figure 3-9: The main Components of the motor system required when preforming voluntary movements, include the premotor cortex, motor cortex, basal ganglia, cerebellar cortex and spinal cord. The green represents descending projection and the purple feedback projections (Kandel et al., 2000)**.**

3.4.3.3 Effects muscle force activation

Siemionow *et al.* (2000) conducted an experiment where the rate of isometric elbow-flexion was contracted at four different intensity levels; 10%, 35%, 60% and 80% of maximum voluntary contraction. It was observed that for an increase in the rate of rising force applied, there was a strong correlation between the magnitude of MRCP in the sensorimotor cortex and SMA. It was suggested that MRCP levels represent motor commands that scale with the level of muscle activation and rate of movement (Siemionow & Yue, 2000). This Indicates more cortical activation of the neurons, and/or that more sensory information is being processed during an increase in muscle force activation (Dai et al., 2001). Ying *et al. (2009)* showed that the speed of the task being performed was encoded in the time delay of the negative peak of the MRCP (Gu et al., 2009) with rapid hand movements resulting in non-continuous activity over the sensorimotor cortex (Kirsch, Hennighausen, & Rösler, 2010). These results indicate that the MRCP levels do not only represent the level of the muscle activation, but also some type of mental component related to the degree of intent for muscle activation. There is also a direct relationship between the force that is applied and the brain volume activations (Dai et al., 2001). A similar force experiment was conducted by Andrej *et al.* (2002), where differences in EEG rhythms were examined for differences in external loads for a brisk voluntary extension of the right index finger. It was observed that for a greater force there was a greater desynchronisation of beta-rhythms in the contralateral sensorimotor area, accompanied by a longer mu-rhythm desynchronisation (Alegre et al., 2002). Fast finger movements have been shown to result in a larger Beta ERS compared to slow finger movements, and wrist movements result in larger Beta

ERS than all finger movements. This means that for greater muscle activation or movement speed there is a direct relationship between the level of MRCPs and the level of beta-rhythm desynchronisation. This was confirmed in an fMRI study by Alegre *et al.* (2002) where there was a direct relationship between the degree of muscle activation and the amplitude of the brain signals. (Alegre et al., 2002; Dai et al., 2001). Dai *et al.* (2001) conducted a similar force *experiment*, where a stronger fMRI output was observed during higher hand grip forces. These studies show that not only does the rate of movement effect brain volume activation, but also the force at which the movement was conducted.

3.4.3.4 Movement Related Coherence

Similarly to PLV (see section 3.4.1.3), event related coherence examines the functional coupling between difference cortical area, unlike ERD/ERS and MRCP which only examine region activation. Changes in the cortical coupling can indicate higher cortical task demand. However, PLV is only affected by the phase difference whereas coherence is known to be affected by both phase and amplitude changed between to cortical areas, refer to section 2.2.4.

Leocani et al (1997), investigated the cortical activation during movement control, by studying event related ERD/ERS and coherence. Similar ERD/ERS result where observed to those discussed in section 3.3.3, with execution and preparation movement resulting in mu and beta ERD, followed by ERS in the sensorimotor cortex. Similar coherence increase was observed to that of ERD, starting frontally in the left central area, becoming more balanced between the left and right area after muscle activation. It was concluded by coherence, that frontal lobes play an important role in movement planning and execution (Leocani et al., 1997).

4. Investigation Methodology

This chapter describes the experimental setup, procedures, and methodology required for studying real, passive and imaginary wrist flexion and extension.

The objectives of this chapter are to:

- Describe the experimental paradigm used for recording EEG during the different wrist movements, including the hand device design, EEG and EMG recording procedure, visual display stimuli and epoch events (see section 4.1).
- Describe the required pre-processing, artefact correction and filtering methods applied to the raw EEG Data (see section 4.2.1).
- Explain the statistical methods used, including the different statistical methods used in the comparison between two movement conditions (see section 4.2.3).
- Give a detailed description of how the analytical methods are calculated. This Includes MRCP, ERDS and PLV analysis between two movement conditions (see section 4.2.4).

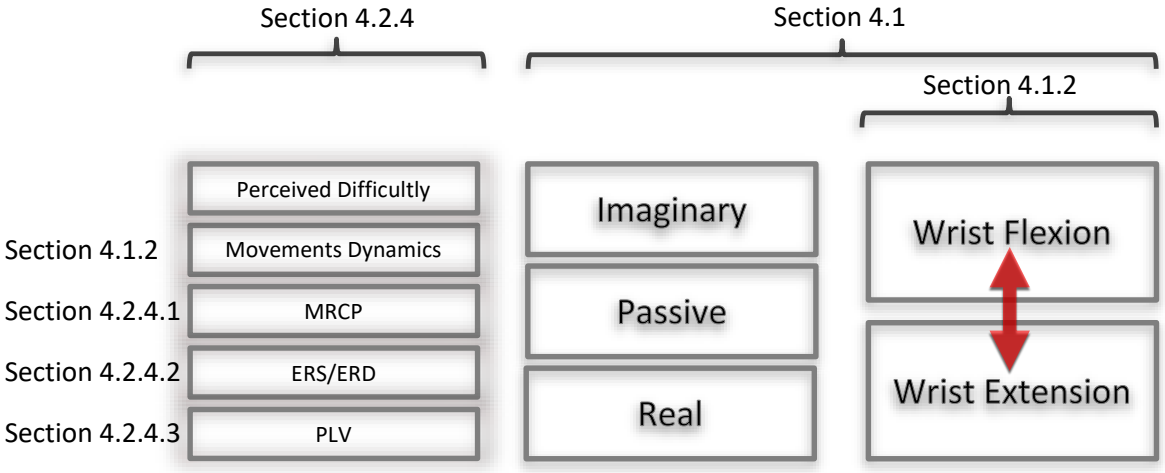

Figure 4-1: Diagram relating methodology section to study sections.

4.1 Experimental Methodology

Following approval by the University of Cape Town (UCT) human ethics committee, written informed consent according to the declaration of Helsinki (World Medical Association, 2008) was given to capture EEG and EMG data on fifteen subjects. Fifteen right handed, neurologically normal subjects (mean age: 25.5 years, standard deviations: 2 years) participated in this study. None of the subjects had previously participated in an EEG recording. The subjects were asked to perform three different tests, broken up into a number of different criteria. A visual displayed program was used to cue and indicate which of the different movements needed to be performed. Refer to APPENDIX A - Subject Consent Form, for the consent form used during the experiments. Refer to APPENDIX A, for age of subjects.

4.1.1 Experimental Paradigm

In the main experiment (Figure 4-2, Main Experiment), subjects were asked to perform real, passive and imaginary repetitive motor movements of the right wrist in flexion and extension. During the imaginary movements, subjects were instructed to perform kinaesthetic motor imagery (first person movement imagery) instead of visual-motor imagery (third-person movement imagery), since the former yields stronger ERD activity (Neuper et al., 2005). Motor imaginary movements were performed at a brisk rate, in a similar manner to the real and passive movements. Visual inspection of the EMG data, displayed through Labview, was used as a way to determine whether the subjects were performing imaginary movements without any muscle activation. For the real movements, the hand device was set to resist the direction of motion with 10% of the MVC value for the particular movement and subject (i.e. real wrist flexion or extension). During the passive experiments, the wrist was moved by the hand device at random, to either the wrist flexion or extension position. This is done at a constant rate for both movements to ensure that the rate of change did not cause a difference in brain volume activation when comparing passive wrist flexion and extension.

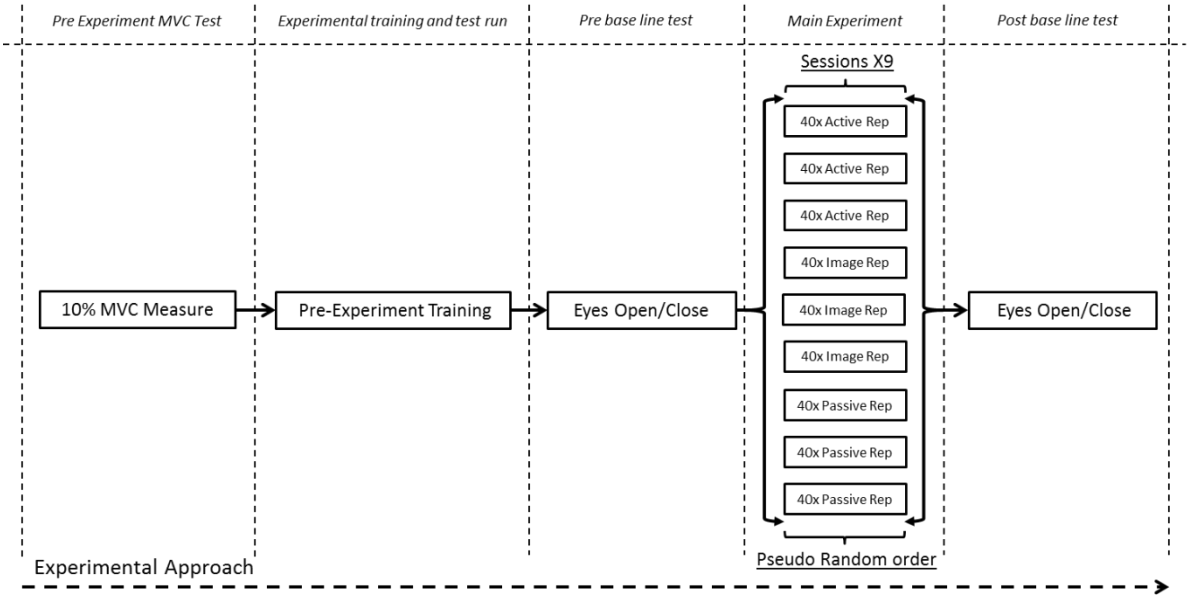

Figure 4-2: Experimental approach. (Active Rep - Real movement Repartition, Image Rep – Imaginary movement repartition, Passive Rep – Passive movement repartition)

The subjects right arm was placed in a hand device (see section 4.1.2, Figure 4-9), that provided forearm and hand support. The arm was positioned with the forearm mid-way between pronation and supination of the wrist, such that the effect of gravity was negated. The hand device was adjusted so that the wrist joint pivoted around the axis of movement. EMG electrodes were positioned on the left and right arm of the subject, corresponding to the prominent muscle groups associated to wrist flexion and extension.

The experimental approach (Figure 4-2), required the subjects to undergo a Maximum Voluntary Contraction (MVC) test (Figure 4-2, Pre Experiment MVC test), training session (Figure 4-2, Experimental training and test run), and baseline EEG recording (Figure 4-2, Pre base line test & Post base line test). The MVC for flexion and extension of the wrist was measured by locking the rotation wheel (Figure 4-9, wheel) of the hand device, so that the wrist was at an angle of 0° (resting position).

To get an accurate MVC measurement, the subject was instructed to perform wrist joint contraction for 5 seconds at the following levels: 100%, 70%, 50%, 30% and 100% of perceived MVC. The highest recorded force for wrist flexion and extension was used to calculate the 10% MVC used in the real movement experiments. This is a similar MVC approach to that used by Slobounov et al. (2002). Before the training session, the subject was first instructed about the experimental procedure with the help of E-prime software (http://www.pstnet.com/eprime.cfm), which display and times the relevant movement cues. This was followed by one full training session of approximately 10 minutes consisting of real, passive and imaginary movements. The baseline recordings performed at the beginning and end of the experiment required the subject to perform an eyes open and eyes closed test, lasting 1 minute each.

Throughout the experiment, subjects were seated in a dimly lit room approximately 1.5m in front of a 17 inch computer monitor, which used E-prime software to cue the movements. To minimize the effect of ocular artefacts, the subjects were instructed not to blink during movements. The right hand was covered with a blackened box (Figure 4-3) to prevent visual access to the on-going movements and to avoid the effect of anticipation (Alegre et al., 2002). Subjects were asked to perform three types of real, imaginary and passive right wrist movements that would correspond to rotation around the wrist extension/flexion axis. During the main experiment, real, imaginary and passive movements were separated into three different sessions (see Figure 4-2) to reduce the strain and fatigue on the subjects (see section 3.2.3). Each session consisted of 20 repetitions of two different movements (wrist flexion and extension), making 40 movements in total. Hence each subject was required to perform 9 sessions consisting of 120 real, 120 passive and 120 imaginary movements, which were each comprised of 60 wrist flexion movements and 60 wrist extensions movements. The order in which wrist flexion and extension occurred was randomized by E-prime. The sessions were pseudo randomized to prevent counterbalancing (carryover effect) and unwanted patterns being embedded in the EEG data. Each session lasted about 10 minutes. Subjects were allowed to take rests between each session, during which the impedance of the EEG system was rechecked. E-prime was used to pseudo randomize the movement type order, randomize the wrist movements, and for marking of the trial cue events in the EEG recording. Refer to APPENDIX A - Experimental Order, for each subject's pseudo random order.

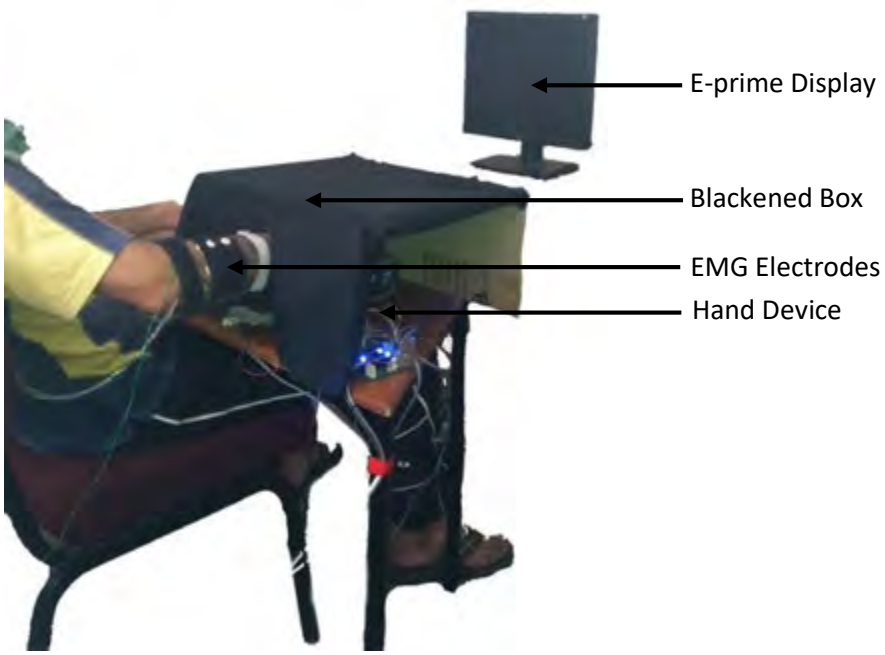

Figure 4-3: Experimental setup in the study, showing the position of the hand device and display.

4.1.1.1 Stimuli

A similar sustained movement approach to Vuckovic *et al (2008)* was used in real, imaginary and passive movement trials (A. Vuckovic & Sepulveda, 2008). At the beginning of each session the subject was instructed on which movement type to perform; real motor movements, passive motor movements or motor imaginary. The sessions consisted of 40 trials each, 10.5±2 seconds in length, consisting of a white fixation cross and white movement cue (Figure 4-5). The trial proceeded as follows: first, at second -2, a fixation cross appeared on the screen coinciding with a beep sound, indicating the beginning of a trial (Figure 4-4). The subject was then required to focus on the fixation cross to prevent eye movement. The preparation period allowed for pre-movements ERD and BP, which can occur 1 to 2s before the onset of the movement. At second 0, an arrow of 5cm in length, pointing right for wrist flexion or left for wrist extension, appeared on the screen and remained there for 1 second. The arrow indicated the movement to be executed. The subject was required to perform the movement type upon the disappearance of the arrow at second 1, and to keep the hand in the required position, i.e. to perform a sustained real, passive or imaginary movement. The total time of the sustained movement was 4 seconds, during which the subject was required to focus on the fixation cross. After the fixation cross disappeared at second 5, the subject made a non-sustained movement to return the hand to the resting position. At second 5 the fixation cross was replaced by a blank screen that remained for a random interval between 3.5 to 5.5 seconds. The purpose of the random interval was to reduce the anticipatory effect between movements (Alegre et al., 2002). The average resting period of 4.5 seconds gave enough time for the clear differentiation of movements in order to calculate the reference state or rest state. This is a similar stimulus approach to that used in other studies (Müller-Putz et al., 2010; Pfurtscheller, Linortner, Winkler, Korisek, & Müller-Putz, 2009; Pfurtscheller, Neuper, Flotzinger, & Pregenzer, 1997; Spiegler et al., 2004).

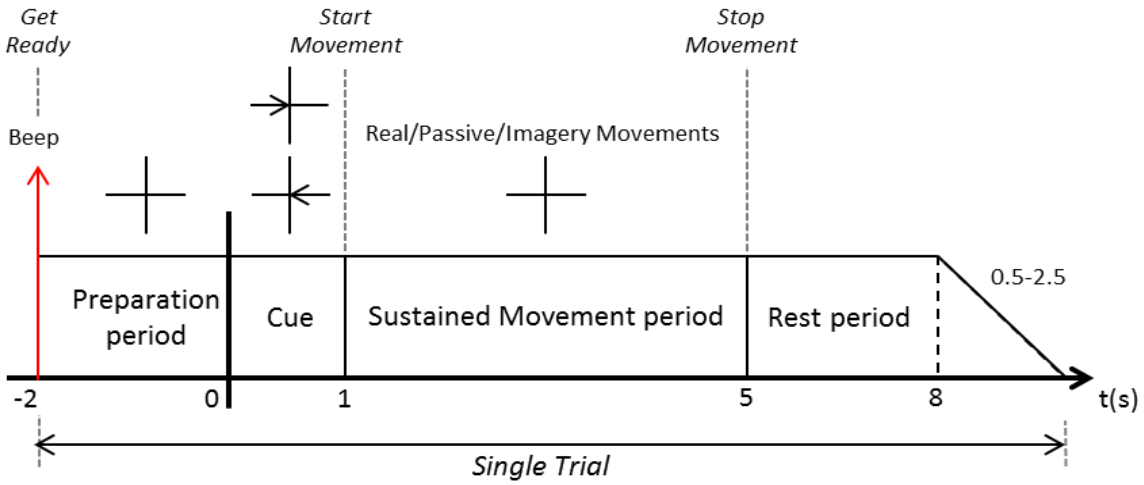

Figure 4-4: Epoch of time sequence and instruction protocol of a single trial for real, imaginary and passive movements.

The subjects were instructed not to blink, swallow, talk, move their eyes or adjust their body during the first 7 seconds of each epoch (Figure 4-4, -2 to 5 seconds), especially prior to performing the movement, in order to reduce muscle movement and eye blink artefacts that might be present during the movement and preparation phases. Subjects were observed throughout the experiment to ensure that the movements where performed as instructed, and any undesired behaviour by the subjects was noted. EMG signals were also observed to ensure that no muscle contraction occurred during the imaginary movements. Subjects were reminded before each session which movements needed to be performed. At the end of all the experiments, subjects were asked to rate the perceived difficulty of the flexion and extension in the real, passive and imaginary tasks using a scale of 1 to 10; where 1 = very easy and 10 = very difficult. Refer to APPENDIX A - Subjects Perceived Difficulty: for the subject experimental ratings.

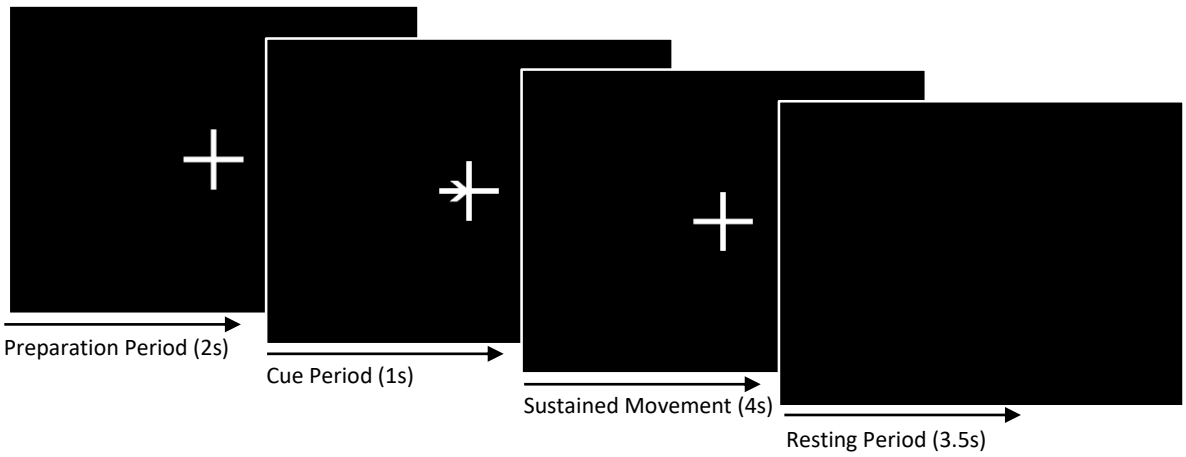

Figure 4-5: Schematically diagram illustrating the visual display in a typical trial. This illustrate is used for real, passive and motor imaginary wrist extension.

4.1.2 Hand Device

During the study of movements, different mechanical designs have been used in the control and monitoring of a particular movement. The hand device used by Yue *et al.* (2000) (Figure 4-6) was designed to study the differences between flexion and extension of the thumb. This device consisted

of a simple rubber band that allowed for an 18N force resistance against thumb flexion and extension. Once the movement had been performed the thumb was passively returned to the resting position with the help of the rubber band. However this design could not allow for thumb flexion and extension to be performed in a random order, due to the adjustment required of the rubber band during the different movements. This design also did not allow for the accurate adjustment of output force relative to each subject, to account for differences in relative muscle force activation during thumb flexion and extension. Another disadvantage of this design was that gravity could have an effect on the movements.

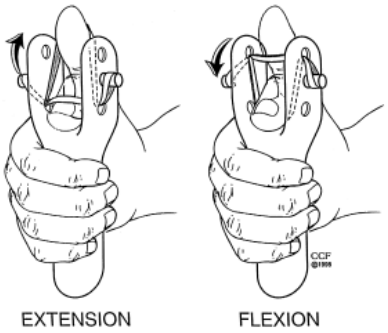

Figure 4-6: Hand device used in thumb flexion extension study (Yue et al., 2000).

Another hand device developed by Mima *et al.* (1999), illustrated in Figure 4-7, implemented a servo motor to control the position of the middle fingers. This device only performed finger flexion, but had the advantage of passive control of the finger position. The device was only designed for passive movements and did not resist against motion. It also did not measure the applied output force during movements. However, this design has the potential to be altered such that it could be used during real movements.

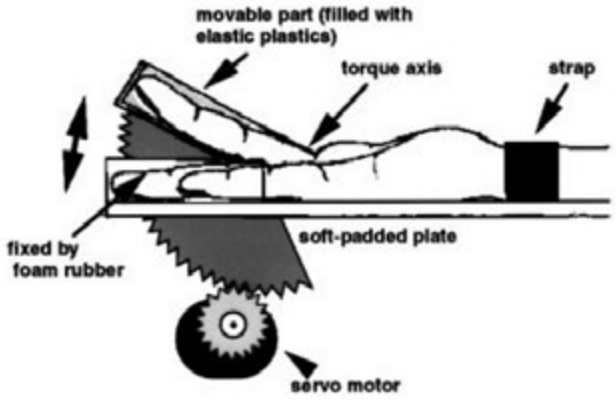

Figure 4-7: Servo controlled finger flexion hand device (Mima et al., 1999)**.**

Another hand device developed by Hidler *et al.* (2005) (Figure 4-8) was designed to be used in static movements, and only measure the torque applied during wrist flexion or extension. The advantage of this hand device is that gravity will not have an effect on the different movements, owing to the position of the hand.

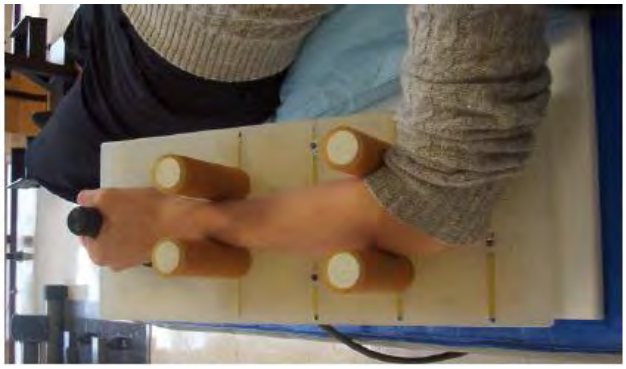

Figure 4-8: Static movement wrist flexion and extension hand device (Hidler, Hodics, Xu, Dobkin, & Cohen, 2006)**.**

The hand device required in the main experiment, needed to perform a combination of the different functions mentioned above. Firstly, it needed to resist the direction of motion with a fixed force that could change depending on the movement being performed. Secondly, it was required to perform passive movements to a predetermined location at a fixed velocity. Finally, the hand device was required to measure the static and dynamic output force being applied during motion. It also had to be designed in such a way that gravity would have an equal effect on the different movements being performed.

The hand device used in the main experiments (see section 4.1) and MVC test (see section 4.1.3.3) is represented in Figure 4-9. The hand device was designed in Solidworks and the main body was milled out of aluminium, refer to Appendix C.1 for more information. The main components of the hand device are the hand grip, arm support, capstan and wheel. The hand grip is where the subject's fingers were placed, and was shaped to match the curvature of human fingers and hand during rest position. The hand grip position could also be adjusted in order to fit the varying arm lengths of subjects (see Appendix C.1.1.2). This allowed the hand to be placed in the device in a rest position to maximize comfort and minimize unnecessary muscle activation. The subject's arm was strapped into the arm support which could be adjusted to match the arm position and was padded for comfort.

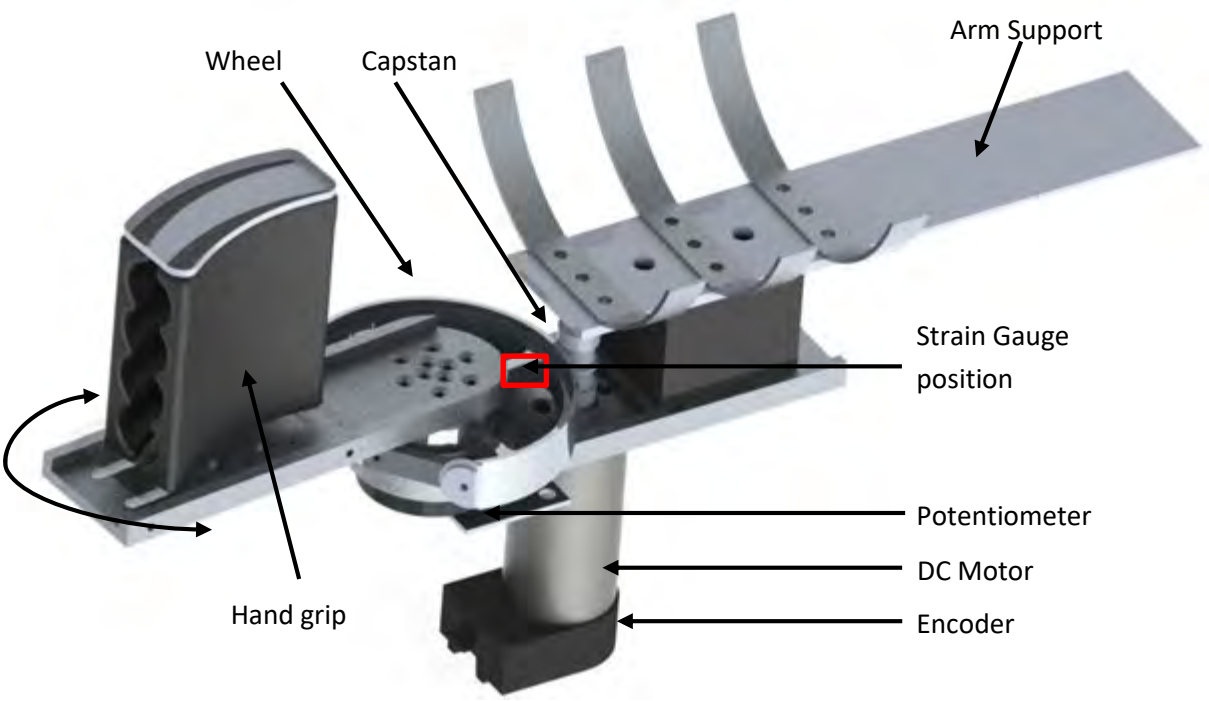

Figure 4-9: Solidworks CAD drawing, illustrating the function assembly of the hand device and its components. The hand device was fixed to a table for support, with the DC motor extruding through the table to minimize the height of the hand device.

Motion was provided to the hand grip by a DC motor through the capstan and wheel (Figure 4-9). This capstan wheel design allowed for high gearing and compliance during wrist movements. The capstan design was based on the Bowden cable actuator, which allowed for the remote actuation and rotation of a joint using a pull-pull configuration (Letier, Pierre A. Schiele, M. Avraam, 2006). A high gearing ratio (10:1) could be incorporated into the design of the hand device through elaboration of the principle Bowden cable actuator (see Figure 4-10).

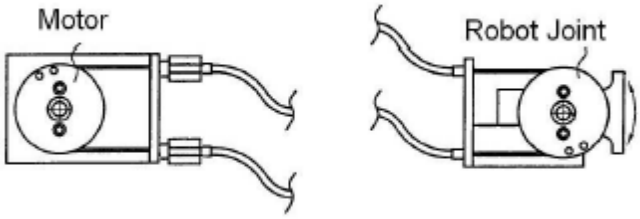

Figure 4-10: Bowden cable actuator principle (Letier, Pierre A. Schiele, M. Avraam, 2006).

The hand device allowed for the subject's wrist to be automatically moved, without human assistance, to either the wrist flexion or extension position during the passive experiments. This device also allowed for automatic resistance against motion with different degrees of output force, which is necessary for real (active) wrist flexion or extension experiments (see section 4.1.1). The ability for the hand device to operate without the need of human intervention increased the accuracy of the experiments, and decreases the probability of human error. The hand device also measured the angle and strain of the wrist during real and passive movements (see section 4.1.3.3). Refer to APPENDIX C - System Design, for a detail design overview of the hand device and system integration. Refer to APPENDIX B - DC Motor for the calibration of the DC motor used in the hand device.

4.1.3 Data Acquisition

On the arrival of subjects to the testing laboratory, the appropriate preparations were made for EEG, EMG, and hand device data acquisition. To prepare the subject for data acquisition the following steps were carried out:

- The subjects' arms were prepared, by cleaning the appropriate areas on the left and right arm where EMG electrodes were placed.
- The head circumference was measured and the vertex of the subject's head located.
- EMG electrode bands were placed onto the left and right arms around the muscle groups associated with flexion and extension of the wrist (see section 4.1.3.2).
- The right hand was strapped into the hand device.
- The MVC values for the subject was determined (see section 4.1.1).
- The EEG net was fitted on the subjects head (see section 4.1.3.1)

4.1.3.1 Electroencephalogram (EEG) online recording

The EEG and EOG were recorded using a 129 electrode, high impedance Electrical Geodesic System (EGS). Prior to recording, the EEG net was soaked in a freshly prepared saline solution for 10 to 15 minutes. The EGI Geodesics sensor net electrodes (Figure 4-11, Top) was mounted on the subjects head according to the international 10-20 system, with the common reference electrode (electrode 129) placed at the vertex, Cz (Figure 4-11, Bottom). The net was then connected to the EGI NetAmp amplifier. The system required electrode impedances to be kept below 50kΩ throughout the recordings. The electrodes were adjusted individually by rocking them, and each electrode's impedance was checked to ensure that it was below 50kΩ. EEG signals were recorded at a sampling rate of 500 samples/s with an on-line hardware band pass filter between 0.1-100Hz. EEG data were continuously recorded throughout the experiment and stored on a Macintosh with NetStation acquisition software. Stimuli trigger and response latencies were recorded online along with the EEG data. The impedances were checked four times throughout the experiment, at the beginning of the experiment and after the 3rd, 6th and 9th sessions. If Impedances were above 50kΩ, the saline solution was added to the problematic electrodes until the impedances were at acceptable levels. The data was then imported into Matrix Laboratory (Matlab) for further offline analysis (see section 4.2). Refer to APPENDIX C - Experimental Setup, for a diagram illustrating how the EEG net station system was incorporated with the EMG recording, Eprime Software and Hand device control.

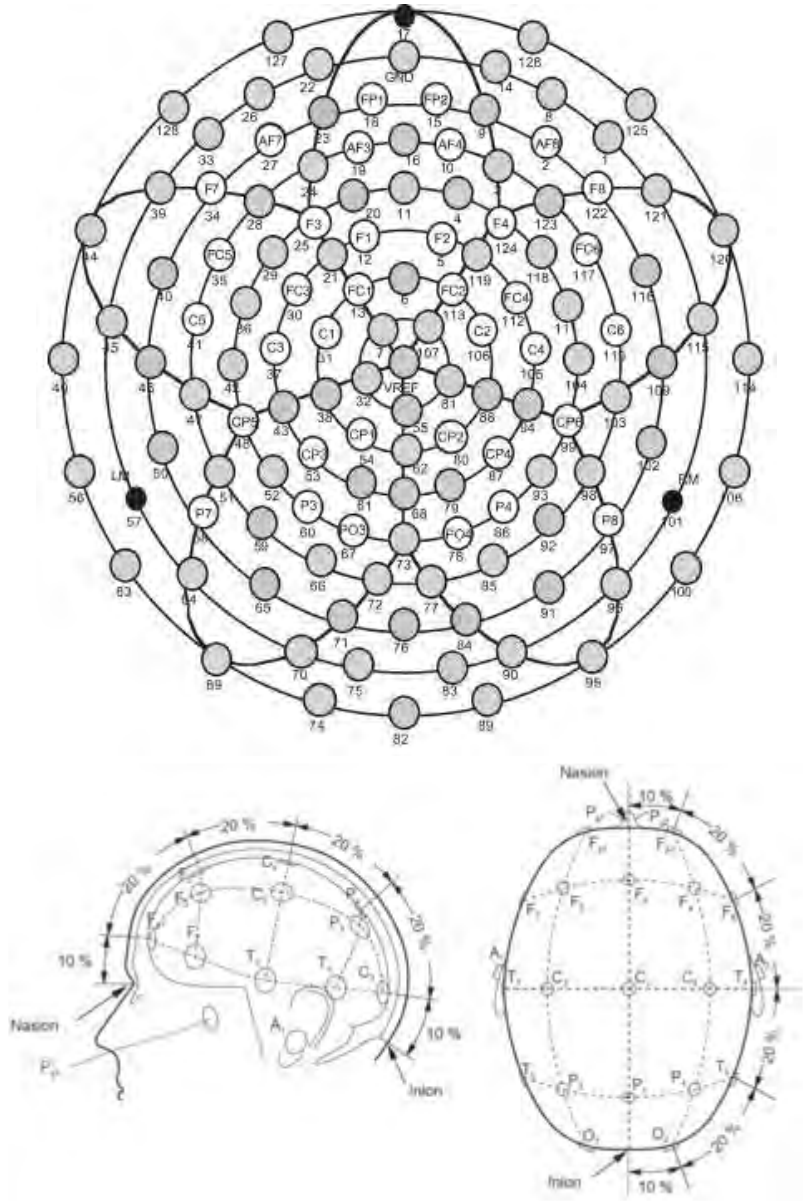

Figure 4-11: Top: electrode position of 128 channel EGI net with 10-20 electrode locations (Zopf, Giabbiconi, Gruber, & Müller, 2004). Bottom: corresponding 10-20 international system electrode placement over scalp (Nicolas-Alonso & Gomez-Gil, 2012).

The EGI Geodesics sensor net electrodes and international 10-10 electrode location montage shown in Figure 4-11 is, associated with the Brodmann sites represented in **Table 4-1** (see section 2.1.1 for Brodmann areas).

Table 4-1: Associating GSN electrode numbers, related to the 10-10 international montage channel position, related to the Brodmann areas.

GSN	*ELECTRODE*	*SITE*	*GSN*	*ELECTRODE*	*SITE*	*GSN*	*ELECTRODE*	*SITE*
E22	FP1	10L, 09L	E6	FCz	06R, 05L	E94	CP4	40R, 01R
E15	FPz	10L, 10R	E119	FC2	06R, 04R	E99	CP6	40R, 42R
E14	FP2	10R, 09R	E112	FC4	06R, 04R	E98	TP8	37R, 21R
E27	AF7	46L, 10L	E117	FC6	44R, 45R	E58	P9	20L, 37L
E24	AF3	09L, 46L	E116	FT8	47R, 38R	E59	P7	37L, 39L
E16	AFz	09L, 09R	E115	FT10	38R, 20R	E52	P5	39L, 19L
E3	AF4	09R, 46R	E46	T7	21L, 42L	E53	P3	39L, 07L
E2	AF8	46R, 10R	E42	C5	42L, 41L	E61	P1	07L, 31L

E34	F7	45L, 47L	E37	C3	02L, 04L	E62	Pz	07R, 07L
E28	F5	45L, 46L	E31	C1	05L, 02L	E79	P2	07R, 31R
E25	F3	08L, 06L	E129	Cz	05L, 05R	E87	P4	39R, 40R
E20	F1	08L, 06L	E106	C2	05R, 01R	E93	P6	39R, 19R
E11	Fz	08L, 08R	E105	C4	04R, 02R	E92	P8	37R, 39R
E4	F2	08R, 06R	E104	C6	42R, 41R	E97	P10	20R, 37R
E124	F4	08R, 09R	E109	T8	21R, 22R	E66	PO7	19L, 18L
E123	F6	46R, 44R	E51	TP7	21L, 42L	E60	PO3	19L, 39L
E122	F8	45R, 47R	E48	CP5	40L, 39L	E68	POz	17L, 17R
E45	FT9	38L, 20L	E43	CP3	40L, 02L	E86	PO4	19R, 39R
E40	FT7	44L, 47L	E38	CP1	05L, 07L	E85	PO8	19R, 18R
E35	FC5	44L, 45L	E55	CPz	05L, 05R	E72	O1	18L, 17L
E30	FC3	06L, 04L	E88	CP2	05R, 07R	E72	Oz	17R, 17L
E21	FC1	06L, 04L				E77	O2	18R, 17R

Table 4-2: Associating brain regions to the corresponding Brodmann Area and the 10-10 international montage channel. Green – Sensory Area, Red – Motor Area, Purple – Association Area.

Brain Regions	Brodmann Area	left Cortex	Right Cortex
Somatosensory cortex	1,2,3	C1, C3	C2, C4
Somatosensory processing and association	5	CPz, CZ, C1, CP1	CPz, Cz, C2, CP2
Primary motor cortex	4	Cz,C1,C3	Cz,C2,C4
Premotor area (SMA)	6	FCz, FC1, FC3	FCz, FC2, FC4
Primary visual cortex	17	Poz, Oz, O1	Poz, Oz, O2
Secondary visual cortex	19	PO7, PO3	PO4, PO8
Parietal Cortex	40	CP3, CP5	CP4, CP6
Posterior parietal Cortex	7	Pz, P1	Pz, P2
Prefrontal Cortex	9	AFz, AF3	Afz, AF4
Anterior prefrontal cortex	10	FPz, FP1	FPz, FP2
Auditory cortex (transverse temporal cortex)	41 & 42	C5	C6
Planning complex movement	8	Fz, F1	Fz, F2

4.1.3.2 Electromyography (EMG) online recording

EMG was recorded using eight modified open EEG boards. Each open EEG board consisted of two EEG amplifiers, which could be used in either unipolar or bipolar configuration. These amplifiers were modified in order to record the necessary EMG signals during a particular hand movement. The open EEG boards were modified so that they could be used for recording the EMG frequency range. The RAW EMG was acquired with a 16 channel National Instruments A/D board with a sampling frequency of 1 kHz at 16 bit resolution. All electrodes that were isolated were from the main power supply with DC to DC isolation (RK-0505S), with an isolation factor of 5kV. The data acquisition board was further isolated from the computer with USB isolation (ADuM4160), with 5000Vrms medical isolation under IEC60601-1. Labview was used to filter the raw EMG data with a 50 Hz notch filter (to remove line noise) and then filtered a second time using a 15-500 Hz band pass filter. This allowed noise or movement interference to be cut out below 15 Hz and above 500 Hz. The data was then smoothed using route mean squared analysis (RMS), which was calculated for a 50ms window.

Table 4-3: Movement types and muscles used in that particular movement (Netter, 2003).

Movement Types	***List of Muscle Activations***
Wrist Flexion	Flexor Carpi Radialis, Palmaris Longus, Flexor Carpi Ulnaris, Flexor Digitorum, Superficialis, Flexor Digitorum Profundus
Wrist Extension	Flexor digitorum superficialis, Flexor digitorum profundus, Extensor indicis, Lumbricals , Dorsal Interossei, Adbuctor pollicis brevis, Opponens pollicis, Adductor pollicis, Abductor pollicis longus, Extensor pollicis brevis, Extensor pollicis longus

The EMG was measured using a bipolar bio-amplifier with a gain of 1800, filtered between 5Hz and 200Hz. EMG was recorded on the left and right forearm with eight pairs of ECI tin electrodes (diameter of 10mm). The tin electrodes were secured in an arm band in the relative positions associated with the muscle groups. Electrodes were placed 2 cm apart, with 2 electrode pairs around the wrist flexor muscle region and 2 electrode pairs around the wrist extensor muscle regions (Table 4-3). Appropriate skin preparation was done before placing the electrode band (Figure 4-12) on the subject. ECI Electro-Gel (Electro-Cap International, Inc. or ECI) was injected into the electrode holders, to reduce the impedance to acceptable levels (< 1kΩ).

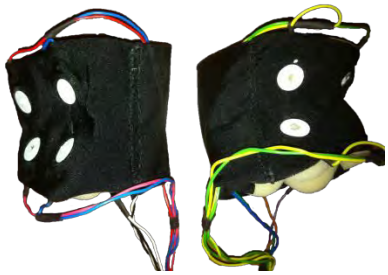

Figure 4-12: EMG electrode arms bands used for recording wrist muscle activation during flexion and extension of the wrist. Each arm band consisted of 4 bipolar EMG electrodes.

In order to check that no muscle activation occurred during imaginary movements, Labview was used to store EMG data, and to visualize the filtered EMG muscle activation for the left and right wrist. Refer to APPENDIX E - Grand Averaged EMG Results for the average rectified EMG results over the left and right hand flexion and extensor muscle groups (Table 4-3) during wrist flexion and extension for imaginary, passive and real movements.

4.1.3.3 Wrist Strain and Angle

The MVC (see section 4.1.1) was measured by the hand device. The applied wrist force (torque), during flexion and extension was measured using four strain gauges (mild steel foil, 5mm, GF 2, 120Ω), connected to a commercial strain gauge amplifier (CMMR>120dB, closed loop gain 3-60000). The angle of the wrist was measured around the pivot point of the hand device, using a precision potentiometer (Precision Pot: 6539S-1-102). See section 4.1.2, Figure 4-9 for the positions of the strain gauge and potentiometer in the hand device. The measured force and angle was recorded with an A/D board (National Instruments) at a sampling frequency of 1 kHz with 16 bit resolution. Before the beginning of the experiment, the MVC was recorded as the maximum torque during the movements, and was used to calibrate the highest torque output (10% MVC) of the hand device for active wrist flexion and extension. Labview was used to store and measure the maximum torque

during the MVC recording, and to set the output torque for the subject's wrist forces. During the experiments, Labview stored and displayed the wrist angle and torque and was also used to visualize whether the subject moved the hand to the required position. Refer to APPENDIX C - Experimental Setup for more details on Labview setup. Refer to APPENDIX B - Strain Gauge for the calibration of the strain gauges used in the experiments.

4.2 Offline Data Analysis

In order for the MRCP, ERDS and PLV analyses to be conducted on the EEG data, the appropriate processing steps needed to be applied to the RAW EEG, to improve the data quality and remove unwanted artefacts. Figure 4-13 represents the processing steps that were applied to the RAW EEG data, including data pre-processing, artefact correction and data analysis. Further sub-steps were required during data analyses, including frequency filtering, spatial filtering, channel referencing, channel rejection, channel interpolation and epoch rejection. Once the appropriate pre-processing and artefact correction steps were applied to the RAW EEG data, cleaning it of all detected artefacts, the relevant analysing techniques were applied.

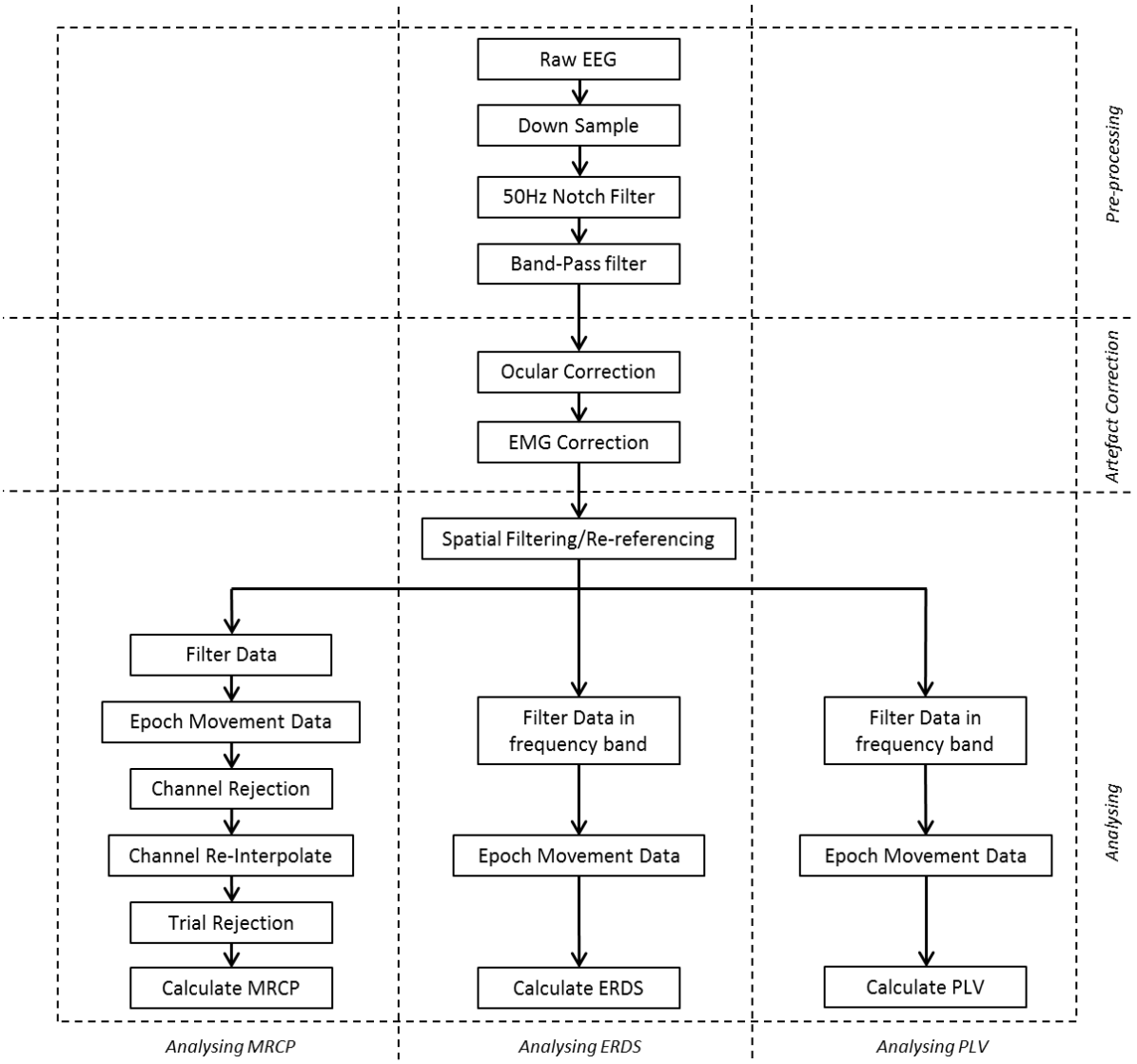

Figure 4-13: Flow diagram showing the procedure followed for pre-processing, artefact correction and data analysis in MRCP, ERDS and PLV calculations.

4.2.1 Pre-processing

The RAW EEG data was down sampled from 500Hz to 250Hz, and then notched filtered at 50Hz, to reduce main line noise. The unipolar EOG channels were separated from the EEG data. The data was then band passed between 0.1-100Hz, in order to remove DC shift and all high frequency components. Linear phase Butterworth finite impulse response (FIR) filters (order of 80) were used to filter the EEG. All data was filtered in the forward and reverse direction in order to eliminate phase shifting.

4.2.1.1 Artefact Correction

Artefacts that may contaminate the EEG signals introduce a significant interference in the measured brain signals, and need to be removed. Such artefacts are typically much larger than the brain signals of interest, and can render these signals uninterpretable. There are many different types of artefacts that can contaminate the spontaneous EEG data; the most common include eye blinks, movement artefacts, heart signals, line noise, and skin potentials. Due to the nature of the experiments and the analyses that needed to be conducted, eye blinks and muscle noise had to be removed.

There is no single method that can be used in the remove all types artefacts. Therefore, ocular and EMG artefact removal had to be dealt with separately. Both Ocular and EMG artefacts are sparsely scattered within EEG signals with infrequent periods of intense activation. A blind source separation (BSS) approach was used in artefact correction, to decompose the artefacts inherent in the EEG signals, into spatially and temporally statistically independent components. Of the many different algorithms that could be used to solve the BSS problem, the extended infomax (information maximization) Independent Component Analysis (ICA) algorithm was used (see section 2.1.5). Extended infomax ICA has already been shown to be a reliable method for detecting a wide variety of artefacts (Jung et al., 2000). The main disadvantage of using BSS techniques for artefact correction in identifying artefact contaminated components is that it is a time consuming process, which usually requires human interpretation through visual inspection of the BSS components (Geetha, 2011). However, Automatic Artifact Removal (AAR) methods have been developed to automatically select and remove or filter unwanted components (Gómez-Herrero, 2007; Joyce, Gorodnitsky, & Kutas, 2004). Two different component selection methods were used during ocular and EMG artefact correction. Ocular components were selected based on their coherency with ocular channels, whilst EEG components where selected based on power difference between EMG and EEG signals.

4.2.1.2 Ocular Artefact Corrections

Ocular movement artefacts were recorded and monitored with 8 electrodes: two positioned horizontally at the outer canthis of both eyes, and six positioned vertically (two upper, and one lower for each eye). The electrode configuration provided sufficient separation of eye movement related components. In order to avoid introducing offsets and slow drifts into the data, unipolar referenced electrooculography (EOG) channels were used in the recordings (Joyce et al., 2004). The relevant unipolar ocular channels were used to calculate the bipolar channels. The vertical EOG (VEOG) and horizontal EOG (HEOG) channels were calculated using the unipolar EOG channels (E1, E8, E26, E33, E125, E126, E127 and E128). The VEOG eye movements were calculated by subtracting the voltages

recorded above and below the eyes (for the left eye, E26 – E127 and E33 – E127, and for the right eye, E8 – E126 and E1 – E126). The HEOG eye-movements were calculated as the difference between the voltage at the left and right outer canthis of the eyes (E128 – E125) (Croft & Barry, 2000). The calculated bipolar EOG channels were then filtered between 0.5-15Hz to remove the higher frequencies derived from the cerebral and ocular activity (Klados, Papadelis, Lithari, & Bamidis, 2008). The original raw unipolar EOG channels were filtered between 0.5-100Hz and added to the EEG data channels, to increase the likelihood of success for ocular correction.

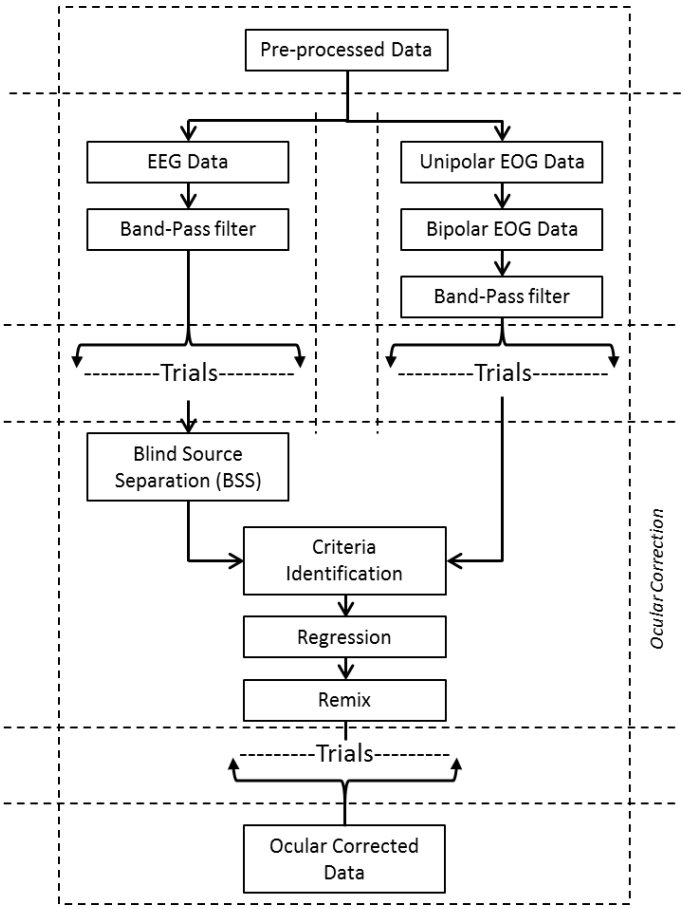

Figure 4-14: Flow diagram of the method used for ocular correction.

In order to perform ocular correction on the pre-processed data, the data was broken up into 36 non overlapping windows, separated by the beginning and end point of every 10th trial throughout the recordings. Each window consisted of 10 trials of about 120 seconds in length. This window size was small enough for the blind source separation technique to converge on a solution, whilst long enough for contaminated ocular ICs to be separated from the data.

A similar method to that used by Klados *et al.* (2011) was adapted to perform ocular correction on the EEG data (Klados, Papadelis, Braun, & Bamidis, 2011). This method uses a regression scheme to filter out the ocular signals. Initially the EEG signals were decomposed into their Independent Components (ICs) using a BSS method. The correlation between all 5 unipolar ocular channels and all IC's was calculated. The contaminated ocular ICs were then identified by their correlation factor to the bipolar ocular signals. IC's with a correlation factor above 0.25 were identified as ICs that contained ocular artefacts. Then, a stable adaptive regression filter based on the Recursive Least Square (RLS) algorithm was applied to the identified components in order to filter out only the ocular

artefacts inherent in the selected ICs, whilst keeping the underlying neural signals intact. Once the ocular artefacts were removed from the contaminated ICs, the processed ICs were then projected back, reconstructing the ocular free EEG signals. This procedure was then repeated for all the windows throughout the recorded time. Refer to APPENDIX D - Ocular Correction, illustrating the ocular artefact correction results.

4.2.1.3 EMG Artefact Correction

The EMG artefacts were rejected from the ocular free EEG data using a similar method to that used for ocular correction. The data was broken up into 72 non overlapping windows, with each window consisting of 5 trials for about 60 seconds in length. A smaller window size was used than for ocular correction as EMG artefacts occur at higher frequencies. This window size was small enough for the blind source separation technique to converge to a solution, whilst long enough for contaminated EMG IC's to be separated from the data. The windowed EEG data was then decomposed into its independent components using the blind source separation method. The contaminated EMG components were detected based on the ratio between the power in the EMG band and the power in the EEG band. The IC whose average powers in the EEG and EMG bands were below a certain ratio was selected as EMG components. These IC's were then rejected whilst the rest of the components were projected back to reconstruct the EMG free EEG signals. Refer to APPENDIX D - EMG Correction, illustrating the EMG artefact correction results.

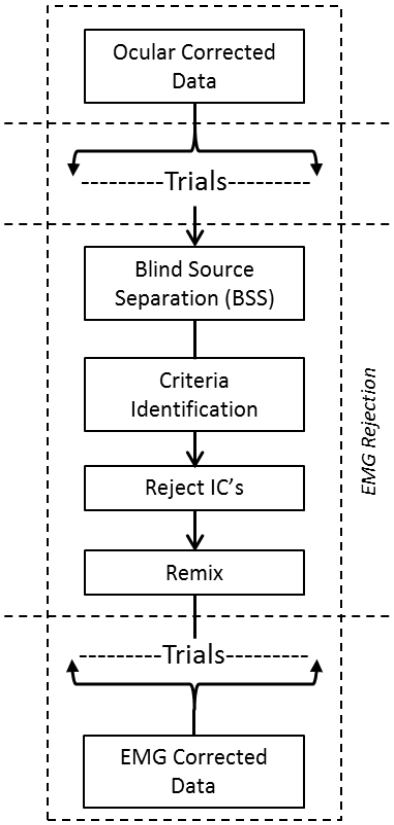

Figure 4-15: Flow diagram of method used for EMG correction

4.2.2 Spatial filtering

When using non-invasive methods such as EEG to record the neurological activity in the brain, the resulting maps of cortical activity are not as well resolved as ECoG, and consequently cross-talk can be present between electrodes. The effect of cross-talk is very sensitive to the location of the sources, and is dependent on the particular head model used (F. Darvas, Ojemann, & Sorensen, 2009). During phase synchrony calculation, the effect of cross-talk can cause unwanted synchronization between adjacent electrodes.

The spatial blurring that occurs on the surface of the scalp results in cross-talk between adjacent electrodes. To get a better estimate of the cortical surface potential and reduce the effect of spatial blurring, a spherical spine Laplacian algorithm (see section 2.1.4) was applied to the measured scalp surface potentials. The surface Laplacian based spherical spline function is considered an excellent interim approach for many research and clinical EEG applications, for which more accurate head models are not practical. In this method the scalp surface Laplacian is represented by the magnitude of the radial current flow leaving and entering the scalp. The surface Laplacian has been shown to estimate cortical surface potential more accuratly than surface EEG, in turn boosting the spatial resolution of the EEG data (Gysels & Celka, 2004). Current source density (CSD) transformation was applied to the artefact corrected, scalp surface potentials in order to sharpen the EEG waveforms. Data was transformed into current density estimates using a spherical spine Laplacian algorithm with standard computation parameters (spline flexibility = 4; lambda = 10^{-5}), and scaled to Laplacian units ($\mu V/cm^2$) with a realistic head radius of 10 cm (Kayser & Tenke, 2006a; Tenke & Kayser, 2012). The Scalp surface Laplacian was calculated with the Current Source Density (CSD) Matlab toolbox (Kayser & Tenke, 2006a, 2006b). The CSD calculation was used during ERDS and PLV calculation, in order to eliminate the effects of spatial blurring, which can result in cross-talk between electrodes, thereby providing a better estimate of the cortical surface potentials.

4.2.3 Statistical Methods

Performing the proper statistical methods on EEG data often poses a considerable challenge. Most case studies involving MRCP and ERP analysis use traditional methods of identifying areas of importance, involving the identification of peak amplitudes and latencies by the visual inspection of particular electrode sites. However, this may not always represent areas of highest significant differences and can often be biased towards selected time regions. Through sample-by-sample time series analysis and exact statistical topographical p-value-maps, a better comparison can be made between two conditions, isolating time regions of statistical significances that might not be identified with traditional methods. This is a similar approach to that used by (Muluh, Vaughan, & John, 2011; Pfurtscheller et al., 2009).

- Sample-by-sample parametric statistics for the time series data analysis, was applied over all subjects and trials, showing the comparison between two conditions. The MRCP analysis was conducted over 15 electrode locations (C5, C6, C3, C4, C1, C2, Cp1, Cp2, Fc3, Fc4, Fz, Fcz, Cz, Cpz and Pz) over the left and right motor cortex and mid line (Figure 4-16). The international 10-20 system was adopted for electrode placement on the scalp. The MRCP and wrist strain, angle and velocity analysis was applied in the comparison between wrist flexion and extension for different movement types. The significant differences of the wrist force, angle and velocity were compared

between the normalized flexion and extension values. Significant differences were represented by a solid bar under the time regions where significance was present. Significant differences of, $p < 0.05$, were displayed for the MRCP analysis, and significant differences of $p < 0.01$ were displayed for wrist strain, angle and velocity analysis. To avoid the effect of multiple comparisons, Bonferronie correction was applied to the p value. The sample-by-sample parametric test was conducted using the EEGLAB, statcond function.

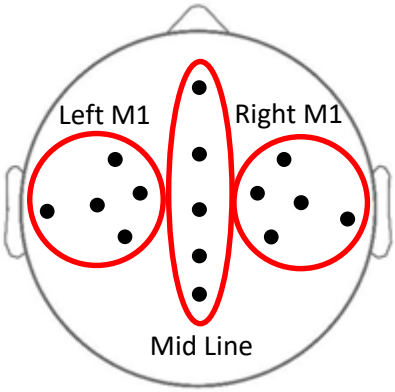

Figure 4-16: MRCP electrode used in sample by sample parametric statistics over the left and right motor cortex and mid line.

- Non-parametric statistics using the permutation test (n = 2000), showed the exact statistical p-value-maps between two conditions. This was conducted over all subjects in 100ms average non overlapping time windows. MRCP, ERDS and PLV coefficient topographical plots showing the exact statistical p-value-maps that were generated between wrist flexion and wrist extension. A colorbar was used to represent different significant levels: red represents areas of high significance ($p < 0.001$) and green represents areas of no significance ($p < 1$). To avoid the effect of multiple comparisons, Bonferronie correction was applied to the exact statistical p-value-maps. The exact statistical non-parametric permutation test was conducted using the EEGLAB statcond function.

- Non-parametric t-percentile bootstrap statistics were applied to the ERDS data, over a given time series and frequency range. The within subjects time frequency statistical maps isolate areas of significance ($p < 0.05$), over all trials for a particular movement type (imaginary, passive, real wrist flexion and extension). The number of bootstrapping resamples was 300, and the mean statistical calculation was performed over the bootstrapped resampled data.

- Within the subject, parametric repeated measures ANOVA, with greenhouse-Geisser correction for spherical assumptions were performed on the MRCP wrist force, strain and velocity data, to quantify the mean amplitudes. The ANOVA analysis was calculated over subjects in particular mean time regions associated with the region of interest. Repeated measured ANVOA analysis was conducted using IMB SPSS 19.0 statistical software.

4.2.4 Flexion and Extension Movement Analysis

After the correction of ocular and EMG artefact (see section 4.2.1.2 & 4.2.1.3), the EEG data was ready for MRCP, ERS/ERD and PLV analysis.

4.2.4.1 Movement Related Cortical Potentials (MRCP)

The following steps were used in the calculation of the MRCP's (see section 2.2.1) for wrist flexion and extension, during motor imaginary, passive movement and voluntary real movements.

The EEG channels were selected according to the 10-20 international montage, reducing the number of electrodes from 128 channels to 64 channels. Spatial filtering methods such as CSD were not used in the MRCP analysis as they are not ideal in the detection of slow cortical potentials, such as in MRCP. Average referencing was applied offline to the data in order, to re-reference the remaining channels and provide a reference free solution for the MRCP analysis.

The MRCP data was found to be located in the 0-4Hz band, however, Vuckovic and Sepulveda showed that the majority of frequencies are in the 0.5Hz to 2Hz range for imaginary wrist movements (Aleksandra Vuckovic & Sepulveda, 2008a). Figure 4-17, shows that the most prominent frequencies over all subjects in the Delta at 2.71Hz (Mean = 2.71Hz; σ = 0.61) and Theta at 5.43Hz (Mean = 5.43Hz; σ = 0.61). The average referenced data was filtered between 0.5-5Hz for the MRCP analysis.

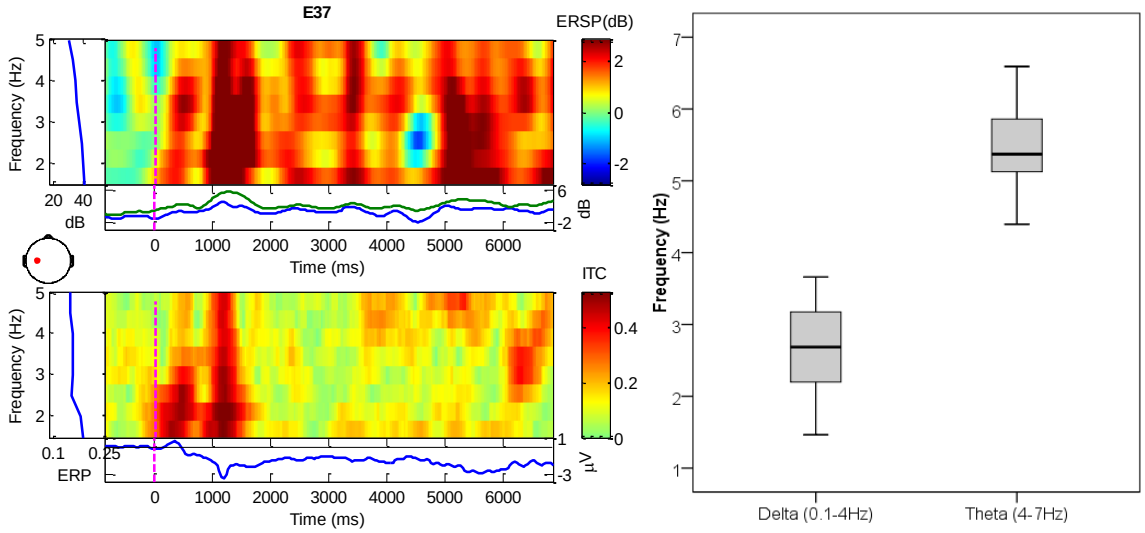

Figure 4-17: Left, ERSP of the MRCP frequencies band for subject 7, at electrode E37 (C1), the most prominent frequencies are present in the Delta band around 2Hz. Right, peak frequencies for Deta and Theta, over all subjects and experiments.

By epoching the filtered data around the get ready stimulus at 0ms (see section 4.1.1.1), with an epoch range of -2000ms to 8000ms, the data was separated into the 6 experiments consisting of Imaginary, Passive and Active wrist flexion and extension. EEG channels within each experiment, with excessive noise corruption were removed. Bad channel selection was based on EEGLAB joint probability channel rejection algorithm. Refer to Table 4-4, for the channel number of the rejected electrode for each subject performing the different experiments. Noisy, rejected channels were then interpolated back into the data with information from the surrounding electrodes, using the EEGLAB spherical interpolation algorithm.

The MRCP for each experiment was calculated using a baseline correction in the preparation interval (see section 4.1.1.1) from -1500ms to -500ms. This is a similar approach to that used by (Bai et al., 2007; S. Slobounov et al., 2002).

Trials showing excessive amplitude were rejected based on a threshold criterion. Trials with potential differences greater than ±100uV and ±250uV in -1500ms to 2000ms and -2000s to 8000s respectively were rejected from each trials segment. Refer to Table 4-4 for the number of rejected trials for each experiment and subject.

Table 4-4: Listing the number of rejected trial and rejected channels for each subject at each movement type.

Subjects	RIWE		RIWF		RPWE		RPWF		RRWE		RRWF	
	Channels	Trials	Channels	Trials	Channels	Trials	Channels	Trials	Channels	Trials	Channels	Trials
S1	22 87	0	22 27 122	0		0		2		0	66	1
S2	35	1	35	3	35	3	22 35 40 87 99	1	35	2	22	2
S3	22 92	3	14	5		2		2	14 22 40	2		6
S4	14	5	14	2	14 22	7	14 22	4	14	4	22	5
S5	22	0	16 22 24 57	1	97	2	97	1	109	3		5
S6	27 121	9	3	7	27 39	8	39 121	9		2		2
S7	22 85 88 93	2	22 93 119	2	43 57 109	2	43	2		2	27 28 45	1
S8	121	6	39 121 122	1	39	2	39	4	46 121 122	3	46 121 122	3
S9	121	1	45 121	2	121 122	2	121 122	2	2 14 115 122	23	2 14 45 79 121	0
S10	2 3 27	5	40	6	14	10	6	10	2 3 27	7	39 53	4
S11	35 40	4	40	2		2	35	2	40	2	35 40 109	5
S12	14 115	0	14	1	14 22 117 122	2		3	14 30	4	105	3
S13	14	3	14 22 27	1	2	5	2	9	46 109	2	101	2
S14	3 16 24	6	14	8	14 45 72	5		9		8		3
S15	45	3		4	45	10		10	22	7	24 25 27	5

Once all the experimental trials with excessive noise were rejected, the remaining trials in each experiment were averaged across all trials and subjects, resulting in the grand average MRCP. A similar method to that used by Fang *et al.* (2011) was used in the MRCP calculation (see Eq 2.5) (Fang, Siemionow, Sahgal, Xiong, & Yue, 2001; Hiroshi Shibasaki & Hallett, 2006). The grand average method is illustrated in Figure 4-18.

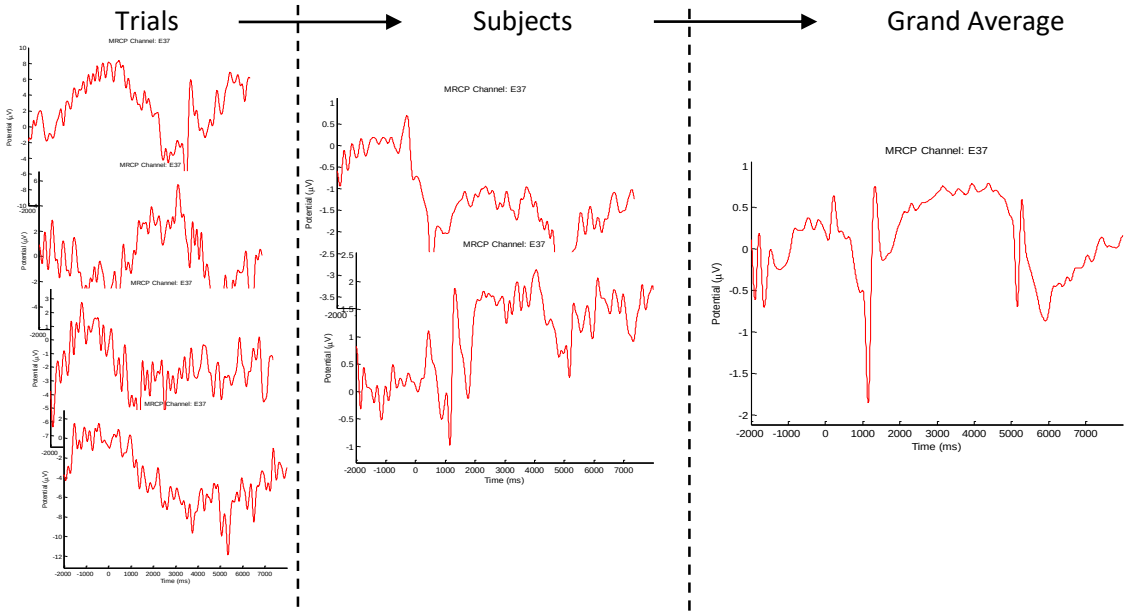

Figure 4-18: Method used in MRCP calculation. First, single trial MRCP are average for each subject (left) then grand average MRCP calculated over all trial (centre) and Subjects (right).

The MRCP statistical comparison between two conditions (wrist flexion and extension) was performed over all trials and subjects, comparing the grand average MRCP's (Figure 4-19) for motor imaginary, real and passive movements. Statistical exact p-value-maps were generated across all subjects and channels in 100ms average non overlapping time regions from 0ms to 7000ms. See Section 4.2.3 for the statistical methods used in the MRCP analysis. Refer to APPENDIX E - Grand Average MRCP Topographical Results for grand average MRCP for imaginary, passive and real movements, showing the exact statistical comparison between wrist flexion and extension.

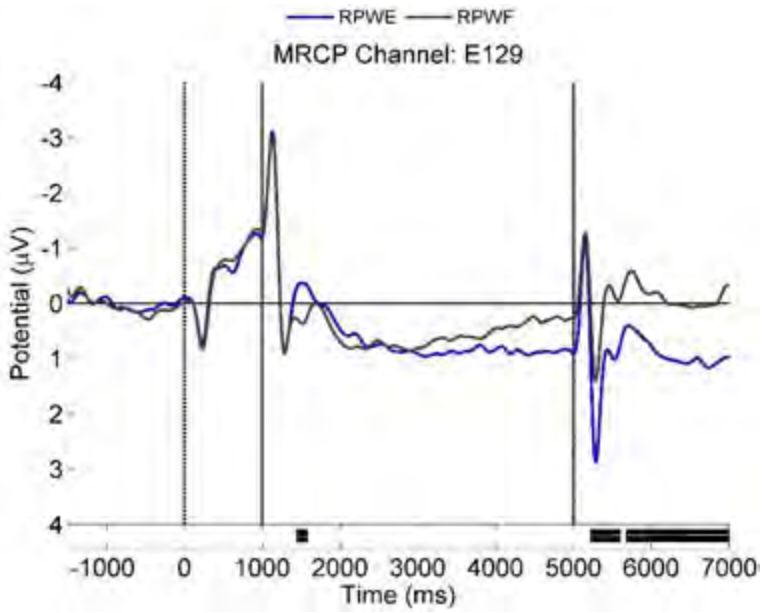

Figure 4-19: Representative grand average MRCP comparing right hand passive wrist flexion and extension.

In summary, the following steps were used in the MRCP analysis:

1. The ocular corrected data was reduced to the international 10-20 montage.
2. Average referencing was performed.
3. The data was filtered between 0.5Hz and 5Hz
4. The data was epoched for each of the six movements.
5. Bad channels were rejected using probability rejection algorithm.
6. Rejected channels were interpolate.
7. Trials containing excessive amplitude were rejected.
8. The grand average MRCP was calculated for each movement by averaging over all trial and subjects (see section 2.2.1).
9. Statistics on the MRCP data was performed, comparing wrist flexion and extension in the different movement types (see section 4.2.3)

4.2.4.2 Event Related De/Synchronization

The spherical Laplacian CSD spatial filter was applied to the artefact corrected data. This spatial filter was useful in two ways: it reduced spatial blurring between adjacent electrodes, resulting in an improved estimate of the cortical activation (see section 4.2.2) and it provided a reference free solution for the ERDS calculations. This is a similar approach to that used by (Pfurtscheller & Lopes Da Silva, 1999; Tenke & Kayser, 2012). The CSD channels were selected according to the 10-10 international montage, reducing the number electrodes from 128 channels to 64 channels. The following steps were used in the ERDS analysis for wrist flexion and extension, during motor imaginary, passive movement and voluntary real movements.

The ERDS analysis was conducted between 0.5Hz and 40Hz. This frequency range contains all mu and Beta frequency components which predominantly contain motor related rhythms (see section 0). The EEG data was filtered in the 0.5Hz narrow band in 0.5Hz increments between 5Hz and 40Hz. In total, the ERDS was calculated over 70 frequencies ranging from 5Hz to 40Hz. The EEG data was filtered

using an FIR filter of order 80, applied in the forward and reverse direction to prevent phase shifting in the data.

A similar method to that of Pfurtscheller *et al.* (2006) was used in the ERDS calculations (Pfurtscheller, Brunner, & Lopes da Silva, 2006). This ERDS analysis is based on the inter-trial variance (iv) method (see Eq 2.7), using the classical referencing method which was applied to the -1500ms to -500ms time interval of each trial. The ERDS referencing interval is located in the preparation period of the epoch. The ERDS was calculated over the whole -2000ms to 8000ms epoch window. See Figure 4-20 Left for the IV ERDS time frequency calculation for all trials over the left M1 area (E37) whilst performing right real wrist extension. Figure 4-20 Left, shows an increase in ERD during wrist extension over the sustained movement period in the mu band. These result are similar to those presented by Pfurtscheller *et al.* (1999) during real hand movments.

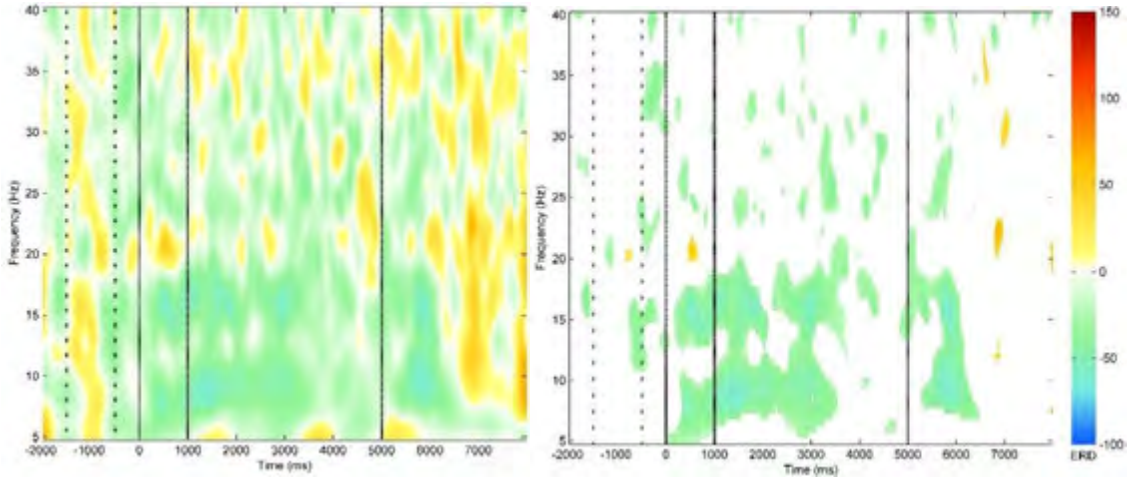

Figure 4-20: The Inter-trial variance ERDS of Subject 6 right hand real wrist extension, frequency 5 – 40Hz, time region -2000ms to 8000ms, with references interval in the -1500ms to -500ms range. Left: EDRS plot over electrode E37. Right: ERDS plot with trial based bootstrapping statistics (P<0.05) only showing significant regions.

The frequency range of each neurological rhythm is known to vary in different subjects (Klimesch, 1999; Pfurtscheller & Lopes Da Silva, 1999). For this reason the peak frequencies in the mu band (8-13Hz), lower beta (12.5-16Hz), midrange beta (16.5–20Hz) and high beta (20-28Hz) were calculated from the power spectral density (PSD) for each band. The ERS/ERD is calculated in the mu band and beta band as they contain movement related rhythms. A similar method to that used by Pfurtscheller *et al.* (1999) was implemented in the ERDS calculation, where subject specific frequency bands were selected. The Topographical ERDS was calculated around the peak frequencies with a bandwidth of 4Hz. (Pfurtscheller & Lopes Da Silva, 1999). The PSD is repressed in Figure 4-21 left showing the peak frequencies for real wrist extension. Refer to APPENDIX A, for the calculated peak frequencies for each subject and movement.

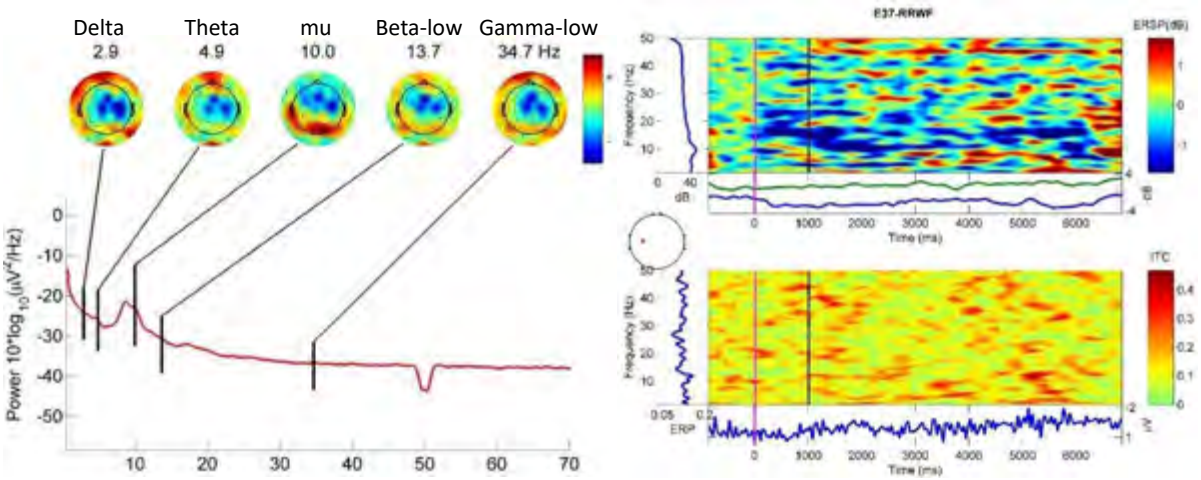

Figure 4-21: Left: PSD of the right hand real wrist extension, illustrating the topographical plots of peak movement frequencies the Delta (0.1-4Hz), Theta (4-7Hz), mu (8-13Hz), beta-low (12.5-16Hz), Gamma-low (30-48Hz). Right: ERSP of subject 6, at electrode E37 (C1).

Bootstrapping statistics (see section 4.2.3) was performed over all trials for each subject and movement experiment, isolating significant regions within the trials lower than $p < 0.05$ (Figure 4-22). This method was repeated over all frequency bands and channels. The grand average ERS/ERD over each peak frequency was calculated in a similar way to the MRCP calculation, but averaging over all subject for each movements type.

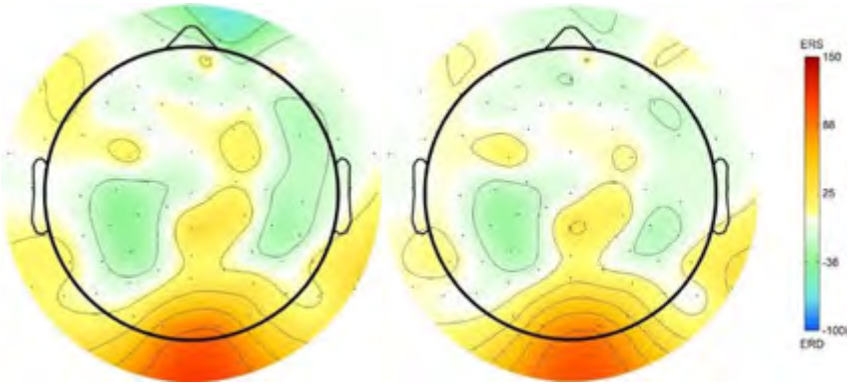

Figure 4-22: ERDS topographical plot of subject 6 performing right hand real wrist extension. This was calculated around the peak mu frequency (10Hz) with a bandwidth of 4Hz, in the sustained movement period, 1000ms-5000ms. The plot on the left illustrated no bootstrapping, while the plot on the right illustrating the bootstrapping statistics.

In summary, the following steps were used in the ERDS analysis:

1. Ocular and EMG artefact correction was performed on the raw EEG data.
2. Data channels were selected on the international 10-20 montage.
3. CSD spatial filtering was applied (see section 4.2.2).
4. Data was filtered between 5Hz and 40Hz in the 0.5Hz band width at 0.5Hz increments.
5. The data was epoched for each of the six movements.
6. The data was referenced to the -1500ms to -500ms time region for each trial.
7. ERDS was calculated using the intertribal variance method (see section 2.2.2).
8. Bootstrapping was performed across all trials for each movement in order to find significant ($p<0.05$) areas of interest.

9. Grand Average ERDS was calculated across all subjects around peak frequencies in the mu, Beta-Low, Beta-Midrange and Beta-High rhythms with a band width of 4Hz.
10. Statistics was performed on the ERDS data comparing wrist flexion and extension for the different movement types (see section 4.2.3)

4.2.4.3 Phase Locking value

The spherical Laplacian CSD spatial filter was applied to the artefact corrected EEG data. All the Phase Locking Value (PLV) analyses were performed using the Hilbert transform (see section 2.2.4.1). The CSD channels were selected according to the 10-20 international montage, reducing the number electrodes from 128 channels to 64 channels.

Two types of PLV calculations were performed, the narrow band frequency analysis between the SMA (E6) and the rest of the 63 channels, over 5Hz to 40Hz in 0.5Hz increments, and the PLV analysis between all channel pairs, over the mu band (8-13Hz).

The first analysis required the CSD artefact corrected EEG data to be filter in narrow band frequencies in 0.5Hz increments with a 0.5Hz band width between 5Hz and 40Hz (Figure 4-23). Calculating the PLV using the Hilbert transform required the use of a narrow bandpass-filter being applied first around the desired frequency range, before calculating the phase synchronization in that band. The EEG signals were filtered with a narrow band filter at frequency f, and the phase was computed by applying the Hilbert transform to the narrow band signal. The phase relation between the channels of the band pass-filtered signals was preserved with a finite impulse response (FIR) filter of order 40, applied in the forward and backward direction to remove phase distortion. Refer to APPENDIX D for the testing of the PLV algorithm with an induced phase synchrony.

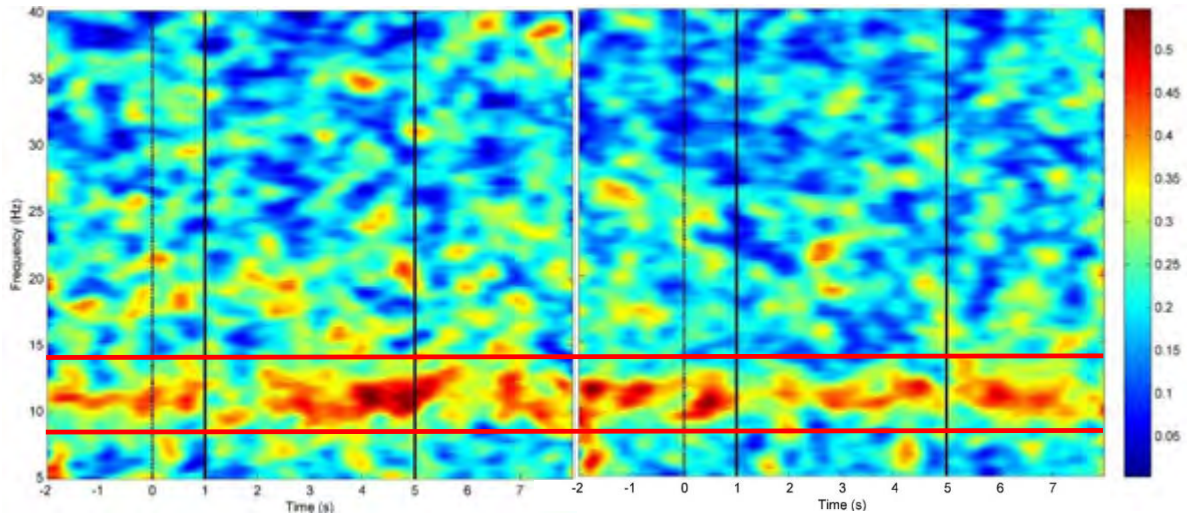

Figure 4-23: PLV for subject 14 for real (left-figure) and imaginary (right-figure) wrist extension, between the SMA (E6) and M1 (E31) in the 5 to 40 Hz band. The mu band (8-13Hz) is indicated by the area between the red lines.

The sample-by-sample statistical differences were calculated over the trials time range (-2000-8000ms) and in the frequency range of 5-40Hz, comparing wrist flexion and extension for the PLV analysis between the SMA and all channels (Figure 4-24). See section 4.2.3 for the statistical methods used in the PLV analysis

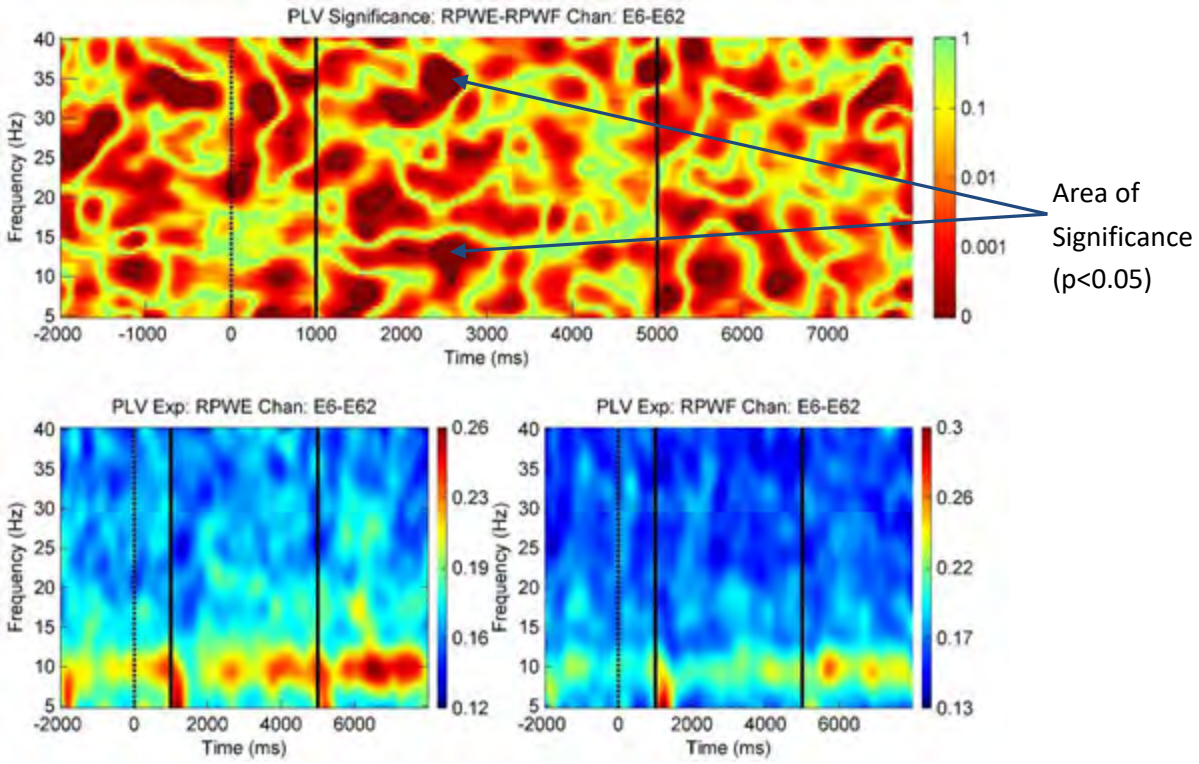

Figure 4-24: Grand average PLV between the SMA (E6) and CPz (E62) comparing passive wrist flexion and extension over the -2000ms to 8000ms time range and 5Hz to 40Hz frequency range. Note: The area inside the black border indicates significant differences, (i.e. $p < 0.05$).

For the mu PLV analysis between all channel pairs, the CSD artefact corrected EEG data was filtered over the mu band, between 8Hz and 13Hz (see Figure 4-23 between the red lines) using an FIR filter of order 80, applied in the forward and reverse directions. The FIR filter preserved the phase relations between channels.

5. Results for Wrist Flexion and Extension

This chapter presents the results required from the objectives (see section 1.1.3), studying the difference between wrist flexion and extension during imaginary, passive and real movements (refer to Figure 5-1, illustrating the different investigation and there corresponding sections), using the methods described in Chapter 4.

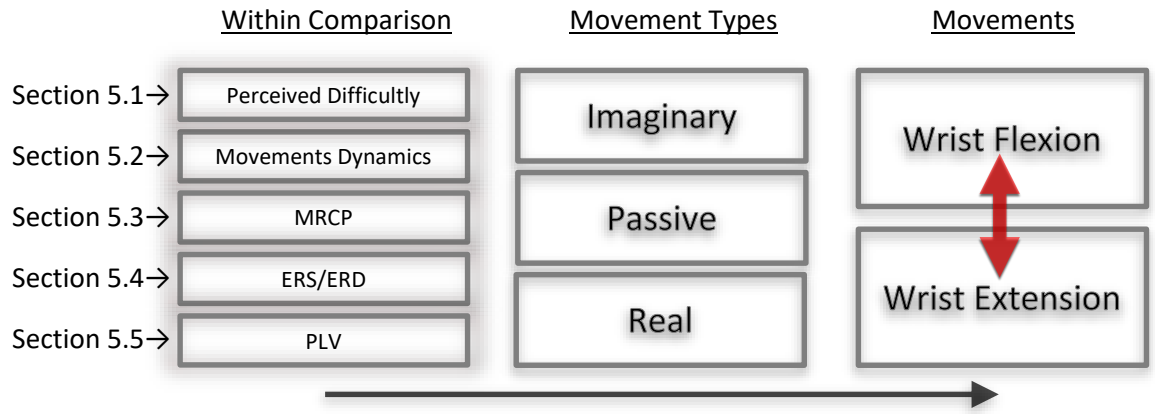

Figure 5-1: Diagram linking study sections to corresponding result sections, using a bottom up approach.

The subjects' perceived movement difficulties are presented in Section 5.1 followed by the strain, angle and velocity of the wrist movements, presented in Section 5.2. The amplitudes and latencies of the MRCP waveforms at 15 standard electrode sites for the left and right motor and sensory cortex and over the midline are presented in Section 5.3. The MRCP latency analysis for selected electrodes that was conducted for imaginary, passive and real movements are presented in Sections 5.3.1, 0 and 5.3.3 respectively. The selected channels represent waveforms from the left motor cortex where high levels of post movement significance occurred between flexion and extension. MRCP p-value-maps comparing flexion and extension from 800 to 2000ms are presented in Section 5.3.4. The MRCP topographical maps are presented in 100ms average time-regions, over the beginning of the sustained movement period. Refer to APPENDIX E - Grand Average MRCP Topographical Results for topographical results over the 0ms to 7000ms region.

ERS/ERD topographical maps for the mu, low-beta, midrange-beta and high-beta are presented in Section 5.4. The ERS/ERD p-value-maps are represented in 100ms average time-regions over the beginning of the sustained movement period from 800ms to 2000ms.

The PLV analysis that can be used for the discrimination of wrist flexion and extension are presented in Section 5.5. The time-frequency maps between the SMA and motor cortex electrodes are presented in Section 5.5.1. The mu band multivariate phase synchrony coefficient PLV topographical maps, including p-value-maps, are presented in APPENDIX E.2. Topographical maps are presented in 100ms average time-regions over the beginning of the sustained movement period from 800ms to 2000ms.

Refer to APPENDIX E.3 for EMG result around the left and right hand wrist muscle group associated with wrist flexion and extension (see Table 4-3).

Refer to APPENDIX D, Sections D.1, D.2 and D.3 for validation of know effect in the MRCP, ERS/ERD and PLV analysis.

5.1 Perceived Movement Difficulty

The significant differences were calculated for the perceived movement difficulties (rated 1-10) of wrist flexion and extension, during real, passive and imaginary movements using repeated measure ANOVA, within subject comparison (Figure 5-2). It was observed that the only significant difference originated from for real movements ($p < 0.01$, $F = 27.4$). Subjects perceived real right wrist flexion to be significantly easier to perform than wrist extension ($F(1,14) = 27.429$, $p < 0.01$). There were no significant perceived movement difficulty between wrist flexion and extension for passive ($F(1,14) = 0.059$, $p > 0.05$) and imaginary movements ($F(1,14) = 0.713$, $p > 0.05$). Real movements were performed at relatively the same perceived movement force. However, subject still perceived real wrist extension was harder to perform than flexion. Refer to APPENDIX A - Subjects Perceived Difficulty, for individual subjects movement ratings.

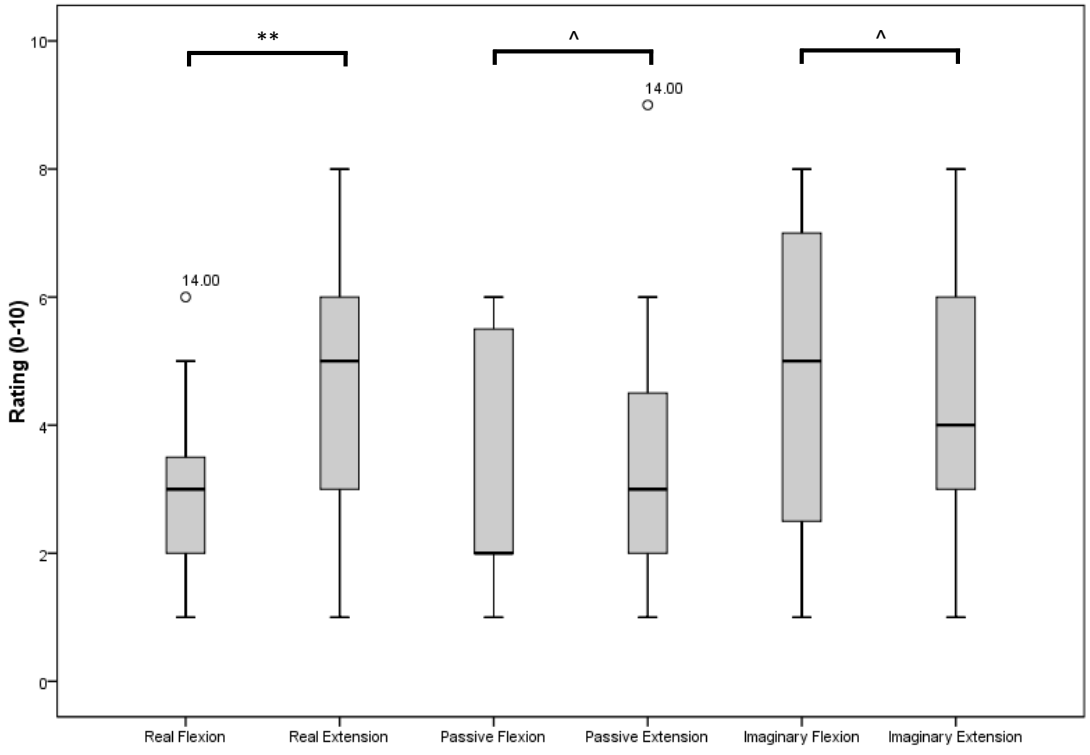

Figure 5-2: Boxplot of subject Perceived difficulties, rated from zero to ten for the different wrist movements types. Significant differences between flexion and extension are illustrated. Note: ^ indicates no significance difference $1 > p > 0.05$; * indicates, $p < 0.05$; ** indicates, $p < 0.01$.

5.2 Wrist Dynamics

During the comparison of different movements, it is important to examine certain movement characteristics, which could be responsible for differences detected in the neurological activation in the brain. The grand average strain, angle and velocity measured (see Section 4.1.3.3) around the pivot point of the hand device (see Section 4.1.2) during wrist flexion and extension is shown in Figure 5-3, where it can be confirmed that no wrist movements were present during imaginary movements. For passive movements the recorded strain represents the force applied by the hand device in order

to move and keep the wrist in the required position. As expected, the strain for passive flexion and extension is opposite in magnitude to that of real flexion and extension. The recorded strain measured from real movements, represent the force applied to the hand device to move it to the required position. Refer to APPENDIX B, Section B.2.1.1 for validation of strain gauge results.

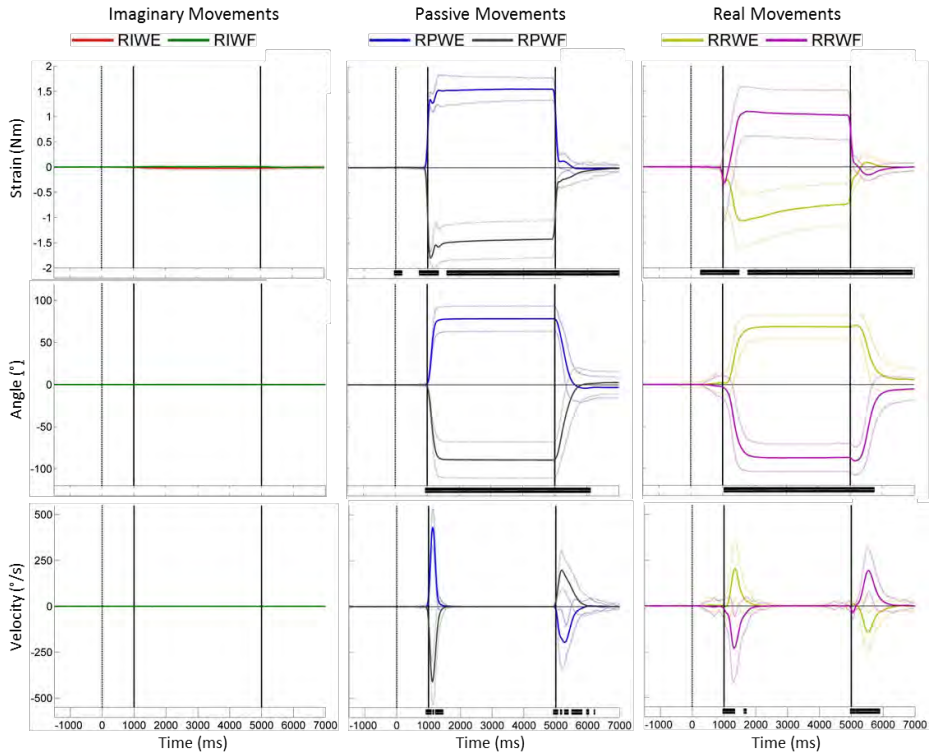

Figure 5-3: The grand average over all subjects showing strain, angle and velocity for imaginary, passive and real wrist flexion and extension movements. The black bar indicates significant ($p<0.01$) regions of differences between flexion and extension for the normalized strain, angle and velocity measurements. Dotted lines indicate standard deviation over all subject and trials for each movement type.

The peak passive strain (Table 5-2) is applied by the hand device to a similar level extent in both flexion and extension. During both passive and real movements the average angle for flexion is always significantly larger than that for extension. This is due to the difference in the range of motions of the wrist for the two movements, even though the subjects were instructed to perform brisk real wrist movement in a similar manner to those observed during passive movements. The velocities of the passive movements are considerably higher than those of real movements.

Table 5-1: Average strain, angle and velocities over the movement period (1000ms – 5000ms).

	Strain (Nm)	**Angle (°)**
RIWE	-0.23 ± 0.03	0.02 ± 0.19
RIWF	0.00 ± 0.02	-0.5 ± 0.36
RPWE	1.54 ± 0.27	77.9 ± 16.48
RPWF	-1.43 ± 0.38	-88.68 ± 22.53
RRWE	-0.86 ± 0.42	67.91 ±13.58
RRWF	1.05 ± 0.47	-86.29 ± 16.21

Table 5-2 Maximum strain, angle and velocities in the movement period (1000ms – 5000ms).

	Strain (Nm)	Angle (°)	Start Velocity (°/s)	End Velocity (°/s)
RIWE	-0.02 ± 0.03	0.23 ± 0.2	0.23 ± 0.28	-0.21 ± 0.26
RIWF	0.00 ± 0.02	-0.11 ± 0.23	0.141 ± 1.66	-0.22 ± 0.27
RPWE	1.55 ± 0.27	78.01 ± 16.48	428.19 ± 106.79	-193.57 ± 115.54
RPWF	-1.5 ± 0.37	-88.87 ± 22.52	-407.7 ± 123.19	197.22 ± 107.52
RRWE	-1.07 ± 0.57	68.89 ± 14.11	203.09 ± 159.15	-143.73 ± 107.91
RRWF	1.10 ±0.49	-87.35 ± 16.34	-230.87 ± 177.59	192.46 ± 117.45

The difference between flexion and extension for strain, angle and velocity were compared using the normalized values in Figure 5-4 and Figure 5-5. The significant differences peak strain and averaged/peak angle in the sustained movement period was present during passive and real movements (Figure 5-4).

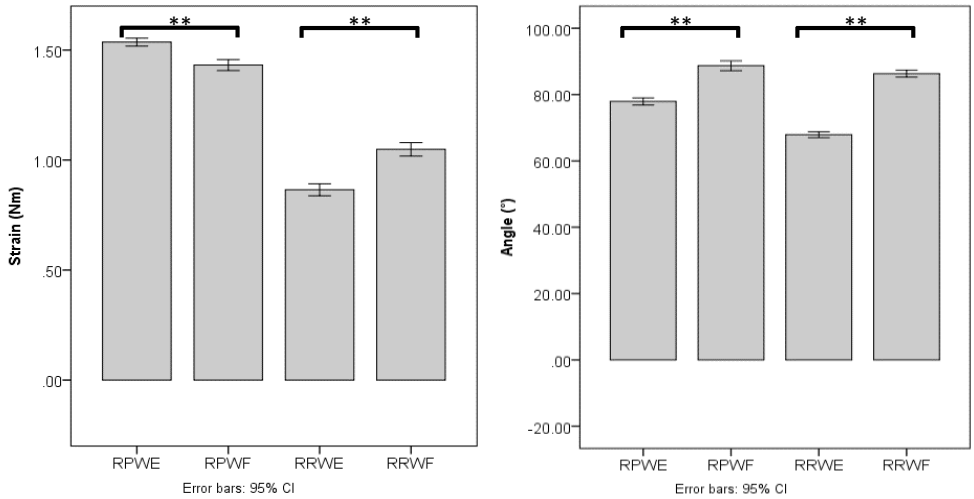

Figure 5-4: Left: grand average peak strain over all subjects, over the movement period (1000-5000ms), comparing wrist flexion and extension for passive and real movements. Right: grand average/peak angle over all subjects, average over the movement period (1000-5000ms), comparing wrist flexion and extension for passive and real movements. Note: ^ indicates, $p > 0.05$; * indicates, $p < 0.05$; ** indicates, $p < 0.01$.

A significant difference was also found for the peak velocity between wrist flexion and extension during passive and real movements, during the start and stop periods of the movements (Figure 5-5). The peak start movement passive extension velocity was significantly higher than that for flexion, while the peak start movement velocity of real extension was significantly lower than that for flexion.

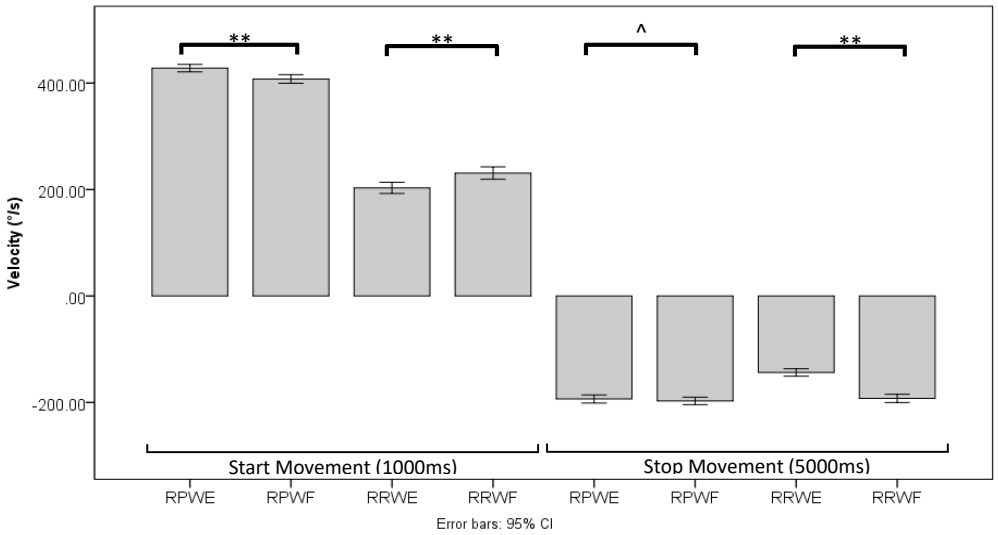

Figure 5-5: Grand average velocity over all subjects, showing peak start (1000ms) and stop (5000ms) velocities and comparing wrist flexion and extension for passive and real movements. Note: ^ indicates, $p > 0.05$; * indicates, $p < 0.05$; ** indicates, $p < 0.01$**.**

5.3 Movement Related Cortical Potentials

The within MRCP significant comparison between wrist flexion and extension was conducted on imaginary, passive and real wrist movements. The movement period can be broken up into six regions of interest (see Section 4.1.1): the preparation period (-2000-0ms), the cue period (0-1000ms), the start movement location (1000ms), the sustained movement period (1000-5000ms), the end movement location (5000ms) and rest period (5000-7000ms) intervals. See Section 2.1.1 for Brodmann Areas and Section 4.1.3.1 for GSN electrode location with respect to Brodmann Areas.

The MRCP at five locations in the left cortex is presented in Figure 5-6, specifically at the left premotor and supplementary motor cortex (FC3), left preparietal somatosensory association cortex (C1, CP1), the left primary somatosensory/motor cortex (C3) and the left transverse temporal cortex (C5). A significant ($p < 0.05$) difference was observed for motor imaginary movements around the start movement period, over the left preparietal somatosensory association cortex (C1, CP1), with a higher level of cortical activation in this area, for imaginary wrist flexion. Passive movements revealed a significant ($p < 0.05$) difference near the end of the cue period, over the left premotor and supplementary motor cortex (FC3), left transverse temporal cortex (C5), left primary somatosensory/motor cortex around the Homunculus wrist area (C3) and the left preparietal somatosensory association cortex (C1). Showing that there is a significantly higher level of cortical activation in all of these areas for passive wrist flexion. There is a similar difference present in the post movement cortical activation over the same cortical areas. This post movement significance ($p < 0.05$), is present in the beginning of the sustained movement period, showing higher passive wrist flexion cortical activation. Towards the end of the sustained movement period there is a significant difference over CP1 and C5, predominantly in the left preparietal somatosensory association cortex. Real movements display a sustained significance over the whole sustained movement period over CP1 and C1, showing higher level of cortical activation for wrist extension. It was also observed that post movement significance was present over the left motor cortex (C3), with higher cortical activation in wrist extension.

The MRCP at five locations in the right cortex is presented in Figure 5-7 at: the right premotor and supplementary motor cortex (FC4), the right preparietal somatosensory association cortex (C2, CP2), the right primary somatosensory/motor cortex (C4) and the right transverse temporal cortex (C6). A significant ($p < 0.05$) difference is present in motor imaginary at the end of the cue period, over the right premotor and supplementary motor cortex (FC4), showing higher cortical activation with wrist extension. A significantly ($p < 0.05$) higher cortical activation in wrist flexion was present at the end of the sustained movement period, over the right transverse temporal cortex (C6). Passive movements displayed no significant differences in the cue period and the beginning of the sustained movement period over all of the five electrode locations. Real movements displayed a sustained significance ($p < 0.05$) around the start movement period, in the C2, C4, CP2, C6 cortical location, with higher cortical activation for wrist extension.

The MRCP at five locations down the midline of the brain is presented in Figure 5-8, at the intermediate frontal cortex (Fz), agranular frontal cortex (Fcz), preparietal somatosensory association cortex and primary motor cortex (Cz), preparietal/superior parietal somatosensory association cortex (CpZ) and superior parietal somatosensory association cortex (Pz). No imaginary movement,

sustained significance was present in any of the movement period over the midline cortical areas. Passive movements displayed a higher level of sustained significance over the intermediate frontal cortex (Fz) over the cue and sustained movement periods, showing higher cortical activation for wrist extension. Real movements displayed a sustained significance in the cue period and in the beginning of the sustained movement period, over the somatosensory association cortex (Cpz, Pz), showing higher cortical activation for wrist extension.

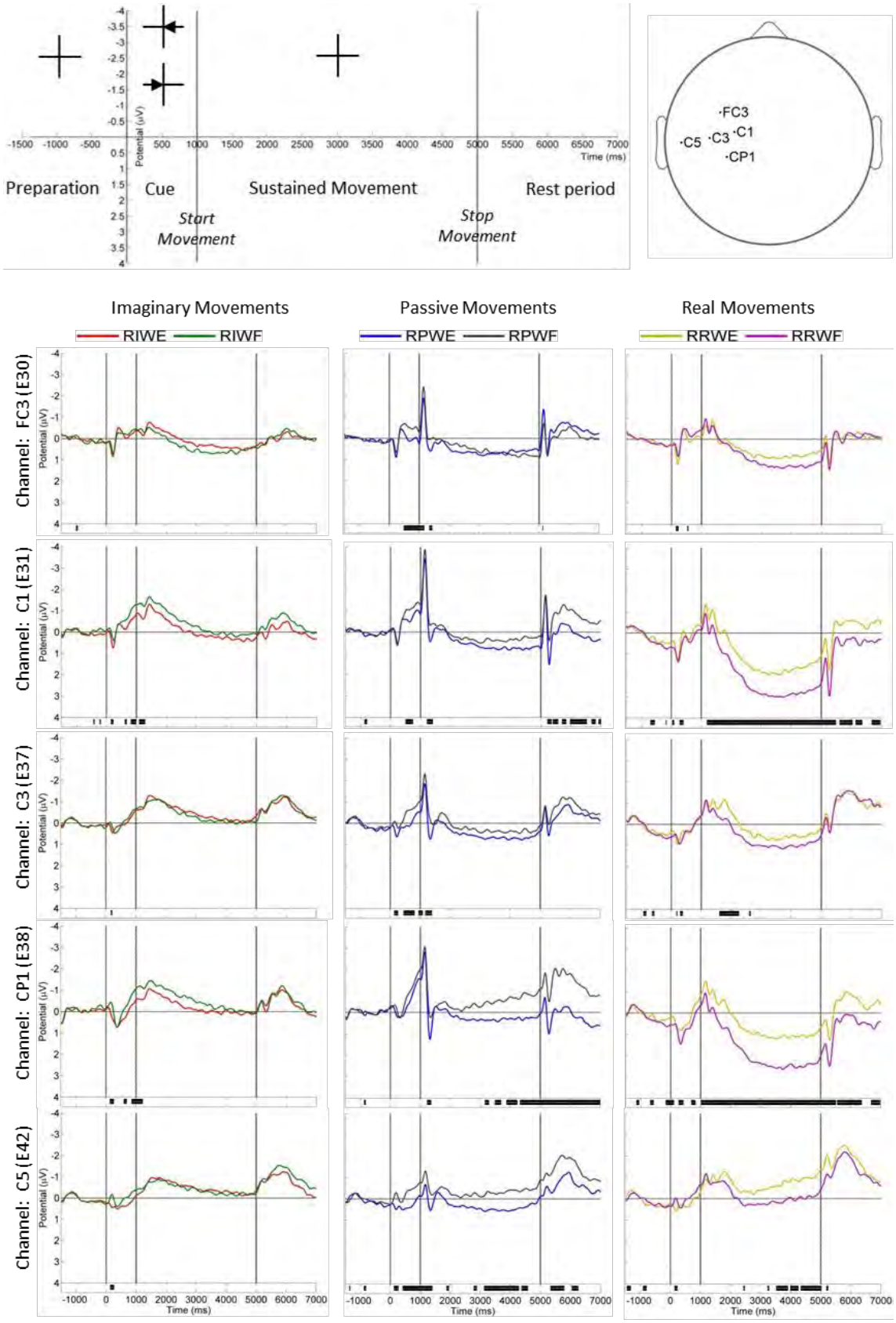

Figure 5-6: Grand Average MRCP waveforms at 5 standard electrode locations over the left primary motor cortex and sensory motor cortex, comparing right wrist flexion and extension in imaginary, passive and real movement types. The solid black bar below the waveforms indicate Significance $p < 0.05$, between flexion and extension.

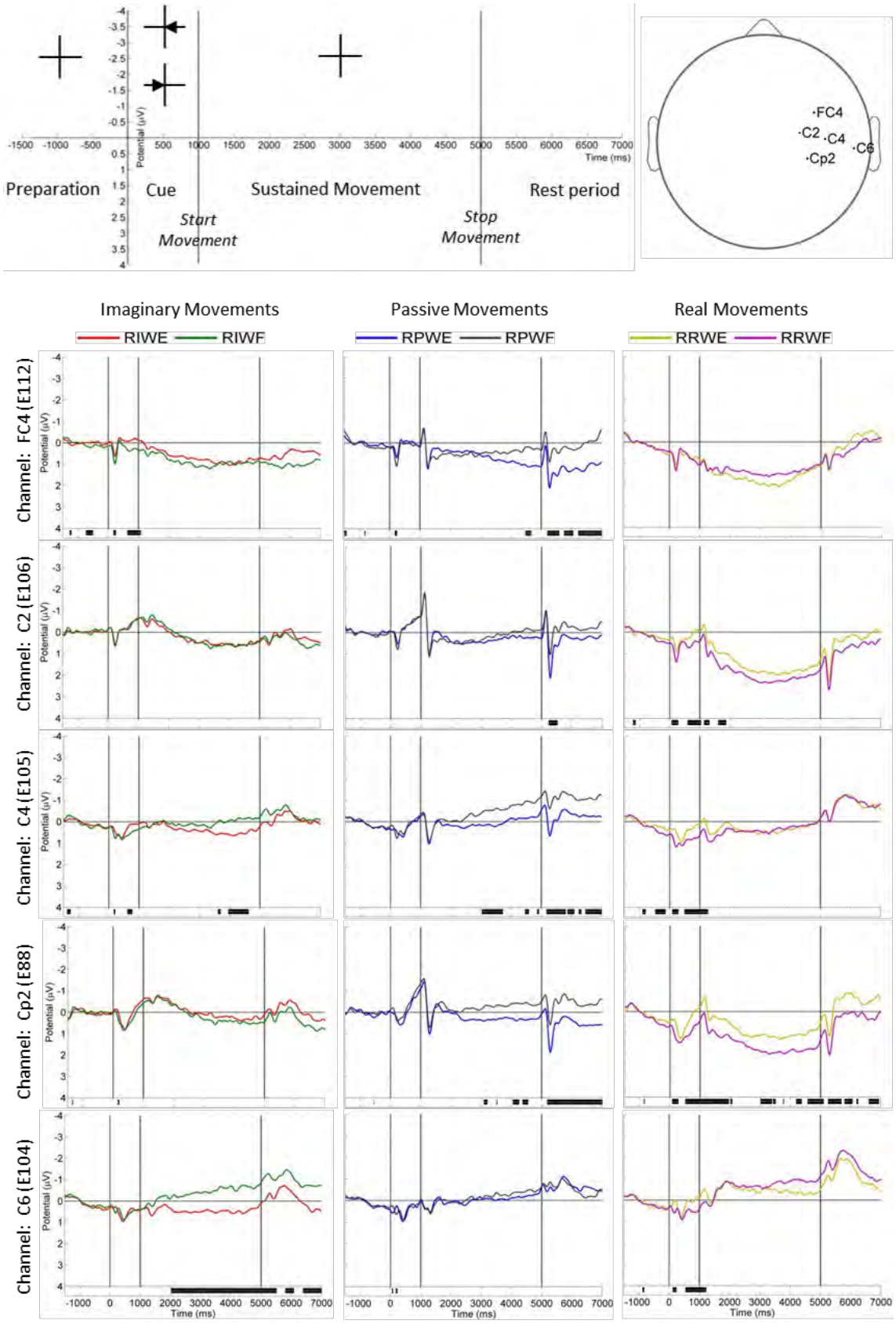

Figure 5-7: Grand Average MRCP waveforms at 5 standard electrode locations over the right primary motor cortex and sensory motor cortex, comparing right wrist flexion and extension in imaginary, passive and real movement types. The solid black bar below the waveforms indicate Significance $p < 0.05$, between flexion and extension.

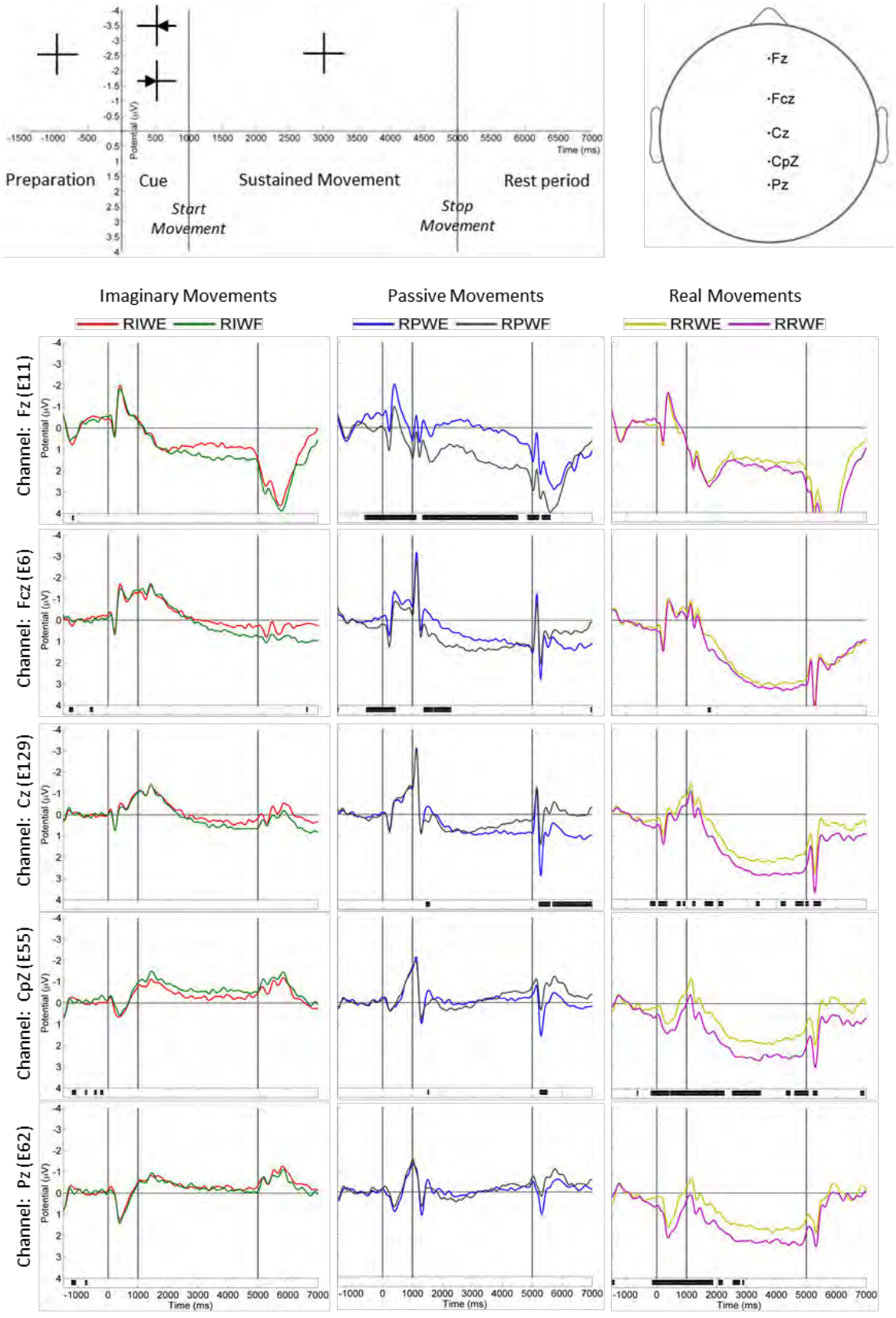

Figure 5-8: Grand Average MRCP waveforms at 5 standard electrode locations over the central line, comparing right wrist flexion and extension in imaginary, passive and real movement types. The solid black bar below the waveforms indicate Significance $p < 0.05$, between flexion and extension.

5.3.1 Imaginary motor cortex activation

The imaginary MRCP waveform over the left cortex was selected from Figure 5-6, at C1 (E31) located around the agranular/preparietal somatosensory associated cortex and primary somatosensory/motor cortex. A significant difference ($p<0.05$) was present between imaginary wrist flexion and extension in the sustain movement period, between 1080ms and 1280ms (Figure 5-9). Post movement imaginary MRCP for wrist flexion was significantly higher than for wrist extension.

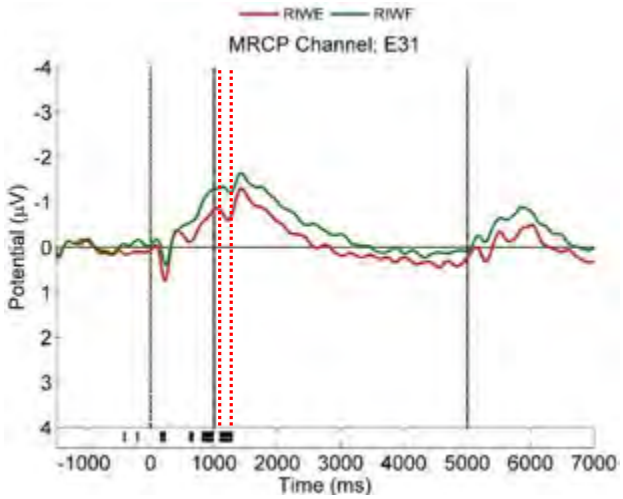

Figure 5-9: Grand average MRCP for motor imaginary wrist flexion and extension for C1 (E31) over -1500ms to 7000ms time regions. Significant regions ($p<0.05$) are indicated below (black regions) between flexion and extension. Between lines (---) illustrating post movement imaginary significant interval (1080-1280ms).

The imaginary movement topographic MRCP plot is presented in Figure 5-10. This plot is averaged over the 1080-1280ms region and shows an increase in the MRCP imaginary wrist flexion activation, predominantly in the left primary motor cortex, and left primary somatosensory cortex around the anterior wall of the central sulcus. A higher level of activation is present in flexion, with a significant difference present in E38 and E61, over the same period (1080-1280ms) as in Figure 5-9.

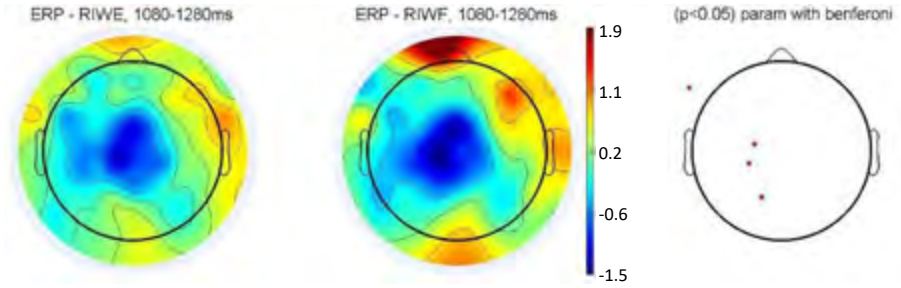

Figure 5-10: Grand average MRCP topographical plot, comparing wrist flexion and extension for post motor imaginary movements, averaged over the C1 (E31) flexion and extension significant region (1080-1280ms). Left cortex electrodes E31, E38 and E61 show significances ($p<0.05$) comparing flexion and extension in the time region 1080ms to 1280ms.

Imaginary movements showed a significant difference between flexion and extension, over the E31 (C1), E38 (CP1) and E61 (P1), with motor imaginary wrist flexion resulting in more cortical activation than motor imaginary wrist extension (Figure 5-11).

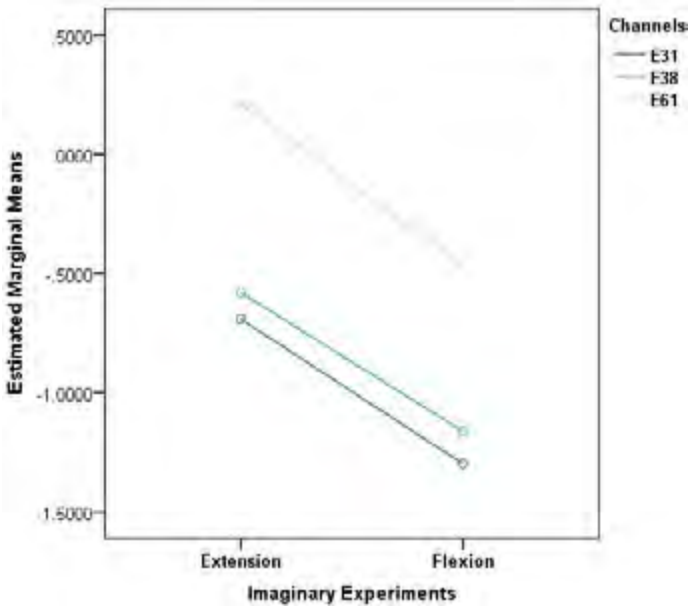

Figure 5-11: Estimated marginal mean for Real wrist flexion and extension, for electrode E31, E38 and E61 averaged over the post movement period 1080ms to 1280ms.

The within subject ANOVA comparison between imaginary flexion and extension over all electrodes showed a significant difference between the two experiments of $F(1,14) = 7.609$, $p < 0.05$. There is also a significant difference between the channels of $F(2,28) = 6.005$, $p < 0.05$, when collapsing the ANOVA over experiments. The experiments and channels do not interact with one another $F(2,28) = 0.071$, $p > 0.05$.

Table 5-3: Within subject, repeated measures ANOVA, with greenhouse-Geisser correction for spherical assumptions showing the channels, experiment and interaction between experiment and channels, between imaginary wrist flexion and extension over channels E31, E38 and E61.

Tests of Within-Subjects Effects

Source		Type III Sum of Squares	df	Mean Square	F	Sig.
Chn	Sphericity Assumed	13.274	2	6.637	6.005	.007
	Greenhouse-Geisser	13.274	1.508	8.800	6.005	.014
Error(Chn)	Sphericity Assumed	30.948	28	1.105		
	Greenhouse-Geisser	30.948	21.116	1.466		
Exp	Sphericity Assumed	8.744	1	8.744	7.906	.014
	Greenhouse-Geisser	8.744	1.000	8.744	7.906	.014
Error(Exp)	Sphericity Assumed	15.484	14	1.106		
	Greenhouse-Geisser	15.484	14.000	1.106		
Chn * Exp	Sphericity Assumed	.039	2	.019	.071	.932
	Greenhouse-Geisser	.039	1.627	.024	.071	.899
Error(Chn*Exp)	Sphericity Assumed	7.705	28	.275		
	Greenhouse-Geisser	7.705	22.778	.338		

5.3.2 Passive motor cortex activation

The passive MRCP waveform over the left cortex was selected from Figure 5-6, C3 (E37) located around the primary somatosensory/motor cortex, at the Homunculus wrist area. A significant difference ($p<0.05$) was observed between passive wrist flexion and extension in the sustain movements period, between 1200ms and 1400ms (Figure 5-12). Post passive MRCP wrist flexion was significantly higher compared with extension.

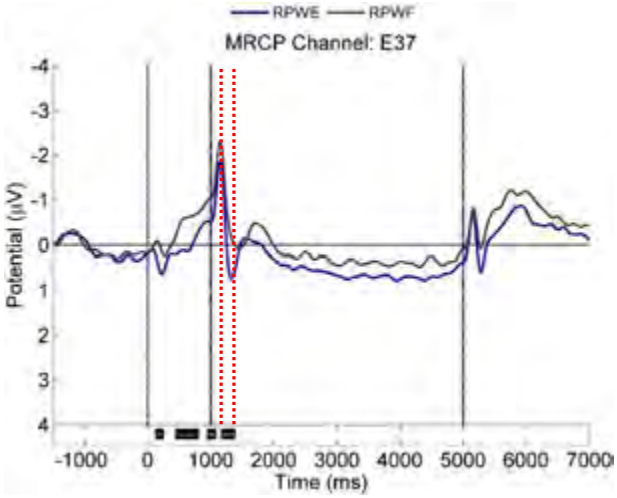

Figure 5-12: Grand average MRCP for passive movement wrist flexion and extension for C3 (E37) over -1500ms to 7000ms time regions. Significant regions ($p<0.05$) are indicated below (black regions) between flexion and extension. Between lines (---) illustrating post passive movement significant interval (1200-1400ms).

The topographic MRCP is presented in Figure 5-13. This plot is averaged over 1080-1280ms region and shows an increase in the MRCP flexion activation, predominantly in the left primary motor cortex, and left primary somatosensory cortex around the central sulcus. A higher level of activation is present in flexion. A significant difference was present in E31, E37, E38 and E42, over the same period (1200-1400ms) as shown Figure 5-12.

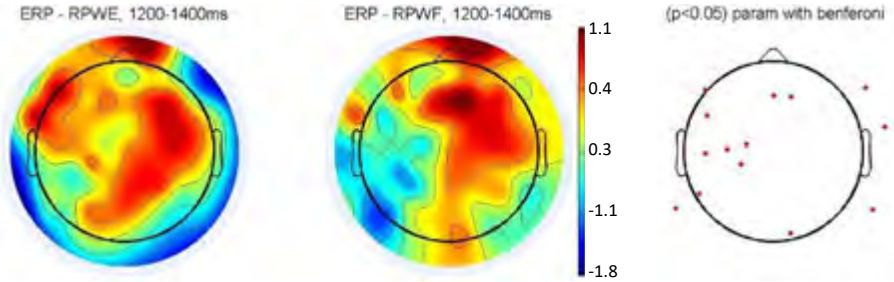

Figure 5-13: Grand average MRCP topographical plot, comparing wrist flexion and extension for post passive movements, averaged over the C3 (E37) flexion and extension significant region (1200-1400ms). Left cortex electrodes E31, E37, E38 and E42 show significances ($p<0.05$) comparing flexion and extension in the time region 1200ms to 1400ms.

Passive movements show a significant difference between flexion and extension, over electrode E31 (C1), E37 (C3), E38 (CP1) and E42 (C5) with passive wrist flexion resulting in more cortical activation as compared to extension over each channel (Figure 5-14).

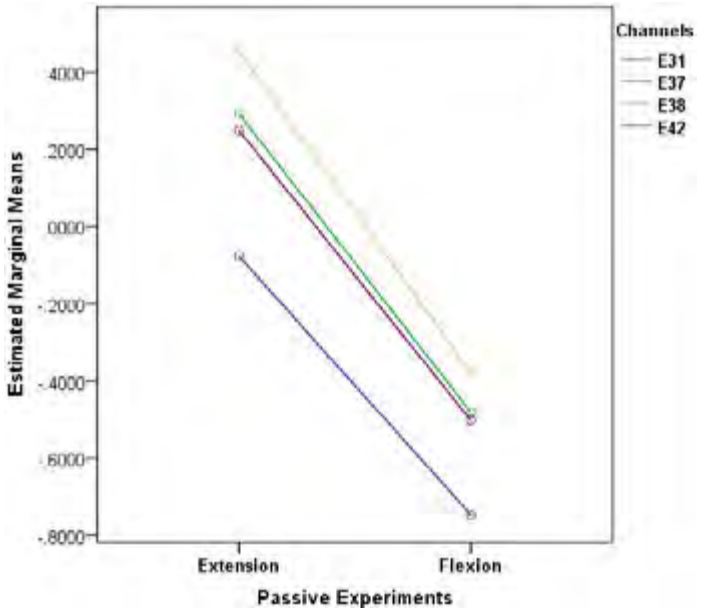

Figure 5-14: Estimated marginal mean for passive wrist flexion and extension, for electrode E31, E37, E38 and E42 averaged over the post movement period 1200ms to 1400ms.

The within subject experimental comparison between imaginary flexion and extension over all electrodes shows a significant different between the two experiments of $F(1,14) = 4.737$, $p < 0.05$. There were no significant differences between the channels of $F(3,42) = 0.494$, $p > 0.05$, when collapsing the ANOVA over experiments. The experiments and channels do not interact with one another $F(3,42) = 0.098$, $p > 0.05$.

Table 5-4: Within subject, repeated measures ANOVA, with greenhouse-Geisser correction for spherical assumptions showing the channels, experiment and interaction between experiment and channels, between passive wrist flexion and extension over channels E31, E37, E38 and E42.

Tests of Within-Subjects Effects

Source		Type III Sum of Squares	df	Mean Square	F	Sig.
Chn	Sphericity Assumed	3.227	3	1.076	.494	.688
	Greenhouse-Geisser	3.227	2.333	1.383	.494	.643
Error(Chn)	Sphericity Assumed	91.394	42	2.176		
	Greenhouse-Geisser	91.394	32.661	2.798		
Exp	Sphericity Assumed	17.216	1	17.216	4.737	.047
	Greenhouse-Geisser	17.216	1.000	17.216	4.737	.047
Error(Exp)	Sphericity Assumed	50.881	14	3.634		
	Greenhouse-Geisser	50.881	14.000	3.634		
Chn * Exp	Sphericity Assumed	.104	3	.035	.098	.960
	Greenhouse-Geisser	.104	1.841	.056	.098	.892
Error(Chn*Exp)	Sphericity Assumed	14.747	42	.351		
	Greenhouse-Geisser	14.747	25.774	.572		

5.3.3 Real motor cortex activation

The real MRCP waveform over the left cortex was selected from Figure 5-6, C3 (E37) located around the primary somatosensory/motor cortex, at the Homunculus wrist area. A significant difference

(p<0.05) was present between real wrist flexion and extension in the sustain movements period, between 1600ms and 2250ms (Figure 4-14). Real MRCP wrist extension was significantly higher compared to real wrist flexion.

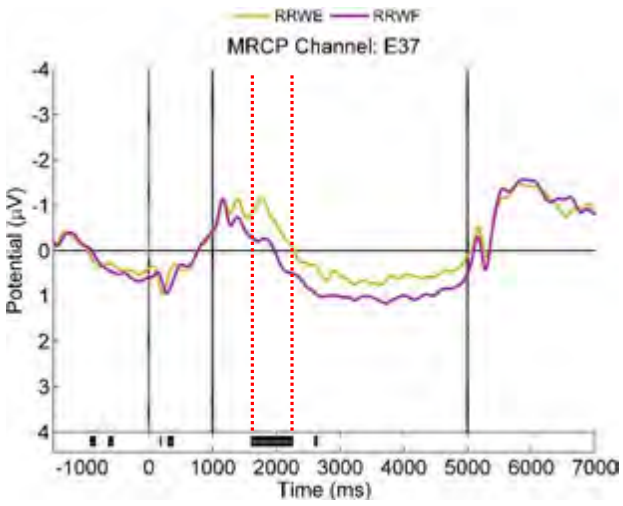

Figure 5-15: Grand average MRCP for real movement wrist flexion and extension for C3 (E37) over -1500ms to 7000ms time regions. Significant regions (p<0.05) are indicated below (black regions) between flexion and extension. Between lines (---) illustrating post movement real significant interval (1600-2250ms).

The topographic MRCP is presented in Figure 5-16. This plot is averaged over 1600-2250ms region and shows and increase in the MRCP extension activation, predominantly in the left primary motor cortex, and left primary somatosensory cortex. The post movement activation during real wrist extension was significantly larger ($p < 0.05$) than that for real wrist flexion. A significant difference was present in E31, E37, E38, E48, E55, E62, E88, E106 and E129, over the same period (1600-2250ms) as shown in Figure 5-15.

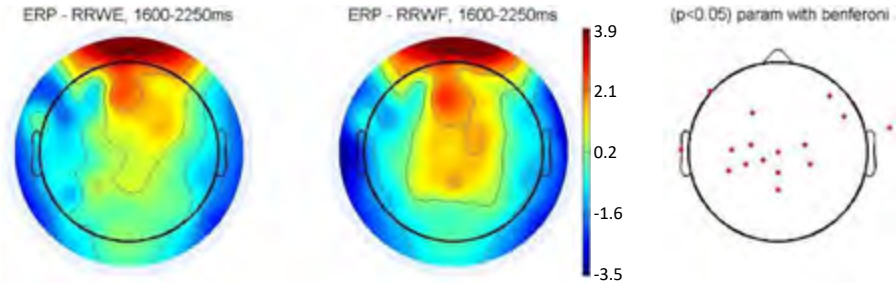

Figure 5-16: Grand average MRCP topographical plot, comparing wrist flexion and extension for post Real movements, averaged over the C3 (E37) flexion and extension significant region (1600-2250ms). Left cortex electrodes E31 (C1), E37 (C3), E38 (CP1), E48 (CP5), E55 (CPz), E62 (Pz), E88 (CP2), E106 (C2) and E129 (Cz) show significances (p<0.05) comparing flexion and extension in the time region 1600ms to 2250ms.

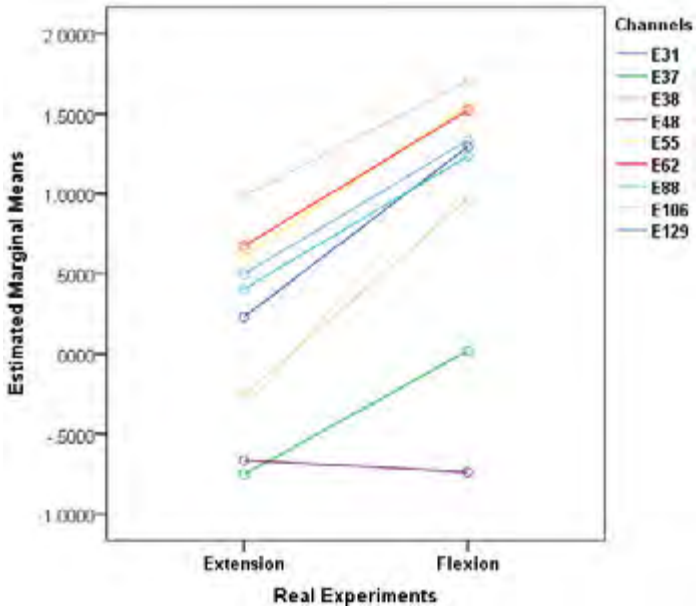

Figure 5-17: Estimated marginal mean for Real wrist flexion and extension, for electrode E31, E37, E38, E48, E55, E62, E88, E106 and E129 averaged over the post movement period 1600ms to 2250ms.

The within subject experimental comparison between real flexion and extension over all electrode shows a significant difference between the two experiments of $F(1,14) = 9.734$, $p < 0.01$. There was a significant difference between the channels of $F(8,112) = 3.975$, $p < 0.05$, when collapsing the ANOVA over experiments. The experiments and channels do not interact with one another $F(8,112) = 1.897$, $p > 0.05$.

Table 5-5: Within subject, repeated measures ANOVA, with greenhouse-Geisser correction for spherical assumptions showing the channels, experiment and interaction between experiment and channels, between real wrist flexion and extension over channels E31, E37, E38, E48, E55, E62, E88, E106 and E129.

Tests of Within-Subjects Effects

Source		Type III Sum of Squares	df	Mean Square	F	Sig.
Chn	Sphericity Assumed	117.104	8	14.638	3.975	.000
	Greenhouse-Geisser	117.104	3.152	37.154	3.975	.012
Error(Chn)	Sphericity Assumed	412.477	112	3.683		
	Greenhouse-Geisser	412.477	44.126	9.348		
Exp	Sphericity Assumed	42.816	1	42.816	9.734	.008
	Greenhouse-Geisser	42.816	1.000	42.816	9.734	.008
Error(Exp)	Sphericity Assumed	61.578	14	4.398		
	Greenhouse-Geisser	61.578	14.000	4.398		
Chn * Exp	Sphericity Assumed	7.924	8	.990	1.897	.067
	Greenhouse-Geisser	7.924	3.474	2.281	1.897	.134
Error(Chn*Exp)	Sphericity Assumed	58.472	112	.522		
	Greenhouse-Geisser	58.472	48.642	1.202		

5.3.4 Topographical MRCP Comparisons

The grand average topographical MRCP statistical comparison between wrist flexion and extension for imaginary, passive and real movements is presented in Figure 5-18, over the end of the cue period and the beginning of the sustained movement period. The majority of motor imaginary post movement significance is in the 1100-1200ms time interval, located around the primary somatosensory/motor cortex at the Homunculus wrist area. Passive movements have shown the highest level of post movement cortical activation around the primary motor cortex and primary somatosensory cortex. However, the majority of significance is located around the frontal cortex (1300-1900ms), anterior transverse primary motor and premotor cortex (1000-1400ms). Passive wrist extension displayed a higher level of MRCP cortical activation in the frontal cortex. Real movements displayed a similar area of significance compared to imaginary movements. However, this occurred for a longer period of time over the sustained movement period, from 1200ms.

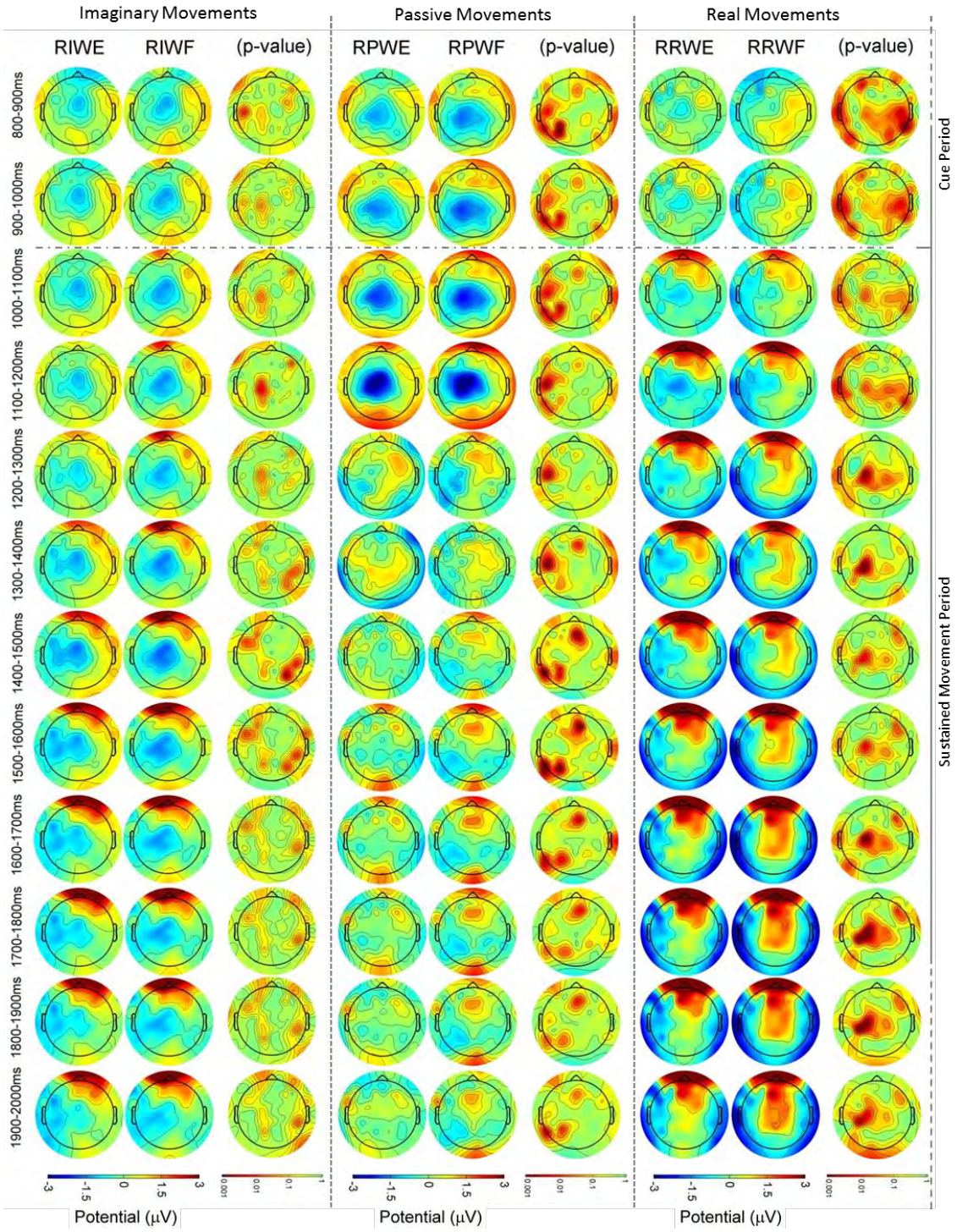

Figure 5-18: Grand average MRCP topographical plots comparing wrist flexion and extension for imaginary, passive and real movements, in the 800ms to 2000ms trial region in 100ms average period windows. The horizontal dotted black line indicated the start movement location. The p-value-maps (colour bar; green & yellow $p>0.05$, red & orange $0.001<p<0.05$) illustrate the comparison between wrist flexion and extension for the different movement types.

5.4 Movements in ERD/ERS

The grand average ERD/ERS topographical maps at peak mu, low-beta, midrange-beta and high-beta for imaginary, passive and real movements, comparing the movement effect of wrist flexion and extension are presented in Figure 5-20, Figure 5-24, Figure 5-25 and Figure 5-26 respectively. The topographical maps are plotted in 100ms averaged windows, from 800ms to 2000ms. The most prominent time series ERS/ERD results for the primary motor cortex, somatosensory association cortex or supplementary motor cortex (SMA) is represented for imaginary, passive and real movements, while comparing wrist flexion and extension movements.

Significant differences, comparing the effects of wrist flexion and extension, are represented as a p-value-map for the grand average topographical maps and black bars for the time series ERS/ERD, illustrating a significance of $p < 0.05$ (see section 4.2.4 for more information on the statistics).

5.4.1 ERD/ERS in the mu band

Motor Imagined mu ERD, present in the sustained movement period over the left somatosensory cortex (C3, CP1), showed a significant higher ERD for wrist flexion (Figure 5-19 – top, left). Passive movements showed high levels of pre and post movements ERS over the left somatosensory cortex, with a significantly ($p<0.05$) higher level of ERS for wrist extension (Figure 5-19 – top, middle), and significant ERD in the left parietal cortex around the start movement period. Real movements showed no significant differences over the left primary motor cortex and left somatosensory association cortex.

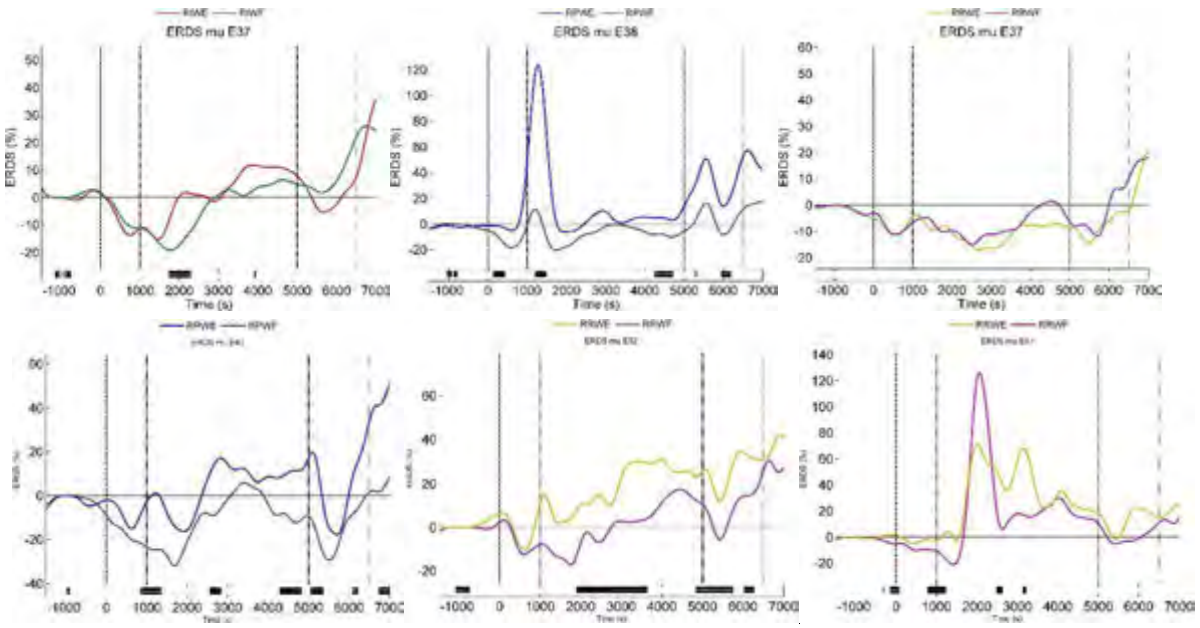

Figure 5-19: Grand average peak mu Beta ERDS for imaginary (C3, E37 - left), passive (CP1, E38 – Top, middle & CP3, E43 – bottom, left) and real movement (C3, E37 – Top, right & Pz, E62 – bottom, middle & PO4, E87 – bottom, right) wrist flexion and extension over -1500ms to 7000ms time regions. Significant regions ($p<0.05$) are indicated below (black regions) between flexion and extension.

The topographical mu ERD/ERS maps in Figure 5-20, show very little significant differences between wrist flexion and extension for imaginary and real movements at the motor cortex. However, real movements show a significant difference for the mu ERD/ERS in the occipital cortex, with higher levels

of ERS for wrist extension. Passive movements show a significantly higher ERS for extension over the left somatosensory association cortex.

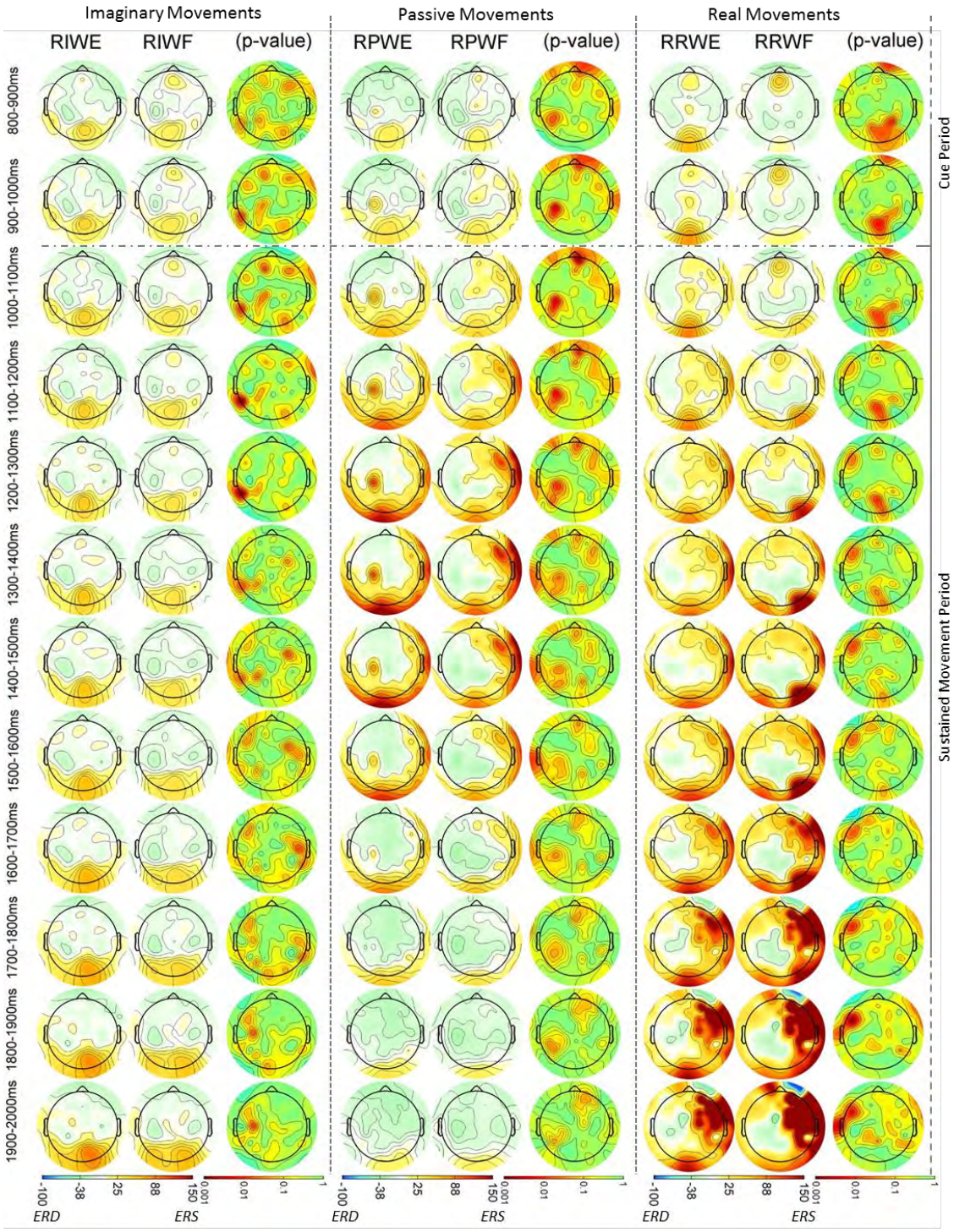

Figure 5-20: Grand average ERDS topographical plots of peak mu rhythms, comparing wrist flexion and extension for imaginary, passive and real movements, in the 800ms to 2000ms trial region in 100ms average period windows. The horizontal dotted black line indicated the start movement location. The p-value-maps (colour bar; green & yellow $p>0.05$, red & orange $0.001<p<0.05$) illustrate the comparison between wrist flexion and extension for the different movement types.

5.4.2 ERD/ERS in the beta band

No sustained significant low-beta ERD/ERS differences were present between wrist flexion and extension for imaginary movements (Figure 5-24). Passive movements only showed a significant difference in the occipital cortex around the start and pre movement period, with higher levels of low-beta ERS for wrist extension (Figure 5-24 – bottom, right). No passive movement significant difference was present around the primary motor cortex (Figure 5-21 – top, middle), somatosensory association cortex or SMA. Real movements showed a significant difference in the left premotor cortex (Figure 5-21 – top, right) around the start movement period, with higher levels of low-beta ERS for wrist flexion.

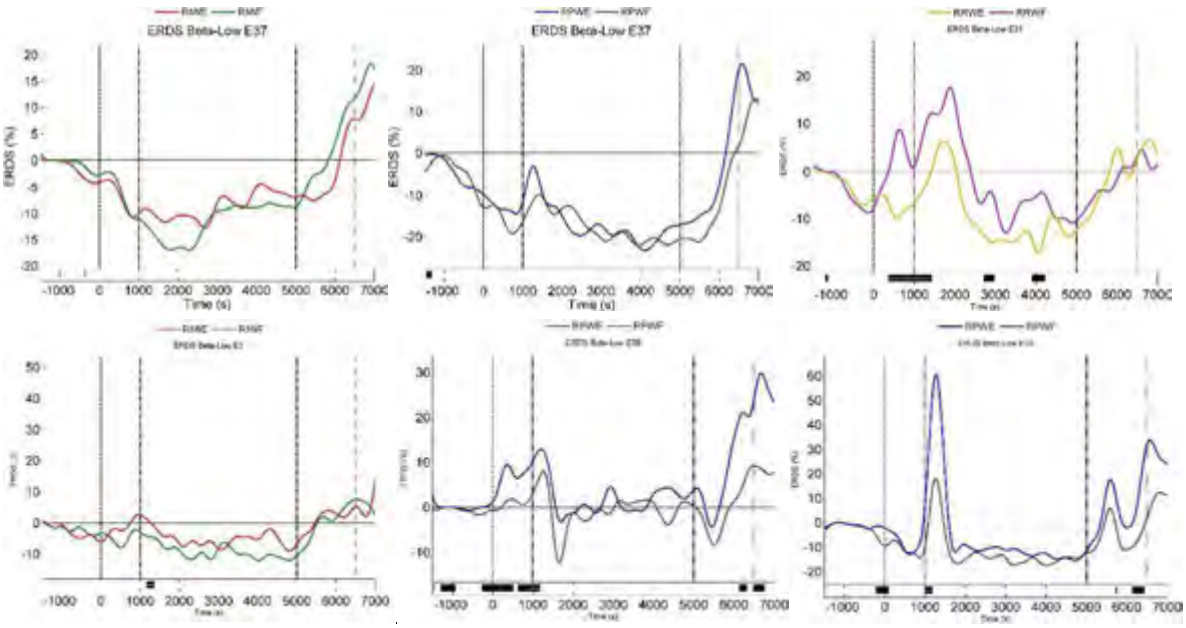

Figure 5-21: Grand average peak low-Beta ERDS for imaginary (C3, E37 – Top, left & FCz, E6 – Left, bottom), passive (C3, E37 – Top, middle & POz, E68 – middle, bottom & CP1, E38 – right, bottom), and real movement (FC1, E21 – Top, right) wrist flexion and extension over -1500ms to 7000ms time regions. Significant regions ($p<0.05$) are indicated below (black regions) between flexion and extension.

The Midrange-Beta imaginary ERD/ERS, showed no sustained significant differences between flexion and extension in the cue period and the sustained movement period, over the primary motor cortex (C3, Figure 5-22 – left), somatosensory association cortex and SMA. Passive movements showed a strong significant difference around the left somatosensory association cortex (CP3, Figure 5-22 - middle), indicating a higher level of ERD for wrist flexion at the end of the cue period and start movement period (Figure 5-25). Real movements showed a significant increase in the ERD for wrist flexion around the somatosensory association cortex (Cpz, Figure 5-22 – right), in the sustained movement period.

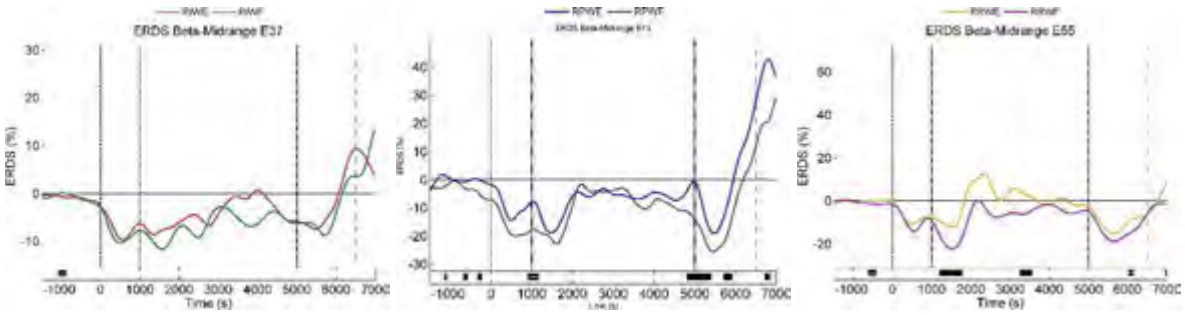

Figure 5-22: Grand average peak midrange-Beta ERDS for imaginary (C3, E37 - left), passive (CP3, E43 - middle) and real movement (Cpz, E55 - right) wrist flexion and extension over -1500ms to 7000ms time regions. Significant regions ($p<0.05$) are indicated below (black regions) between flexion and extension.

High-beta ERD/ERS showed no sustained significant differences, when comparing imaginary wrist flexion and extension over the cue period and the sustained movement period (Figure 5-26). Significantly high-beta ERD was observed for passive flexion movements over the left primary motor and somatosensory cortex (C3, Figure 5-23 – top, middle) at the start movement location, and the central somatosensory cortex, during the pre and post movements period (Figure 5-26, bottom, middle). Real movements showed a high-beta significance in the central premotor area (FCz, Figure 5-23 – top, right) and scattered throughout the sustained movement period for the left premotor area (FCz, Figure 5-23 – bottom, right) , with higher levels of ERD for wrist extension, around the start movements location.

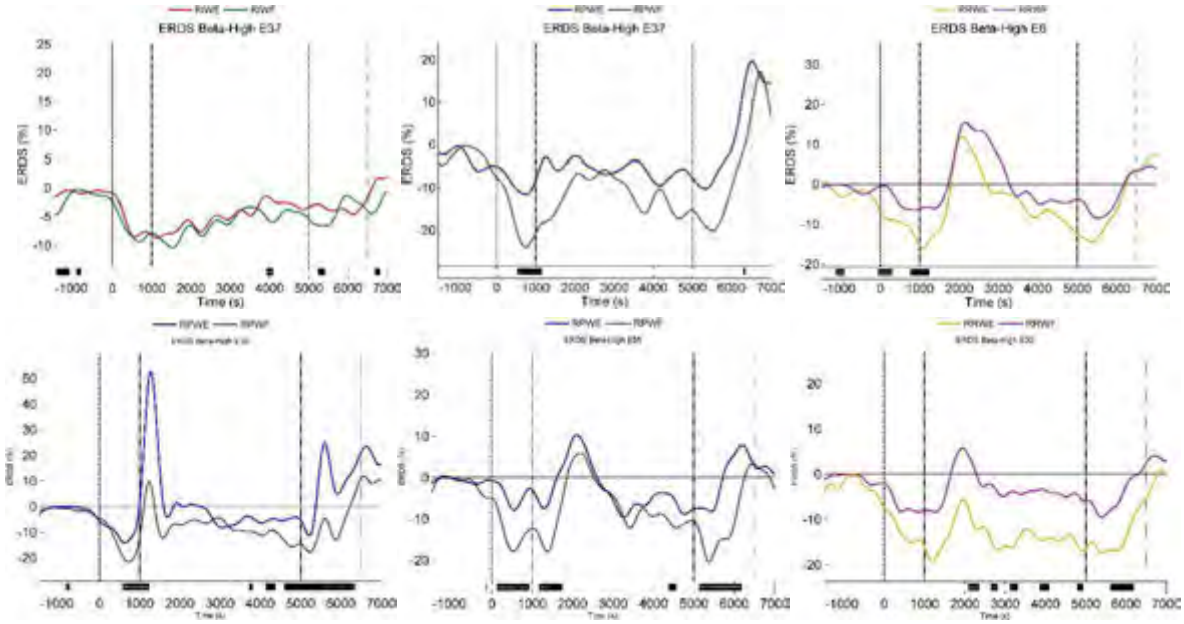

Figure 5-23: Grand average peak high-Beta ERDS for imaginary (C3, E37 – top, left), passive (C3, E37 – top, middle & CP1, E38 – bottom, left & Cpz, E55 – bottom, middle) and real movement (FCz, E6 – Top, right, FC3, E30 – Bottom, right) wrist flexion and extension over -1500ms to 7000ms time regions. Significant regions ($p<0.05$) are indicated below (black regions) between flexion and extension.

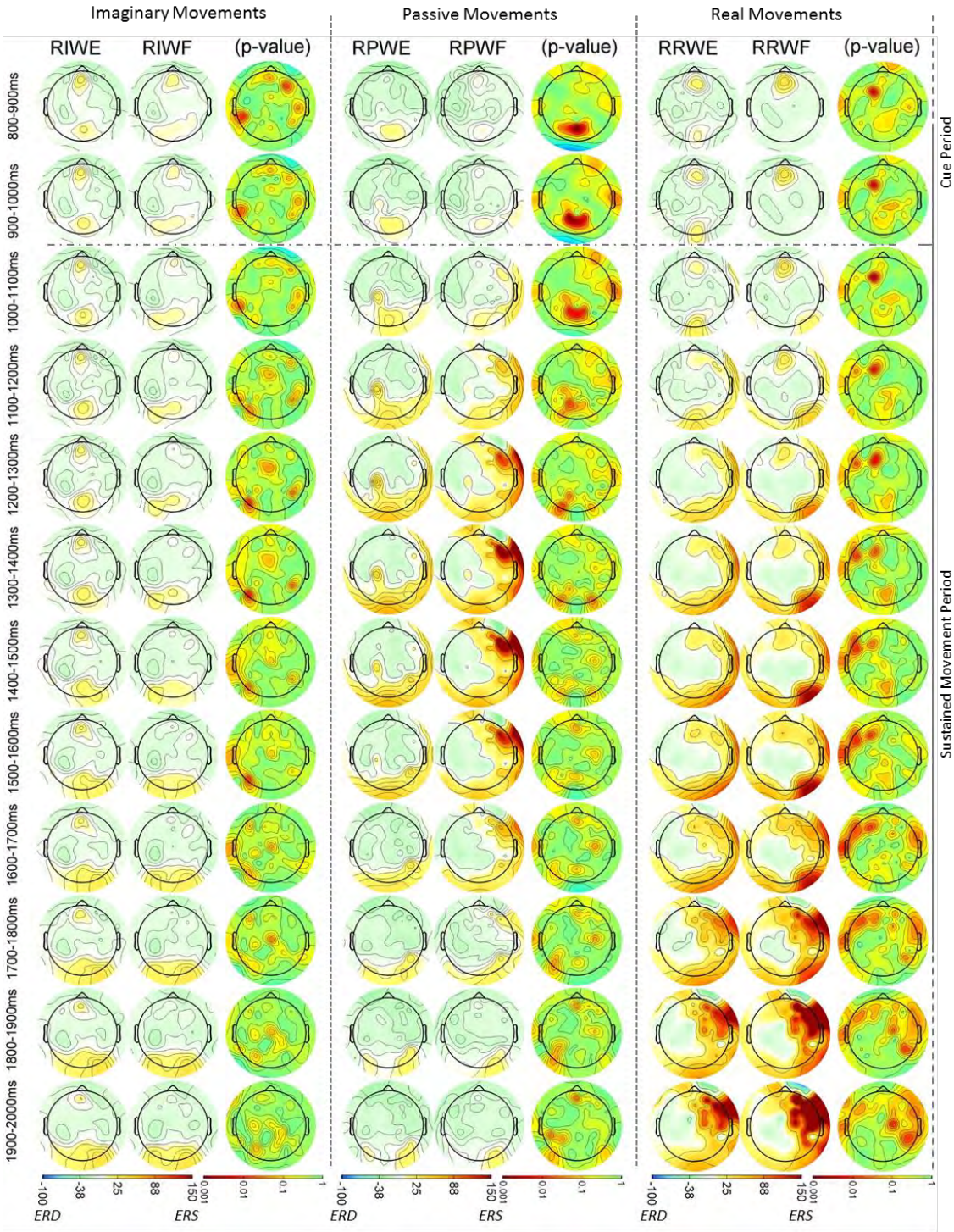

Figure 5-24: Grand average ERDS topographical plots of peak low-beta rhythms, comparing wrist flexion and extension for imaginary, passive and real movements, in the 800ms to 2000ms trial region in 100ms average period windows. The horizontal dotted black line indicated the start movement location. The significant p-value-maps (colour bar; green $p<1$, red $p>0.001$) illustrated the significant comparison between wrist flexion and extension for the different movement types.

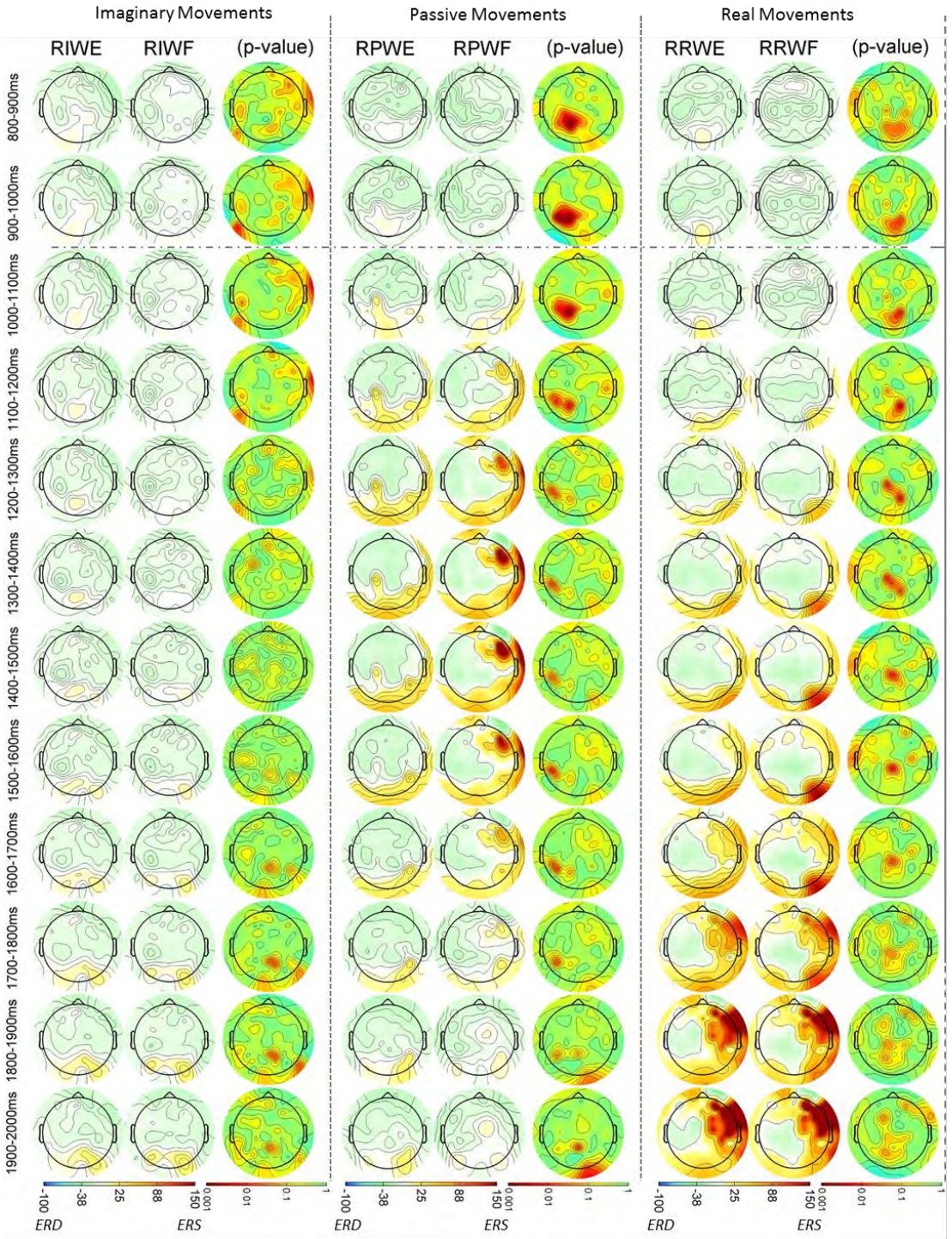

Figure 5-25: Grand average ERDS topographical plots of peak midrange-beta rhythms, comparing wrist flexion and extension for imaginary, passive and real movements, in the 800ms to 2000ms trial region in 100ms average period windows. The horizontal dotted black line indicated the start movement location. The p-value-maps (colour bar; green & yellow $p>0.05$, red & orange $0.001<p<0.05$) illustrate the comparison between wrist flexion and extension for the different movement types.

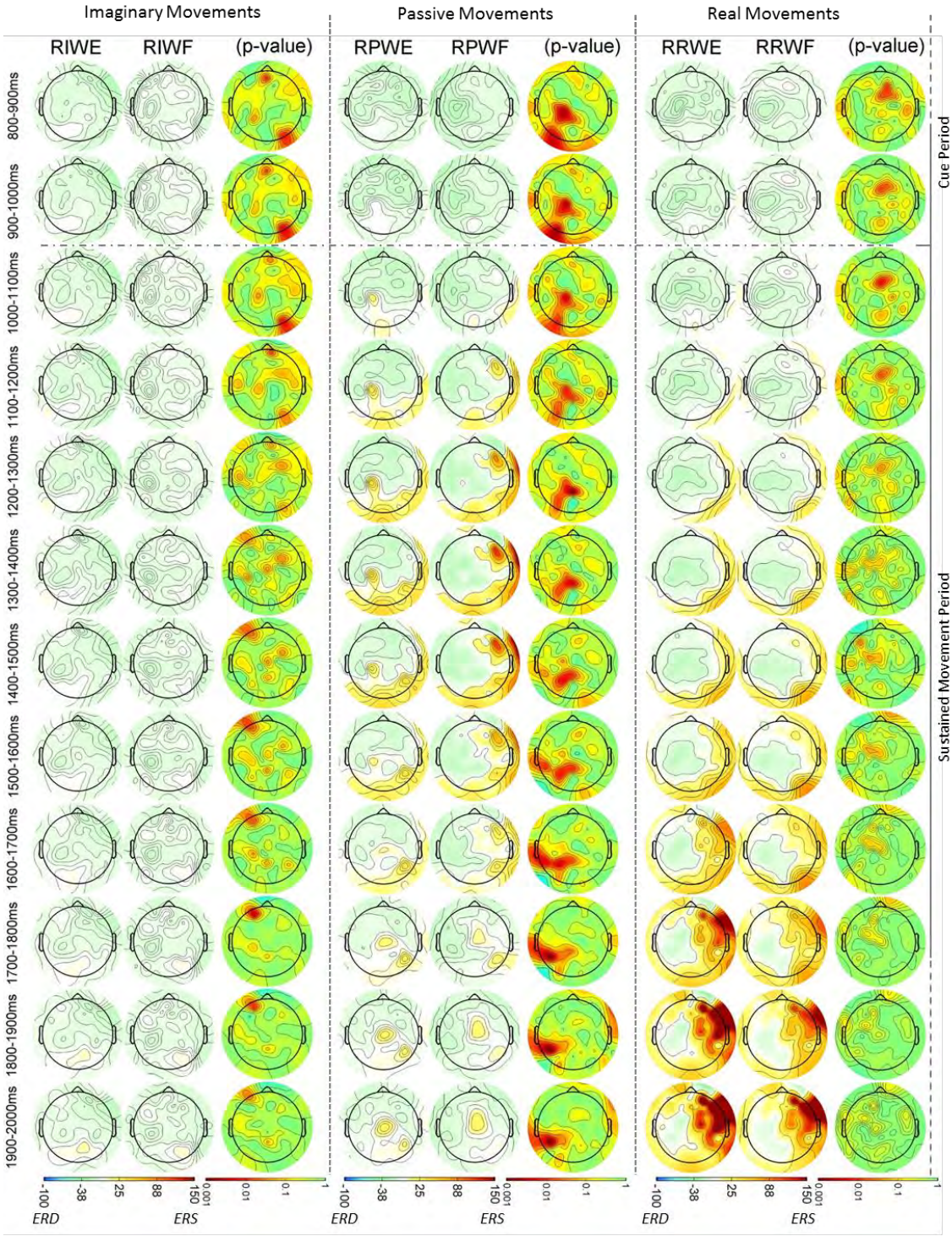

Figure 5-26: Grand average ERDS topographical plots of peak high-beta rhythms, comparing wrist flexion and extension for imaginary, passive and real movements, in the 800ms to 2000ms trial region in 100ms average period windows. The horizontal dotted black line indicated the start movement location. The p-value-maps (colour bar; green & yellow $p>0.05$, red & orange $0.001<p<0.05$) illustrate the comparison between wrist flexion and extension for the different movement types.

5.5 Phase Locking Value

5.5.1 Phase Locking Value with SMA

The grand average PLV results calculated between the SMA and primary motor cortex is presented below for imaginary, passive and real movements, and display the statistical comparison between wrist flexion and extension. The sample-by-sample time and frequency statistical comparison is represented over the -2000ms to 8000ms trial region and 5Hz to 40Hz frequency range.

5.5.1.1 Imaginary movements

Imaginary PLV between the contralateral primary motor cortex (C3) and SMA (Pcz), in the comparison of wrist flexion and extension showed significant differences around 3000ms in the mu band (Figure 5-27 – top, left), with a higher level of PLV for imaginary wrist flexion. A significantly higher level of post movement imaginary PLV wrist flexion over the sustained movement period in the mu band, was present over the central primary motor cortex (Figure 5-27 – top, right). The left parietal cortex shown a significantly higher pre-movement mu band PLV for wrist flexion (Figure 5-27 – bottom, left). The left visual cortex also showed a significantly higher mu band PLV for wrist flexion (Figure 5-27 – bottom, right).

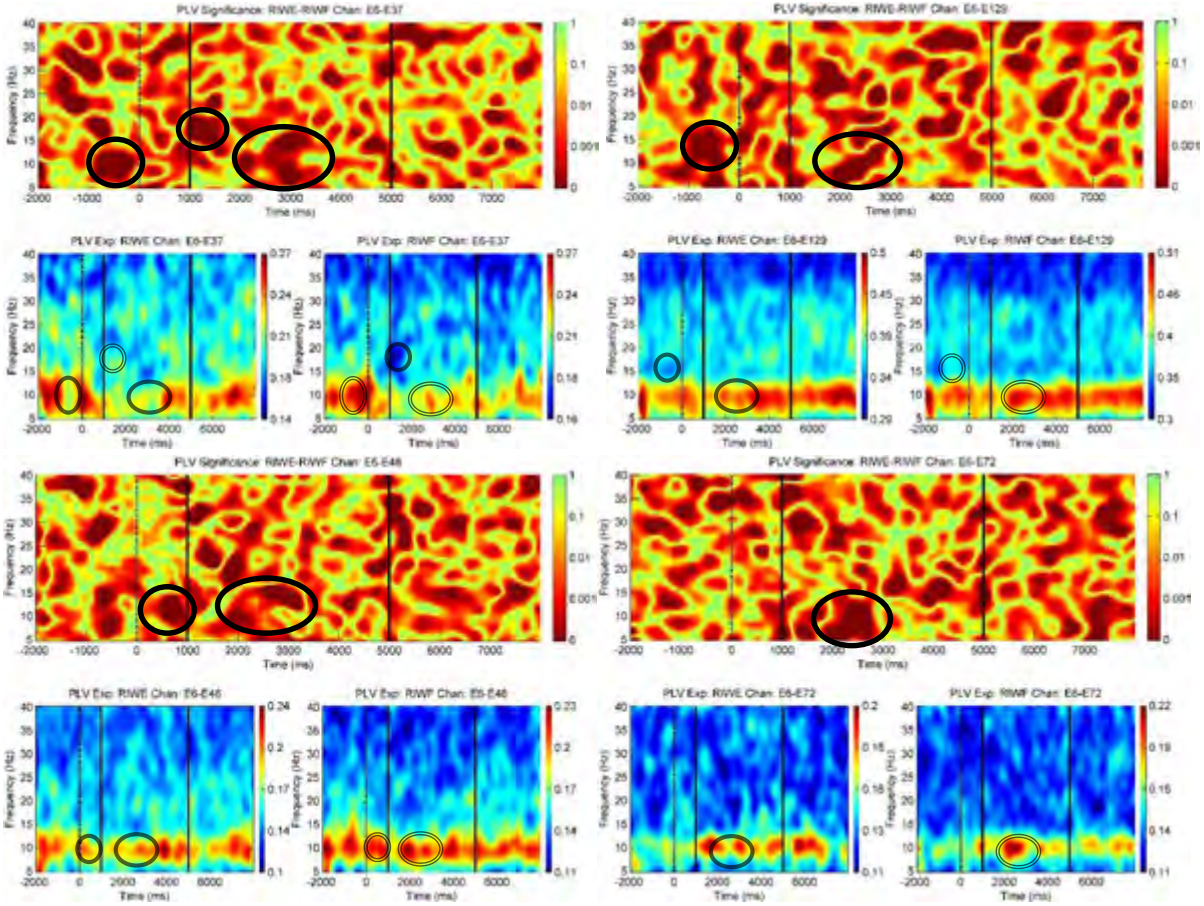

Figure 5-27: The grand average PLV for Imaginary wrist movements between showing the phase locking between the primary motor cortex (Top, left image – E37, C3 & Top, right image – E129, Cz), Left Parietal Cortex (Brodmann area 40, Bottom, Left – E48, CP5), left primary visual cortex (Bottom, right – E72, O1) and SMA (Pcz), over the -2000ms to 8000ms trial range and 5Hz to 40Hz frequency range. The PLV time-frequency-p-map showing the significance difference between wrist flexion and extension is illustrated at the top. Black circle indicate areas of significance ($p < 0.05$), with double dash circle indicating movement with the highest PLV.

5.5.1.2 Passive movements

Passive PLV showed a significant difference in a similar time and frequency location to imaginary PLV: with a significant mu PLV between the contralateral primary motor (C3) and SMA (Pcz) cortex for passive wrist movements in the sustained movement period (Figure 5-28 – top, left). The left premotor cortex also showed a significantly higher level of beta PLV in the sustained movement period for wrist extension.

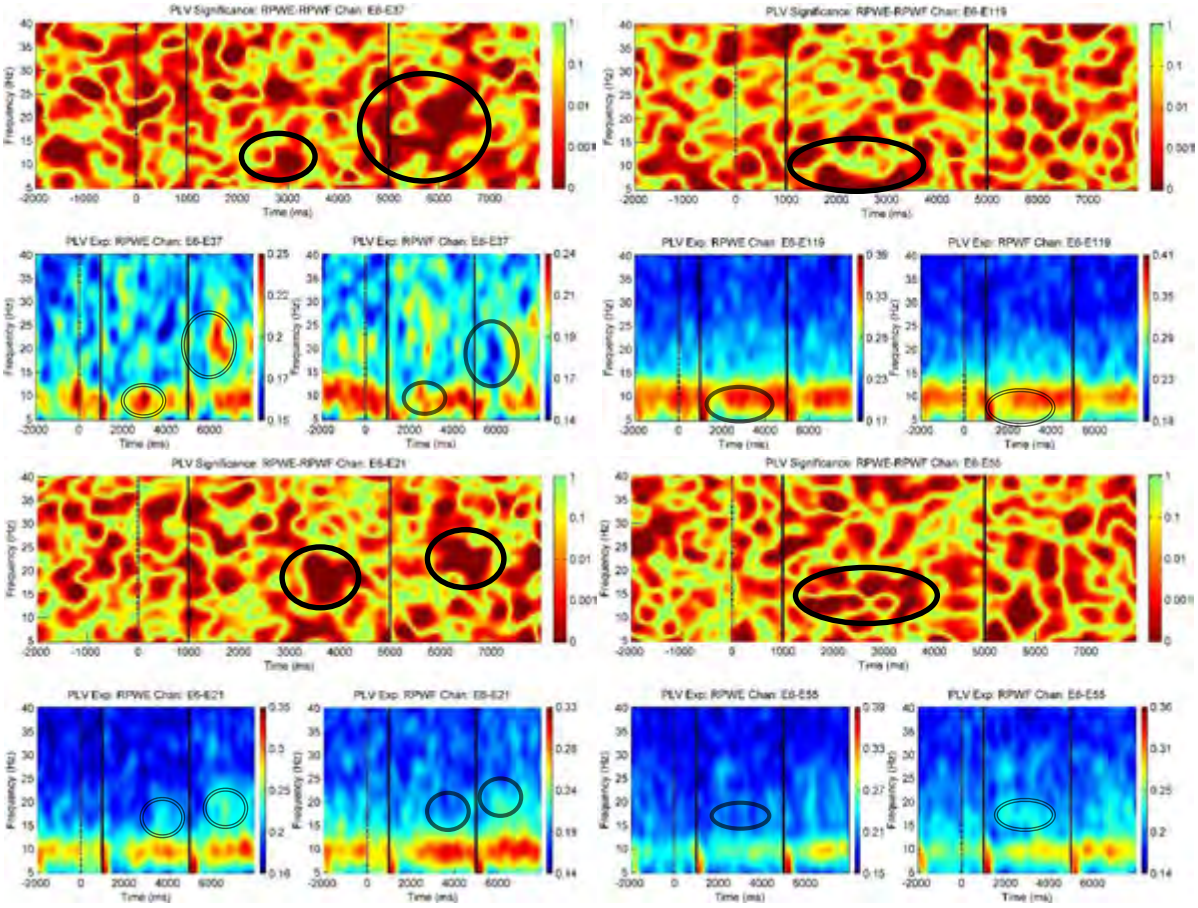

Figure 5-28: The grand average PLV for passive wrist movements between showing the phase locking between the Left primary motor cortex (Top left image – E37, C3), right premotor cortex (Top right image – E119, FC2), left Premotor cortex (Bottom middle image – E21, FC1), central somatosensory cortex (Bottom left – E55, Cpz) and SMA (Pcz), over the -2000ms to 8000ms trial range and 5Hz to 40Hz frequency range. The PLV time-frequency-p-map showing the significance difference between wrist flexion and extension is illustrated at the top. Black circle indicate areas of significance ($p < 0.05$), with double dash circle indicating movement with the highest PLV.

5.5.1.3 Real Movements

There were no significant sustained mu-band PLV difference between real wrist flexion and extension, in the sustained movement period, between the contralateral primary motor cortex (C3, C4) and the SMA (Pcz), refer to Figure 5-29 – top, left. However, there is a significantly higher PLV for wrist flexion between the SMA and right pre-motor cortex during the pre and post movement interval (refer to Figure 5-29 – top, right: 500ms, 2000ms 10Hz). Significant higher wrist flexion PLV is also present at start movement interval between the SMA and left pre-motor cortex, (refer to Figure 5-29 – bottom, left: 1000ms 15Hz).

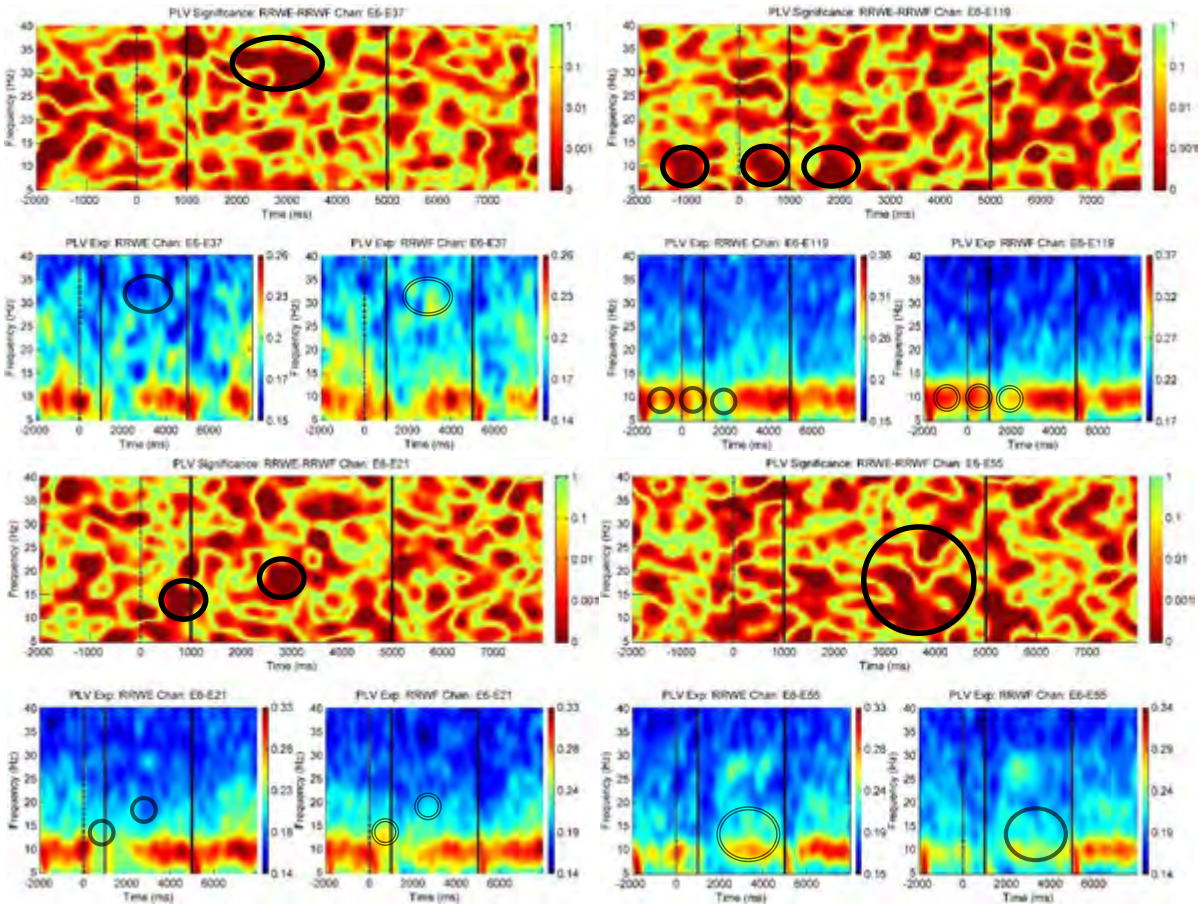

Figure 5-29: The grand average PLV for real wrist movements between showing the phase locking between the Left primary motor cortex (Top left image - C3), right premotor cortex (Top right image – E119, FC2), left premotor cortex (bottom left image – E21, FC1), central somatosensory cortex (bottom right image – E55, Cpz), and SMA (Pcz), over the -2000ms to 8000ms trial range and 5Hz to 40Hz frequency range. The PLV time-frequency-p-map showing the significance difference between wrist flexion and extension is illustrated at the top. Black circle indicate areas of significance ($p < 0.05$), with double dash circle indicating movement with the highest PLV.

5.6 Overview of main results

The most significant findings of the within comparison between wrist flexion and extension for imaginary (see section 5.6.1), passive (see section 0) and real movements (see section 0) are summarized below, and categorized into their investigation subsections as illustrated in Figure 5-30.

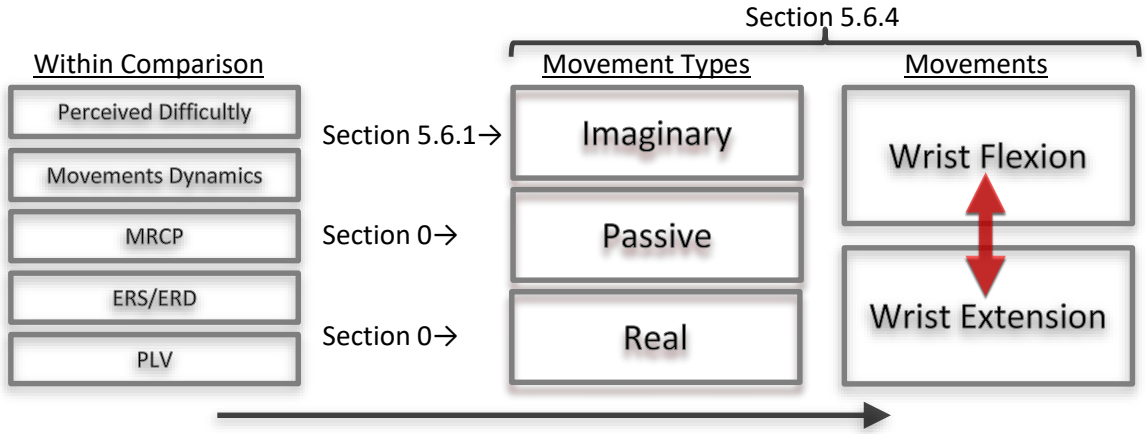

Figure 5-30: Overview of results section for movement types; motor imaginary, passive movements and real (active) movements including the summary of all significant results.

5.6.1 Motor imaginary wrist flexion and extension comparison

Table 5-6: Significant findings between motor imaginary wrist flexion and extension for perceived, MRCP, ERD/S and PLV analysis over the pre and post movement periods, around prominent cortical areas (see Figure 4-2). Significant finding related to movements and/or sensory feedback is highlighted in bold.

Wrist Flexion and Extension within Comparison Significant	**Motor Imaginary** – Perceived	• **No subject perceived movement differences (F(1,14) = 0.713, p > 0.05), see Figure 5-2.**
	Motor Imaginary – MRCP	• **Significant flexion (p < 0.05), pre- post- movement (800-1200ms), C1 – contralateral primary motor cortex and somatosensory cortex, see Figure 5-6 left column & Figure 5-9.** • **Significant flexion (p < 0.05), start movement (~1000ms), CP1 – contralateral somatosensory processing and association, see Figure 5-6 left column.** • Significant extension (p < 0.05), pre-movement (800-1000ms), FC4 – right premotor area, see Figure 5-7 left column. • Significant flexion (p < 0.05), sustained-movement (2000-5500ms), C6 – right Auditory cortex, see Figure 5-7 left column. • Within subject comparison (F(1,14) =7.609, p < 0.05) between flexion and extension over electrode over the E31 (C1), E38 (CP1) and E61 (P1) within the period 1080-1280ms, showed more cortical activation for wrist flexion, with a significant difference between channels of F(2,28) = 6.005, p < 0.05, see Figure 5-10.
	Motor Imaginary – ERS/ERD	• **Significant flexion mu-band ERD (p < 0.05), sustained-movement (~2000ms), C3 – contralateral primary motor cortex and somatosensory cortex, see Figure 5-19-top left.** • Significant flexion low beta-band ERD (p < 0.05), post-movement (~1100ms), FCz – central premotor area, see Figure 5-21-bottom left.

		PLV	• Significant flexion (p < 0.05), mu-band (10Hz), pre-cue (-1000-0ms), SMA to C3 – contralateral primary motor cortex and somatosensory cortex, see Figure 5-27-top left. • Significant extension (p < 0.05), beta-band (18Hz), post movement (1200ms), SMA to C3 – contralateral primary motor cortex and somatosensory cortex, see Figure 5-27-top left. • **Significant flexion (p < 0.05), mu-band (10Hz), sustained movement (2000-3000ms), SMA to C3 – contralateral primary motor cortex and somatosensory cortex, see Figure 5-27-top left.** • Significant flexion (p < 0.05), mu-band (10Hz), sustained movement (2000-3000ms), SMA to Cz – central primary motor cortex and somatosensory cortex, see Figure 5-27-top right. • Significant flexion (p < 0.05), mu-band (10Hz), pre-cue (-1000 - 0ms), SMA to Cz – central primary motor cortex and somatosensory cortex, see Figure 5-27-top right. • Significant flexion (p < 0.05), mu-band (10Hz), pre movement (~800ms), SMA to Cp5 – left parietal cortex cortex, see Figure 5-27-bottom left. • Significant flexion (p < 0.05), mu-band (10Hz), sustained movement (2000ms-3000ms), SMA to O1 – left primary visual cortex, see Figure 5-27-bottom right.

5.6.2 Passive movement wrist flexion and extension comparison

Table 5-7: Significant findings between passive wrist flexion and extension movements for perceived, Dynamic, MRCP, ERD/S and PLV analysis over the pre and post movement periods, around prominent cortical areas (see Figure 4-2). Significant finding related to movements and/or sensory feedback is highlighted in bold.

Wrist Flexion and Extension within Comparison Significant Differences		
Passive Movements	Perceived	• **No subject perceived movements differences (F(1,14) = 0.059, p > 0.05), see Figure 5-2.**
	Dynamics	• **Normalized average (1000-5000ms) wrist strain was significantly (p < 0.01) higher for extension, see Figure 5-3 and Figure 5-4, left.** • Peak wrist strain was significantly (p < 0.01) higher for extension, see • • • **Normalized average (1000-5000ms) wrist angles was significantly higher (p<0.01) for flexion, with a maximum extension angle of 78˚ and a maximum flexion angle of 88˚, see Figure 5-3 and Table 5-1** • **Peak start (~1000ms) wrist velocity was significantly (p<0.01) higher for extension and peal end velocity (~5000ms) show no significant difference, see Table 5-1 and Figure 5-3.**
	MRCP	• **Significant flexion (p < 0.05), pre- post- movement (400-1200ms), FC3 – contralateral premotor area, see Figure 5-6 middle column.** • **Significant flexion (p < 0.05), pre- post- movement (~800ms ~1200ms), C1 – contralateral primary motor cortex and somatosensory cortex, see Figure 5-6 middle column.** • **Significant flexion (p < 0.05), pre- post- movement (200-1400ms), C3 – contralateral primary motor cortex and somatosensory cortex, see Figure 5-6 middle column.** • Significant flexion (p < 0.05), pre- post- sustained- movement (200-1400ms), C5 – left auditory cortex, see Figure 5-6 middle column. • Significant extension (p < 0.05), pre- post- sustained- movement (-200-4000ms), Fz – frontal cortex, see Figure 5-8 middle column. • Significant extension (p < 0.05), cue- post- movement (~0ms ~2000ms), Fcz – central premotor cortex, see Figure 5-8 middle column. • Within subject comparison (F(1,14) =4.737, p < 0.05) between flexion and extension over electrode over the E31, E37, E38 and E42 within the period 1080-1280ms, showed more cortical activation for wrist flexion, with a no significant difference between channels of F(2,28) = 0.494, p > 0.05, see Figure 5-13.

		ERS/ERD	• **Significant extension mu-band ERS (p < 0.05), pre- post- movement (~200ms ~14000ms), CP1 – contralateral somatosensory processing and association area, see Figure 5-19-top middle.** • Significant flexion mu-band ERD (p < 0.05), start movement (~1000ms), CP3 – contralateral parietal cortex, see Figure 5-19-bottom left. • Significant extension low beta-band ERS (p < 0.05), pre- movement (~-200 -1200ms), POz – central primary visual cortex, see Figure 5-21-bottom middle. • **Significant flexion low beta-band ERS (p < 0.05), post- movement (1000ms-1200ms), CP1 – central somatosensory processing and association area, see Figure 5-21-right, bottom.** • Significant flexion midrange beta-band ERD (p < 0.05), start movement (~1000ms), CP3 – left parietal cortex, see Figure 5-22-middle. • **Significant flexion high beta-band ERD (p < 0.05), start movement (500 -1100ms), C3 – contralateral primary motor cortex and somatosensory cortex, see Figure 5-23-middle, top.** • **Significant flexion high beta-band ERD (p < 0.05), pre- movement (0- 1200ms), Cpz – central somatosensory processing and association area, see Figure 5-23-middle, bottom.** • **Significant flexion high beta-band ERS (p < 0.05), post- movement (1100ms-1600ms), Cpz – central somatosensory processing and association area, see Figure 5-23-middle, bottom.** • **Significant flexion high beta-band ERD (p < 0.05), pre- movement (500ms-1000ms), CP1 – central somatosensory processing and association area, see Figure 5-23-left, bottom.** • **Significant flexion high beta-band ERS (p < 0.05), post- movement (1000ms-1200ms), CP1 – central somatosensory processing and association area, see Figure 5-23-left, bottom.**
		PLV	• **Significant extension (p < 0.05), mu-band (10Hz), sustained movement (~3000ms), SMA to C3 – contralateral primary motor cortex and somatosensory cortex, see Figure 5-28-top left.** • **Significant extension (p < 0.05), beta-band (20Hz), relax period (~6000ms), SMA to C3 – contralateral primary motor cortex and somatosensory cortex, see Figure 5-28-top left.** • **Significant extension (p < 0.05), beta-band (20Hz), sustained movement (3500-4000ms), SMA to FC1 – contralateral premotor area, see Figure 5-28-bottom, left**. • Significant flexion (p < 0.05), mu-band (8Hz), sustained movement (1700-3000ms), SMA to FC2 – right premotor area, see Figure 5-28-top, right. • **Significant flexion (p < 0.05), beta-band (15Hz), sustained movement (1500-3800ms), SMA to CPz – central somatosensory area, see Figure 5-28-bottom, right**.

5.6.3 Real movement wrist flexion and extension comparison

Table 5-8: Significant findings, between real (active) wrist flexion and extension movements for perceived, Dynamic, MRCP, ERD/S and PLV analysis over the pre and post movement periods, around prominent cortical areas (see Figure 4-2). Significant finding related to movements and/or sensory feedback is highlighted in bold.

Wrist Flexion and Extension within Comparison Significant Differences	**Real Movements**	Perceived	• **Higher subject perceived movement difficulty for extension (F(1,14) = 27.429, p < 0.01), see Figure 5-2.**
		Dynamics	• **Greater sustained movement strain for wrist extension (0.86Nm) compared to wrist flexion (1.05Nm), (p < 0.05), see Figure 5-3, Figure 5-4 and Table 5-1.** • **Greater maximum relative extension angle (68.89˚) compared to Flexion angle (87.35˚), (p < 0.05), see Figure 5-3, Figure 5-4 and Table 5-1.**
		MRCP	• Significant extension (p < 0.05), sustained movement (~1000ms-5000ms), C1 – contralateral primary motor cortex and somatosensory cortex, see Figure 5-6 right column. • **Significant extension (p < 0.05), sustained movement (1800ms-2300ms), C3 – contralateral primary motor cortex and somatosensory cortex, see Figure 5-6 right column.** • **Significant extension (p < 0.05), sustained movement (1000ms-5000ms), CP1 – contralateral somatosensory processing and association area, see Figure 5-6 right column.** • Significant extension (p < 0.05), pre- post- movement (600ms-1100ms), C2 – right primary motor cortex and somatosensory cortex, see Figure 5-6 right column. • Significant extension (p < 0.05), pre- post- movement (500ms-1200ms), C4 – right primary motor cortex and somatosensory cortex, see Figure 5-6 right column. • Significant extension (p < 0.05), pre- post- movement (500ms-2000ms), CP2 – right somatosensory processing and association area, see Figure 5-6 right column. • Significant extension (p < 0.05), pre- post- sustained movement (0ms-2200ms), CP2 – central somatosensory processing and association area, see Figure 5-6 right column. • Significantly (F(1,14) = 9.734, p < 0.01) higher levels of cortical activation was present for wrist extension as compared to flexion, predominantly around the left primary motor cortex and left primary somatosensory cortex in the 1600-2250ms epoch region, see Figure 5-15 and Figure 5-16.
		ERS/ERD	• Significant extension mu-band ERD (p < 0.05), start movement (~1000ms), Pz – central parietal cortex, see Figure 5-19-bottom middle. • **Significant extension low beta-band ERD (p < 0.05), pre- post- movement (400-1300ms), FC1 – contralateral premotor cortex, see Figure 5-21-top right.** • Significant flexion midrange beta-band ERD (p < 0.05), post- movement (1100-1800ms), Cpz – central somatosensory processing and association area, see Figure 5-22-right. • Significant extension high beta-band ERD (p < 0.05), pre- post movement (~0ms 800ms-1200ms), FCz – central premotor area, see Figure 5-23-top right. • **Significant extension high beta-band ERD (p < 0.05), sustained movement (scattered 2000ms-5000ms), FC3 – contralateral premotor area, see Figure 5-23-bottom right.**

		PLV	• **Significant flexion (p < 0.05), gamma-band (33Hz), sustained movement (3000ms), SMA to C3 – right premotor area, see Figure 5-29-top left.** • Significant flexion (p < 0.05), mu-band (10Hz), pre-cue pre- post- movement (~-1000ms ~500ms ~2000ms), SMA to FC2 – right premotor area, see Figure 5-29-top right. • **Significant flexion (p < 0.05), mu-band (10Hz), pre- movement (800-1000ms), SMA to FC1 – left premotor area, see Figure 5-29-top left.** • **Significant flexion (p < 0.05), beta-band (10Hz), sustained movement (3000ms), SMA to FC1 – left premotor area, see Figure 5-29-bottom left.** • Significant Extension (p < 0.05), beta-band (10Hz), sustained movement (scattered 3000-4500ms), SMA to Cpz – central somatosensory processing and association area, see Figure 5-29-bottom right.

5.6.4 Summary

The main results, illustrated in **Table 5-9**, display the significant differences between wrist flexion and extension for motor imaginary, passive movements and real (active) movements for subject perceived difficult, movement dynamic (strain, velocity, angle), MRCP, ERD/ERS and PLV analysis (see **Table 5-9**, analysis column) for the pre-, pro- and sustained movement periods (refer to Figure 5-31). Cortical areas of interest are limited to the somatosensory cortex, primary motor cortex, premotor cortex, auditory cortex, parietal cortex and visual cortex (see Table 4-2) by associating EEG electrodes to the corresponding Brodmann areas (see section 4.1.3.1).

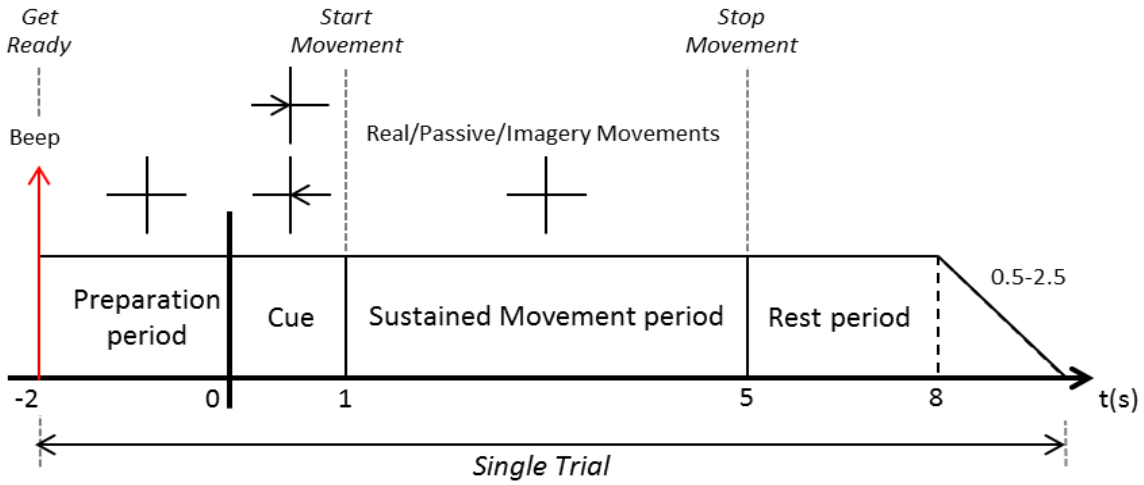

Figure 5-31: An illustration of the different movement epoch time regions in relation to the acronyms used in the summary of result. Acronyms: Pre-cue < 0ms, 0ms <pre < 1000ms, stat – around 1000ms, 0ms <post < 2000ms, 2000ms < sus < 5000ms;

Table 5-9: Significant result (* < 0.05; ** < 0.01) of the within comparison between flexion and extension for perceived, dynamic, MRCP, ERDS, and PLV analysis over the pre-, post- movement and sustained periods around prominent left, right and central cortical areas in the brain (See Figure 4-2).

				Imaginary		Passive		Real	
Analysis	Type	Cortex	Region	Flexion	Extension	Flexion	Extension	Flexion	Extension
Perceived:	Subjects								**
Dynamics:	Strain	Normalized					**	**	
		Peak					**	**	
	Angle	Normalized				**		**	
		Peak				**		**	
	Velocity	Start					**	**	
		Stop						**	
MRCP:	Somatosensory Cortex		Left	* (start)		* (pre, post)			* (pre,post,sus)
			Central						*(pre, post, sus)
			Right						* (pre,post)
	Pirmary Motor Cortex		Left	* (pre, post)		* (pre, post)			* (pre,post,sus)
			Right						* (pre,post)
	Premotor Cortex		Left			* (start)			* (pre,post,sus)
			Right						* (pre,post)
			Central			* (pre, sus)	* (cue, sus)		
			Right	* (sus)	* (pre)				
	Auditory cotrex		Left			* (start, sus)			
			Right	* (sus)					* (start)
ERDS:	Mu	Somatosensory Cortex	Left	* (ERD, sus)		* (ERD, cue)	* (ERS, pre, post)		
		Pirmary Motor Cortex	Left	* (ERD, sus)					
		Parietal Cortex	Left			* (ERD, start)			* (ERD, sus)
		Visual cortex	Right						* (ERD, start)
	Low-Beta	Premotor Cortex	Central	* (ERD, post)					
		Somatosensory Cortex	left			* (ERD, pre)	* (ERS, post)		
		Primary Visual Cortex	Central				* (ERS, start)		
		Premotor Cortex	Left						* (ERD, pre)
	Midrange-Beta	Somatosensory Cortex	Central					* (ERD, post)	
		Parietal Cortex	Left			* (ERD, start)			
	High-Beta	Somatosensory Cortex	Central			* (ERD, pre)	* (ERS, post)		
			Left			* (ERD, pre)	* (ERS, post)		
		Pirmary Motor Cortex	Central			* (ERD, pre)			
			Left			* (ERD, start)			
		Premotor Cortex	Central						* (ERD, start)
			Left						* (ERD, sus)
PLV:		Somatosensory Cortex	Central	* (10Hz, sus)		* (15Hz, sus)			* (10Hz, sus)
			Left	* (10Hz, sus)	* (18Hz, post)		* (10Hz, sus)	* (33Hz, sus)	
		Pirmary Motor Cortex	Central	* (10Hz, post)					
			Left	* (10Hz, pre-cue)	* (18Hz, post)		* (10Hz, sus)	* (33Hz, sus)	
		Premotor Cortex	Left				* (20Hz, sus)	* (15Hz, start)	
			Right			* (8Hz, sus)		* (8Hz, pre, post)	
		Primary Visual Cortex	Left	* (8Hz, sus)					

6. Discussion

The main findings of this study report that stronger cortical activation was present during active real movements of wrist extension compared to flexion by MRCP and ERDS analysis, performed at subject specific 10% relative muscle force activation. These results confirm previous observations conducted by Yue et al. (2000) on thumb flexion and extension. Corticospinal pathways, sensory pathways and/or structural and possible functional differences in the brain may affect the cortical differences observed between flexion and extension. Other important findings include the relationship observed during passive and motor imaginary movements, as wrist flexion was performed with significantly higher levels of cortical activation, by MRCP and ERDS analysis, when compared to wrist extension. These results seem to be contradictory to prior literature, which indicate that higher cortical activation is present due to flexor muscles being more facilitated or less inhibited by the cortical spinal and sub-cortical motor control systems (Robichaud et al., 2004; Yue et al., 2000).

The motor imaginary and passive results seem to disprove the initial hypothesis (see section 1.1.4), which predicted that higher cortical activation is required for extension, due to the corticospinal and sub-cortical motor control systems of flexor muscles being more facilitating or less inhibiting. Various factors can influence the cortical activation detected for wrist related movements, and may have caused the observed differences during the MRCP, ERDS and PLV analysis. The results are explored in section 6.1, and include the effects of perceived difficulty, strain, angle and EMG. In this chapter, the investigations will be critically discussed. Each investigation type is discussed separately for real, passive and imaginary movements in section 6.1.1, 6.1.2 and 6.1.3 respectively, with each section followed by subsections discussing potential factors that could account for the detected differences. These sections are followed by global wrist flexion and extension differences (which looks at possible effects across all movement types, see section 6.2), validation of existing analysis in section 6.3, and recommendation for future work in section 6.5.

The following objectives are discussed, investigating the corticospinal and neurological differences between flexion and extension of the upper extremities, and their effect on the cortical activation of the brain. These objectives are summarized below:

- Real (active movements) wrist flexion and extension applied at the same relative muscle force activation of 10% MVC.
- Passive (active movements) wrist flexion and extension, investigating the effect of somatosensory (afferent) pathways.
- Motor imaginary wrist flexion and extension, investigating frequency use of movement, without the effect of corticospinal and somatosensory pathway.

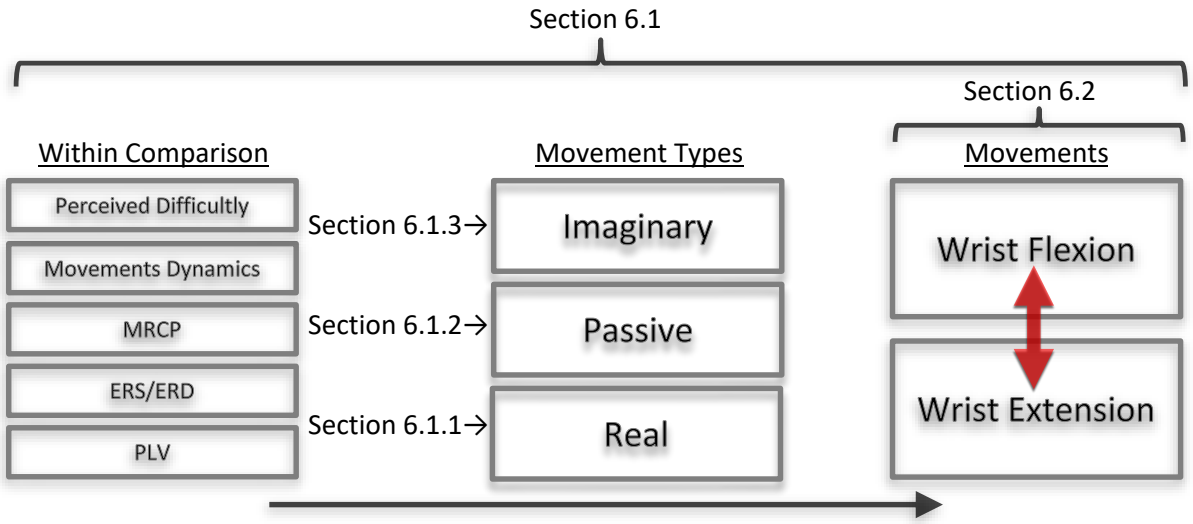

Figure 6-1: Diagram illustrating the flow of the discussion, starting with the different analysis; subject perceived difficulty, movements dynamics, MRCP, ERDS and PLV for each movements type; motor imaginary, passive movements and real movements within comparison between wrist flexion and extension.

The various investigations into motor imaginary, passive movements and real movements between wrist flexion and extension, were associated with differences in the time course analysis for movement dynamics (strain, angle, velocity), MRCP, ERDS and PLV as showed in Figure 6-1.

6.1 Movement specific wrist flexion and extension differences

This section discusses the differences between wrist flexion and extension for real (active) movements, passive (active) movements and motor imaginary movements as illustrated in Figure 6-1.

6.1.1 Real (Active) wrist differences

Significant differences between real (active) wrist flexion and extension are discussed in the below subsection, for movement dynamics, perceived difficulty, MRCP, ERDS and PLV analysis in order to ascertain the effect of relative muscle force activation.

6.1.1.1 Flexion and extension significant results

Stronger cortical activation was reported for voluntary execution of right wrist extension in comparison to wrist flexion (see Figure 5-15), for a similar relative muscle force activation of 10% MVC, applied with the aid of a servo controlled hand device (see section 4.1.2). The calibration of the 10% relative muscle force is apparent in the 10% higher strain output for wrist flexion (see Figure 5-4, left RRWE/F). However, even with subject specific muscle strain calibration, and the effect of gravity accounted for, wrist extension was still perceived to be more difficult to perform by the subject (see Figure 5-2), and wrist flexion was executed with higher level of movement velocity (Figure 5-5).

The MRCP analysis (see section 2.2.1), over the contralateral motor cortex (C3, Figure 5-15) and somatosensory cortex (C1, Figure 5-6, left row) showed significant differences in the sustained movement period with higher level of cortical activation present for wrist extension. These results are

in agreement with previous observations conducted by Yue et al. (2000) on thumb flexion and extension. However, unlike the study by Yue et al. (2000), which consisted of no sustained movement period, and passive returning movement shortly after the initial movements, the MRCP in this investigation shows post movement cortical differences in the sustained movement period with no significant pre-movement differences detected in the contralateral primary motor cortex, somatosensory cortex and premotor area (respectively C1, C3, FC3 – see Figure 5-6). This indicates that there are no differences in movement preparation or planning between either flexion or extension.

Unlike MRCP which shows phase locked responses of cortical neurons, ERD/ERS (see section 2.2.2) shows both phase-locked and no phased locked changes between neurons and interneurons at a particular, frequency component. The ERDS analysis, showed similar results to MRCP in the high-beta band, with significantly higher wrist extension ERD in the sustained movement at the contralateral premotor area (FC3, Figure 5-23 – bottom, right), and in the central premotor cortex around the start movements period (FCz, Figure 5-23 – top, right). The mid-range beta showed significantly lower post movements ERD for wrist flexion around the central somatosensory cortex (CPz, Figure 5-22, right). The low-beta showed significantly lower ERD for wrist extension around the start movement period in the contralateral premotor cortex (FC, Figure 5-21 – top, right). The beta rhythms in the real active movements are associated with muscle contraction for isotonic movements (movements which keep force constant while velocity changes, see section 2.1.2.1). These results are in agreement with finding by Neuper et al. (2006) for left and right hand movements, showing ERD in the primary motor cortex region.

The mu band PLV analysis (see section 2.2.4.1) shows contradictory results to that observed by MRCP and ERDS. Significantly higher levels of cortical phase locking were observed, between the SMA and the left (FC1, Figure 5-29 – bottom, left) and right (FC2, Figure 5-29 – top, right) premotor cortex for wrist flexion in the pre and post movement interval. The central somatosensory cortex showed a significant mu PLV during the sustained movement period with higher PLV for wrist extension (Cpz, Figure 5-29 – bottom, right).

6.1.1.2 Potential factors influencing real flexion extension difference

Based on the above findings a number of factors might have influenced the difference in cortical activation, resulting in greater activation for extension of the wrist, compared to flexion:

i. The angles to which the movements were performed resulted in about a 20˚ greater range of motion in real wrist flexion. This is due to the difference in the voluntary range of motion (ROM) of the wrist during flexion and extension (Delp et al., 1996). However, the firing of the primary motor cortex neurons are only affected by the force of the movement and not the displacement (Kandel et al., 2000). This means the MRCP for real (active) movements will not be affected by the difference in the angle between flexion and extension. However, even if the difference in the angle did affect the cortical activation, this would only be present during the movement interval and would not account for the significant MRCP differences over the sustained period, where higher levels of cortical activation were present for wrist extension.

ii. The rate of change for each movement was not the same. Speed of movement is known to affect the onset of the MRCP (Hiroshi Shibasaki & Hallett, 2006). However, the speed of movement would only account for the difference in the movement period of the wrist and would not explain the MRCP differences in the sustained period, where no movements are performed. Also, higher movement velocity was present for wrist flexion, and not wrist extension. Therefore movement velocity can be eliminated as a cause for the higher cortical activation, by MRCP and ERD/ERS.

iii. The subject perceived movement differences could account for the cortical differences detected. Wrist extension was perceived to be of greater difficulty, even though the relative difference in the muscle force activation was accounted for in each subject. This perceived difficulty difference could explain the cortical differences detected between flexion and extension. However, this could also be due to subject perceiving the difference in strain between the movement, and not due to perceived cortical differences, refer to (iv).

iv. The wrist flexion and extension movements cannot be accomplished with the activation of a single muscle, and groups of muscles are required for each movement. The EMG activation over the extensor muscles during wrist extension is considerably higher compared to the EMG activation over the flexion muscles, during wrist flexion, even though the difference in relative muscle force was accounted for in each subject (refer to APPENDIX E.3 for grand average EMG results). Another observation was that wrist extension required a higher level of sustained EMG activation during the sustained movement period. The difference in muscle force activation could be due to the larger grouping of extensor muscles required when performing wrist extension. The stabilization muscles are also required during the wrist movements, however the effect of these muscles might have been reduced due to the support of the hand device.

v. Sensory information may have affected the cortical activation. However, the hand and surrounding fingers in contact with the hand grip (Refer to APPENDIX C, section C.1.1.2) are in the same position for both flexion and extension of the wrist. No contact was made with the finger tips and no adjustment was made to the hand during either of the two movements for each subject. Under these conditions, a similar level of sensory information to the hand is expected for both wrist flexion and extension.

vi. Visual sensory information could also account for differences in cortical activation. However, the subject's hand was covered and had no visual input from the movement, and had a random interval between movements. Therefore there was minimal influence with the ongoing cortical activity for the movements (Alegre et al., 2002).

6.1.2 Passive wrist differences

Significant differences between passive wrist flexion and extension are discussed in the below subsection for movement dynamics, perceived difficulty, MRCP, ERDS and PLV analysis in order to ascertain the effects of reflex.

6.1.2.1 Flexion and extension significant results

The servo controlled hand device (see section 4.1.2) induced passive wrist flexion and extension, resulting in a significantly higher level of strain for passive extension (Figure 5-4, left RPWE/F). This could indicate higher flexor muscle reflex resistance during passive extension. However, passive extension also showed higher movement velocity (Figure 5-5), and subjects perceived no noticeable differences between passive wrist flexion and extension (Figure 5-2). These results are contradictory to those observed during real wrist flexion and extension.

Strong cortical differences were present between passive movements, showing higher levels of MRCP activation for passive wrist flexion during pre and post movement period over the contralateral somatosensory cortex, primary motor cortex (C3, Figure 5-12, Figure 5-6 – middle row) and pre-motor cortex (FC3, Figure 5-6 – middle row). During passive wrist movements, one would expect flexion and extension to have similar brain activation to real (active) movements. There was also a significantly higher MRCP for wrist flexion during the pre and sustained period at central frontal cortex (Fz, Figure 5-8, middle), which is associated with planning of complex movements (see section 2.1.1). However, the contralateral primary motor cortex activation elicited by passive wrist flexion was significantly higher compared to extension, during pre and post MRCPs. The passive MRCP result showed a greater increase in the Bereitschaftpotential and a negative slope (refer to section 2.2.1) at the start of the passive movement in comparison to real movements.

The passive movements ERS/ERD over the pre and post movements are good indicators of the difference in the cortical activation of the brain (Cassim et al., 2000). The phase synchronization between wrist flexion and extension showed similar results to the MRCP for passive movements around the onset of the movements, with significantly higher levels of high-beta ERD for wrist flexion over the contralateral primary motor cortex. Similar ERD differences were present in the midrange and high beta band for passive movements, displaying significantly higher ERD for passive wrist flexion at the start of the movement in the contralateral primary motor cortex (C3, Figure 5-23-top, middle). However, post movement extension showed a significant ERS in the central somatosensory (Cpz, Figure 5-23-bottom, middle). Significantly higher mu and beta ERS are also present in the post movement period for passive extension over the contralateral somatosensory cortex, which is responsible for processing and association of movements (CP1, Figure 5-19-top, middle & Figure 5-20).

Contradictory PLV results were also observed for passive wrist movements, when compared to MRCP and ERDS analysis. The PLV between contralateral primary motor/somatosensory cortex and SMA (C3, Figure 5-28-top, left) shows significantly higher passive wrist extension in the sustained period (3000ms) mu band. Similar Beta band PLV findings were present between left premotor cortex and SMA (C3, Figure 5-28-bottom, left) during the sustained period and also during the rest period. However, the significant differences were only present for a short period of time, during the mid-

sustained movement period, showing a greater period of significance during the rest period. The rest period difference could be due to cortical phase locking during movement relaxation. Similar PLV result to that observed by ERD/ERS and MRCP where observed between the SMA and central somatosensory processing and association area (CPz, Figure 5-28-bottom, right), showing higher levels of cortical phase locking for passive wrist flexion over the sustained movement period in the beta band.

6.1.2.2 Potential factors influencing passive flexion-extension difference

Based on the above findings, a number of possible reasons could account for the differences detected between passive wrist flexion and extension:

i. One possible explanation for the post movement differences is that the activation of extensors stretch reflexes during passive flexion. The afferent inputs from those muscle spindles are projected to the area in the cortex responsible for the excitation of neurons that produce the contraction of the same muscles (Weiller et al., 1996). This means that passive wrist flexion could cause the activation of sensory areas associated with wrist extension muscle spindles and stretch reflexes. This in turn, will activate the area in the brain that is responsible for execution of that movement, i.e. similar area of the brain that would be activated during voluntary wrist extension is activated during passive flexion. This is apparent in the MRCP results, which show higher levels of post movement activation in the primary motor cortex, premotor cortex and somatosensory cortex from passive wrist flexion. As expected due to reflex, this is opposite to those results observed during real, active wrist movements (see section 6.1.1.2).

ii. Another observation is the strong mu band ERS in the somatosensory cortex. Cassim et al. (2001) showed that ERS activation is not only as a result of termination of movement commands, but can also reflect movement related somatosensory processing. This could indicate that higher levels of sensory feedback (association) is present during passive extension. The higher level of somatosensory processing associated with passive extension, could cause a higher primary motor cortex activation for flexion via the inter-cortical tract (refer to section 2.1.1). This observation supports the explanation in paragraph (i), and also can explain the observed PLV between the SMA and primary motor/somatosensory cortex, which shows significantly higher passive extension during the sustained movement period. This indicates that stronger cortical coupling is present for wrist extension. However, the PLV significant were only present for a short period of time in the mid-sustained movement period, and implies that the cortical phase coupling differences, between passive flexion and extension are not present during the post movement period, as shown by the ERS result.

iii. The difference in the wrist tendon force and position could contribute to the cortical differences observed between flexion and extension in the primary motor cortex. Lieber et al. (1996) showed that the flexor tendon force was two to three times greater than that for wrist extension, indicating that greater resistance is encountered during passive wrist extension from flexor tendons. Higher levels of strain were measured when performing passive wrist extension, which support the observation made by Lieber et al. (1996). Who indicating that higher level movement resistance, caused by flexor tendon was present during passive wrist extension. Therefore, differences in tendon force between the wrist movements may result in an increase in the afferent

feedback (stretch reflex), causing higher levels of cortical activation in the somatosensory cortex. This could be explained by the above results (ii), showing higher levels of mu and beta band contralateral somatosensory cortical ERS for wrist extension. However, this result could also be explained due to a difference in the somatosensory pathway, resulting in sensory feedback being less inhibited for passive extension.

iv. There is a significantly higher movement velocity for wrist extension; therefore one would expect this to indicate least amount of resistance for that movement. However, movement strain is shown to be greatest during passive wrist extension. Which concurs with result observed by Lieber et al. (1996) (see section 3.2.2). This could be due to the difference in the ROM of the movements, with passive flexion having the greater ROM, therefore encountering the least amount of movement resistance and velocity.

v. The pre MRCP and pre ERD differences between passive flexion and extension could be explained as a result of the pre movements cue, in the 0ms – 1000ms epoch period. Similar pre-movement differences were observed in motor imagined movements (see Figure 5-9). However, this is expected due to general preparation for planned movements (see section 2.2.1). The passive movement differences could also be due to general preparation, but this was not expected. Another supporting observation is that passive pre-movement show beta-band ERS around the occipital region (POz, Figure 5-21-bottom, right), indicating that the movements cue, might have caused general preparation for the oncoming passive movement.

vi. PLV is a result of the phase synchronization between different cortical areas, and not as a result of amplitude changes in the brain. Higher levels of mu phase locking are displayed for passive extension between the SMA and contralateral primary motor cortex and premotor cortex in the sustained movement period. However, as illustrated in section 2.1.1, the somatosensory cortex is communicated directly to the primary motor cortex, and the primary motor cortex connected to the SMA. The PLV is calculated between the SMA and primary motor cortex and somatosensory cortex. The PLV result could indicate a difference in coupling for flexion and extension between the SMA and primary motor cortex, due to reflex. Refer to paragraph (ii).

vii. Visual sensory information about the hand position during passive movements could not account for the cortical differences detected, as no visual input of the hand was present during the passive movement study (see section 4.1.1). Experiments were also pseudo-randomised, with a random timing intervals between movements to eliminate anticipation of the passive movements and counterbalancing.

6.1.3 Motor imaginary wrist differences

Significant differences between motor imagined wrist flexion and extension is discussed in the below subsection for perceived difficulty, MRCP, ERDS and PLV analysis in order to investigate the cortical activation without any overt movements. It was observed that motor imaginary movements can produce similar cortical activation to that which would be produced if the movement was real.

6.1.3.1 Flexion and extension significant results

The subjects perceived no difference between motor imaginary wrist flexion and extension (Figure 5-2). As expected, no movements took place during the motor imagery, with no angle (Figure 5-3), strain or EMG (see Appendix E.3.1) activation detected throughout the imaginary investigation.

Significantly higher MRCP for post and pre motor imagined wrist flexion is detected over the contralateral wrist representation areas in the primary motor cortex and somatosensory processing cortex (C1, Figure 5-9). MRCP showed higher extension pre movement cortical activation over the right premotor cortex (FC4, Figure 5-7 left row).

Even though significant MRCP differences were detected, ERD/ERS are the proven techniques for analysis motor imagery (Wolpaw et al., 2002). Higher sustained movement mu band ERD for flexion was present in the contralateral somatosensory cortex and primary motor cortex (C3, Figure 5-19-top, left). Significantly higher low beta post movements ERD for flexion was present around the central premotor cortex (Fcz, Figure 5-21-bottom, left). No significant differences were present for imaginary midrange and high beta ERS/ERD.

Motor imaginary wrist movement PLV show similar activation to motor imagined MRCP and ERDS results. Cortical phase locking between contralateral somatosensory/primary motor cortex (C3, Cz, Figure 5-27-top) and SMA showed higher levels for motor imaginary wrist flexion in the pre, post and sustained movements period.

6.1.3.2 Potential factors influencing motor imaginary flexion and extension difference

Based on the above findings, a number of possible reasons could account for the analytical differences detected between motor imagined wrist flexion and extension:

i. Unlike passive and real movements, motor imaginary wrist movement cortical activation, by MRCP and ERDS analysis, is not affected by force or angle. Subjects also perceived no difference between the motor imagination of wrist flexion or extension, indicating that similar levels of mental concentration were required for both movements.

ii. Frequency of use of a particular movements can affect the motor imagined cortical differences, similar to the effect that may be present during passive and voluntary movements. However, the lack of the effect of afferent and effect pathways, for movements that are more frequently used, result in less cortical activity needed to induce that movement. On the other hand, this would have resulted in higher cortical activation for wrist extension.

iii. Visual sensory information about the hand position during motor imaginary movements could not account for the cortical differences detected, as no visual input was present during the hand movements (see section 4.1.1). Experiment were also pseudo-randomised with a random timing interval between movements to eliminate anticipation and counterbalancing.

6.2 Global wrist flexion and extension differences.

There are a number of factors that could explain the differences detected between wrist flexion and extension for the different movements types. These include the frequency of movements, rate of movements, force of movement, corticospinal pathways and somatosensory pathways, as explored in section 6.1. These factors could also explain why passive and motor imaginary movements give rise to contradictory results to those observed in real active movements, by MRCP, ERDS and PLV. These differences represent structural and possible functional differences in the movement related control systems of the brain.

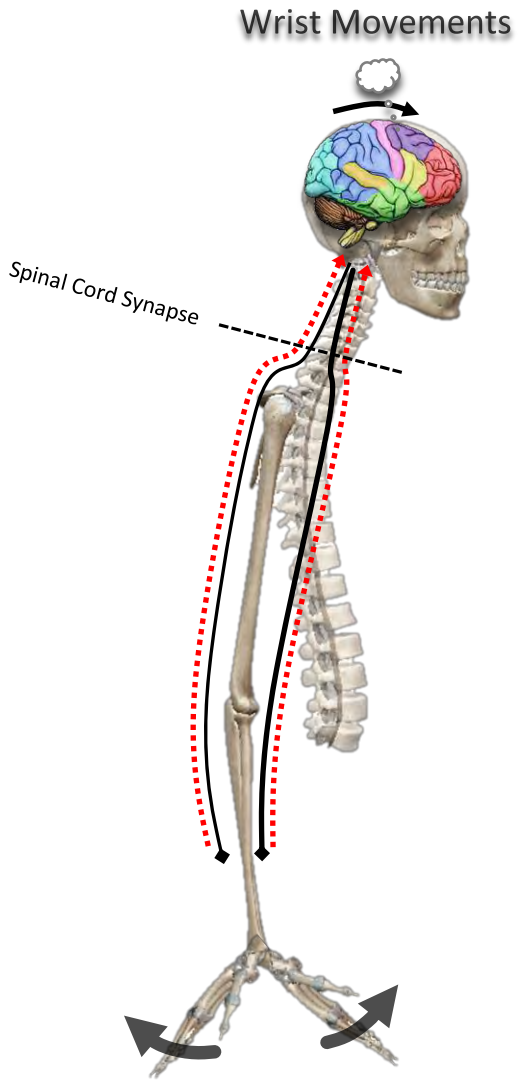

Figure 6-2: Solid lines indicated efferent pathways, for motor control. Dotted lines indicated afferent pathways for sensory feedback.

Each objective looks at a different movement type and its effect on the cortical activation between wrist flexion and extension. The movement types explored were real movements and the effects of relative muscle force activation and efferent and afferent pathways, passive movements and the

effects of reflex and afferent pathways, and motor imaginary movements and the effects of frequency of movement, without the effect of affect and efferent and afferent pathways. As indicated in the above illustration (Figure 6-2), each movement type is a combination of one or more motor systems. Real movements involve efferent, afferent pathways (corticospinal projection) and the cortical aspect. Passive movements are similar to real movements, but are more affected by afferent pathways and reflex stimulation. Motor imaginary movements have no movements and are minimally affected by afferent and efferent pathways.

6.2.1 Unexpected Findings

A number of initial unexpected finding are listed below:

- Passive movements resulted in the reverse flexion and extension cortical difference to those observed in real movements, with higher cortical activation present for flexion movements. Refer to Figure 5-12. However, this could be explained due to reflex, refer to section 6.1.2.2-(i).

- Passive movements had a significant difference in the pre-movements MRCP, showing higher levels of cortical activation for wrist flexion (refer to Figure 5-12). This result is unexpected, as no movements by the hand device occurred prior to the start interval. Refer to section 6.1.2.2-(v).

- Motor imaginary movements resulted opposite differences to those observed in real movements, with higher cortical activation for flexion wrist movements, by mu ERD. Refer to Figure 5-19 top left and by MRCP refer to Figure 5-9.

- Real movements show opposing PLV results, with significantly higher levels of phase synchrony between the SMA and left and right premotor cortex in the pre and post movement intervals. Refer to Figure 5-29.

6.2.2 Involvement of relative muscle force activation

As discussed in section 3.4.3.3, muscle force activation is known to affect the level of cortical activation around the contralateral motor cortex, with an increase in motor unit firing rate, which requires an increase in cortical activation in the cortex area associated with that motor unit (Siemionow & Yue, 2000). Real (active) wrist flexion and extension movements, being performed at 10% subject relative MVC showed significantly higher cortical activation for real wrist extension when compared to real wrist flexion, by MRCP and ERD analysis. This shows that muscle force activation did not play a role in the differences detected between flexion and extension, and indicates that some other factor may influence the cortical activation, such as the corticospinal pathway or/and structural and function differences in the brain and motor control.

These results are in agreement with the findings of Yue et al. (Yue et al., 2000), which show that thumb extension results in higher cortical activation in the brain, by MRCP and fMRI. As a result, the extensors are less facilitated by these systems and a higher level of brain activation may be needed to activate the extensor muscles (Yue et al., 2000).

An important observation is that the subject still perceived real wrist extension to be considerably harder to perform during real movements and the extensor muscles are less extensively used in comparison to flexion. Therefore the CNS could adapt to the more extensively used motor task, making wrist flexion more automatic with less cortical activation (refer to Section 6.2.5).

6.2.3 Involvement of movements rate

As discussed in section 2.2.1 and 2.2.2, the movement rate is known to affect both MRCP and ERD/ERS results. Higher level of MRCP and ERD were observed in the motor cortex for both real and imaginary movements, for an increase in the movement rate (Doležal et al., 2006; Hiroshi Shibasaki & Hallett, 2006). However, this would not apply for real movement, as wrist flexion is shown to have higher level of movement velocity, whereas wrist extension was shown to have higher levels of contralateral primary motor cortex activation, by MRCP (refer to section 6.1.1.2-(ii)). Real wrist flexion also shows higher level of MRCP, throughout the sustained movement period, which would not be affected by the rate of movement.

Motor imagined wrist flexion showed significantly higher MRCP and ERD around the primary motor cortex. Although though all subjects received similar amounts of motor imagined training for both movements and perceived no movement differences (see section 6.2.4), it is unknown if these results were affected by the rate of motor imagination. However, PLV results, which are insensitive to amplitude changes, showed similar observation to ERD and MRCP, with higher level of cortical phase coupling between the SMA and primary motor cortex for motor imagined wrist flexion.

Passive results might have also been affected by the rate of the movements in the primary motor cortex. However, passive extension showed higher movements velocity, whereas passive flexion shows higher levels of cortical activation around the primary motor cortex, by MRCP and ERDS. The effect that this has on passive movements and sensory feedback, remains unclear.

The above observation indicates that movement rate has no effect on real, passive and motor imagined wrist flexion and extension.

6.2.4 Effect of no movement

There was a significant difference in the somatosensory association area (C1, MRCP) for motor imaginary movements, showing similar cortical activation differences to those observed in passive wrist flexion and extension. These motor imaginary movement results are not affected by differences in tendon forces, muscle force activation and/or corticospinal tract, as no movement was performed during the motor imaginary wrist movements. This could indicate that differences in imaginary movements are as a result of cortical differences only. It is also important to note, that unlike the real wrist movements, the subjects perceived no movement difficulty difference between the two passive and imaginary movements (i.e. wrist flexion and extension).

6.2.5 Involvement of frequency of movement

Another possible explanation for the observed result is that wrist flexion movements are performed more frequently (refer to section 3.4.3.1). Due to the greater adaption of flexor muscle in day to day

activities, a higher level of cortical activation could be required for extensor movements (Seitz et al., 1990; Yue et al., 2000). However, passive and imaginary movements resulted in a higher level of cortical activation for flexion wrist movements. The passive movement results could be explained due to afferent pathways and reflex. However, motor imagined movements would be expected to process similar results to those observed in real movement, if the frequency of movements played a role in affecting cortex differences between flexion and extension. This could indicate that the difference detected between flexion and extension are primarily due to corticospinal and/or sensory pathways differences, which can also be affected by frequency of movements. Motor imaginary movements are known to be affected by training. However both movements where trained for the same duration and subjects perceived no difference in difficulty between the flexion and extension movements.

6.2.6 Involvement of reflex and afferent ascending pathways

Similar sensorimotor/primary motor cortex cortical activation (by MRCP, CP1 & C3) was observed during passive and real active movements, around the post-movements period (see Figure 5-18 & Figure 5-6, 1100ms – 1200ms). Passive movements resulted higher levels of cortical activation, which could be due to the different movement types and/or higher levels of movement velocity (see Figure 5-3). However, the opposite wrist flexion and extension cortical differences, by MRCP and beta-band ERD, were observed for passive movements, compared to real active movements. As discussed in section 3.4.2.1, a compelling explanation for the differing results, is the role that stretch reflexes play during passive movements (as discussed in section 6.1.2.2-i & ii). Similar observations were detected by Weiller et al. (1996), when comparing active and passive right elbow flexion-extension movements. Their results showed that coupling exists between the afferent somatosensory inputs and efferent primary cortex motor output, with the SMA retaining a complete somatotopic representation of their own direct somatosensory inputs and corticospinal projection. This somatotopic representation in the SMA could explain the PLV result between the SMA and somatosensory cortex, where significant higher PLV occurred for passive flexion in the post-movement period between the SMA and central somatosensory cortex. PLV is insensitive to the amplitude changes, and only related to the phase changes between two signals (Wei et al., 2007). Therefore the PLV results are insensitive to the motor force and unit firing rate difference between wrist flexion and extension.

The higher sensory feedback association (somatosensory cortex) for extension (refer to section 6.1.2.2-ii & iii), could indicate that extension afferent pathways are more facilitated or less inhibited, in comparison to flexion. One possible explanation is that flexion is more extensively used, resulting in extension afferent reflex pathways to becoming more automatic, in turn resulting in high cortical stimulation. This could indicate that frequency of movements (refer to section 6.2.5), not only affects corticospinal tract, but also the afferent sensory tract, used during reflex and movement control. Due to flexion being more frequently used, extension feedback pathways might also be more frequently used during control of flexion movement. Another possible explanation is that higher levels of passive movement velocity was present during wrist extension, which could have resulted in an increase somatosensory cortical activation (refer to section 6.1.2.2-iv). However, the increase in velocity is due to the difference in angle between the movements.

6.2.7 Involvement of Cortiospinal descending pathways

As discussed in Section 3.4.3.2, corticospinal tracts play an important role in voluntary movements, making them accurate and precisely timed, through the modulation of sensory and motor information, including tactile, visual and proprioceptive information (Kandel et al., 2000; Raptis et al., 2010). The motor neurons can be influenced by corticospinal pathways being facilitated by reflex loop inside the spine (Raptis et al., 2010). There have been many studies showing that higher levels of motor neuron activation is present during extension, due to extension corticospinal pathways being more inhibited and/or less facilitated compared to flexion (Palmer & Ashby, 1992; Yue et al., 2000). Based on the above result, real wrist movements of the upper extremities seem to be affected by differences in the corticospinal pathway to the respective motor neurons, thereby requiring higher levels of cortical activation to perform wrist extension. In this study, rate of movements and muscle force activation have been illuminated as possible reasons for the cortical activation differences detected between real flexion and extension. However, differences in afferent sensory pathways may also play a role in the detected differences.

6.3 Validation of Existing Features

The results for MRCP, ERDS analysis are shown in APPENDIX D and validated with existing knowledge. Different analysis methods are compared with proven waveforms from similar movements. Known features of MRCP waveforms, focusing on the Bereitschaftpotential are reproved to existing findings. Other literature finding for ERDS are validated with waveforms from the existing movement types, followed by the breakdown of the ocular and EMG correction, before and after ERSP waveforms showing the effect of the artifact correction (section D.4). The measurement calibration of the hand device are validated and shown in APPENDIX B. These validations confirm that the analysis and experimental setup used in this study do not contain any fundamental errors, which could have influenced the above investigations.

6.4 Clinical Relevance

Patients suffering from disease or insult, such as stroke, often have some form of motor impairment, resulting in a significant reduction in their gait performance. The most common form of motor impairment is Hemiplegia, in which stroke can affect the corticospinal tracks in the brain. Hemiplegia often results in the paralysis of muscles in the face, arm, leg or trunk on one side of the body, which can affect motor activities such as holding and grasping (Belda-Lois et al., 2011). In order for patients to relearn how to function successfully in a daily capacity, the rehabilitation process often focuses on intensive physical therapy. This can help to minimize motor deficits through the reorganization of neural networks around damaged areas in the brain, due to the mechanisms of neural plasticity. These traditional rehabilitation methods focus on a bottom-top approach, which acts on the physical (bottom) manipulation of motor movements in order to influence the neural systems (top). However, very little is known as to how the neural plasticity mechanisms are established, and rehabilitation is often built on the assumption that practice and training leads to the improvement of skills (Krakauer, 2006). Only through the study of normal neuromuscular pathways and pathological patterns in the brain of healthy individuals (present study), can the mechanism of gait control be clearly understood, making it possible to maximize the recovery of gait related functions after a stroke. Increasingly more researchers are looking into the top-bottom approach in order to define the rehabilitation therapies based on the state of the brain after stroke. The use of neuroimaging techniques to get a deeper understanding into the neurological differences related to movements and their corticospinal pathways could help improve the rehabilitation process in patients suffering from brain injuries. This could help in giving a better understanding of why patients suffering from stroke find it more difficult to relearn movements involving extension of the upper extremities, compared to flexion. The detection of differences in passive movements could also be useful in neuro-feedback brain computer interface (BCI) driven assistive devices, which could be used in stroke rehabilitation for inducing activity-dependent brain plasticity, and in the monitoring of stroke rehabilitation progress.

6.5 Recommendations for future work

Based on the findings and discussion in this section, a number of recommendations can be made for future studies and investigations into the differences between flexion and extension.

6.5.1 Improved Analysis

6.5.1.1 Phase Locking

In many EEG applications and methods, the ability to detect real and imaginary motor movement is still somewhat limited, due to the difficulties in extracting movement rhythms. The difficulty only increases as the movement type becomes finer. In a recent Electrocorticography (ECoG) study for consistent thumb movement, it was concluded that there is a non-linear cross frequency coupling between premotor and primary motor area (Felix Darvas et al., 2009).

Phase Locking Value (PLV – see section 4.2.4.3) and bi-Phase Locking Value (bPLV) are two types of phase synchronization methods. Both methods are important due to the fact that they look at the interaction of frequencies. While bPLV cannot distinguish between single frequency interaction and is not sensitive to crosstalk, PLV can detect harmonic coupling but is blind to cross frequency interaction (F. Darvas et al., 2009). In the current PLV analysis, phase locking was calculated for each frequencies band between the SMA and remaining EEG electrodes, while being insensitive to the non-linear frequency coupling that may occur during wrist movements. Refer to APPENDIX E.2.1.1 for more information on bPLV calculation.

Another disadvantage to the current PLV analysis is that only the interaction between the SMA and remaining locations were calculated. A more intensive approach would be to calculate the PLV between all groups of electrodes. However, this possesses an analytical problem in finding areas of significance. Multivariate phase synchrony coefficient, as shown in APPENDIX E.2, would simplify this problem by showing cortical areas where phase locking with the remaining electrode would be significant. The multivariate phase locking coefficient, showed a large amount of phase locking occurring with the somatosensory cortex during the post-movements period, with a significantly higher level for passive wrist movements (refer to APPENDIX E.2, Figure E-8). These results could possible tie into the ERS somatosensory result observed during passive extension. Future studies into multivariate PLV could help in investigating the differences detected between flexion and extension.

6.5.2 Experimental Improvements

6.5.2.1 Length of Experiment

Due to the large number of movements that each subject need to perform as indicated in section 4.1, it was noted by the participants that the experiments were lengthy. Although the movements were counterbalanced between subjects to decrease the effect of mental fatigue (Appendix A.3) and the subjects were allowed to take breaks if required between movements groups, it would have been ideal to break the experiment up into a number of sessions, to eliminate any possible effect of muscle and mental fatigue.

6.5.2.2 Improved hand device control

Better PID control of the hand device (see APPENDIX C.1.1) movement angle would be ideal during passive movements, keeping the relative angle and movement velocity during wrist flexion and extension the same. This would eliminate any cortical differences that may be present due to differences in the angle and movements velocity between passive wrist flexion and extension. Refer to Section 5.2, Figure 5-3 for the differences in the angle between passive wrist flexion and extension.

6.5.2.3 Movement Feedback

Movement feedback for motor imaginary movement and real active movements would assist the subject in sustaining the movements correctly during the sustained movement period. For motor imaginary movements, contralateral cortical power could be displayed indicating correct movement imagination. This could also be used in the training session. For real active movement, wrist angle could be displayed, requiring the subject to keep the movement at the same relative angle.

7. Conclusion

This study set out to investigate the central nervous system (CNS) differences between wrist flexion and extension of the upper extremities, through the EEG feature analysis of real, passive and motor imagined movements. It was hypothesized that the corticospinal differences between flexion and extension do indeed play a role, with substantially greater cortical activation required during wrist extension. Such an understanding into the neurological and corticospinal differences could help to improve the rehabilitation process by giving a better understanding of why patients suffering from stroke find it more difficult to relearn movements involving extension of the upper extremities in comparison to flexion.

For each movement type a number of observations could be made on the neurological and/or corticospinal difference that may affect the cortical activation present during wrist flexion and extension:

- During real movements the cortical activation was still higher during wrist extension even with relative muscle force being accounted for. This indicated that muscle force activation does not contribute to the neurological differences detected between flexion and extension. However, this does not rule out the effect of corticospinal projection density, movement frequency and/or functional differences.

- Passive movements resulted in the opposite primary motor cortex difference than those detected in real movements. It was theorized that this is due to reflex, activating areas in the motor cortex responsible for opposing the passive movements. However, sensory association area showed higher cortical activation for extension, implying that the extensor somatosensory pathway causes higher cortical activation in the sensory cortex compared to flexion.

- The motor imaginary movements resulted in similar difference to those observed during passive movements. Similar differences to those present during real movement would have been present for imaginary movements if the differences between flexion and extension was due to neurological differences in the brain. This indicates that the cortical differences between real flexion and extension is related to the movement control system pathways.

Therefore, it can be concluded, based on the results and data in the literature, that there is a difference between the cortical muscular and somatosensory pathway used in the cortical control of the upper extremities during flexion and extension movements. Noticeably greater cortical activation is needed to activate to extensor muscles and higher cortical activation is present due to extension sensory feedback, deeming the hypothesis partially valid.

8. References

Alary, F., Doyon, B., Loubinoux, I., Carel, C., Boulanouar, K., Ranjeva, J. P., … Chollet, F. (1998). Event-related potentials elicited by passive movements in humans: characterization, source analysis, and comparison to fMRI. *NeuroImage*, *8*(4), 377–390. http://doi.org/10.1006/nimg.1998.0377

Alegre, M., Labarga, A., Gurtubay, I. G., Iriarte, J., Malanda, A., & Artieda, J. (2002). Beta electroencephalograph changes during passive movements: Sensory afferences contribute to beta event-related desynchronization in humans. *Neuroscience Letters*, *331*(1), 29–32. http://doi.org/10.1016/S0304-3940(02)00825-X

Allefeld, C., & Kurths, J. (2004). An approach to multivariate phase synchronization analysis and its application to event-related potentials. *International Journal of Bifurcation and Chaos*, *14*(2), 417–426. http://doi.org/10.1142/S0218127404009521

Angelaki, D. E., & Bergman, H. (2010). Motor systems. *Current Opinion in Neurobiology*, *20*(6), 687–688. http://doi.org/10.1016/j.conb.2010.09.009

Babiloni, F. (2001). Recognition of imagined hand movements with low resolution surface Laplacian and linear classifiers. *Medical Engineering and Physics*, *23*, 323–328. http://doi.org/10.1016/S1350-4533(01)00049-2

Bai, O., Lin, P., Vorbach, S., Li, J., Furlani, S., & Hallett, M. (2007). Exploration of computational methods for classification of movement intention during human voluntary movement from single trial EEG. *Clinical Neurophysiology*, *118*(12), 2637–2655. http://doi.org/10.1016/j.clinph.2007.08.025

Baker, S. N. (2007). Oscillatory interactions between sensorimotor cortex and the periphery. *Current Opinion in Neurobiology*, *17*(6), 649–655. http://doi.org/10.1016/j.conb.2008.01.007

Behrens, M., Mau-Moeller, A., Wassermann, F., & Bruhn, S. (2013). Effect of Fatigue on Hamstring Reflex Responses and Posterior-Anterior Tibial Translation in Men and Women. *PLoS ONE*, *8*(2). http://doi.org/10.1371/journal.pone.0056988

Belda-Lois, J.-M., Mena-del Horno, S., Bermejo-Bosch, I., Moreno, J. C., Pons, J. L., Farina, D., … Rea, M. (2011). Rehabilitation of gait after stroke: a review towards a top-down approach. *Journal of Neuroengineering and Rehabilitation*, *8*(1), 66. http://doi.org/10.1186/1743-0003-8-66

Brazier, M. A. B. (1963). the History of the Electrical Activity of the Brain As a Method for Localizing Sensory Function. *Medical History*, *7*(3), 199–211. http://doi.org/10.1017/S0025727300028350

Brunner, C., Scherer, R., Graimann, B., Supp, G., & Pfurtscheller, G. (2006). Online control of a brain-computer interface using phase synchronization. *IEEE Transactions on Biomedical Engineering*, *53*(12), 2501–2506. http://doi.org/10.1109/TBME.2006.881775

Byrne, J. H. and Dafny, N. (1997). Neuroscience Online: An Electronic Textbook for the Neurosciences. Retrieved from http://nba.uth.tmc.edu/neuroscience/

C. Büchel, J.T. Coull, K. J. F. (1999). The Predictive Value of Changes in Effective Connectivity for Human Learning. *Science*, *283*(5407), 1538–1541. http://doi.org/10.1126/science.283.5407.1538

Cassim, Ë., Monaca, C. A. C., Szurhaj, W., Bourriez, J.-L., Defebvre, L., Derambure, P., … Cassim, F.

(2001). Does post-movement beta synchronization reflect an idling motor cortex? *Neuroreport*, *12*(17), 3859–3863. http://doi.org/10.1097/00001756-200112040-00051

Cassim, Ë., Szurhaj, W., Sediri, H., Devos, D., Bourriez, J., Poirot, I., … Guieu, J. (2000). Brief and sustained movements : differences in event-related (de) synchronization (ERD / ERS) patterns Franc, *111*, 2032–2039.

Croft, R. J., & Barry, R. J. (2000). Removal of ocular artifact from the EEG: A review. *Neurophysiologie Clinique*, *30*(1), 5–19. http://doi.org/10.1016/S0987-7053(00)00055-1

Dai, T. H., Liu, J. Z., Saghal, V., Brown, R. W., & Yue, G. H. (2001). Relationship between muscle output and functional MRI-measured brain activation. *Experimental Brain Research*, *140*(3), 290–300. http://doi.org/10.1007/s002210100815

Darvas, F., Miller, K. J., Rao, R. P. N., & Ojemann, J. G. (2009). Nonlinear Phase–Phase Cross-Frequency Coupling Mediates Communication between Distant Sites in Human Neocortex. *The Journal of Neuroscience*, *29*(2), 426–435. http://doi.org/10.1523/JNEUROSCI.3688-08.2009

Darvas, F., Ojemann, J. G., & Sorensen, L. B. (2009). Bi-phase locking - a tool for probing non-linear interaction in the human brain. *NeuroImage*, *46*(1), 123–132. http://doi.org/10.1016/j.neuroimage.2009.01.034

Delorme, A., & Makeig, S. (2004). EEGLAB: An open source toolbox for analysis of single-trial EEG dynamics including independent component analysis. *Journal of Neuroscience Methods*, *134*(1), 9–21. http://doi.org/10.1016/j.jneumeth.2003.10.009

Delp, S. L., Grierson, A. E., & Buchanan, T. S. (1996). Maximum isometric moments generated by the wrist muscles in flexion-extension and radial-ulnar deviation. *Journal of Biomechanics*, *29*(10), 1371–1375. http://doi.org/10.1016/0021-9290(96)00029-2

Descarreaux, M., Lafond, D., Jeffrey-Gauthier, R., Centomo, H., & Cantin, V. (2008). Changes in the flexion relaxation response induced by lumbar muscle fatigue. *BMC Musculoskeletal Disorders*, *9*, 10. http://doi.org/10.1186/1471-2474-9-10

Divekar, N. V., & John, L. R. (2013). Neurophysiological, behavioural and perceptual differences between wrist flexion and extension related to sensorimotor monitoring as shown by corticomuscular coherence. *Clinical Neurophysiology*, *124*(1), 136–147. http://doi.org/10.1016/j.clinph.2012.07.019

Doležal, J., Štastný, J., & Sovka, P. (2006). Modelling and recognition of movement related EEG signal. *International Conference on Applied Electronics 2006, AE*, 27–30. http://doi.org/10.1109/AE.2006.4382955

Drouin, C., & Tassin, J.-P. (2002). Encyclopedia of the Human Brain. *Encyclopedia of the Human Brain*, 625–646. http://doi.org/10.1016/B0-12-227210-2/00254-5

Edwards, E. (2007). *Electrocortical Activation and Human Brain Mapping*. ProQuest. Retrieved from http://books.google.co.za/books?id=YV0Zn68UX-YC

Fang, Y., Siemionow, V., Sahgal, V., Xiong, F., & Yue, G. H. (2001). Greater movement-related cortical potential during human eccentric versus concentric muscle contractions. *Journal of Neurophysiology*, *86*(4), 1764–1772. http://doi.org/Article

Ferree, T. C., & Ph, D. (1996). Spline Interpolation of the Scalp EEG. *Electrical Geodesics*, (1990), 1–5. Retrieved from ftp://128.223.180.15/pub/documentation/technotes/SplineInterpolation.pdf\npapers2://publ

ication/uuid/5053BC59-7D7C-46B4-A0A9-D99A0F33D188

Formaggio, E., Storti, S. F., Boscolo Galazzo, I., Gandolfi, M., Geroin, C., Smania, N., … Manganotti, P. (2013). Modulation of event-related desynchronization in robot-assisted hand performance: brain oscillatory changes in active, passive and imagined movements. *Journal of Neuroengineering and Rehabilitation*, *10*(1), 24. http://doi.org/10.1186/1743-0003-10-24

Fründ, I., Busch, N. A., Schadow, J., Körner, U., & Herrmann, C. S. (2007). From perception to action: phase-locked gamma oscillations correlate with reaction times in a speeded response task. *BMC Neuroscience*, *8*, 27. http://doi.org/10.1186/1471-2202-8-27

Geetha, G. (2011). Scrutinizing different techniques for artifact removal from EEG signals. *International Journal of Engineering Science*, *3*(2), 1167–1172.

Geodesics, E., Note, T., Ferree, T. C., & Srinivasan, R. (2000). Theory and Calculation of the Scalp Surface Laplacian. *Electrical Geodesics, Inc*, 1–6.

Gómez-Herrero, G. (2007). Automatic Artifact Removal (AAR) toolbox v1.3 (Release 09.12.2007) for MATLAB. *Technology*, *3*, 1–23. Retrieved from http://www.cs.tut.fi/~gomezher/projects/eeg/aar/aardoc.pdf

Granacher, U., Wolf, I., Wehrle, A., Bridenbaugh, S., & Kressig, R. W. (2010). Effects of muscle fatigue on gait characteristics under single and dual-task conditions in young and older adults. *Journal of Neuroengineering and Rehabilitation*, *7*(1), 56. http://doi.org/10.1186/1743-0003-7-56

Gu, Y., Dremstrup, K., & Farina, D. (2009). Single-trial discrimination of type and speed of wrist movements from EEG recordings. *Clinical Neurophysiology*, *120*(8), 1596–1600. http://doi.org/10.1016/j.clinph.2009.05.006

Gu, Y., Farina, D., Murguialday, A. R., Dremstrup, K., Montoya, P., & Birbaumer, N. (2009). Offline identification of imagined speed of wrist movements in paralyzed ALS patients from single-trial EEG. *Frontiers in Neuroscience*, *3*(AUG), 1–7. http://doi.org/10.3389/neuro.20.003.2009

Gysels, E., & Celka, P. (2004). Phase Synchronization for the Recognition of Mental Tasks in a Brain – Computer Interface. *Rehabilitation*, *12*(4), 406–415.

Hidler, J., Hodics, T., Xu, B., Dobkin, B., & Cohen, L. G. (2006). MR compatible force sensing system for real-time monitoring of wrist moments during fMRI testing. *Journal of Neuroscience Methods*, *155*(2), 300–307. http://doi.org/10.1016/j.jneumeth.2006.01.016

Hyvärinen, A., & Oja, E. (2000). Independent component analysis: Algorithms and applications. *Neural Networks*, *13*(4–5), 411–430. http://doi.org/10.1016/S0893-6080(00)00026-5

James, C. J., & Hesse, C. W. (2005). Independent component analysis for biomedical signals. *Physiological Measurement*, *26*(1), R15-39. http://doi.org/10.1088/0967-3334/26/1/R02

Joyce, C. A., Gorodnitsky, I. F., & Kutas, M. (2004). Automatic removal of eye movement and blink artifacts from EEG data using blind component separation. *Psychophysiology*, *41*(2), 313–325. http://doi.org/10.1111/j.1469-8986.2003.00141.x

Judith Hall, Judith Allanson, Karen Gripp, A. S. (2006). *Handbook of physical measurements - Limbs 8*. *Handbook of Physical Measurements (Oxford Handbook Series)* (2nd ed.). Oxford University Press, USA. Retrieved from http://www.amazon.com/dp/0195301498

Jung, T. P., Makeig, S., Westerfield, M., Townsend, J., Courchesne, E., & Sejnowski, T. J. (2000). Removal of eye activity artifacts from visual event-related potentials in normal and clinical

subjects. *Clinical Neurophysiology*, *111*(10), 1745–1758. http://doi.org/10.1016/S1388-2457(00)00386-2

Jung T., Makeig S., Lee T., McKeown M., Brown G., Bell A., & Sejnowski T. (2000). Independent component analysis of biomedical signals, (1), 224.

Kalcher, J., & Pfurtscheller, G. (1995). Discrimination between phase-locked and non-phase-locked event-related EEG activity. *Electroencephalography and Clinical Neurophysiology*, *94*(5), 381–384. http://doi.org/10.1016/0013-4694(95)00040-6

Kandel, E., Jessel, T., & Schwartz, J. (2000). *Principles of Neural Science*. *McGraw Hill Publishing*. McGraw-Hill, Health Professions Division. Retrieved from http://books.google.co.za/books?id=yzEFK7Xc87YC

Kayser, J., & Tenke, C. E. (2006a). Principal components analysis of Laplacian waveforms as a generic method for identifying ERP generator patterns: II. Adequacy of low-density estimates. *Clinical Neurophysiology*, *117*(2), 369–380. http://doi.org/10.1016/j.clinph.2005.08.033

Kayser, J., & Tenke, C. E. (2006b). Principal components analysis of Laplacian waveforms as a generic method for identifying ERP generator patterns: II. Adequacy of low-density estimates. *Clinical Neurophysiology*, *117*(2), 369–380. http://doi.org/10.1016/j.clinph.2005.08.033

Keinrath, C., Wriessnegger, S., M??ller-Putz, G. R., & Pfurtscheller, G. (2006). Post-movement beta synchronization after kinesthetic illusion, active and passive movements. *International Journal of Psychophysiology*, *62*(2), 321–327. http://doi.org/10.1016/j.ijpsycho.2006.06.001

Kirsch, W., Hennighausen, E., & Rösler, F. (2010). ERP correlates of linear hand movements in a motor reproduction task. *Psychophysiology*, *47*(3), 486–500. http://doi.org/10.1111/j.1469-8986.2009.00952.x

Klados, M. A., Papadelis, C., Braun, C., & Bamidis, P. D. (2011). REG-ICA: A hybrid methodology combining Blind Source Separation and regression techniques for the rejection of ocular artifacts. *Biomedical Signal Processing and Control*, *6*(3), 291–300. http://doi.org/10.1016/j.bspc.2011.02.001

Klados, M. A., Papadelis, C., Lithari, C. D., & Bamidis, P. D. (2008). The removal of ocular artifacts from EEG signals: A comparison of performances for different methods. *IFMBE Proceedings*, *22*, 1259–1263. http://doi.org/10.1007/978-3-540-89208-3_300

Klimesch, W. (1999). EEG alpha and theta oscillations reflect cognitive and memory performance: A review and analysis. *Brain Research Reviews*, *29*(2–3), 169–195. http://doi.org/10.1016/S0165-0173(98)00056-3

Krakauer, J. W. (2006). Motor learning: its relevance to stroke recovery and neurorehabilitation. *Current Opinion in Neurology*, *19*(1), 84–90. http://doi.org/10.1097/01.wco.0000200544.29915.cc

Leocani, L., Toro, C., Manganotti, P., Zhuang, P., & Hallett, M. (1997). Event-related coherence and event-related desynchronization / synchronization in the 10 Hz and 20 Hz EEG during self-paced movements. *Electroencephalography and Clinical Neurophysiology*, *104*, 199–206.

Letier, Pierre A. Schiele, M. Avraam, M. H. and A. P. (2006). Bowden Cable Actuator for Torque-Feedback in Haptic Applications. *Proc. Eurohaptics 2006*, (July).

Letier, P., Avraam, M., Horodinca, M., Schiele, A., & Preumont, A.́. (2006). Survey of Actuation Technologies for Body-Grounded Exoskeletons. *CiteSeerx*.

Lieber, R. L., Amiel, D., Kaufman, K. R., Whitney, J., & Gelberman, R. H. (1996). Relationship between joint motion and flexor tendon force in the canine forelimb. *Journal of Hand Surgery*, *21*(6), 957–962. http://doi.org/10.1016/S0363-5023(96)80299-1

Lotze, M., Braun, C., Birbaumer, N., Anders, S., & Cohen, L. G. (2003). Motor learning elicited by voluntary drive. *Brain*, *126*(4), 866–872. http://doi.org/10.1093/brain/awg079

Lowe, W. (2006). *Orthopedic Assessment In Massage Therapy*. *Orthopedic Assessment in Massage Therapy*. Daviau Scott. Retrieved from http://www.amazon.com/Orthopedic-Assessment-Massage-Therapy-Whitney/dp/0966119630

Martini, F., Marieb, E. N., Wilhelm, P. B., Timmons, M. J., Tallitsch, R. B., & Mallatt, J. (2014). *Human Anatomy*. Pearson. Retrieved from https://books.google.com/books?id=uX8eYgEACAAJ&pgis=1

Mima, T., Sadato, N., Yazawa, S., Hanakawa, T., Fukuyama, H., Yonekura, Y., & Shibasaki, H. (1999). Brain structures related to active and passive finger movements in man. *Brain*, *122*(10), 1989–1997. http://doi.org/10.1093/brain/122.10.1989

Müller, G. R., Neuper, C., Rupp, R., Keinrath, C., Gerner, H. J., & Pfurtscheller, G. (2003). Event-related beta EEG changes during wrist movements induced by functional electrical stimulation of forearm muscles in man. *Neuroscience Letters*, *340*(2), 143–147. http://doi.org/10.1016/S0304-3940(03)00019-3

Müller-Putz, G. R., Kaiser, V., Solis-Escalante, T., & Pfurtscheller, G. (2010). Fast set-up asynchronous brain-switch based on detection of foot motor imagery in 1-channel EEG. *Medical and Biological Engineering and Computing*, *48*(3), 229–233. http://doi.org/10.1007/s11517-009-0572-7

Müller-Putz, G. R., Zimmermann, D., Graimann, B., Nestinger, K., Korisek, G., & Pfurtscheller, G. (2007). Event-related beta EEG-changes during passive and attempted foot movements in paraplegic patients. *Brain Research*, *1137*(1), 84–91. http://doi.org/10.1016/j.brainres.2006.12.052

Muluh, E. T., Vaughan, C. L., & John, L. R. (2011). High resolution event-related potentials analysis of the arithmetic-operation effect in mental arithmetic. *Clinical Neurophysiology*, *122*(3), 518–529. http://doi.org/10.1016/j.clinph.2010.08.008

Nashmi, R., Mendon??a, A. J., & MacKay, W. A. (1994). EEG rhythms of the sensorimotor region during hand movements. *Electroencephalography and Clinical Neurophysiology*, *91*(6), 456–467. http://doi.org/10.1016/0013-4694(94)90166-X

Netter, F. H. (2003). *Atlas of human anatomy*. *Exp Neurol* (Vol. 97). http://doi.org/10.1017/CBO9781107415324.004

Neuper, C., Scherer, R., Reiner, M., & Pfurtscheller, G. (2005). Imagery of motor actions: Differential effects of kinesthetic and visual-motor mode of imagery in single-trial EEG. *Cognitive Brain Research*, *25*(3), 668–677. http://doi.org/10.1016/j.cogbrainres.2005.08.014

Neuper, C., W??rtz, M., & Pfurtscheller, G. (2006). Chapter 14 ERD/ERS patterns reflecting sensorimotor activation and deactivation. *Progress in Brain Research*, *159*, 211–222. http://doi.org/10.1016/S0079-6123(06)59014-4

Niazi, I. K., Jiang, N., Tiberghien, O., Nielsen, J. F., Dremstrup, K., & Farina, D. (2011). Detection of Movement Intention from Single-Trial Movement-Related Cortical Potentials. *Journal of Neural Engineering*, *8*(6), 66009. http://doi.org/10.1088/1741-2560/8/6/066009

Nicolas-Alonso, L. F., & Gomez-Gil, J. (2012). Brain computer interfaces, a review. *Sensors*, *12*(2),

1211–1279. http://doi.org/10.3390/s120201211

Palmer, E., & Ashby, P. (1992). Corticospinal projections to upper limb motoneurones in humans. *The Journal of Physiology*, *448*, 397–412. http://doi.org/10.1113/jphysiol.1992.sp019048

Pereda, E., Quiroga, R. Q., & Bhattacharya, J. (2005). Nonlinear multivariate analysis of neurophysiological signals. *Progress in Neurobiology*, *77*(1–2), 1–37. http://doi.org/10.1016/j.pneurobio.2005.10.003

Pfurtscheller, G., Brunner, C., & Lopes da Silva, F. H. (2006). Mu rhythm (de)synchronization and EEG single-trial classification of different motor imagery tasks. *NeuroImage*, *31*(1), 153–159. http://doi.org/10.1016/j.neuroimage.2005.12.003

Pfurtscheller, G., Brunner, C., & Lopes da Silva, F. H. (2006). Mu rhythm (de)synchronization and EEG single-trial classification of different motor imagery tasks. *NeuroImage*, *31*(1), 153–159. http://doi.org/10.1016/j.neuroimage.2005.12.003

Pfurtscheller, G., Linortner, P., Winkler, R., Korisek, G., & Müller-Putz, G. (2009). Discrimination of motor imagery-induced EEG patterns in patients with complete spinal cord injury. *Computational Intelligence and Neuroscience*, *2009*. http://doi.org/10.1155/2009/104180

Pfurtscheller, G., & Lopes Da Silva, F. H. (1999). Event-related EEG/MEG synchronization and desynchronization: Basic principles. *Clinical Neurophysiology*, *110*(11), 1842–1857. http://doi.org/10.1016/S1388-2457(99)00141-8

Pfurtscheller, G., Neuper, C., Brunner, C., & Lopes Da Silva, F. (2005). Beta rebound after different types of motor imagery in man. *Neuroscience Letters*, *378*(3), 156–159. http://doi.org/10.1016/j.neulet.2004.12.034

Pfurtscheller, G., Neuper, C., Flotzinger, D., & Pregenzer, M. (1997). EEG-based discrimination between imagination of right and left hand movement. *Electroencephalography and Clinical Neurophysiology*, *103*(6), 642–651. http://doi.org/10.1016/S0013-4694(97)00080-1

Quyen, M. L. Van, Foucher, J., Lachaux, J., Rodriguez, E., Lutz, A., Martinerie, J., & Varela, F. J. (2001). Comparison of Hilbert transform and wavelet methods for the analysis of neuronal synchrony. *Journal of Neuroscience Methods*, *111*, 83–98.

Rapid Prototyping for Microcontrollers | mbed. (n.d.). Retrieved from http://mbed.org/

Raptis, H., Burtet, L., Forget, R., & Feldman, A. G. (2010). Control of wrist position and muscle relaxation by shifting spatial frames of reference for motoneuronal recruitment: possible involvement of corticospinal pathways. *The Journal of Physiology*, *588*(Pt 9), 1551–70. http://doi.org/10.1113/jphysiol.2009.186858

Robichaud, J. A., Pfann, K. D., Comella, C. L., Brandabur, M., & Corcos, D. M. (2004). Greater impairment of extension movements as compared to flexion movements in Parkinson's disease. *Experimental Brain Research*, *156*(2), 240–254. http://doi.org/10.1007/s00221-003-1782-0

Sanei, S., & Chambers, J. a. (2007). *EEG Signal Processing*. *John Wiley &Sons*. Wiley-Interscience. http://doi.org/10.1002/9780470511923

Schneider, C., Lavoie, B. a, Barbeau, H., & Capaday, C. (2004). Timing of cortical excitability changes during the reaction time of movements superimposed on tonic motor activity. *Journal of Applied Physiology (Bethesda, Md. : 1985)*, *97*(6), 2220–2227. http://doi.org/10.1152/japplphysiol.00542.2004

Seitz, R. J., Roland, E., Bohm, C., Greitz, T., & Stone-Elander, S. (1990). Motor learning in man: a positron emission tomographic study. *Neuroreport*, *1*(1), 57–60.

Seki, K., & Fetz, E. E. (2012). Gating of Sensory Input at Spinal and Cortical Levels during Preparation and Execution of Voluntary Movement. *Journal of Neuroscience*, *32*(3), 890–902. http://doi.org/10.1523/JNEUROSCI.4958-11.2012

Shibasaki, H., Barrett, G., Halliday, E., & Halliday, A. M. (1980). Cortical potentials following voluntary and passive finger movements. *Electroencephalography and Clinical Neurophysiology*, *50*(3–4), 201–2013. http://doi.org/10.1016/0013-4694(80)90147-9

Shibasaki, H., & Hallett, M. (2006). What is the Bereitschaftspotential? *Clinical Neurophysiology*, *117*(11), 2341–2356. http://doi.org/10.1016/j.clinph.2006.04.025

Siemionow, V., & Yue, G. H. (2000). Relationship between motor activity-related cortical potential and voluntary muscle activation. *Medicine*, 303–311.

Siemionow, V., Yue, G. H., Ranganathan, V. K., Liu, J. Z., & Sahgal, V. (2000). Relationship between motor activity-related cortical potential and voluntary muscle activation. *Experimental Brain Research. Experimentelle Hirnforschung. Experimentation Cerebrale*, *133*(3), 303–311. http://doi.org/10.1007/s002210000382

Slobounov, S., Chiang, H., Johnston, J., & Ray, W. (2002). Modulated cortical control of individual fingers in experienced musicians: An EEG study. *Clinical Neurophysiology*, *113*(12), 2013–2024. http://doi.org/10.1016/S1388-2457(02)00298-5

Slobounov, S., Hallett, M., & Newell, K. M. (2004). Perceived effort in force production as reflected in motor-related cortical potentials. *Clinical Neurophysiology*, *115*(10), 2391–2402. http://doi.org/10.1016/j.clinph.2004.05.021

Song, L., & Epps, J. (2006). Improving Separability of Eeg Signals During Motor Imagery With An Efficient Circular Laplacian. *2006 IEEE International Conference on Acoustics Speed and Signal Processing Proceedings*, (2), II-1048-II-1051. http://doi.org/10.1109/ICASSP.2006.1660526

Spiegler, A., Graimann, B., & Pfurtscheller, G. (2004). Phase coupling between different motor areas during tongue-movement imagery. *Neuroscience Letters*, *369*(1), 50–54. http://doi.org/10.1016/j.neulet.2004.07.054

Stancák, A. (2000). The electroencephalographic β synchronization following extension and flexion finger movements in humans. *Neuroscience Letters*, *284*(1–2), 41–4. Retrieved from http://www.sciencedirect.com/science/article/pii/S0304394000009538

Stancak, A., Riml, A., & Pfurtscheller, G. (1997). The effects of external load on movement-related changes\rof the sensorimotor EEG rhythms. *Electroencephalogr Clin Neurophysiol*, *102*, 495–504.

Tenke, C. E., & Kayser, J. (2012). Generator localization by current source density (CSD): implications of volume conduction and field closure at intracranial and scalp resolutions. *Clinical Neurophysiology : Official Journal of the International Federation of Clinical Neurophysiology*, *123*(12), 2328–45. http://doi.org/10.1016/j.clinph.2012.06.005

Thatcher, R. W., Biver, C. J., & North, D. M. (2004). EEG and Brain Connectivity: A Tutorial . *Bio-Medical.Com*, 110. Retrieved from http://bio-medical.com/media/support/dynbi.pdf\npapers2://publication/uuid/0E63543D-6BA4-430C-B16D-E8BE67294CCE

Thickbroom, G. W., Byrnes, M. L., & Mastaglia, F. L. (2003). Dual representation of the hand in the cerebellum: Activation with voluntary and passive finger movement. *NeuroImage*, *18*(3), 670–674. http://doi.org/10.1016/S1053-8119(02)00055-1

Vuckovic, A., & Sepulveda, F. (2008a). Delta band contribution in cue based single trial classification of real and imaginary wrist movements. *Medical and Biological Engineering and Computing*, *46*(6), 529–539. http://doi.org/10.1007/s11517-008-0345-8

Vuckovic, A., & Sepulveda, F. (2008). Quantification and visualisation of differences between two motor tasks based on energy density maps for brain-computer interface applications. *Clinical Neurophysiology*, *119*(2), 446–458. http://doi.org/10.1016/j.clinph.2007.10.015

Wahba, G., & Wendelberger, J. (1980). Some new mathematical methods for variational objective analysis using splines and cross validation. *Monthly Weather Review*, *108*(8), 1122–1143. http://doi.org/10.1175/1520-0493(1980)108<1122:SNMMFV>2.0.CO;2

Wang, Y., Hong, B., Gao, X., & Gao, S. (2006). Phase synchrony measurement in motor cortex for classifying single-trial EEG during motor imagery. *Annual International Conference of the IEEE Engineering in Medicine and Biology - Proceedings*, 75–78. http://doi.org/10.1109/IEMBS.2006.259673

Wasaka, T., Nakata, H., Kida, T., & Kakigi, R. (2005). Gating of SEPs by contraction of the contralateral homologous muscle during the preparatory period of self-initiated plantar flexion. *Cognitive Brain Research*, *23*(2–3), 354–360. http://doi.org/10.1016/j.cogbrainres.2004.11.002

Wei, Q., Wang, Y., Gao, X., & Gao, S. (2007). Amplitude and phase coupling measures for feature extraction in an EEG-based brain-computer interface. *Journal of Neural Engineering*, *4*(2), 120–129. http://doi.org/10.1088/1741-2560/4/2/012

Weiller, C., Jüptner, M., Fellows, S., Rijntjes, M., Leonhardt, G., Kiebel, S., … Thilmann, a F. (1996). Brain representation of active and passive movements. *NeuroImage*, *4*(2), 105–110. http://doi.org/10.1006/nimg.1996.0034

Williams, E. R., Soteropoulos, D. S., & Baker, S. N. (2009). Coherence between motor cortical activity and peripheral discontinuities during slow finger movements. *Journal of Neurophysiology*, *102*(2), 1296–1309. http://doi.org/10.1152/jn.90996.2008

Wojtys, E. M., Wylie, B. B., & Huston, L. J. (1996). The effects of muscle fatigue on neuromuscular function and anterior tibial translation in healthy knees. *The American Journal of Sports Medicine*, *24*(5), 615–621. http://doi.org/10.1177/036354659602400509

Wolpaw, J., Birbaumer, N., McFarland, D. J., Pfurtscheller, G., & Vaughan, T. M. (2002). Brain Computer Interfaces for communication and control. *Clinical Neurophysiology*, *113*, 767–791. http://doi.org/10.3389/conf.fnins.2010.05.00007

Yue, G. H., Liu, J. Z., Siemionow, V., Ranganathan, V. K., Ng, T. C., & Sahgal, V. (2000). Brain activation during human finger extension and flexion movements. *Brain Research*, *856*(1–2), 291–300. Retrieved from http://www.ncbi.nlm.nih.gov/pubmed/10677638

Zhou, Z., Wan, B., Ming, D., & Qi, H. (2010). A novel technique for phase synchrony measurement from the complex motor imaginary potential of combined body and limb action. *Journal of Neural Engineering*, *7*(4), 46008. http://doi.org/10.1088/1741-2560/7/4/046008

Zopf, R., Giabbiconi, C. M., Gruber, T., & Müller, M. M. (2004). Attentional modulation of the human somatosensory evoked potential in a trial-by-trial spatial cueing and sustained spatial attention

task measured with high density 128 channels EEG. *Brain Research. Cognitive Brain Research*, *20*(3), 491–509. http://doi.org/10.1016/j.cogbrainres.2004.02.014

APPENDIX A - **SUBJECT INFORMATION**

A.1 Subject Consent Form

Definitions

Electrodes: Small metal caps placed on the skin to measure bio-electrical signals.

Surface Electromyography (sEMG): Study of bio-electrical signals which can be measured with electrodes on the skin surface near a muscle and represent the muscles activity.

Electroencephalography (EEG): Study of bio-electrical signals which can be measured on the scalp by electrodes and which are representative of cortical activity.

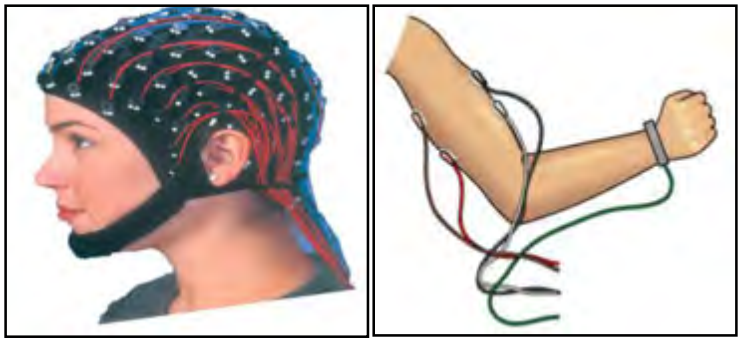

Figure 5: High Resolution EEG cap (Left), EMG recording from muscles (Right)

Informed consent

Researchers at the MRC/UCT Medical Imaging Research Unit are developing a brain computer interface. Brain and muscle function would be measured by recording high resolution electroencephalographic (EEG) and electromyographic (EMG) waveforms from participants whilst they are required to perform or imagine a series of hand movements. Both EEG and EMG are safe non-invasive recording techniques that require the placement of a net of sponge covered electrodes on the head of a participant for EEG, and the placement of disposable electrodes on the forearm for EMG.

Testing procedure

All testing will be carried out at the UCT Faculty of Health Sciences, and has been pre-approved by the Human Ethics committee. You will be required to wash your hair with shampoo prior to testing. For good electrical conductivity, your skin will be first cleaned with alcohol; this causes miniscule discomfort, if any. Electrodes will be covered with a layer of conducting gel; this causes no discomfort. Participants will be seated in a chair facing a computer monitor, and will be fitted with a high resolution EEG net (see Figure 5 left) and EMG electrodes (see Figure 5 right). A series of instructions for real and imagined movement will be presented on a computer screen. Testing should take approximately 1 hour. You will be paid R50 on successful completion of the recording. There will be no direct benefit to participating subjects but the results of the research will be used to further develop a brain-computer interface that will be used to assist the medically disabled.

Possible risks associated with participation

The EEG and EMG equipment is inherently safe. Temporary mild skin sensitivity may result from the salt solution used with the electrode sponge. In the unlikely case of any subject experiencing discomfort, the subject should alert the investigator. The University of Cape Town has a public liability cover should some unforeseen event occur whilst you are participating in this study

Statement of understanding and consent

I confirm that I am over 18 years of age, and the exact procedure and techniques and the possible complications of the above tests have been thoroughly explained to me. I am free to withdraw from the study at any time should I choose to do so. I understand that I may not go through with the testing procedure if I suffer from epilepsy of any kind, and may ask questions at any time during the testing procedure. I know that the personal information required by the researchers and derived from the testing procedure will remain strictly confidential and will only be revealed as a number in classification analysis. I have carefully read this form and understand the nature, purpose and procedures of this study. I agree to participate in this research project conducted by the MRC/UCT Medical Imaging Research Unit.

Subject Information Sheet

Name of volunteer / guardian (if necessary):_____

Signature:_____

Name of investigator:_____

Signature:_____

Date:_____

Research Team

Principal Investigator: Dr LR John (Lecturer, UCT)

Co-Investigators: Mr S. Stoeckigt (MSc (Med) (BME) student, UCT)

Contact details:

Principal Investigator contact:	UCT Research Ethics Committee contact:
Lester John, BScEng, PhD Electronic & Biomedical Engineer MRC/UCT Medical Imaging Research Unit Department of Human Biology Faculty of Health Sciences University of Cape Town Observatory 7925 South Africa Tel: +27 21 406-6548 Fax: +27 21 448-7226 Lester.John@uct.ac.za http://www.uct.ac.za/departments/humanbio	UCT Research Ethics Committee Health Sciences Faculty E53 Room 44.1 Old Main Building Groote Schuur Hospital Observatory 7925 South Africa Tel: +27 21 406-6338 Fax: +27 21 406-6411 Sumayah.Ariefdien@uct.ac.za

A.2 Ethics Approval

UNIVERSITY OF CAPE TOWN
Faculty of Health Sciences
Human Research Ethics Committee

Room E52-24 Old Main Building
Groote Schuur Hospital
Observatory 7925
Telephone [021] 406 6338 • **Facsimile** [021] 406 6411
Email: lamees.emjadi@uct.ac.za
Website: www.health.uct.ac.za/fhs/research/humanethics/forms

18 March 2015

HREC REF: 465/2009

Dr L John
Human Biology
Anatomy Building

Dear Dr John

PROJECT TITLE: TOWARDS A COHERENCE-BASED SENSORIMOTOR BRAIN-COMPUTER INTERFACE (MMED CANDIDATE STEFAN STOECKIGT)

Thank you for submitting your study to the Faculty of Health Sciences Human Research Ethics Committee for review.

The HREC approved the above-study until **30 November 2010.** The HREC notes that the above-study has been completed.

We acknowledge that the following MMed Candidate Stefan Stoeckigt was also involved in the above-mentioned study.

Please note that the ongoing ethical conduct of the study remains the responsibility of the principal investigator.

Please quote the HREC reference no in all your correspondence.

Yours sincerely

Signed by candidate

PROFESSOR M BLOCKMAN
CHAIRPERSON, FHS HUMAN ETHICS

A.3 Experimental Information

Thirteen right handed male subjects' ages ranged from 24 to 30 years old, with a mean age of 25ys were used in the experiments (Table A-1).

Table A-1: Experimental subject age

Subjects	Age
S1	24
S2	24
S3	22
S4	25
S5	23
S6	26
S7	25
S8	25
S9	24
S10	26
S11	27
S12	28
S13	30
S14	26
S15	27
Mean	25.46667
SD	2.030717

A.3.1 Experimental Order

In order to prevent counter balancing the experimental groups order is pseudo randomized. The experimental groups are represented in Table A-2, for each of the 15 subjects. Each of the three movement types are broken up into three groups. Each movements group consists of 20 wrist flexion and 20 wrist extension movements in a random order. The random order of the wrist flexion and extension is not pseudo randomized.

Table A-2: Pseudo randomization order of the movement type for each subject.

Subjects	Movement Type Pseudo Randomization Order →								
S1	Imaginary	Real	Real	Imaginary	Real	Passive	Imaginary	Passive	Passive
S2	Imaginary	Real	Imaginary	Real	Passive	Passive	Imaginary	Passive	Real
S3	Imaginary	Real	Passive	Imaginary	Passive	Passive	Imaginary	Real	Real
S4	Real	Imaginary	Passive	Real	Imaginary	Passive	Passive	Real	Imaginary
S5	Real	Imaginary	Real	Imaginary	Passive	Imaginary	Passive	Passive	Real
S6	Real	Passive	Imaginary	Passive	Imaginary	Real	Passive	Real	Imaginary
S7	Passive	Imaginary	Passive	Imaginary	Real	Passive	Real	Real	Imaginary
S8	Passive	Imaginary	Real	Imaginary	Real	Imaginary	Passive	Passive	Real
S9	Passive	Real	Imaginary	Real	Imaginary	Imaginary	Passive	Real	Passive
S10	Real	Passive	Real	Passive	Imaginary	Passive	Imaginary	Real	Imaginary
S11	Real	Passive	Real	Imaginary	Passive	Passive	Imaginary	Imaginary	Real
S12	Real	Imaginary	Passive	Imaginary	Real	Passive	Real	Passive	Imaginary
S13	Passive	Real	Imaginary	Real	Real	Imaginary	Passive	Passive	Imaginary
S14	Passive	Imaginary	Real	Passive	Passive	Real	Imaginary	Imaginary	Real
S15	Passive	Real	Passive	Real	Passive	Real	Imaginary	Imaginary	Imaginary

A.3.2 Maximum Voluntary Contraction

The Maximum Voluntary Contraction (MVC) results for all thirteen subjects, performing 100%, 70%, 50%, 30% and then again 100% of perceived MVC for wrist flexion and extension is given in Table A-3. The maximum force output is used for the 10% MVC calibration of the hand device for flexion and extension.

Table A-3: Maximum voluntary contraction (MVC) value for the first 100% MVC, 70% MVC, 50% MVC, 30% MVC and end 100% MVC for the real flexion and extension movements.

Subjects		MVC (Nm)	70% MVC (Nm)	50% MVC (Nm)	30% MVC (Nm)	MVC (Nm)	Max MVC (Nm)
S1	Flexion	9.03	5.55	4.26	2.89	11.03	11.03
	Extension	-4.58	-2.40	-2.08	-1.25	-6.47	-6.47
S2	Flexion	18.16	11.22	10.36	6.66	15.84	18.16
	Extension	-8.62	-7.80	-6.80	-6.38	-11.57	-11.57
S3	Flexion	9.74	5.37	2.98	3.05	7.77	9.74
	Extension	-7.42	-3.97	-2.69	-1.77	-5.73	-7.42
S4	Flexion	7.65	2.48	0.99	0.20	9.43	9.43
	Extension	-7.80	-5.73	-3.97	-3.34	-8.99	-8.99
S5	Flexion	5.80	2.77	2.84	2.53	5.27	5.80
	Extension	-4.49	-2.34	-2.52	-1.52	-4.10	-4.49
S6	Flexion	13.99	8.26	6.28	3.42	12.32	13.99
	Extension	-6.84	-4.65	-3.15	-2.27	-5.34	-6.84
S7	Flexion	12.42	5.66	4.07	3.27	9.50	12.42
	Extension	-6.60	-3.03	-2.56	-1.64	-8.18	-8.18
S8	Flexion	11.66	5.88	4.74	4.09	12.31	12.31
	Extension	-8.35	-5.68	-4.49	-3.69	-8.65	-8.65
S9	Flexion	6.35	5.46	2.96	1.73	6.16	6.35
	Extension	-6.32	-4.16	-3.91	-2.40	-5.26	-6.32
S10	Flexion	9.99	7.03	5.24	3.78	12.21	12.21
	Extension	-6.45	-3.78	-2.30	-1.64	-6.32	-6.45
S11	Flexion	19.66	7.77	3.95	1.85	15.72	19.66
	Extension	-5.80	-4.03	-2.69	-1.90	-6.79	-6.79
S12	Flexion	6.35	3.09	2.78	2.16	5.30	6.35
	Extension	-5.48	-3.28	-2.59	-2.02	-5.66	-5.66
S13	Flexion	6.78	2.53	1.53	0.50	2.90	6.78
	Extension	-4.35	-2.40	-1.71	-0.87	-5.65	-5.65
S14	Flexion	9.80	4.75	2.66	1.42	8.24	9.80
	Extension	-4.87	-2.46	-2.21	-1.39	-4.10	-4.87
S15	Flexion	12.21	6.81	5.65	3.01	15.84	15.84
	Extension	-10.92	-4.05	-3.70	-2.27	-9.18	-10.92

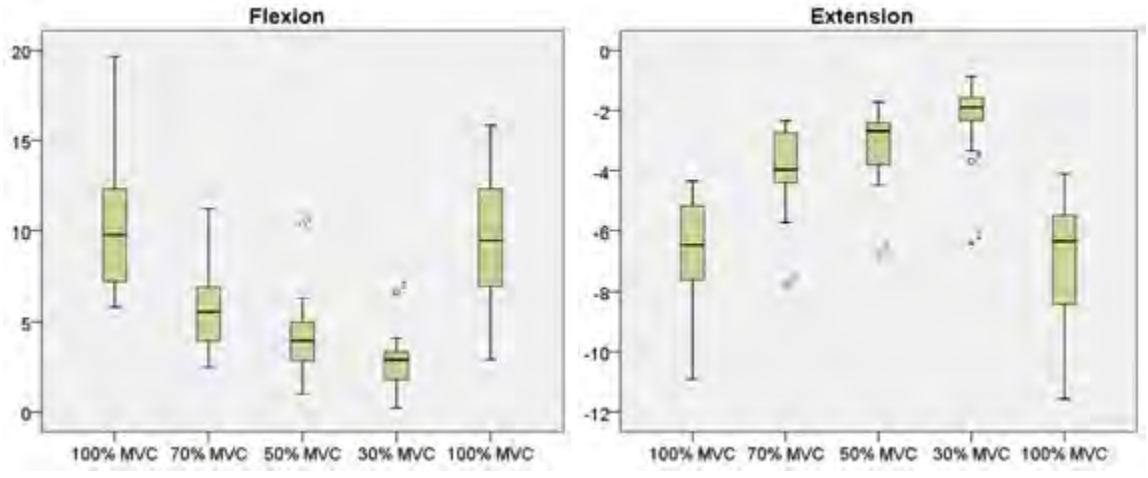

Figure A-1: Flexion and Extension, Maximum Voluntary Contraction (MVC) over all subjects.

A.3.3 Subjects Perceived Difficulty

The subjects were asked to rate each of the different movements types on a scale from 1-10, where 1 represents easy to perform, and 10 represents difficult to perform (**Table A-4**). The subjects were then asked again to rate the different movements types, by selecting whether one movement was harder than the other, or if they were equal in difficulty (Neutral). These results were used as a check, to insure that the rating score was in agreement.

Table A-4: Subject perceived difficulty, comparing wrist flexion and extension for each of the different movement types (Real, Passive and Imaginary movements). Including the perceived difficulty rated from 0-10 (Right column).

Subjects		Flexion	Neutral	Extension	Flexion	Extension
	Real		✓		3	3
S1	Passive	✓			6	3
	Imaginary	✓			6	4
	Real			✓	2	4
S2	Passive		✓		1	1
	Imaginary			✓	1	1
	Real			✓	4	6
S3	Passive			✓	2	3
	Imaginary		✓		1	1
	Real		✓		2	3
S4	Passive	✓			4	3
	Imaginary		✓		4	5
	Real			✓	2	6
S5	Passive	✓			5	3
	Imaginary	✓			7	3
	Real		✓		3	3
S6	Passive	✓			2	1
	Imaginary		✓		2	2
	Real			✓	3	6
S7	Passive		✓		2	2
	Imaginary		✓		3	3
	Real			✓	4	5
S8	Passive		✓		2	2
	Imaginary			✓	2	3
	Real			✓	2	5
S9	Passive		✓		2	2
	Imaginary		✓		7	7
	Real		✓		1	1
S10	Passive	✓			1	1
	Imaginary		✓		8	8
	Real	✓			2	3
S11	Passive		✓		6	4
	Imaginary	✓			7	7
	Real			✓	3	5
S12	Passive			✓	3	6
	Imaginary		✓		3	3
	Real			✓	5	7
S13	Passive	✓			6	5
	Imaginary		✓		8	8
	Real			✓	6	8
S14	Passive			✓	6	9
	Imaginary		✓		5	5
	Real			✓	1	2
S15	Passive			✓	1	6
	Imaginary		✓		5	5

A.4 Peak Frequencies

A.4.1 Power Spectrum Density

Power Spectrum Density (PSD) will be applied to the CSD EEG data to extract frequencies of interest before calculating ERS/ERD. The PSD was calculated using EEGLAB spectopo function using the pwelch method (Delorme & Scott Makeig, 2004). The PSD for each of the six movement types are represented in Figure A-2, for subject 7 over channel E31. The peak frequencies for each subject and each movement type (RRWE, RRWF, RIWE, RIWF, RPWE, RPWF) is represented in Table A-5. The peak frequencies average over all subjects is represented in Table A-5, for all movements.

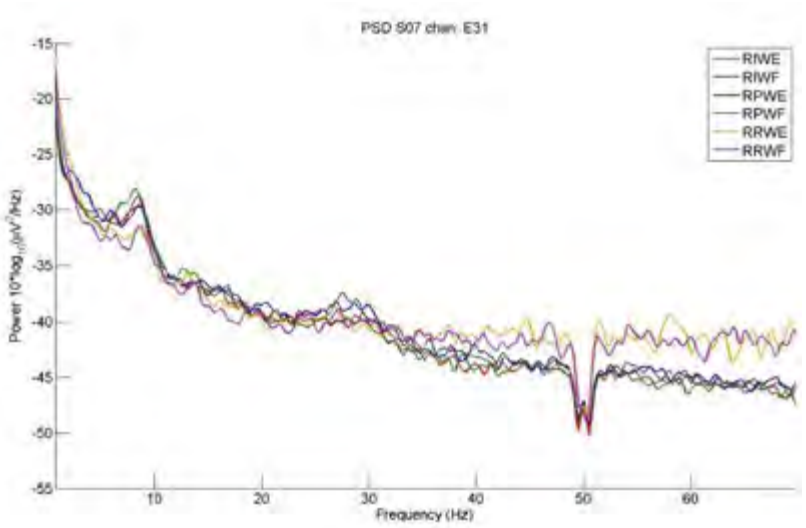

Figure A-2: Power Spectral density of Subject 7 channel E37 (C3) for all the movements. RIWE = Imaginary right wrist Extension; RIWF = Imaginary right wrist flexion; RPWE = Passive right wrist extension; RPWF = Passive right wrist flexion; RRWE = Real right wrist extension; RRWF = real right wrist flexion.

The peak PSD frequencies are isolated over all channels for each movement type and grouped into bins for each of the EEG rhythms; Delta (0.1-4Hz), Theta (4-7Hz), Alpha (8-12Hz), mu (8-13Hz), Beta (13-30Hz), Low-Beta (12.5-16Hz), Midrange-Beta (16.5-20Hz), High-Beta (20.5-28Hz), Gamma-Low (30-48Hz) and Gamma-High (52-70Hz). The histogram for all the EEG rhythms is represented in Figure A-3. Each colour illustrates a different EEG rhythms, and the peak bin in each rhythms represents the most prominent frequency for that subject and movement. These peak frequencies are box plotted in Figure A-4, aver all thirteen subjects and six movements types.

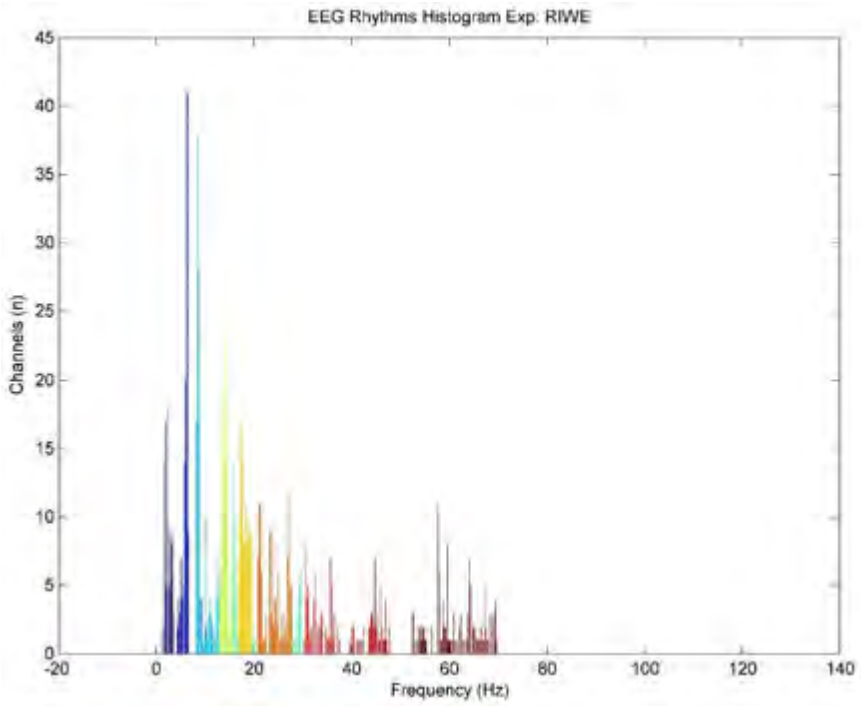

Figure A-3: Histogram for peak frequencies in Delta, Theta, mu, Beta-Low, Beta-middle and Beta-High rhythms within 0-5000ms time region over all channels, for RIWE.

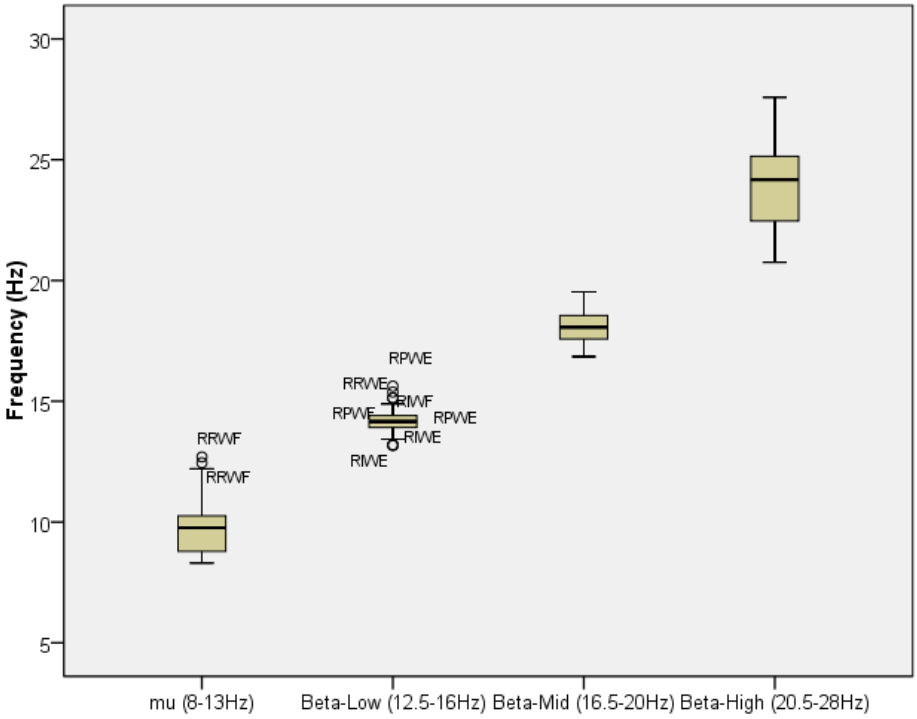

Figure A-4: Box plot of mu, Beta-Low, Beta-middle and Beta-High brain rhythms across all subjects and experiments.

Table A-5: Peak frequencies in the Delta (0.1-4Hz), Theta (4-7Hz), Alpha (8-12Hz), mu (8-13Hz), Beta (13-30Hz), Low-Beta (12.5-16Hz), Midrange-Beta (16.5-20Hz), High-Beta (20.5-28Hz), Gamma-Low (30-48Hz) and Gamma-High (52-70Hz) for each subject (1-15) and each experiment type.

Subject	Exp	Delta (0.1-4Hz)	Theta (4-7Hz)	Alpha (8-12Hz)	mu (8-13Hz)	Beta (13-30Hz)	Beta-Low (12.5-16Hz)	Beta-Mid (16.5-20Hz)	Beta-High (20.5-28Hz)	Gamma-low (30-48Hz)	Gamma-high (52-70Hz)
S1	RIWE	2.0	4.4	10.0	10.0	13.4	13.4	17.6	25.1	30.5	60.1
	RIWF	2.4	4.6	10.0	10.0	13.7	15.6	17.3	26.6	30.3	64.5
	RPWE	2.2	5.1	10.0	10.0	13.4	13.9	19.0	26.9	31.3	68.6
	RPWF	2.9	5.4	10.0	10.0	13.4	14.2	18.6	26.4	30.3	56.4
	RRWE	3.2	5.4	10.0	10.0	13.9	14.6	17.3	24.7	34.7	68.8
	RRWF	2.2	5.6	10.0	10.3	13.7	13.9	17.6	24.4	31.5	60.3
S2	RIWE	3.2	5.1	10.7	10.7	13.7	13.7	18.6	22.5	39.6	64.7
	RIWF	2.7	4.6	10.0	10.0	13.4	13.9	18.3	22.7	35.2	61.0
	RPWE	3.7	5.9	10.3	10.3	13.7	14.4	17.3	24.9	30.3	61.0
	RPWF	1.7	4.6	9.5	10.0	14.2	14.2	18.1	22.5	47.4	59.8
	RRWE	2.0	4.4	10.0	11.7	13.7	13.9	18.3	24.4	45.4	60.5
	RRWF	2.0	5.4	9.5	9.5	13.9	14.2	17.8	26.9	30.3	53.5
S3	RIWE	2.7	5.1	9.8	9.8	25.1	13.2	17.8	25.1	40.8	66.4
	RIWF	2.0	4.9	9.8	9.8	13.7	14.9	18.1	25.4	47.1	59.3
	RPWE	2.0	5.4	9.8	9.8	14.2	14.2	19.5	24.7	45.9	62.5
	RPWF	2.9	4.4	9.5	9.5	14.2	14.2	18.8	20.8	42.7	65.7
	RRWE	3.7	5.1	9.8	9.8	13.9	13.9	18.3	25.1	30.3	58.1
	RRWF	2.0	5.4	9.8	9.8	13.4	13.7	18.6	27.3	32.2	53.2
S4	RIWE	3.2	4.4	8.8	8.8	13.9	14.2	18.6	25.6	31.3	67.4
	RIWF	3.2	6.6	11.2	11.2	13.4	13.4	17.3	21.7	31.5	59.6
	RPWE	2.4	6.3	9.5	9.5	14.2	14.2	17.8	22.9	31.0	62.0
	RPWF	3.7	6.3	9.8	9.8	14.2	14.2	18.8	23.9	31.0	53.2
	RRWE	1.7	5.6	9.3	9.5	13.7	15.1	18.1	24.2	31.5	59.8
	RRWF	3.7	4.6	9.5	9.5	13.9	14.4	18.1	22.9	30.3	58.1
S5	RIWE	2.9	5.9	8.8	8.8	15.1	14.9	18.6	24.2	41.7	60.1
	RIWF	2.4	5.6	8.8	8.8	13.9	13.9	18.1	25.1	33.7	62.5
	RPWE	2.7	5.9	8.8	8.8	14.2	14.2	17.6	26.9	45.9	66.4
	RPWF	2.2	5.6	8.8	8.8	17.3	13.9	17.6	24.7	30.3	60.5
	RRWE	2.7	5.6	8.8	8.8	13.7	13.7	17.8	24.2	31.3	64.2
	RRWF	2.2	5.9	9.0	8.8	13.4	14.2	17.8	23.9	45.9	65.2
S6	RIWE	2.4	4.4	10.3	10.3	13.9	14.2	18.3	27.6	31.3	60.1
	RIWF	2.7	4.4	10.3	10.3	13.7	14.4	17.8	21.2	37.4	63.7
	RPWE	3.4	5.4	10.0	8.8	13.4	13.4	18.3	20.8	46.6	65.4
	RPWF	2.9	4.4	9.0	9.0	14.2	14.2	17.8	25.6	33.4	69.1
	RRWE	2.9	4.9	10.0	10.0	13.7	13.7	17.3	26.1	34.7	66.7
	RRWF	2.0	4.4	10.3	10.3	13.7	14.2	18.8	23.7	45.7	55.4
S7	RIWE	2.4	6.3	8.5	8.5	15.9	14.2	17.3	27.1	30.5	57.6
	RIWF	3.7	6.1	8.3	8.3	13.9	13.9	18.6	26.4	36.1	66.7
	RPWE	2.9	6.1	8.5	8.5	13.4	15.4	17.6	24.7	34.2	59.6
	RPWF	2.9	6.3	8.3	8.3	13.9	13.9	18.8	25.4	42.2	62.3
	RRWE	2.7	6.1	8.8	8.8	13.7	13.7	17.6	24.2	38.6	54.7
	RRWF	2.7	6.3	10.3	12.7	25.6	14.4	19.0	25.6	43.2	59.8
S8	RIWE	3.7	4.6	8.8	8.8	17.3	14.6	17.6	22.5	34.7	59.6
	RIWF	3.7	5.9	9.0	8.8	17.8	14.9	17.8	23.4	34.4	64.9
	RPWE	2.2	5.6	8.8	8.8	15.9	13.9	18.1	22.5	45.7	67.1
	RPWF	2.2	5.6	8.8	8.8	15.4	14.4	17.6	21.7	42.7	60.8
	RRWE	3.7	4.9	8.8	8.8	17.6	14.4	17.6	22.2	41.5	66.4
	RRWF	2.7	5.4	8.8	8.8	14.9	14.9	19.0	22.7	42.2	54.9
S9	RIWE	3.2	5.6	8.5	8.5	13.4	13.4	18.6	23.2	42.5	55.4
	RIWF	2.2	5.6	9.0	9.0	13.9	13.9	18.8	23.4	45.7	54.9
	RPWE	1.5	5.9	8.5	8.5	25.9	14.2	19.3	21.2	46.6	60.8
	RPWF	3.7	5.1	11.0	11.0	21.0	15.1	16.8	27.1	47.4	64.7
	RRWE	2.7	5.6	8.8	8.8	18.6	13.9	18.6	21.2	41.3	62.7
	RRWF	2.9	6.6	9.0	12.5	14.9	14.9	17.3	24.4	43.0	65.9
S10	RIWE	3.7	4.9	10.7	10.7	13.4	13.7	17.6	22.2	31.3	64.5
	RIWF	2.2	5.6	10.7	10.7	22.5	13.9	18.6	22.2	39.1	61.5
	RPWE	2.4	5.1	10.7	10.7	13.4	13.4	18.1	21.5	44.7	57.4
	RPWF	3.2	5.1	10.7	10.7	13.4	14.6	17.3	21.7	31.3	59.1
	RRWE	3.4	5.1	10.7	10.7	14.6	14.6	18.6	21.5	45.4	64.9
	RRWF	3.2	5.1	10.7	10.7	21.7	14.4	18.3	21.7	45.9	64.9
S11	RIWE	2.7	4.9	10.3	10.3	14.2	14.4	17.6	21.2	31.0	63.5
	RIWF	2.7	6.6	10.3	10.3	13.9	13.9	17.8	21.5	43.5	62.3
	RPWE	3.7	5.1	10.0	10.3	14.2	14.2	18.6	22.5	30.5	58.6
	RPWF	2.7	5.4	9.8	10.5	13.4	13.9	18.3	22.0	30.5	52.2
	RRWE	3.4	5.4	10.3	10.3	13.4	14.4	19.0	22.0	41.3	57.9
	RRWF	2.9	5.9	10.0	10.3	13.4	13.4	19.5	24.9	47.1	63.7
S12	RIWE	2.0	6.6	9.0	10.5	13.9	13.9	18.3	26.6	46.1	59.1
	RIWF	3.7	4.9	10.3	10.3	14.4	14.4	19.5	22.9	31.0	54.7
	RPWE	2.7	4.4	9.5	9.3	13.9	14.2	17.8	24.2	36.6	64.0
	RPWF	3.2	5.6	8.8	8.8	13.7	14.2	18.8	24.2	37.6	68.8
	RRWE	2.4	6.3	10.0	10.0	14.6	14.6	17.8	25.1	33.2	60.5
	RRWF	2.0	5.6	9.3	12.2	13.4	14.4	17.3	24.7	46.9	63.7
S13	RIWE	2.9	5.1	8.8	8.8	14.4	14.4	19.0	25.9	31.0	64.7
	RIWF	3.2	6.1	10.0	10.0	14.2	14.4	19.5	24.9	40.5	56.4
	RPWE	2.7	5.1	11.0	11.0	13.7	13.7	18.3	20.8	45.7	54.7
	RPWF	3.7	5.4	8.8	8.8	13.9	13.9	18.6	25.1	47.6	64.2
	RRWE	2.9	5.6	9.5	8.8	13.9	13.7	18.1	23.2	33.4	69.3
	RRWF	3.2	6.3	10.7	10.7	14.2	14.4	18.1	23.7	34.4	57.9
S14	RIWE	3.4	6.1	10.5	10.5	13.9	13.2	17.8	22.7	36.1	53.7
	RIWF	2.4	6.1	10.3	10.3	13.7	14.9	18.1	24.7	42.5	69.3
	RPWE	2.7	5.4	10.3	10.3	13.7	13.2	19.0	22.7	30.3	64.7
	RPWF	1.5	5.4	10.7	10.7	13.7	14.4	17.3	24.2	44.2	54.7
	RRWE	3.2	4.9	10.5	10.7	14.2	14.2	18.3	24.2	30.3	53.7
	RRWF	3.2	5.9	10.7	10.7	13.7	14.4	18.6	24.9	30.3	58.8
S15	RIWE	3.2	5.9	9.3	8.5	14.2	14.2	17.3	21.2	30.3	65.7
	RIWF	1.5	4.6	8.8	8.8	13.4	14.2	18.1	27.6	33.9	60.1
	RPWE	1.7	5.9	9.3	9.3	13.9	14.2	18.3	24.4	30.5	58.3
	RPWF	2.7	5.1	9.3	9.3	13.9	13.9	19.0	22.7	47.4	55.9
	RRWE	2.7	5.9	9.3	9.3	13.7	13.7	18.1	25.4	33.2	54.2
	RRWF	2.4	5.6	9.3	9.3	18.3	14.2	18.3	23.7	30.8	61.3

Table A-6: Mean frequencies in the Delta (0.1-4Hz), Theta (4-7Hz), Alpha (8-12Hz), mu (8-13Hz), Beta (13-30Hz), Low-Beta (12.5-16Hz), Midrange-Beta (16.5-20Hz), High-Beta (20.5-28Hz) for each experiment type. The total mean frequency across all experiments is also calculated.

		Delta (0.1-4Hz)	Theta (4-7Hz)	Alpha (8-12Hz)	mu (8-13Hz)	Beta (13-30Hz)	Beta-Low (12.5-16Hz)	Beta-Mid (16.5-20Hz)	Beta-High (20.5-28Hz)
RIWE	Mean	2,90	5,29	9,52	9,57	15,06	13,96	18,03	24,19
	N	15	15	15	15	15	15	15	15
	STDV (σ)	0,54	0,73	0,83	0,90	2,99	0,52	0,54	2,12
RIWF	Mean	2,70	5,49	9,78	9,77	14,63	14,31	18,25	23,99
	N	15	15	15	15	15	15	15	15
	STDV (σ)	0,66	0,75	0,82	0,84	2,42	0,57	0,66	1,99
RPWE	Mean	2,59	5,50	9,67	9,59	14,73	14,03	18,31	23,42
	N	15	15	15	15	15	15	15	15
	STDV (σ)	0,65	0,50	0,77	0,81	3,14	0,51	0,67	2,00
RPWF	Mean	2,80	5,32	9,52	9,60	14,65	14,21	18,15	23,86
	N	15	15	15	15	15	15	15	15
	STDV (σ)	0,67	0,58	0,82	0,86	2,02	0,34	0,69	1,90
RRWE	Mean	2,88	5,39	9,64	9,73	14,45	14,14	18,05	23,84
	N	15	15	15	15	15	15	15	15
	STDV (σ)	0,57	0,52	0,66	0,89	1,52	0,47	0,48	1,50
RRWF	Mean	2,60	5,60	9,80	10,40	15,48	14,26	18,28	24,37
	N	15	15	15	15	15	15	15	15
	STDV (σ)	0,56	0,60	0,66	1,24	3,63	0,39	0,65	1,48
Total	Mean	2,75	5,43	9,65	9,78	14,83	14,15	18,18	23,94
	N	90	90	90	90	90	90	90	90
	STDV (σ)	0,61	0,61	0,75	0,95	2,66	0,48	0,61	1,82

APPENDIX B - **CALIBRATION**

B.1 E-Prime and EGI (Net station) Synchronization

In order to accurately synchronize the EGI machine with the E-prime pc, a scaling factor needs to be calculated. The scaling factor represents the amount of drift that occurs between the E-prime pc and EGI system (Net station) clocks. Without adjusting the scaling clock, timing drifts are likely to accumulate between the different clocks. Although each clock is very precise, there exists very small error in the designated frequency of each clock. When timing events over prolonged periods of time these very small differences in frequencies can accumulate to hundreds of thousands of milliseconds. E-prime scales its internal clock to correct for the error in drift between the clocks.

The following timing experiment is conducted to calculate the scaling factor. A photodiode is place on the E-Prime monitor in the top left hand corner. The photodiode is triggered by a flashing square in precise increments and sent to the Net Station system though one of the digital inputs. At the same time E-Prime is communicates the same trigger to the Net station system by means the network peripherals. Table B-1 represents the difference in the photodiode and network communication. This difference represents a combination of the starting difference and clock drift.

Table B-1: Latency between EGI and Eprime PC (Scaling factor = 1).

	Start	*15min*	*30min*	*45min*	*1hour*
E-prime	00:00:02.661	00:15:03.339	00:30:02.998	00:45:02.741	01:00:01.517
Netstation	00:00:02.601	00:15:03.292	00:30:02.932	00:45:02.656	01:00:01.412
Difference	00:00:00.060	00:00:00.047	00:00:00.066	00:00:00.085	00:00:00.105
Latency		00:00:00.031	00:00:00.050	00:00:00.069	00:00:00.089

The scaling factor is calculated in Table B-2 by extracting the drift that occurs between the E-prime and Net station trigger points. This drift represents the accumulated difference that occurs between the netstation and E-prime pc clocks.

Table B-2: Scaling factor Calculations

	Time (min)
	00:59:58.856
	00:59:58.811
Scaling factor	0.999987496

To correct for the drift that occurs between the two systems a scaling factor of 0.999987496 is used. In Table B-3 the differences in the E-prime and Netstation clock is accounted for, as you can see the difference in the latency is significantly smaller compared to Table B-1: Latency between EGI and Eprime PC (Scaling factor = 1).

.

Table B-3: latency between EGI and Epime PC's with correction scaling factor (Scaling factor = 0.999987496).

	Start	*15min*	*30min*	*45min*	*1hour*
E-prime	00:00:02.588	00:15:03.278	00:30:03.987	00:45:03.679	01:00:01.404
Netstation	00:00:02.572	00:15:03.261	00:30:03.967	00:45:03.656	01:00:01.377
Difference	00:00:00.016	00:00:00.017	00:00:00.020	00:00:00.023	00:00:00.027
Latency		00:00:00.001	00:00:00.004	00:00:00.007	00:00:00.011

B.2 Calibration of Hand device

In order to calibrate the hand device for experimental recording, the amplified strain gauge values need to be related to applied force, and the DC motor output force need to be related to input current. The section below shows the calibration values and procedure for the strain gauge and DC motor used in the hand device.

B.2.1.1 Strain Gauge

Calibration of the strain gauges was done by simulating forces that would be applied during wrist flexion and extension. The force was applied tangentially, increasing from no load to 60.8N, at a point, 150mm from the pivot point of the hand device.

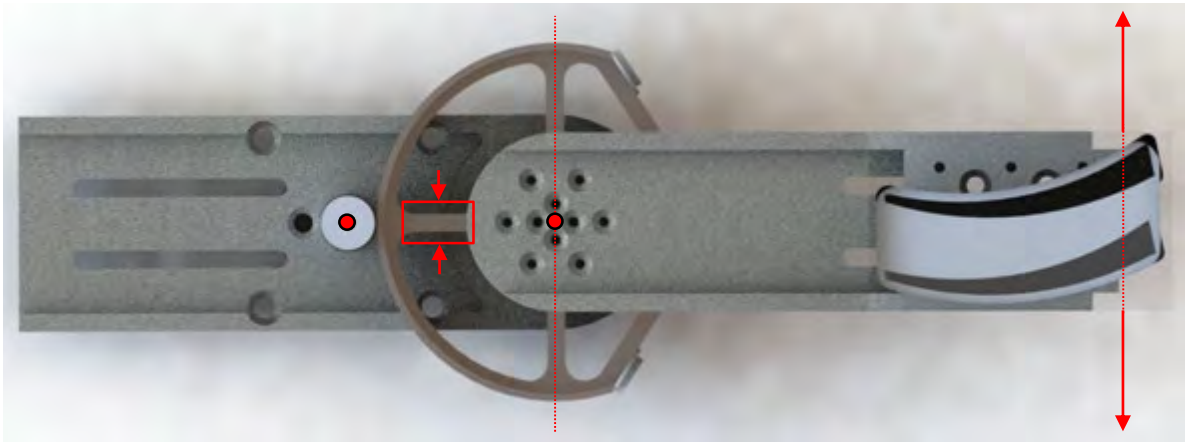

Figure B-1: CAD drawing illustrating the strain gauge position and where the calibration force is applied.

The amplified strain gauge voltages was recorded and used to calibrate the output forced for flexion and extension (Table B-4).

Table B-4: Force verse Strain in the direction of flexion and extension.

Number	*Mass (kg)*	*Force at 150mm (N)*	*Moment (Nm)*	*Strain Extension (V)*	*Strain Flexion (V)*
1	0	0	0	0	0
2	0.7	6.867	1.03005	-0.158	0.164
3	1.2	11.772	1.7658	-0.295	0.283
4	1.7	16.677	2.50155	-0.449	0.439
5	2.2	21.582	3.2373	-0.556	0.547
6	2.7	26.487	3.97305	-0.695	0.692
7	3.2	31.392	4.7088	-0.792	0.800
8	3.7	36.297	5.44455	-0.924	0.934
9	4.2	41.202	6.1803	-1.020	1.030
10	4.7	46.107	6.91605	-1.152	1.173
11	5.2	51.012	7.6518	-1.253	1.262
12	5.7	55.917	8.38755	-1.355	1.360
13	6.2	60.822	9.1233	-1.418	1.450

B.2.1.2 DC Motor

In order for the 10% MVC to be set during active (real) wrist flexion and extension, the output force for of the DC motor needs to be calculated for different DC motor current values. This is done by relating the applied current to the DC motor to the measured output force, during stall conditions. The output force is measured with the calibrated strain gauges. The hand device was locked at it pivots point in the rest position, whilst slowly increasing the current applied to the motor. The corresponding force/strain values are recorded for both flexion and extension.

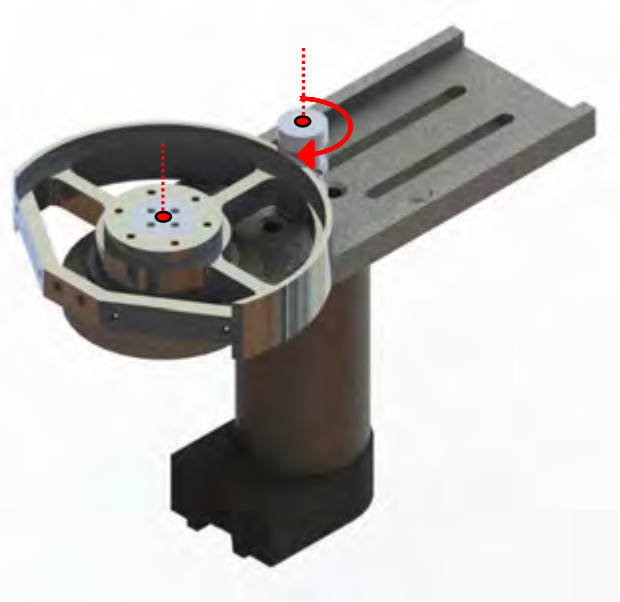

Figure B-2: Position of central axis in the hand device.

Table B-5 shows the motor current to force/strain voltages, with the corresponding computer number required to apply the necessary current.

Table B-5: Computer output value that is sent to the hand device related to current values and equivalent strain output form the DC motor.

Num	Computer Number	Extension		Flexion	
		Current (A)	Force/Strain (V)	Current (A)	Force/Strain (V)
1	60	0.06	-0.0003	-0.05	-0.0003
2	1016	0.22	-0.07	-0.21	0.03
3	1510	0.3	-0.06	-0.3	0.06
4	2047	0.39	-0.065	-0.38	0.07
5	3040	0.57	-0.1	-0.57	0.1
6	3998	0.73	-0.145	-0.73	0.11
7	4948	0.9	-0.16	-0.89	0.155
8	6122	1.09	-0.21	-1.09	0.2
9	6915	1.22	-0.23	-1.27	0.22
10	8052	1.39	-0.28	-1.4	0.25
11	9094	1.55	-0.29	-1.55	0.26
12	10271	1.69	-0.31	-1.69	0.3
13	10916	1.67	-0.32	-1.77	0.31
14	11959	1.72	-0.34	-1.79	0.31
15	13102	1.7	-0.32	-1.87	0.31

APPENDIX C - **SYSTEM DESIGN**

This section will give a detailed view into the system setup required to conduct the necessary experiments. This will include the design and construction of the hand device used in the experiments and how this hand device is integrated into the EMG and EEG recordings. This section will also include the system setup of the EMG recording, which is based on modular open source EEG amplifier (http://openeeg.sourceforge.net/doc).

C.1 Hand Device Specifications

There are many different approaches that can be used in the design of the hand device. In order to be used in this experiment the device needs to be designed in a way to meet certain safety, mechanical and functional criteria. From an ethical perspective the system setup needs to be safe to be used on subjects throughout experiment.

The following hand device design specifications need to be met in order to conduct the experiments:

- Safety criteria:
  - Must not hurt or be uncomfortable to the subject during movements.
  - If failure occurs, must fail in safe way.
  - Adequate support of hand and arm for prolong period.
- Movement criteria:
  - Allowing for wrist flexion and extension.
  - Apply a force up to 10% of the subject MVC.
  - Resist the direction of motion with a fixed force.
  - Move the wrist in flexion and extension.
- Mechanical Design criteria:
  - One degree of freedom at wrist pivot point.
  - Allows for maximum wrist flexion and extension angles.
  - Fits different hand and arm sizes.
  - Adjustable wrist pivot point.
  - Support hand and wrist in natural position.
- Recording criteria:
  - Maximum Voluntary Contraction (MVC) forces of wrist flexion and extension movements around one DOF.
  - Angle of wrist flexion and extension.

C.1.1 Movements Criteria

There are three types of wrist movements that the hand device is used in; passive, active and imaginary movements.

The active movements are broken up into four different phases consisting of the movement, sustained, returning and resting periods. During the different phases the hand device is required to operate in different modes.

- For the movement period the hand device needs to resist the direction of motion with a fixed torque while the subject performs wrist flexion or extension. Once the movement is sustained

the hand device continuously pushes back on the wrist with a fixed force trying to return the wrist to the resting position.

- During the returning period, the subject will start to return the wrist to the resting position. In response to this, the resisting force against motion is removed allowing the subject wrist to move more freely while hand device guides the hand back to the resting position.
- For the resting period the hand device remains in the free moving state.

In the case of passive movements there are three different phases consisting of the movement, returning and resting periods.

- In the first period (movement period) the hand device is required to move the wrist to its maximum flexion or extension angle, similar to the angle in the active movements, and sustain it at this position.
- During the returning and resting period for the active movements the hand device operates in the same way as in the active movements.

For imaginary experiments the hand device does not apply any force and remains at the resting position. This allows the device to move freely and is a good way to indicate if any movements occurred during imagery experiments. The different modes in the hand device for the active, passive and imaginary movements are control by an external addressing system through E-prime.

C.1.1.1 Design Approach

The hand device requires accurate control of the motion, position and torque. There are several types of actuators that can be used, including Direct Current (DC), Alternating Current (AC), Servo and Stepper Motors, each with its own operating characteristics inherent to its basic design. Thus, the selection of the motor is a procedure of matching the application requirements to the performance parameters of the motor, then selecting the most compatible. Stepper motors have the advantage of having easy angle and speed control, but the non-linear relationship between the rotors angular velocity and speed make difficult to control torque. Resonance can also occur in stepper motor, which can cause interference and noise during operation. AC motors are usually a fairly large and difficult to control with a non-linear relationship between speed and torque. The DC motors are currently the most common motor used in robotic actuators. The fact that they are easy to control and that they operation quietly makes the DC motor the ideal actuators for the hand device. The low noise operation reduces the distractions to the subjects making it ideal for EEG recordings. The output torque of DC motors varies with speed, ranging from maximum at zero speed, to zero torque at maximum speed. An increase in torque requires a decrease in angular velocity and vice versa. This means the toques is inversely proportion to the speed and proportional to the input current. The rotational speed of a DC motor is determined by the input voltage while the torque is determined by the current. Figure C-1 shows the relationship between the DC motors' speed, current and torque. There are three main types of DC motors; permanent-magnet, shunt-wound and series-wound DC motors. Permanent magnet DC motors have similar characteristics to DC shunt wound motors in terms of torque and speed characteristics. However, PM DC motors are more compact in size, have a much higher starting torque and their speed load characteristics are more linear and predictable over electromagnetically-excited motors. The PM DC motors linear relationship between voltage and

speed, and torque and current allows for easy control of the force and speed applied during the active and passive movements. Also the high torque-to-inertia ratio of the permanent-magnet DC motors allowing for quick response to control signal changes, allowing for position control to be achieved with close loop Proportional Integral Differential (PID) control.

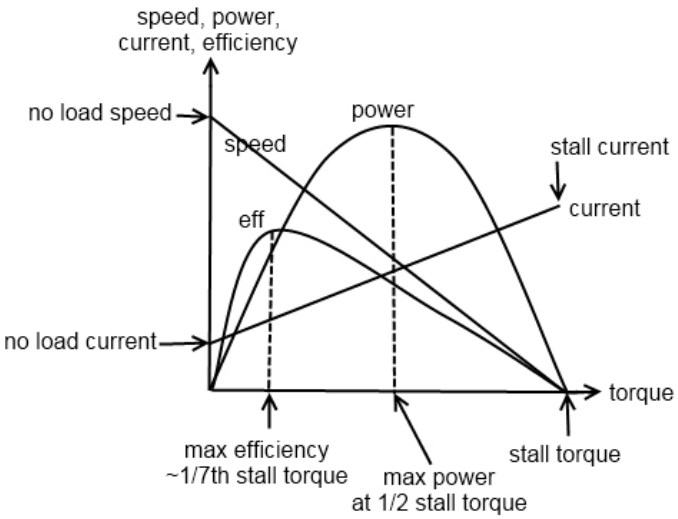

Figure C-1: The Forward Motoring region of a DC motor, showing the relationship between speed, power, current, efficiency and output torque of the motor.

There are four regions that the motor can operate in, forward motoring, forward braking, reverse motoring and reverse braking. For each phase in the active and passive experiments the motor will operated in a different region depending on the movements (rotation in the direction of wrist flexion is positive speed).

Table C-1: Showing what operating regions the DC motor is running in for the different Experiments and movement phases.

Movement Phases	**Active Movements**			**Passive Movements**		
	Wrist Flexion	Wrist Extension	Control	Wrist Flexion	Wrist Extension	Control
movement	Forward Braking	Reverse Braking	Current	Forward Motoring	Reverse Motoring	Position
sustained	Stall torque	Stall torque	Current	Stall torque	Stall torque	Position
returning	Reverse Motoring	Forward Motoring	Position	Reverse Motoring	Forward Motoring	Position
resting	None	None	None	None	None	None

When operating a DC motor in the forward or reverse motoring regions there is a direct relationship between the motor speed and output torque. As the load increases the speed drops, vice-versa. There is also a direct linear relationship between the output torque and the amount of current drawn by the motor. The linear relationship between the torque and speed of a DC motor during the motoring regions (Figure C-1) makes torque control difficult. If a DC motor is driven with current limiting active there is an equivalent maximum torque that the motor can produce. When the load torque exceeds that maximum torque of the motor, it can no longer create an equal and opposite force and the motor will be pushed backward in the opposite direction. The motor will be operating in the reverse braking or forward braking regions. In this region the motor is operating in the negative speed and its output torque is directly proportional to the current limiting. For this reason torque control is only used during reverse braking and forward braking regions, allows for easy control of the force applied during

the active movements, regardless of the motion of the wrist or rotational speed of the motor. Therefore the force of the hand device is control by current limiting the DC motor. While position control is achieved with a PID controller, through pulse width modulation (PWM) control of the DC motors input voltage. Since voltage is proportional to the output speed of the motor, the PWM control will affect the power output of the motor. For this reason the PID control is only used in the passive movements and for guiding the subject wrist back to resting position. It will be disabled during movements that require a constant resisting force.

C.1.1.2 Mechanical Design

To perform the desired experiments, a right hand mechanical device needs to be designed, that can comfortably fit subjects of different physical characteristics and provide support for the arm, hand and fingers (Figure C-2). The forearm needs to be positioned in the device with the wrist mid-way between the pronation and supination of the wrist, to cancel out the effect of gravity on the different movements. It must allow for wrist flexion and extension, but limit finger, arm and other wrist movements. During the real (active) experiment the hand device is required to move the wrist whilst providing a force of 10% MVC feedback. During the passive experiments the hand device is required to passively move the wrist to either the wrist flexion or extension position.

Figure C-2: Rendered view of 3D printed hand support, one side.

The MVC force produced during wrist flexion and extension is affected by the muscle strength and the hand size of the subject. The maximum isometric and passive moments generated by 10 healthy males, ages 23-33, range anywhere from 3.4Nm to 18.7Nm for isometric wrist flexion and extension. While passive moments remain near zero and increased at the end of the range of motion, with the average passive flexion moments of 0.5Nm at 90° flexion and 1.2Nm at 90° extension (Delp et al., 1996). The male hand length, distance from the bass of the hand at the wrist crease to the tip of the middle finger, ranges from 173mm, 1st percentile to 219mm, 99th percentile. The breadth, measured across the ends of the metacarpal bones, ranges from 81mm, 1st percentile to 100mm, 99th percentile (Judith Hall, Judith Allanson, Karen Gripp, 2006). For 10% MVC contraction, the hand device needs to apply a torque ranging between 1.8Nm and 0.34Nm at a maximum hand length of 219mm. The hand

device can be adjusted to fit subject of different sizes, by adjusting the position of the hand grip and arm support (Figure C-3).

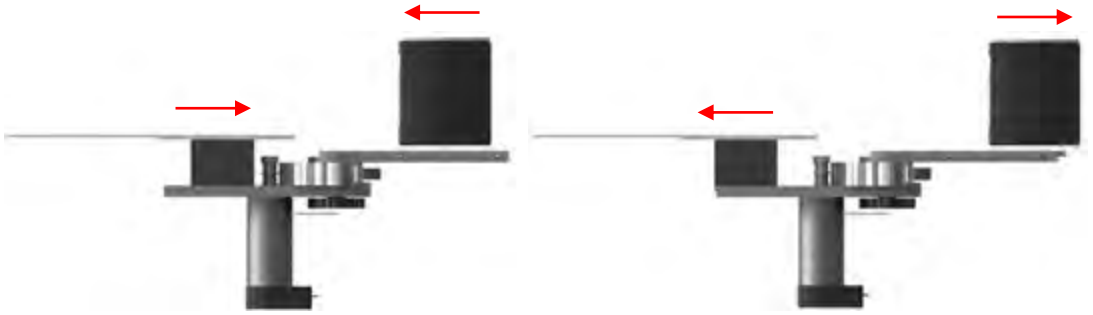

Figure C-3: Illustrating the maximum (right) and minimum (left) allowed adjustment of the hand device at the arm rest and hand support.

Stand-alone DC motor directly located on the joint axes results in quite heavy and bulky actuators with very inefficient in haptic working condition. The use of a smaller dc motor in combination with a reducer is preferred, even though it can affect the off-state friction and dynamic range of the system. In order to reduce the effect of friction and backlash inherent in conventional reducers, a cable capstan reducer is used. This reducer allows for zero backlash transmission and low friction, although its lower torque/volume ratio means it requires a larger area (Letier, Avraam, Horodinca, Schiele, & Preumont, 2006). Its working principle is based on capstan located on a motor shaft, on which a cable is wrapped around and attached to both end of a large diameter wheel (Figure C-4, right). The motor translates is rotational motion through the capstan into the cable, which is attached the wheel. The diameter of the wheel and capstan determine the gearing ratio of the cable capstan reducer. With a gearing ratio of 10:1 the motor maximum stalling torque need to be at least 0.18Nm. Running a DC motor at its maximum stalling toque is not idea; therefore a larger and more powerful motor is needed.

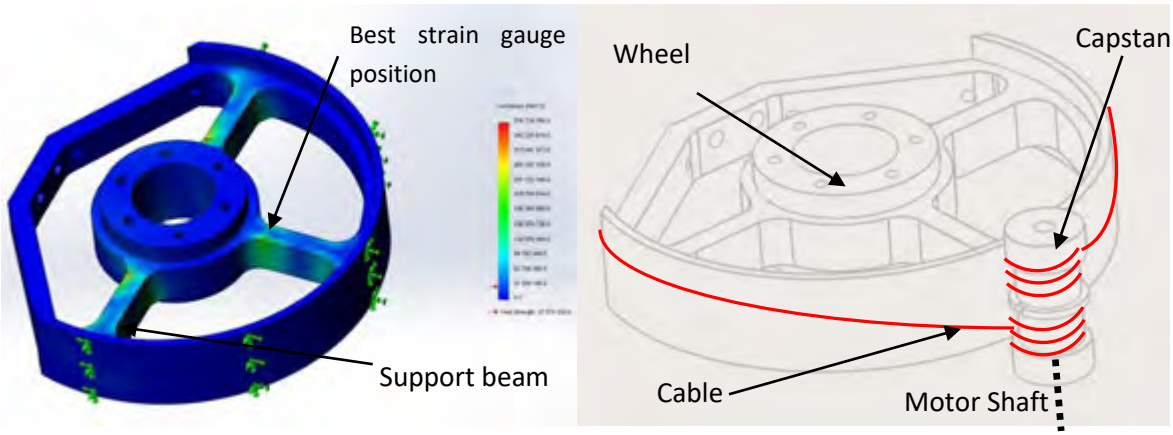

Figure C-4: Right - Diagram of the cable capstan reducer and wheel designed used in the hand device. Left - Finite Element model of wheel used in the cable capstan reducer, showing the optimal position for the strain gauge. Strain calculated with a 19Nm torque applied to the hand grip.

The cable capstan reducer has one degree of freedom (DOF) around the centre axis of the wheel. This limits the motion of movements pivoted around the wheels axis. By positioning the hand midway between supination and pronation with the wrist joint aligned with the wheel axis, only wrist flexion or extension can be performed. Since the wheel only rotates around its axis, the strain measured on

the wheel, tangential to its axis will only be affected by wrist flexion and extension. The finite element model in Figure C-4 left, represents the stress that occurs in the wheel, when a simulated wrist flexion of 19Nm is applied to the hand grip. The three support beams connecting the outside of the wheel to the inner shaft show the maximum stress nearest to the inner shaft. Strain gauges at this position allow for the best translation of force from the hand to the wheel, resulting in the finest force measurement with the best accuracy.

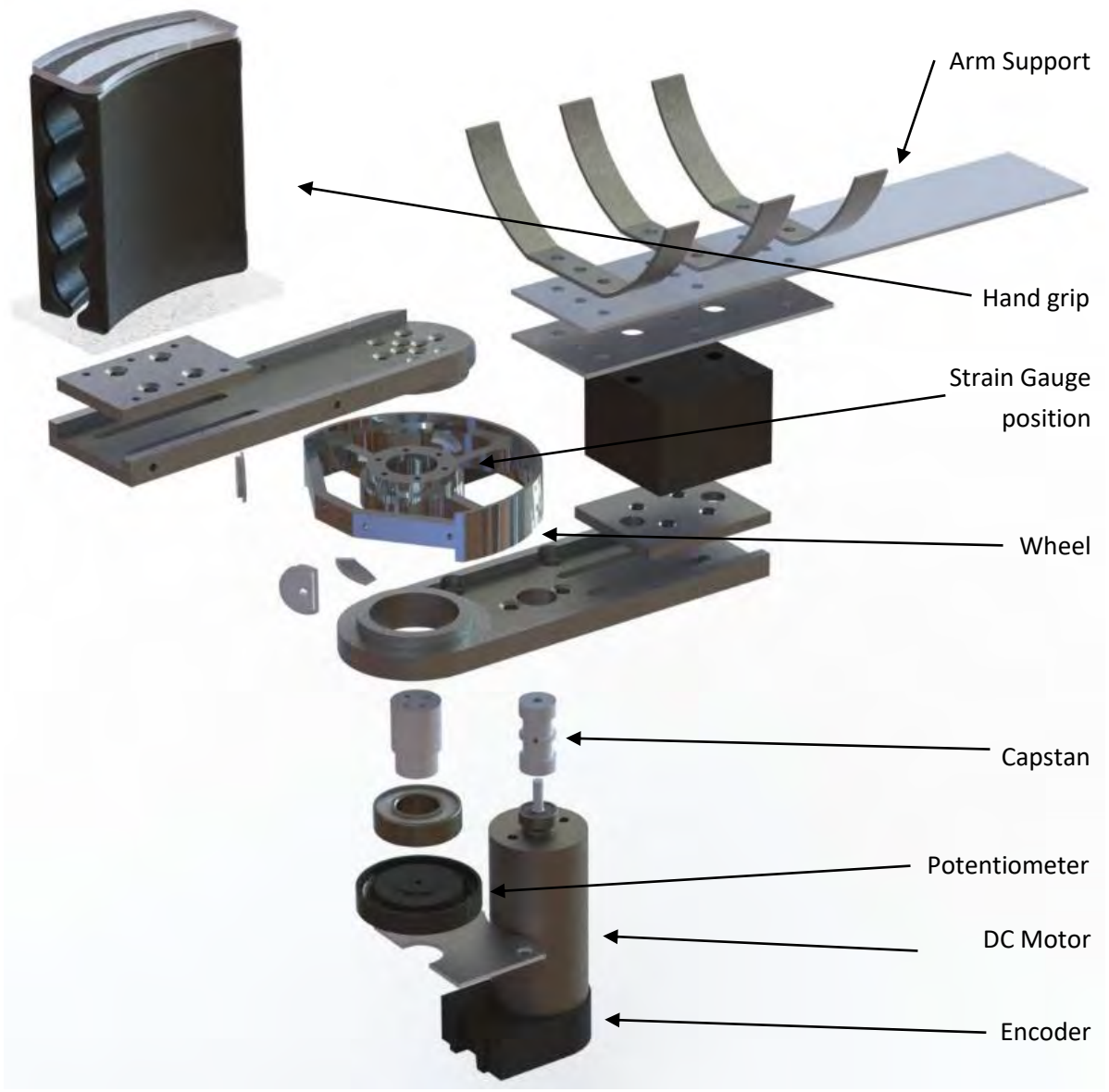

Figure C-5: Exploded view of the hand device.

The hand device in Figure C-5 is designed to support the hand during flexion and extension of the wrist. The subject hand is place in the "hand grip" from the base of the proximal phalanges to the end of the fingers at a slight angle. This is to ensure that neither flexor nor extensor muscles are activated and that the hand is in its natural resting position. The lower arm is strapped onto the device so that the pivot point of the wrist is at the centre of rotation of the force transducer. The angle of the wrist is measured with the potentiometer and is used to move the wrist to the correct positions during passive and real wrist flexion and extension. The DC motor transfers its motion and torque through the capstan to the wheel via a 2mm cable attached at either end of the wheel.

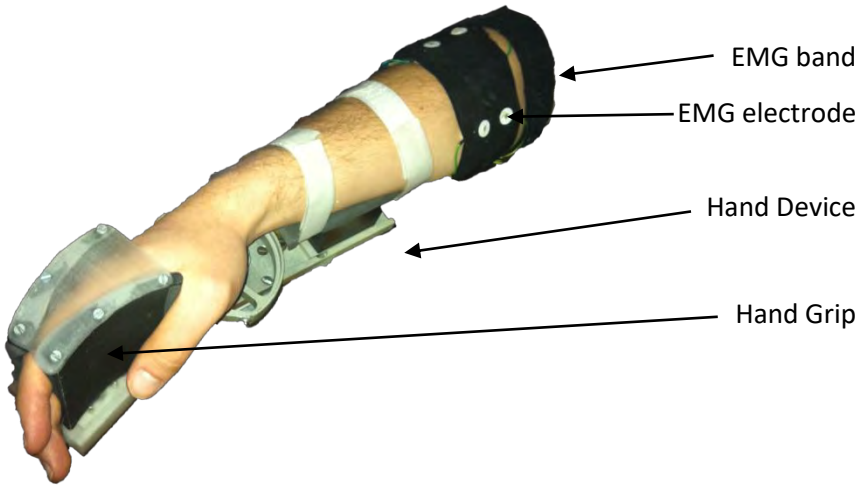

Figure C-6: Right hand Strapped in hand device, with EMG electrode arm band.

The hand device is also limited with:

- The range of motions is not limited between flexion and extension for active passive and active real movements
- The rate of the movements is not restricted during real movements, only the force.
- The rate of movements applied for passive movements is not controlled.
- The height of the table was not adjusted for each subject, only the position and length of the hand device.

C.1.1.3 Motion and Force Control

PID control was used to control the hand device position during real and passive wrist movements. This is done with pulse width modulation (PWM) through the Mbed controller ("Rapid Prototyping for Microcontrollers | mbed," n.d.), with the potentiometer used for feedback. The torque of the motor is controlled with current, which is set in Labview prior to the experiments (i.e. current relating to 10% MVC for flexion and extension). All forces are read from the strain gauges into a strain gauge amplifier that is recorded in Labview. Figure C-7 shows the control setup of the hand device.

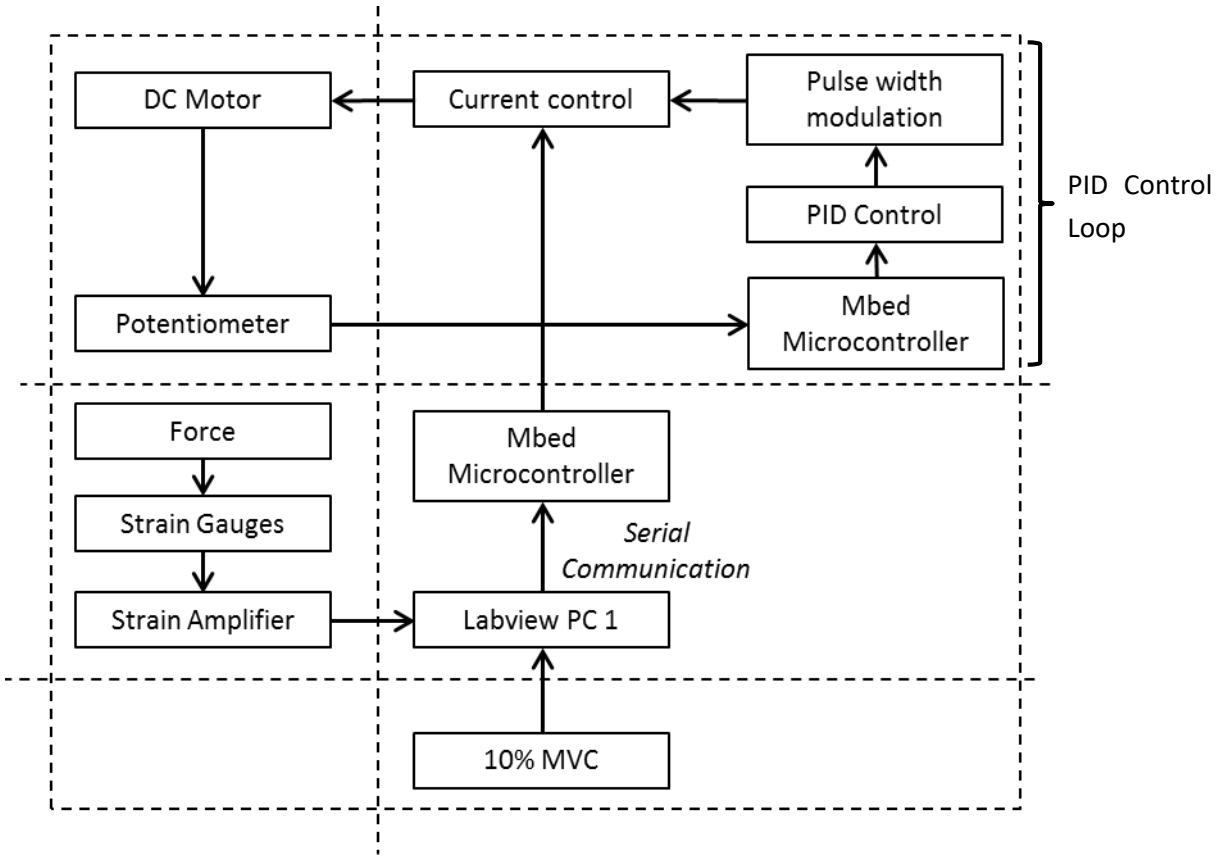

Figure C-7: Control setup of hand device, showing how all the subsystem was connected together in order to conduct the necessary experiments.

The PCB layout of the control circuit used to control the hand device position, speed, direction and torque. The interface board for the MBED controller (Figure C-8), and torque control (Figure C-9, Right) and speed and direction control (Figure C-9, Left) board.

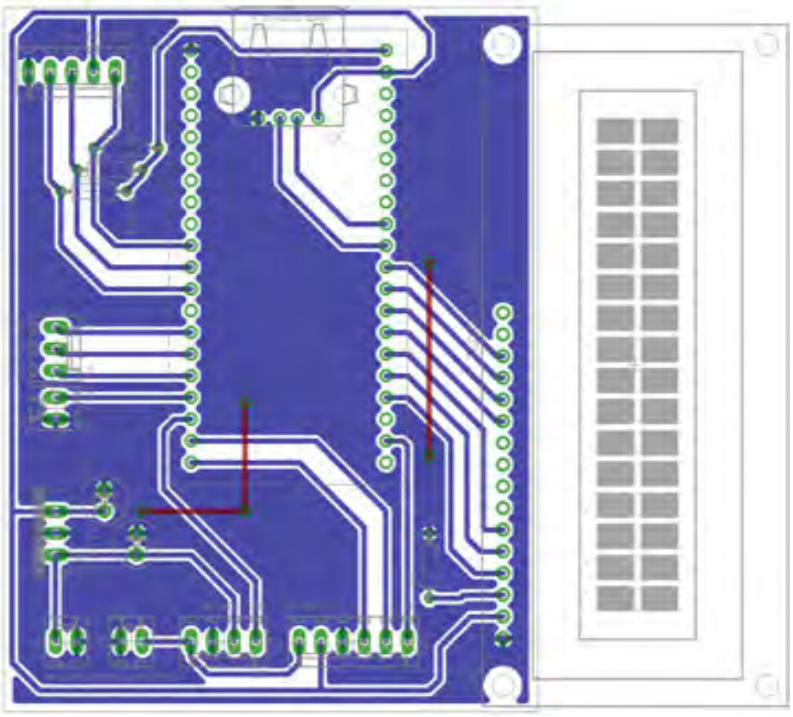

Figure C-8: PCB layout (Eagle CAD) of MBED interface board for hand device control processing.

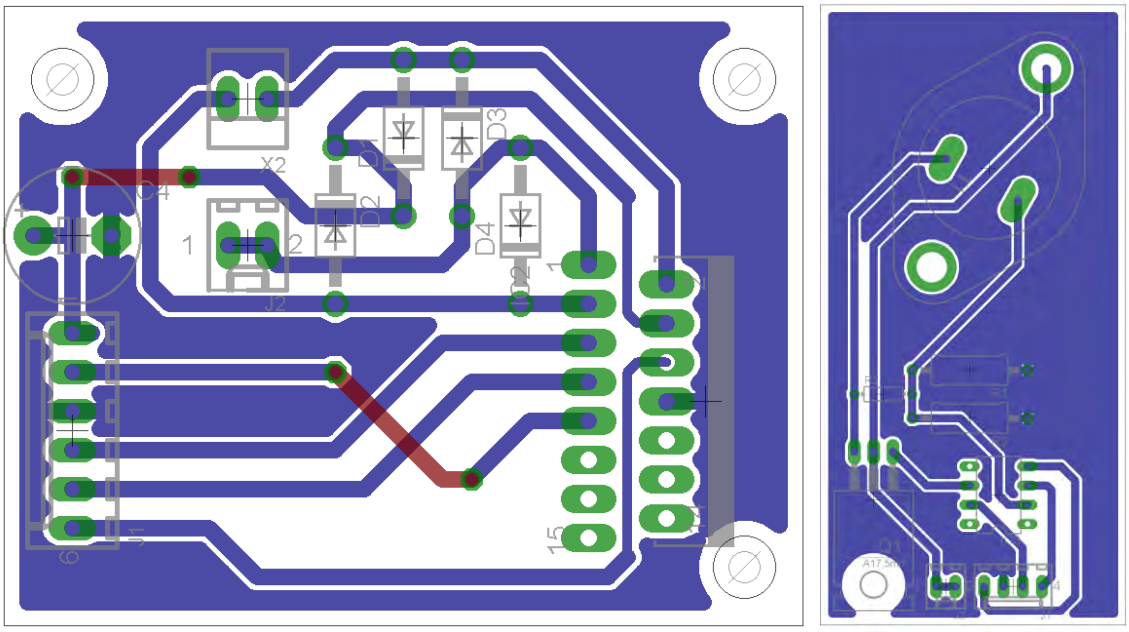

Figure C-9: Left, PCB layout (Eagle CAD) of motor direction and speed control board. Right, PCB layout (Eagle CAD) of motor current and torque control board.

C.1.1.4 Verification

The hand device was verified by comparing the applied torque to output strain (Figure C-10, left) and using this to compare the hand device output torque to motor input current (Figure C-10, right). The motor output torque was measured at the maximum hand length. The maximum torque that the DC motor can apply is ±8Nm of force in flexion and extension position. This force is directly related to

the current applied to the DC motor. This is well within the range of the 10% MVC required (1.8Nm flexion and 0.34Nm extension) to resist active movements over a large range of subjects (Delp et al., 1996). This means that the DC motor will be able to supply adequate amount of torque resisting the direction of motion during real flexion and extension of the wrist. It is also important that the motor is able to overcome the passive moments required to move the wrist to either the flexion or extension position. With a passive moment of 0.5Nm at 90° flexion and 1.2Nm at 90° extension, the hand device has more than enough torque to move the subject wrist to either position (Delp et al., 1996).

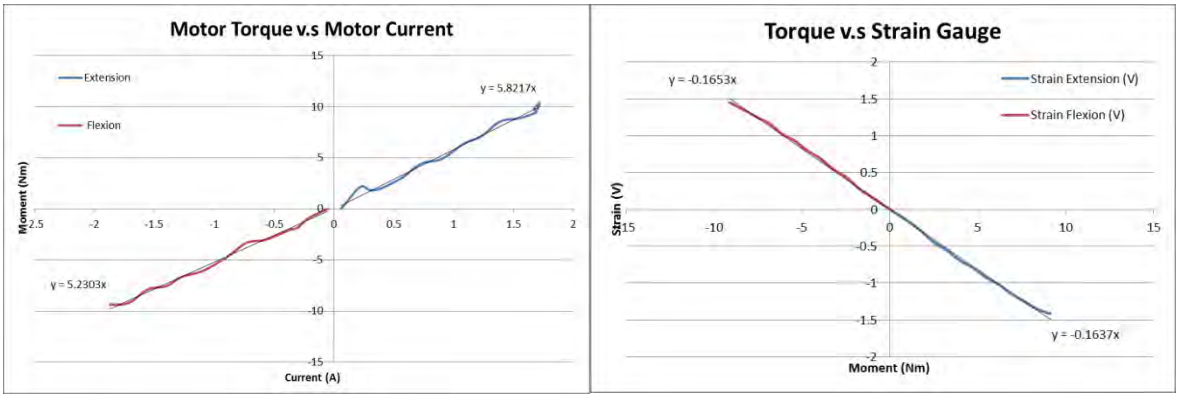

Figure C-10: left image: DC motor torque, verse current output during stall operation of the DC motor during flexion and extension operation. Right image: Torque verse Strain for different forces applied to the hand device at a distance of 15cm from DOF, with equations of the linear trend line for flexion and extension movements.

C.1.2 Experimental Setup

In order to get a reliable EEG, EMG recording it is important that the proper calibration and system setup was performed. There are a number of sub systems that needs to be synchronized to ensure that the recording and triggers all occur at the same time. The EEG, EMG, Eprime and hand device all need to be synchronized with one another. Figure C-11, shows the experimental recording configuration and how the EMG, EEG and Hand Device systems are connected together. To make sure both the EEG and EMG system recorded in synchronicity, a 1 kHz clock generated by the EGI system was used to synchronize the EMG data acquisition device (DAC). The Erpime system was synchronized with the EGI system over a network trigger. The Eprime Trigger was also generated and shared between the E-prime, EMG and EEG systems and was used as a check for synchronicity. To ensured that the hand movements occur in sync with the rest of the system. The hand device was triggered through a parallel interface from the Eprime machine that would indicate which movement the hand device needs to be configured for. Refer to APPENDIX B - Calibration, for the calibration procedure of the EGI machine with Eprime.

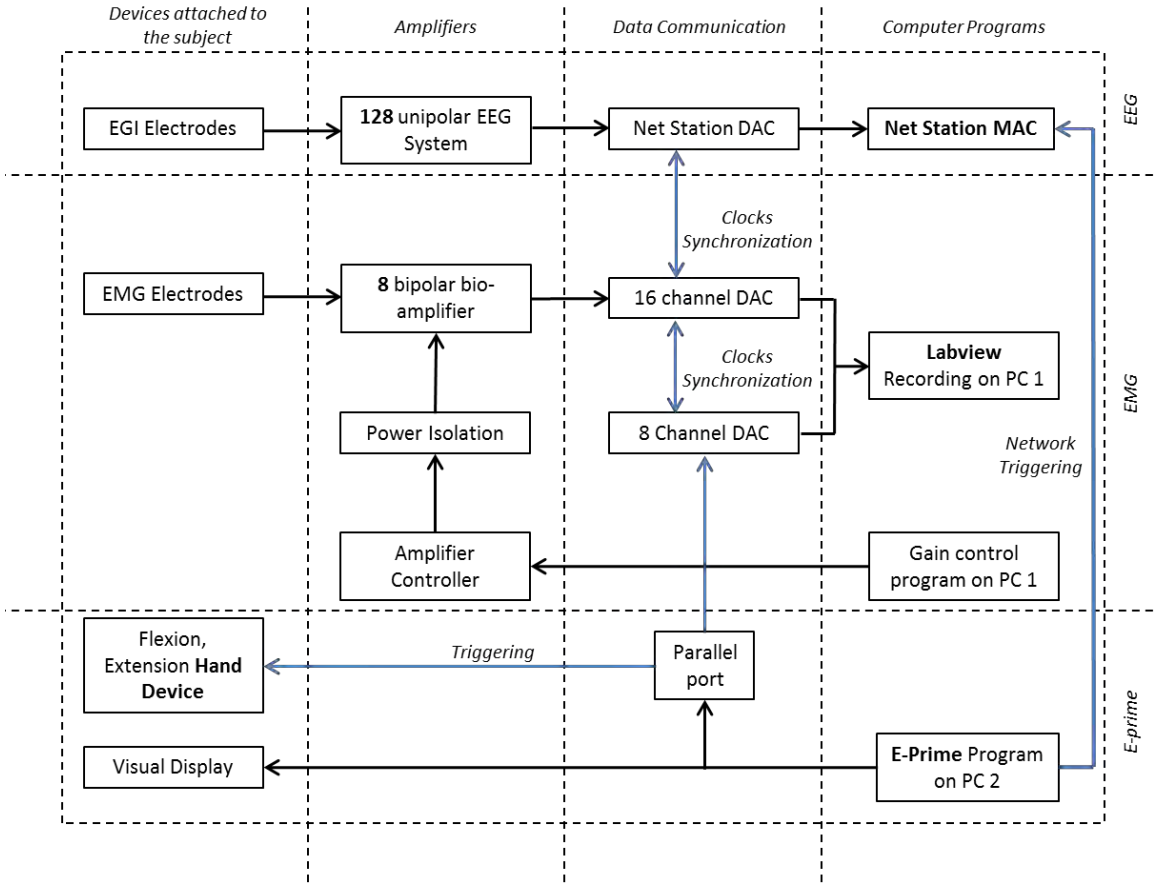

Figure C-11: System Connection diagram of the EGI, EMG and Eprime systems, plus how the hand device is incorporated into the design

Labview is used to display the filtered EMG signals and output strain, including the experimental address and progress. The angle of the wrist and strain applied to the hand device is displayed, and the output force applied against motion is set in the Labview display (Figure C-12).

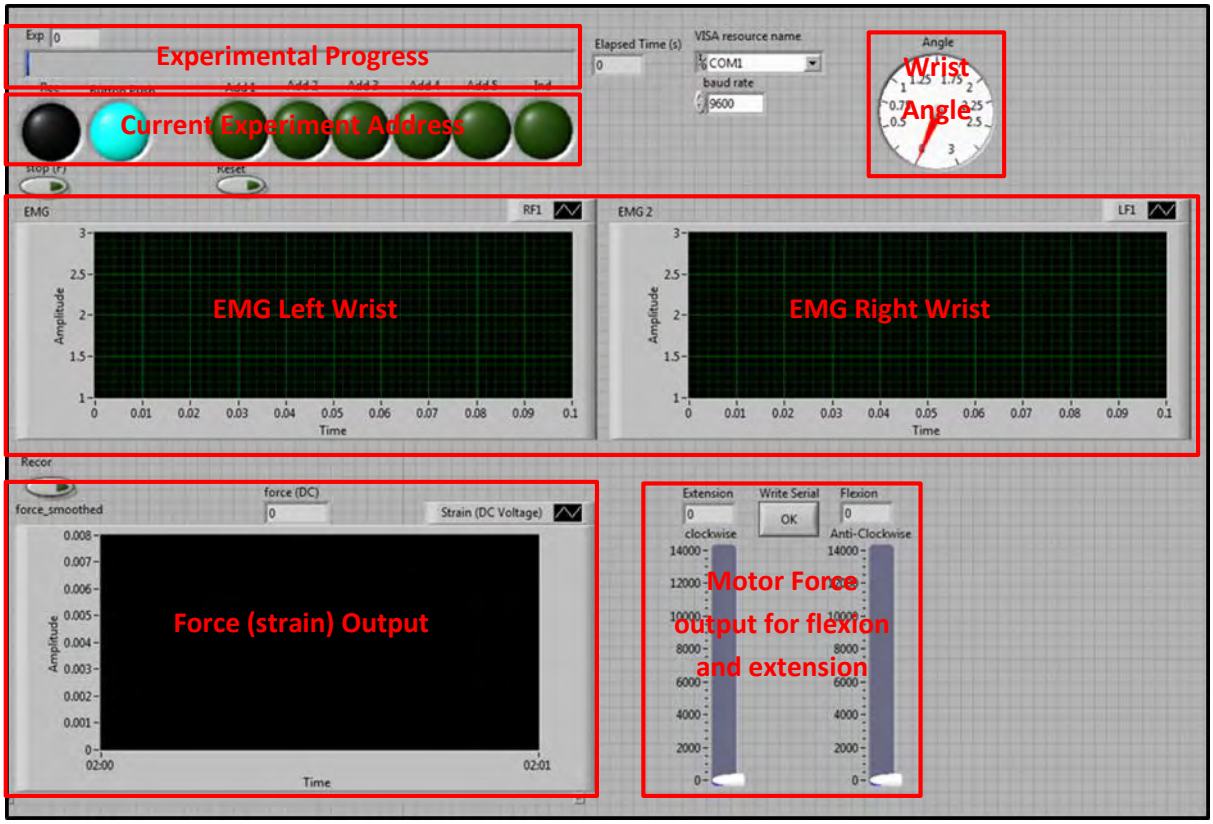

Figure C-12: Labview display output image, illustration how the EMG, Wrist Angle, Output Force (Strain), Experimental progress and Current experimental address was displayed during to the examiner during experiments.

APPENDIX D - **PROVEN TECHNIQUES**

The following section validated the MRCP (see section D.1) and ERDS (see section D.2) waveforms/features for motor imagined, passive and real movement to existing literature results. The PLV analysis is evaluated by inducing an artificial phase synchronization between tow signals, as shown in section D.3. Finally the effectiveness of the artefact correction (see section D.4) is visually inspected for EMG correction and ocular correction.

D.1 Movement related cortical potentials (MRCP)

The MRCP result for imaginary, passive and real wrist movements is reproved to those result found in the literature. The below MRCP result show similar wave to that observed during movements at the contralateral motor cortex. The Bereitschaftpotential (BP) show similar response to that seen in section 2.2.1, with a pre-motor event related negativity occurring prior to the onset of the movement, as shown in Figure D-1, Figure D-2 and Figure D-3 at the left and right primary motor cortex (C3, C4).

D.1.1 Imaginary Movements

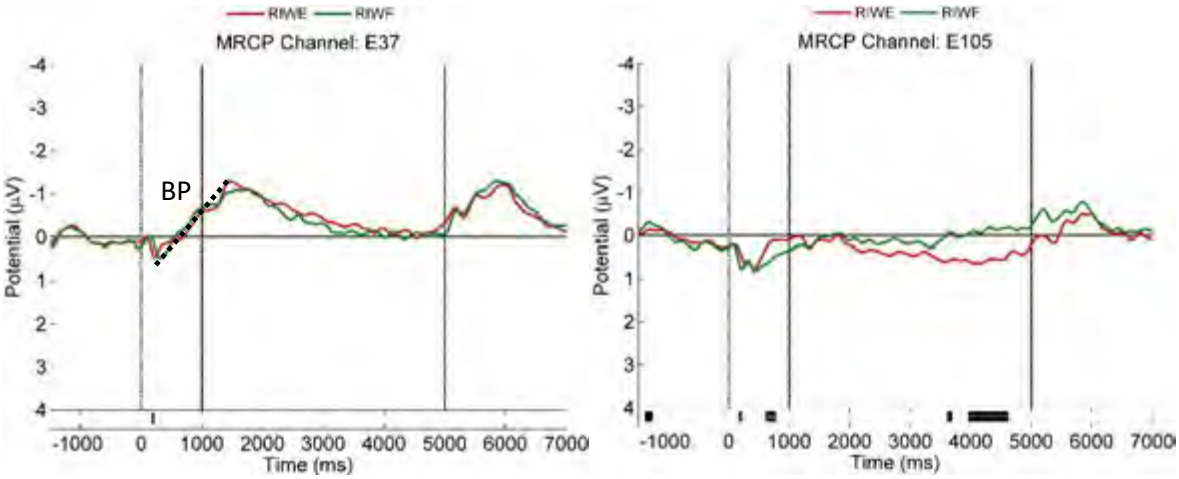

Figure D-1: The grand average imaginary MRCP over the left primary motor cortex (left figure - E37, C3) and right primary motor cortex (right figure – E105, C4), illustrating the Bereitschaftpotential (BP).

D.1.2 Passive Movements

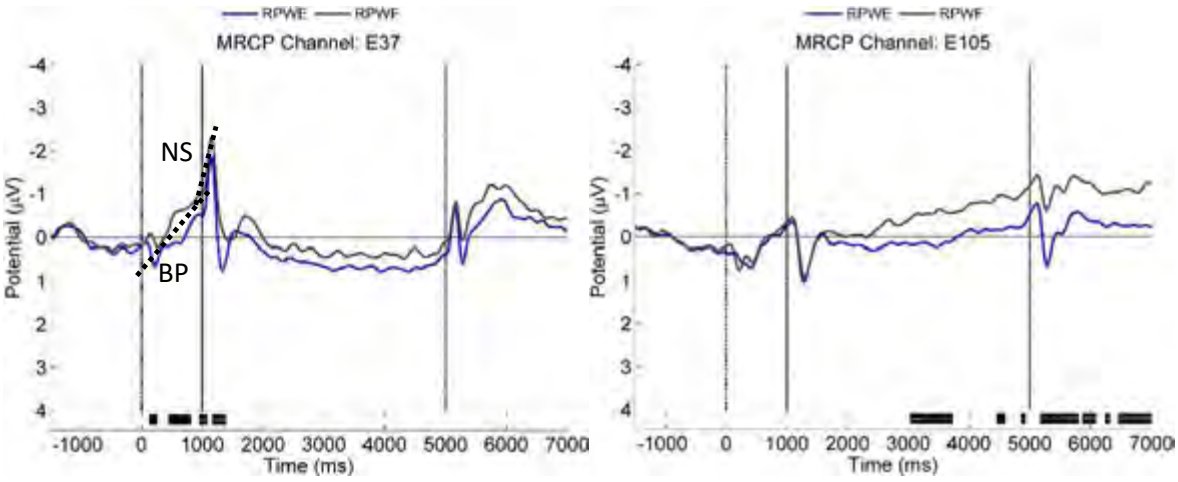

Figure D-2: The grand average passive MRCP over the left primary motor cortex (left figure - E37, C3) and right primary motor cortex (right figure – E105, C4), illustrating the Bereitschaftpotential (BP).

D.1.3 Real Movements

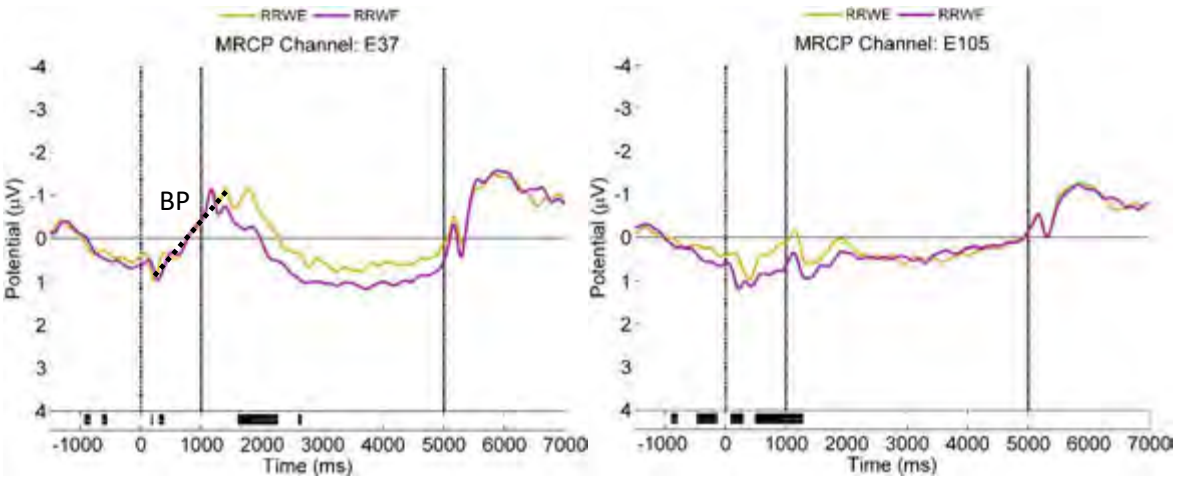

Figure D-3: The grand average real MRCP over the left primary motor cortex (left figure - E37, C3) and right primary motor cortex (right figure – E105, C4), illustrating the Bereitschaftpotential (BP).

D.2 Event related de/synchronization (ERS/ERD)

The ERS/ERD result for imaginary, passive and real wrist movements are compared to result obtained in the literature for ERS/ERD movements.

D.2.1 Imaginary Movements

The motor imaginary ERD/ERS result observed between wrist flexion and extension in the beta bands (see Figure D-5) are compared to Muller et al. (Müller-Putz et al., 2007) finding (see Figure D-4). Similar ERD result are present for motor imagined to those observed in the literature, showing a beta band desynchronization in the primary motor cortex during the sustained period. The mu band topographical plot also shows desynchronization around the contralateral primary motor cortex (see Figure D-6).Refer to section 2.2.2 for an in-depth review of ERD/ERS.

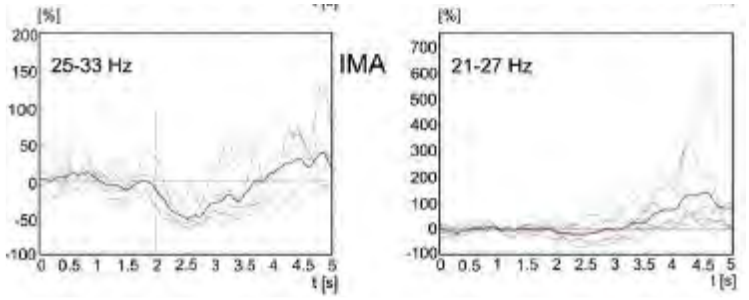

Figure D-4: Grand average (solid line - red) time series beta band ERD and ERS from channel Cz, motor imaginary (IMA) movements (Müller-Putz et al., 2007).

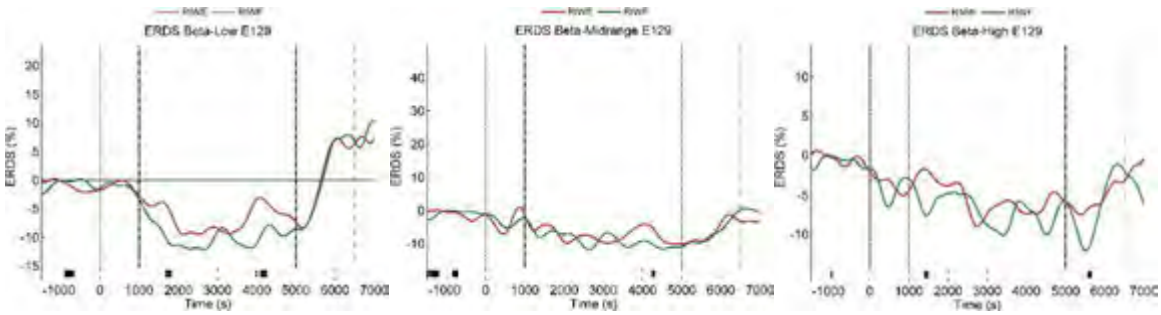

Figure D-5: The grand average ERS/ERD time series plot for channel Cz, for motor imaginary wrist flexion (green) and extension (red) movement average over the peak Beta-Low (Left figure), peak Beta-midrange (middle figure) and peak Beta-high (right figure) bands.

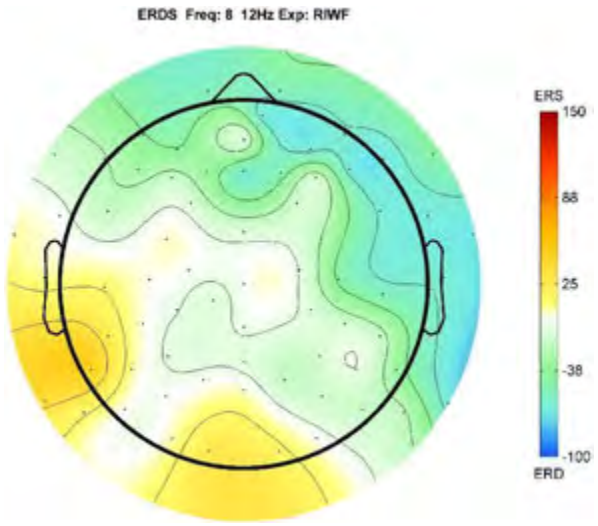

Figure D-6: The grand average ERS/ERD topographical plot averaged over the sustained movement period (1000-5000ms) for motor imaginary wrist movement average over the mu band (8-12Hz).

D.2.2 Passive Movements

The passive movement beta band ERD/ERS result observed during wrist flexion and extension (see Figure D-8) are compared to know literature by Muller et al. (Müller-Putz et al., 2007), as shown in Figure D-7. Similar low-beta (Figure D-8, left) and midrange-beta (Figure D-8, middle) result are observed around the central primary motor cortex (Cz) in comparison to the results observed by Muller et al. (Müller-Putz et al., 2007), showing ERD and ERS result. The topographical mu band plot (see Figure D-9) also shows ERD around the contralateral primary motor cortex for passive movements.

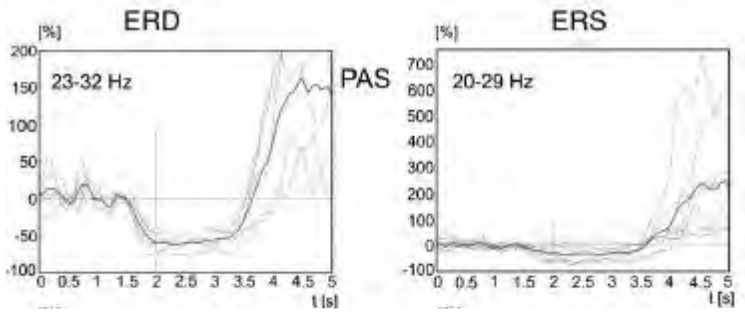

Figure D-7: Grand average (solid line - red) time series beta band ERD and ERS from channel Cz, for passive (PAS) movements (Müller-Putz et al., 2007).

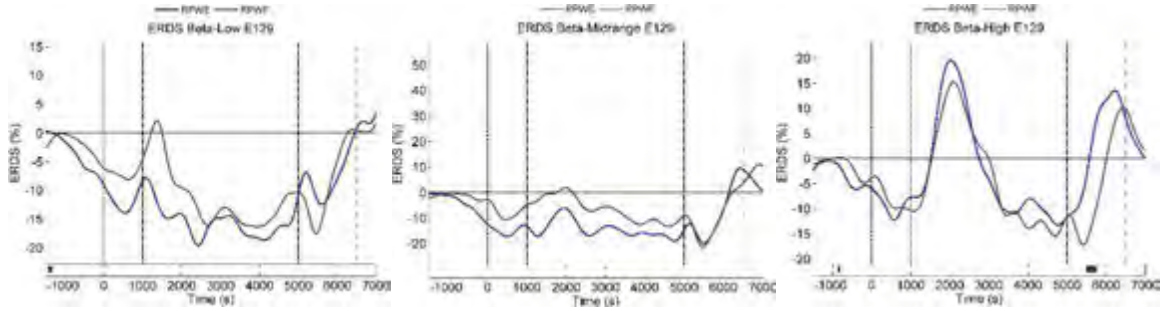

Figure D-8: The grand average ERS/ERD time series plot for channel Cz, for motor imaginary wrist flexion (grey) and extension (blue) movement average over the peak Beta-Low (Left figure), peak Beta-midrange (middle figure) and peak Beta-high (right figure) bands.

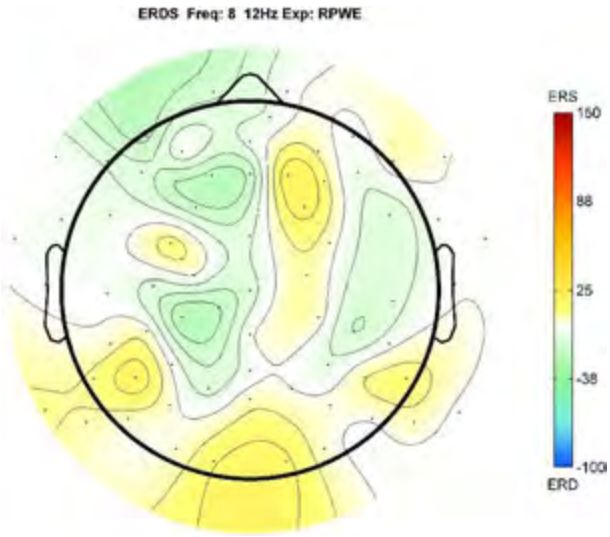

Figure D-9: The grand average ERS/ERD topographical plot averaged over the sustained movement period (1000-5000ms) for passive wrist movement average over the mu band (8-12Hz).

D.2.3 Real Movements

The real movement mu and beta band ERD/ERS result observed during flexion and extension are compared to know literature by Cassim et al. (2000) for mu/beta-band (wrist movement, see Figure D-11) Muller et al. (Müller-Putz et al., 2007) for beta-band (foot movement, see Figure D-10) . Similar mu-band ERD (Figure D-12) low-beta (Figure D-13, left) and midrange-beta (Figure D-13, middle) result are observed around the central primary motor cortex (Cz) in comparison to Muller et al. (Müller-Putz et al., 2007) and Cassim et al. (2000) finding, for the ERD and ERS during real movements. The topographical mu band plot (see Figure D-14) also shows ERD around the contralateral primary motor cortex for passive movements.

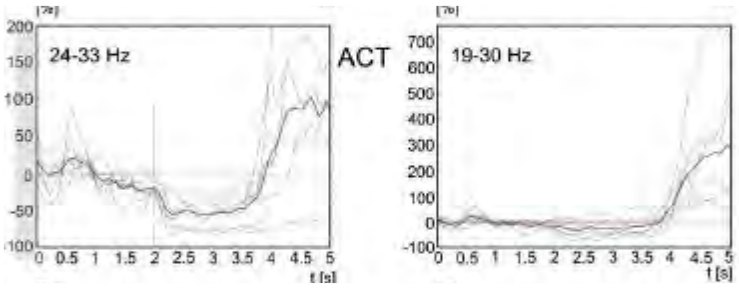

Figure D-10: Grand average (solid line - red) time series beta band ERD and ERS from channel Cz, Active (ACT) foot movements (Müller-Putz et al., 2007).

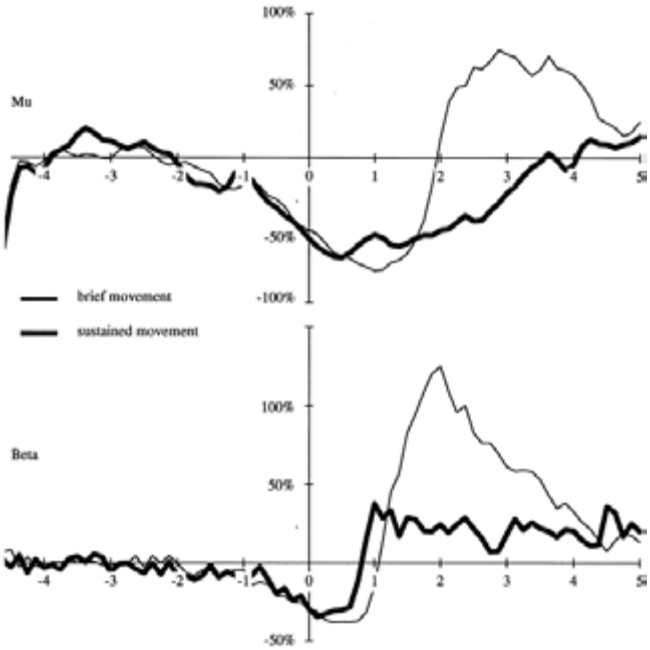

Figure D-11: ERS/ERD grand average time series of the mu (upper trace) beta (bottom trace) for wrist extension during brief and sustained movements (Cassim et al., 2000).

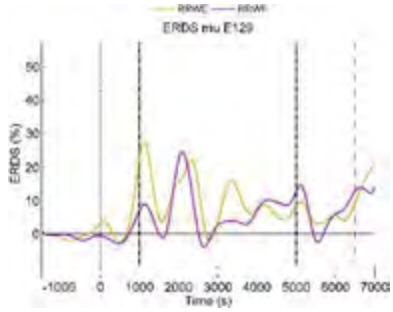

Figure D-12: The grand average ERS/ERD time series plot for channel Cz, for real wrist flexion (purple) and extension (yellow) movement average over the peak mu band.

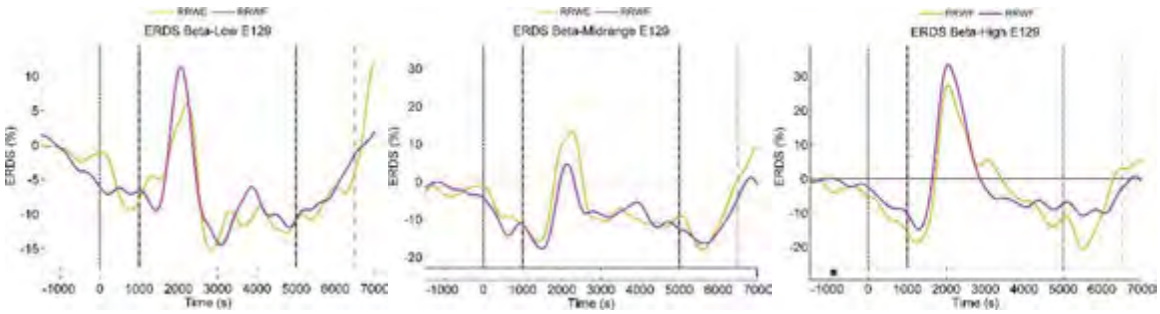

Figure D-13: The grand average ERS/ERD time series plot for channel Cz, for real wrist flexion (purple) and extension (yellow) movement average over the peak Beta-Low (Left figure), peak Beta-midrange (middle figure) and peak Beta-high (right figure) bands.

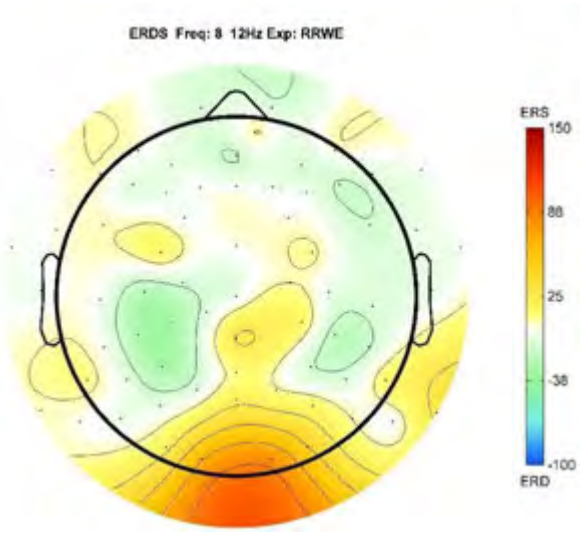

Figure D-14: The grand average ERS/ERD topographical plot averaged over the sustained movement period (1000-5000ms) for real wrist movement average over the mu band (8-12Hz).

D.3 Phase Locking Value (PLV)

In order to test that the Phase Locking Value (PLV) is working correctly, a method similar to that used by Darvas *et al.* (2009) is implemented (F. Darvas et al., 2009).

For the reconstruction of Phase Locking between two signals, EEG signals that have very little phase coupling between them are used. The coupling between the two signals X and Y is reconstructed by subtracting from Y the narrow band component $Y(f,t)$ and then adding the narrow band components $X(f,t)$ normalized by $\sqrt{A_x(f,t)A_y(f,t)}$ in a time interval t around frequency f. This makes a new signal, $Y_{couple} = Y - Y(f,t) + X(f,t)/\sqrt{A_x(f,t)A_y(f,t)}$, that will phase couple with signal X around a particular frequency *f* in a time *t*. Figure D-15 represents the PLV between two signals X and Y_{couple}, where Y_{couple} is a signal containing $X(f,t)$ around 20Hz in the time interval [0,1]s. As can be seen in Figure D-15 strong phase coupling is present around 20Hz between 0 and 1 seconds. This shows that the PLV method being used can accurately calculate the phase locking between two signals.

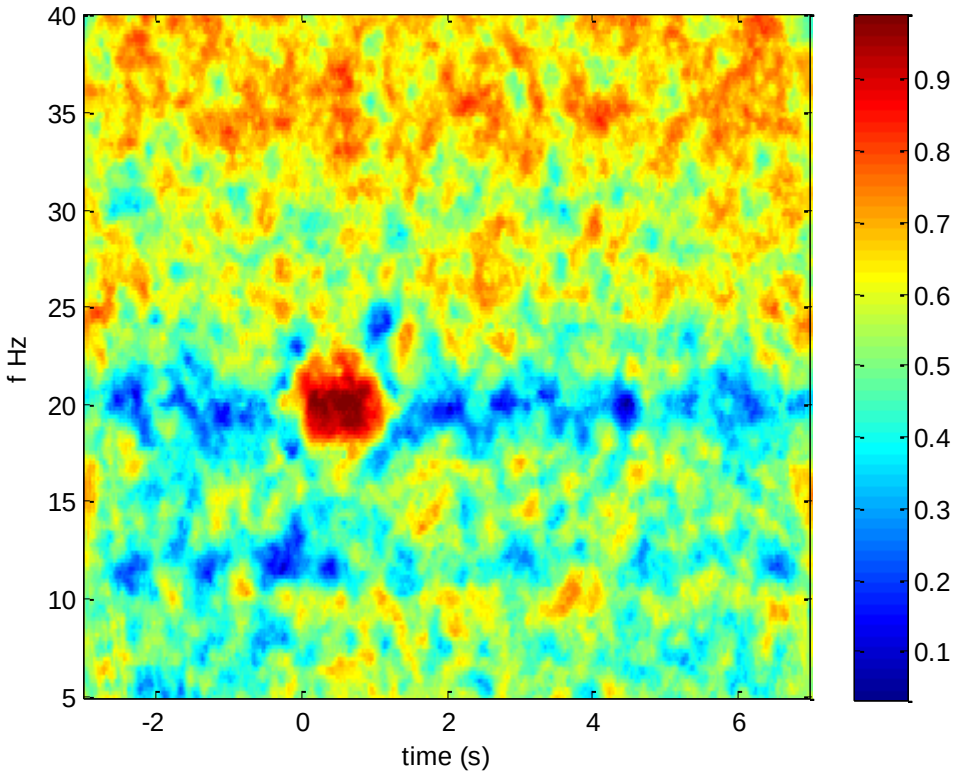

Figure D-15: PLV artificial phase coupling between signal X and $\boldsymbol{Y_{couple}}$ between time interval [0,1]s at 20Hz.

D.4 Artefact Correction

The figures below represent the recorded data of 8 unipolar ocular channels (E1, E8, E26, E33, E125, E126, E127, E128) from Subject 7. The RAW data in Figure E-16, represents raw unfiltered artefact (shaded area) contaminated EEG data. In this section of the data the subject was preforming a passion wrist flexion. The ocular corrected data is shown in Figure D-19, and the combination of EMG and ocular correction is shown in Figure D-20.

D.4.1 EMG Correction

The ocular artefact (single dash, red square, Figure D-16) at 1200 seconds occurs at the starts of the passive wrist movements, followed by the EMG artefacts (double dash, blue square-Figure D-16) during the wrist movements. The following two figures will illustrate the ocular and EMG artefact correction algorithms.

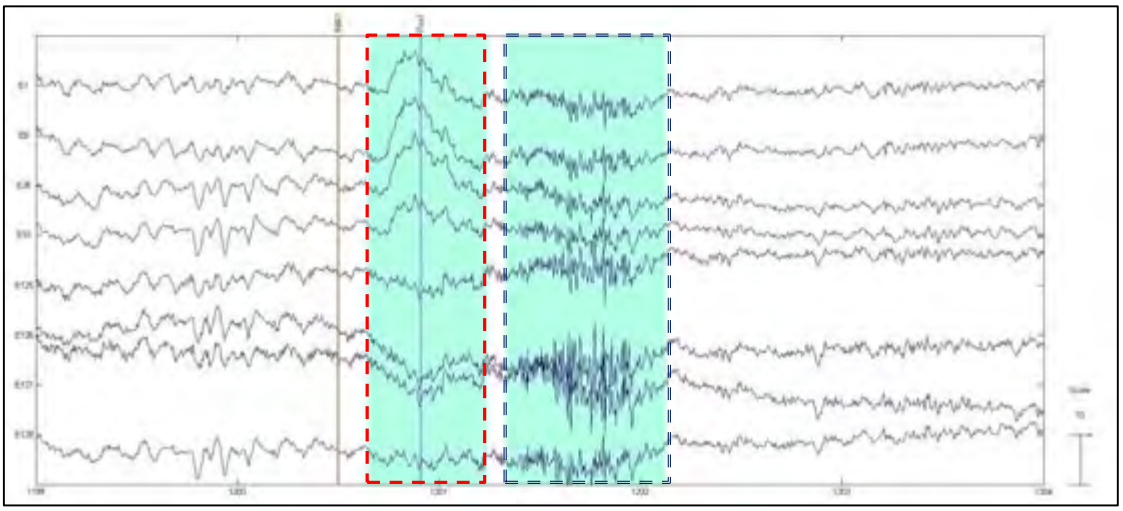

Figure D-16: RAW unprocessed unipolar ocular channels (E1, E8, E26, E33, E125, E126, E127, E128) illustrating ocular artefacts (single dash, red square) and EMG artefacts (double dash, blue square).

D.4.1.1 Ocular Correction

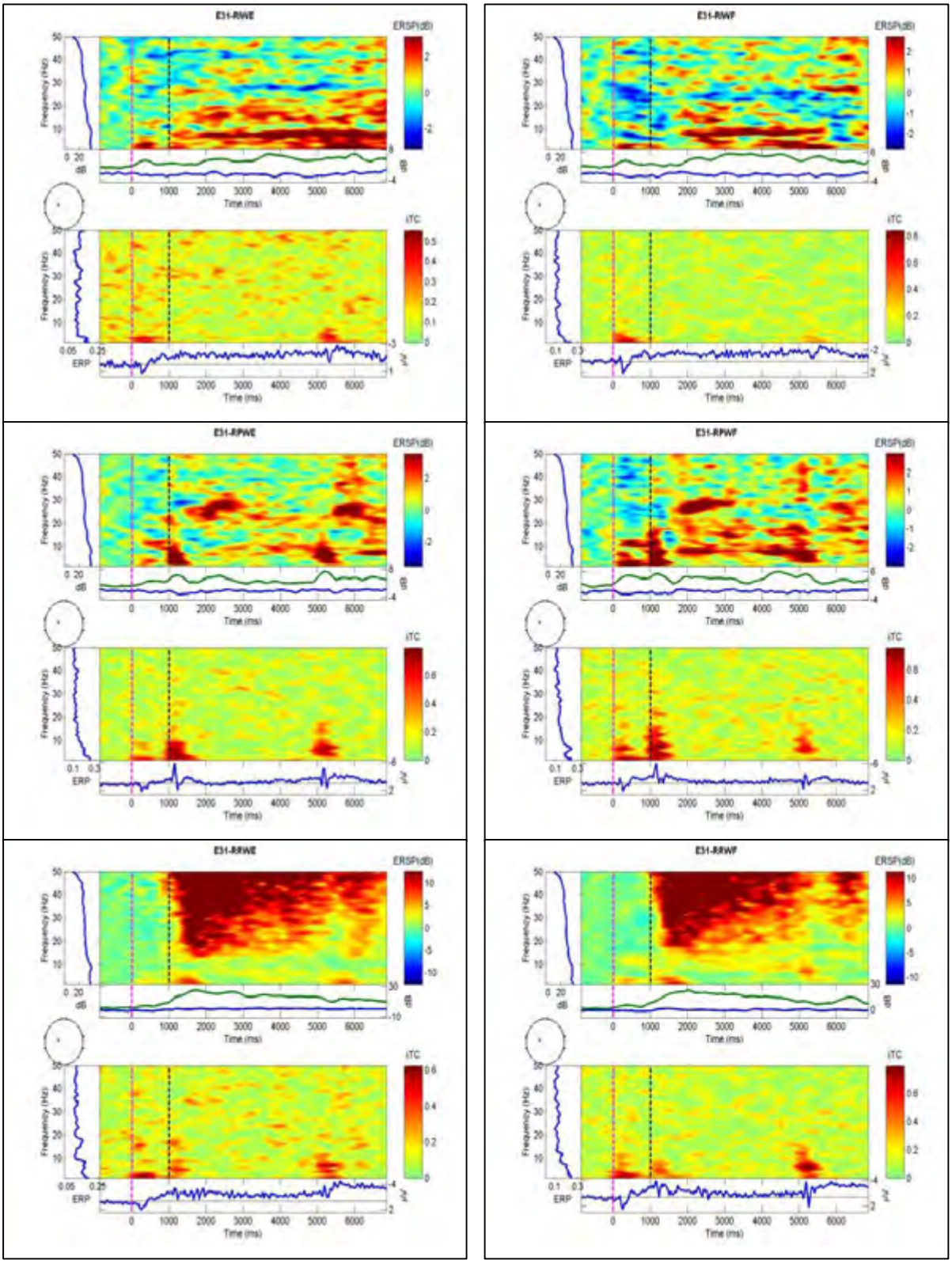

Figure D-17: ERSP plots of the RAW EEG data over electrode C1 (E31) for right wrist; imaginary, passive and real, flexion and extension.

The figure below shows the success of the automated ocular correction algorithms. The ocular artefacts have been successfully removed from the data, whilst still retaining the EEG rhythms. As you can see the EMG artefact are still present.

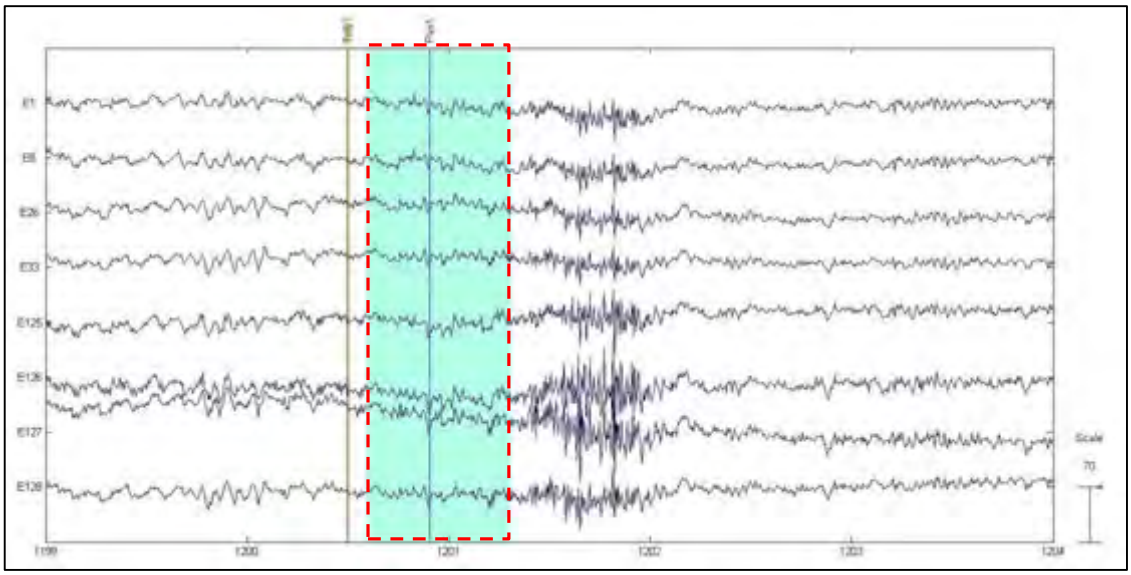

Figure D-18: Prepressed ocular corrected data for eight unipolar ocular channels (E1, E8, E26, E33, E125, E126, E127, E128), illustrating the removal of ocular artefacts (single dash, red square) from the contaminated RAW unprocessed data.

D.4.1.2 EMG Correction

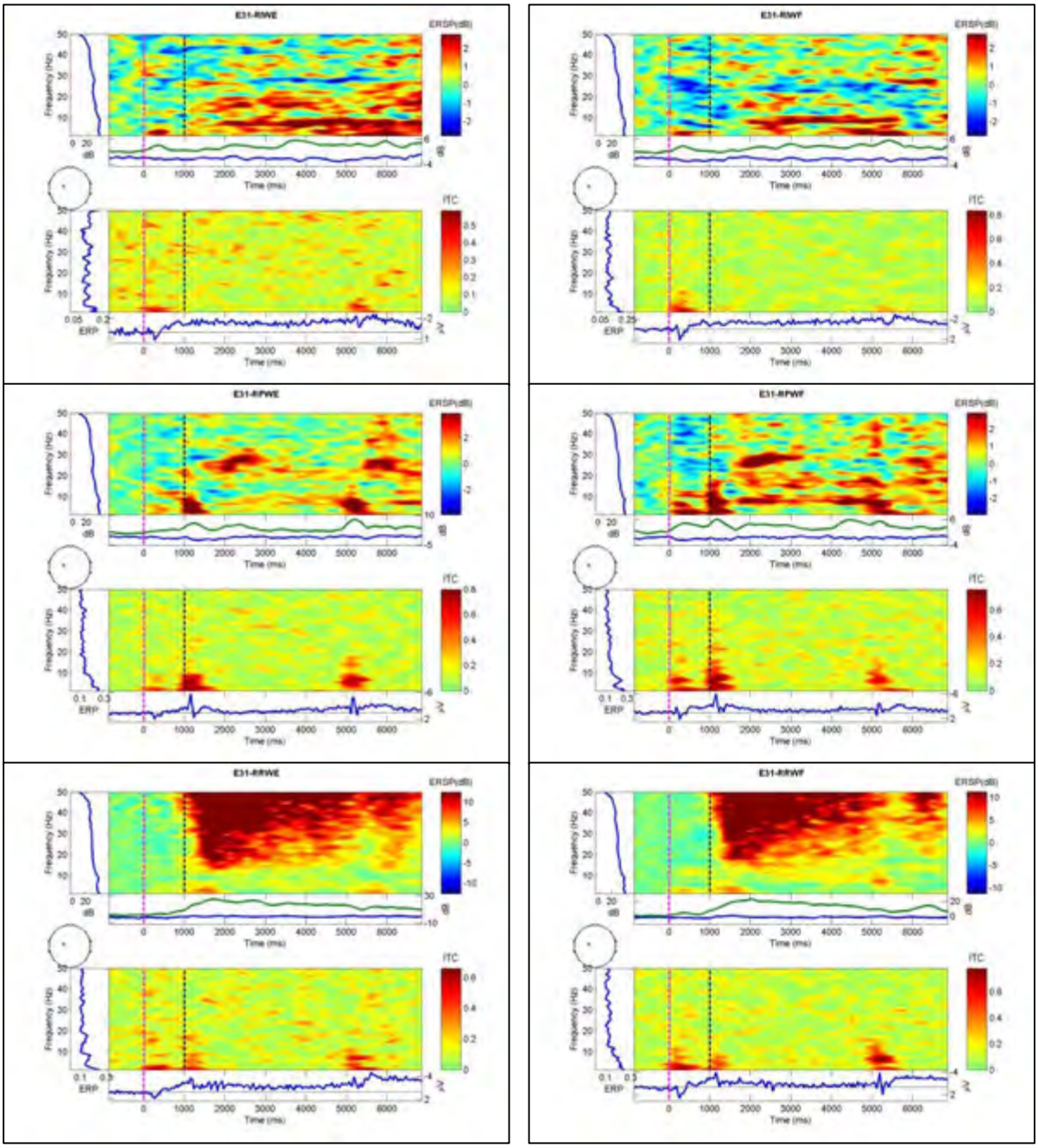

Figure D-19: ERSP plots of the ocular corrected EEG data over electrode C1 (E31) for right wrist; imaginary, passive and real, flexion and extension.

The figure below illustrated the effect of the EMG artefact correction algorithm that was applied to the ocular corrected data. This algorithm is not 100% successful in rejecting all the EMG artefacts present in the data, but it does substantially reduce its impact.

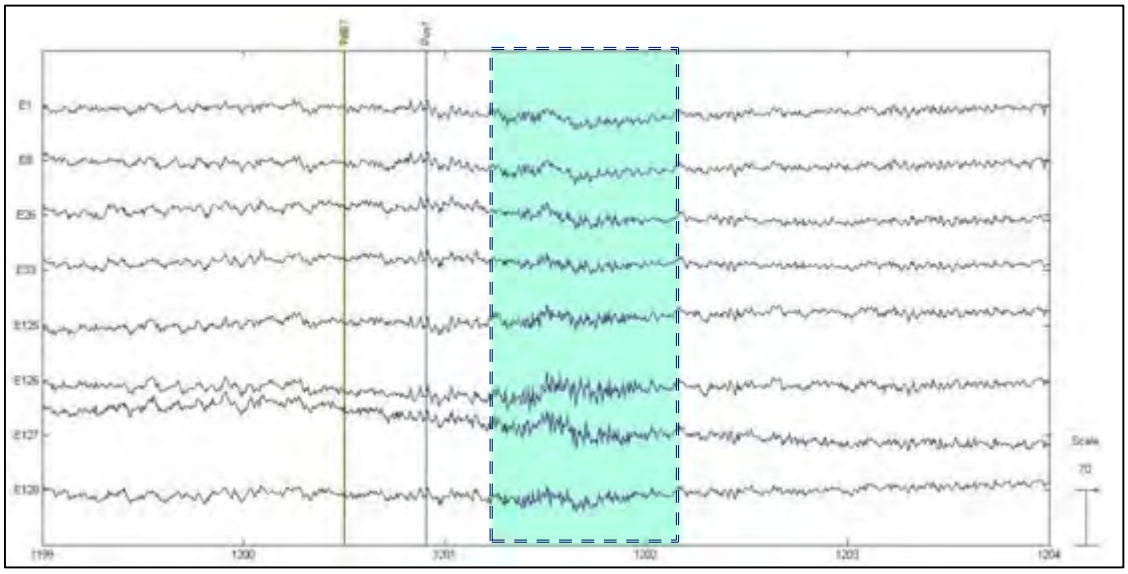

Figure D-20: Prepressed ocular and EMG corrected data for eight unipolar ocular channels (E1, E8, E26, E33, E125, E126, E127, E128), illustrating the removal of EMG artefact (single dash, red square) from the contaminated ocular corrected data.

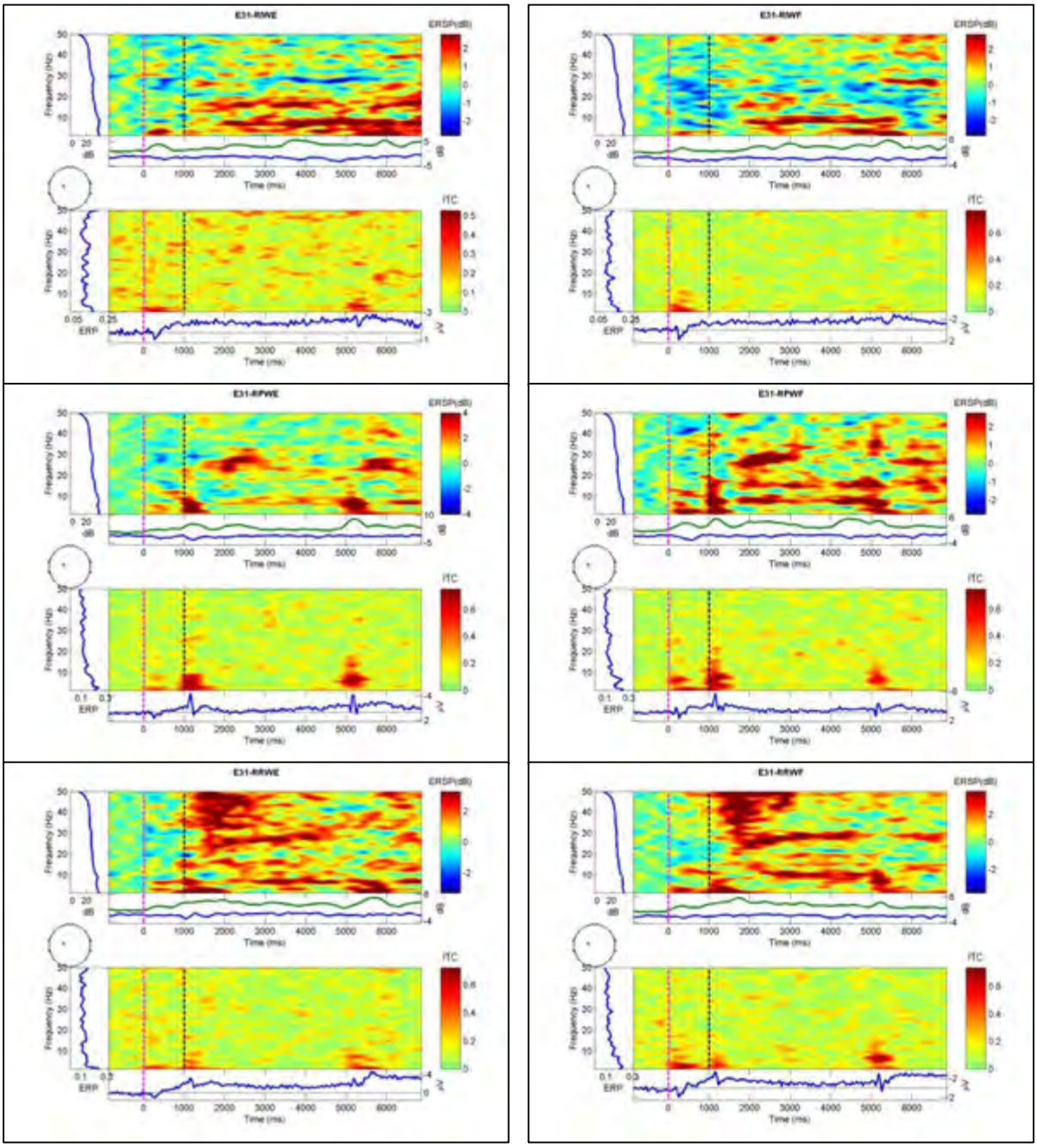

Figure D-21: ERSP plots of the ocular and EMG corrected EEG data over electrode C1 (E31) for right wrist; imaginary, passive and real, flexion and extension.

APPENDIX E – **MORE RESULTS**

E.1 Grand Average MRCP Topographical Results

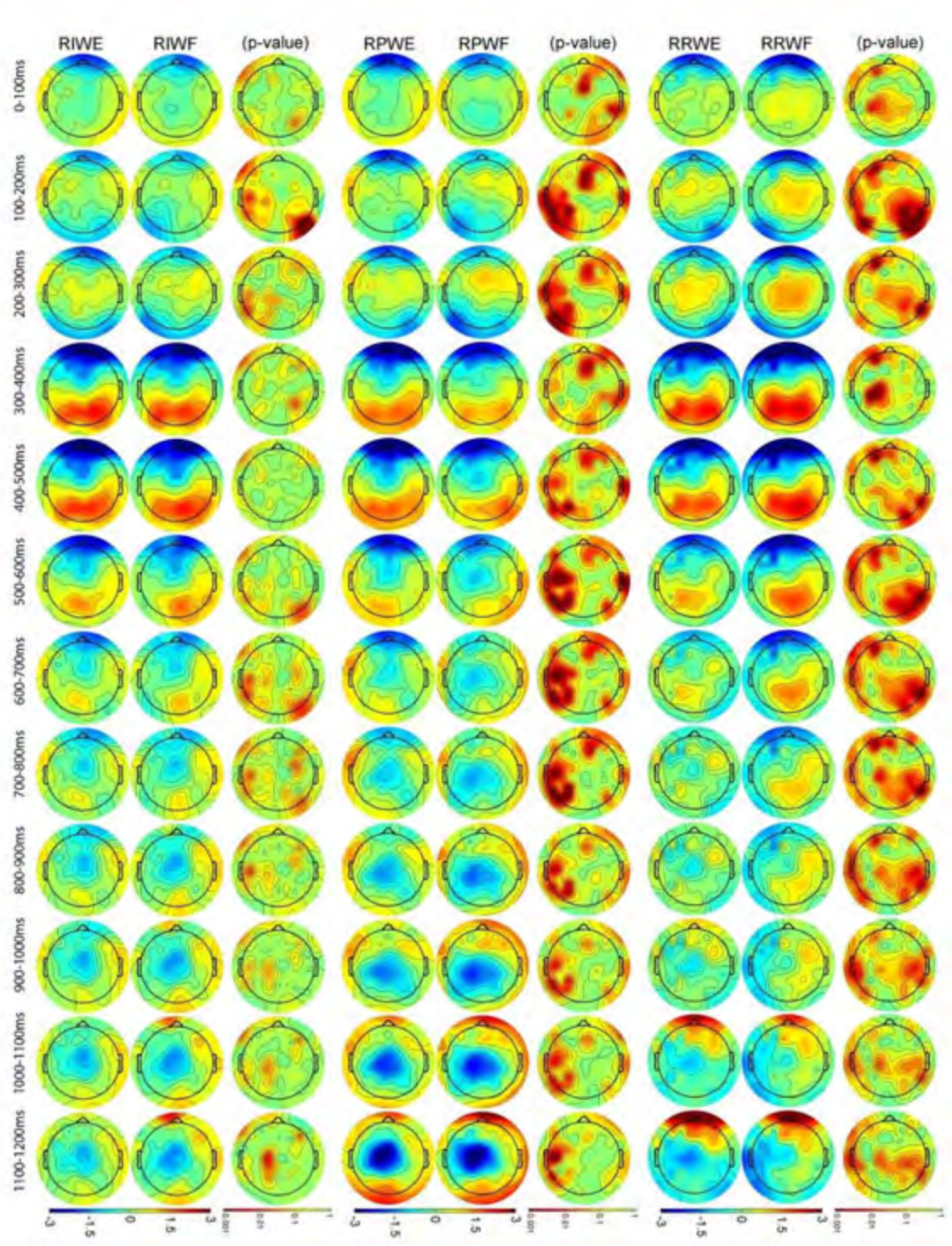

Figure E-1: Grand average MRCP topographical plots comparing wrist flexion and extension for imaginary, passive and real movements, in the 0ms to 1200ms trial region in 100ms average period windows. The horizontal dotted black line indicated the start movement location. The p-value-maps (colour bar; green & yellow $p>0.05$, red & orange $0.001<p<0.05$) illustrate the comparison between wrist flexion and extension for the different movement types.

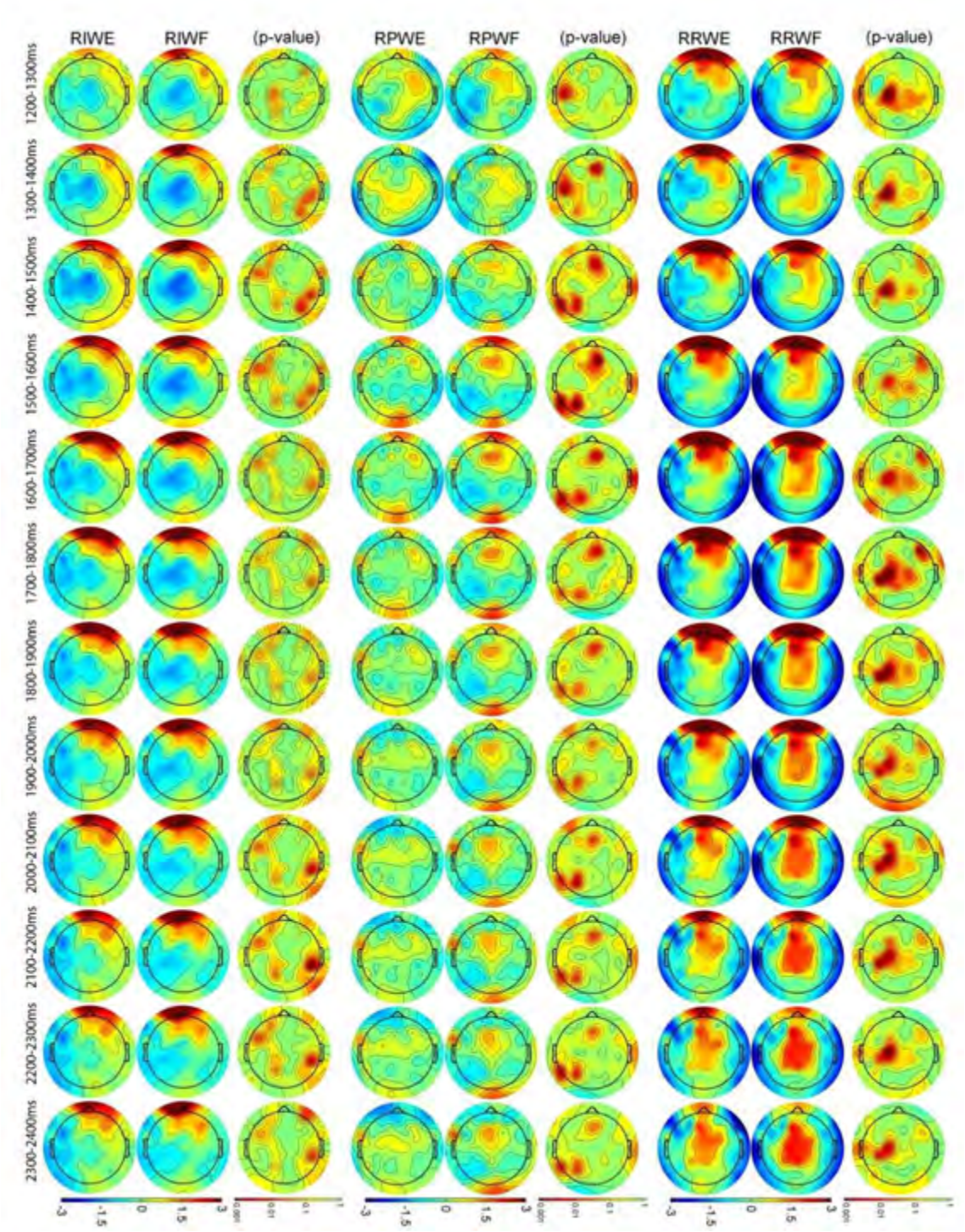

Figure E-2: Grand average MRCP topographical plots comparing wrist flexion and extension for imaginary, passive and real movements, in the 1200ms to 2400ms trial region in 100ms average period windows. The horizontal dotted black line indicated the start movement location. The p-value-maps (colour bar; green & yellow $p>0.05$, red & orange $0.001<p<0.05$) illustrate the comparison between wrist flexion and extension for the different movement types.

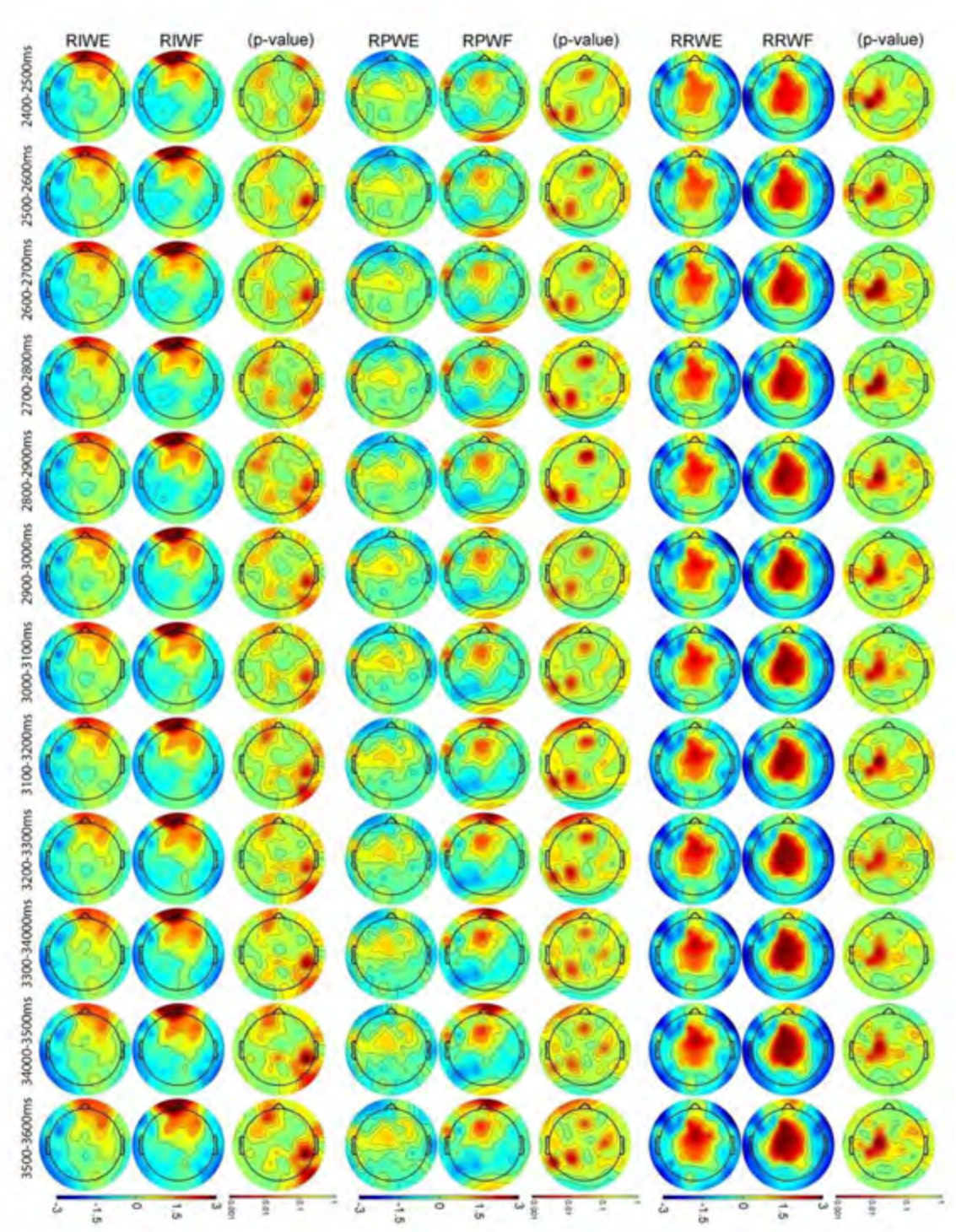

Figure E-3: Grand average MRCP topographical plots comparing wrist flexion and extension for imaginary, passive and real movements, in the 2400ms to 3600ms trial region in 100ms average period windows. The horizontal dotted black line indicated the start movement location. The p-value-maps (colour bar; green & yellow $p>0.05$, red & orange $0.001<p<0.05$) illustrate the comparison between wrist flexion and extension for the different movement types.

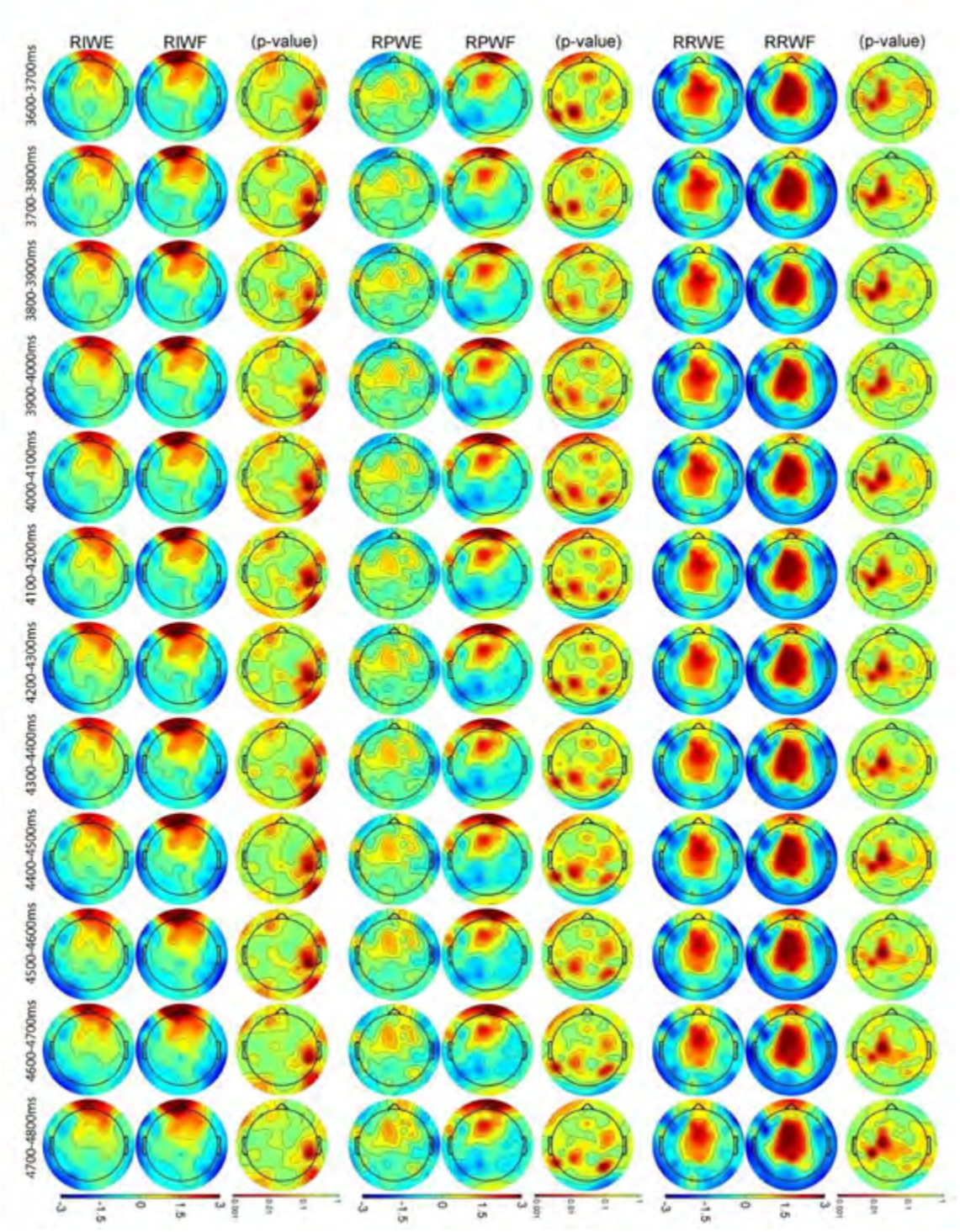

Figure E-4: Grand average MRCP topographical plots comparing wrist flexion and extension for imaginary, passive and real movements, in the 3600ms to 4800ms trial region in 100ms average period windows. The horizontal dotted black line indicated the start movement location. The p-value-maps (colour bar; green & yellow $p>0.05$, red & orange $0.001<p<0.05$) illustrate the comparison between wrist flexion and extension for the different movement types.

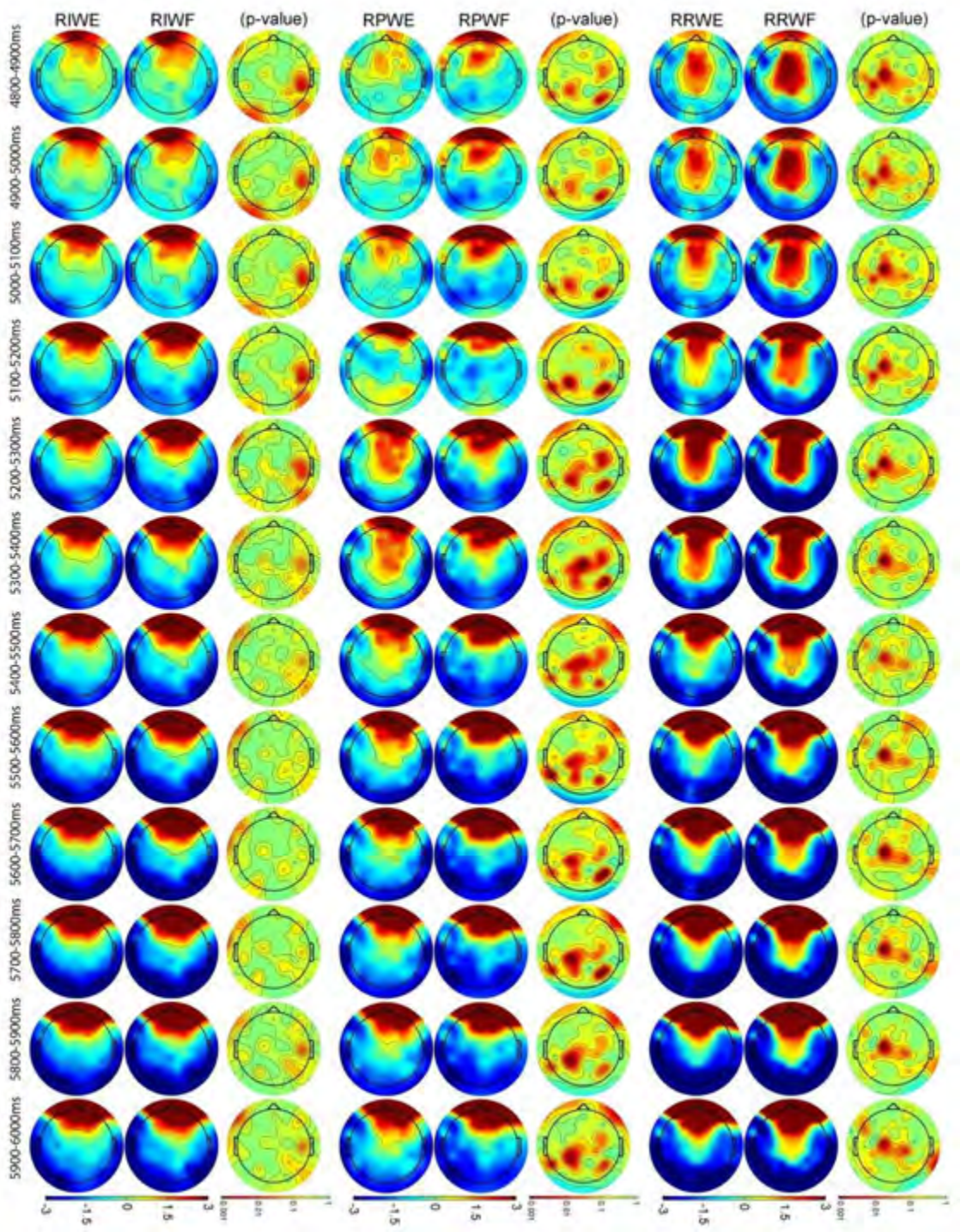

Figure E-5: Grand average MRCP topographical plots comparing wrist flexion and extension for imaginary, passive and real movements, in the 4800ms to 6000ms trial region in 100ms average period windows. The horizontal dotted black line indicated the start movement location. The p-value-maps (colour bar; green & yellow $p>0.05$, red & orange $0.001<p<0.05$) illustrate the comparison between wrist flexion and extension for the different movement types.

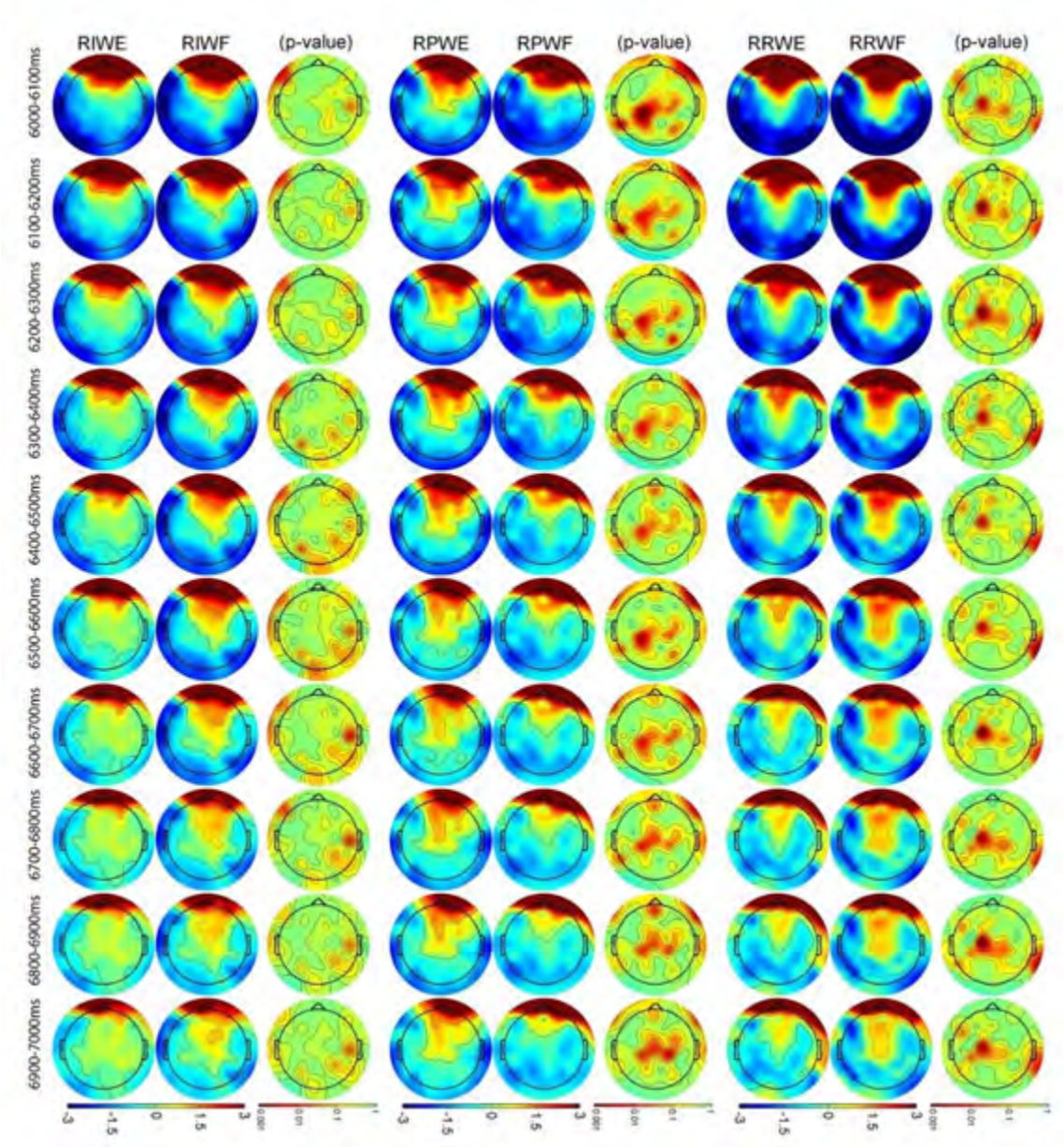

Figure E-6: Grand average MRCP topographical plots comparing wrist flexion and extension for imaginary, passive and real movements, in the 6000ms to 7000ms trial region in 100ms average period windows. The horizontal dotted black line indicated the start movement location. The p-value-maps (colour bar; green & yellow $p>0.05$, red & orange $0.001<p<0.05$) illustrate the comparison between wrist flexion and extension for the different movement types.

E.2 Mu band multivariate phase synchrony coefficient

The multivariate phase synchrony coefficient ((Quyen et al., 2001)) as illustrated in Figure E-7 is calculated over all the mu band PLV pairs, comparing the difference between wrist flexion and extension (Allefeld & Kurths, 2004). The multivariate phase synchrony coefficient (P_i) for the *i*th electrode was calculated as follows:

$$\boldsymbol{P_i = \frac{1}{M}\sum_{k=1}^{M} r_{ik}} \qquad \textbf{Equation 8.1}$$

Between the *i*th and *k*th oscillators, where *M* is the total number of *k* oscillators.

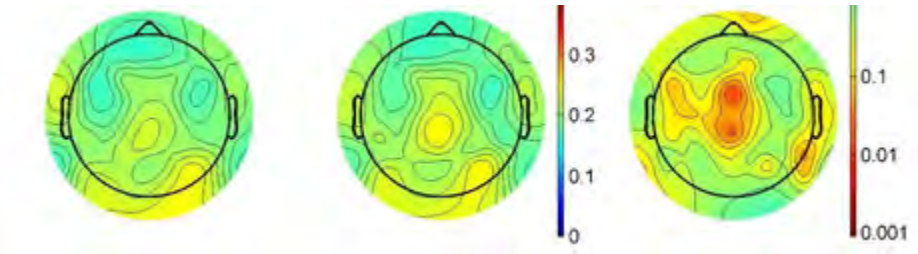

Figure E-7: The grand average multivariate phase synchrony coefficients PLV, comparing passive wrist flexion and extension over all channels, including the significant p-value-map (red $p < 0.05$).

The multivariate phase synchrony coefficient in the mu band, shows no sustained significant differences between wrist flexion and extension for imaginary and real movements in the pre-movements period or the sustained movement period (Figure E-8). However, there was a passive post movement (1000-1300ms) significant difference around the center somatosensory association area and right primary motor area, with higher level of passive flexion.

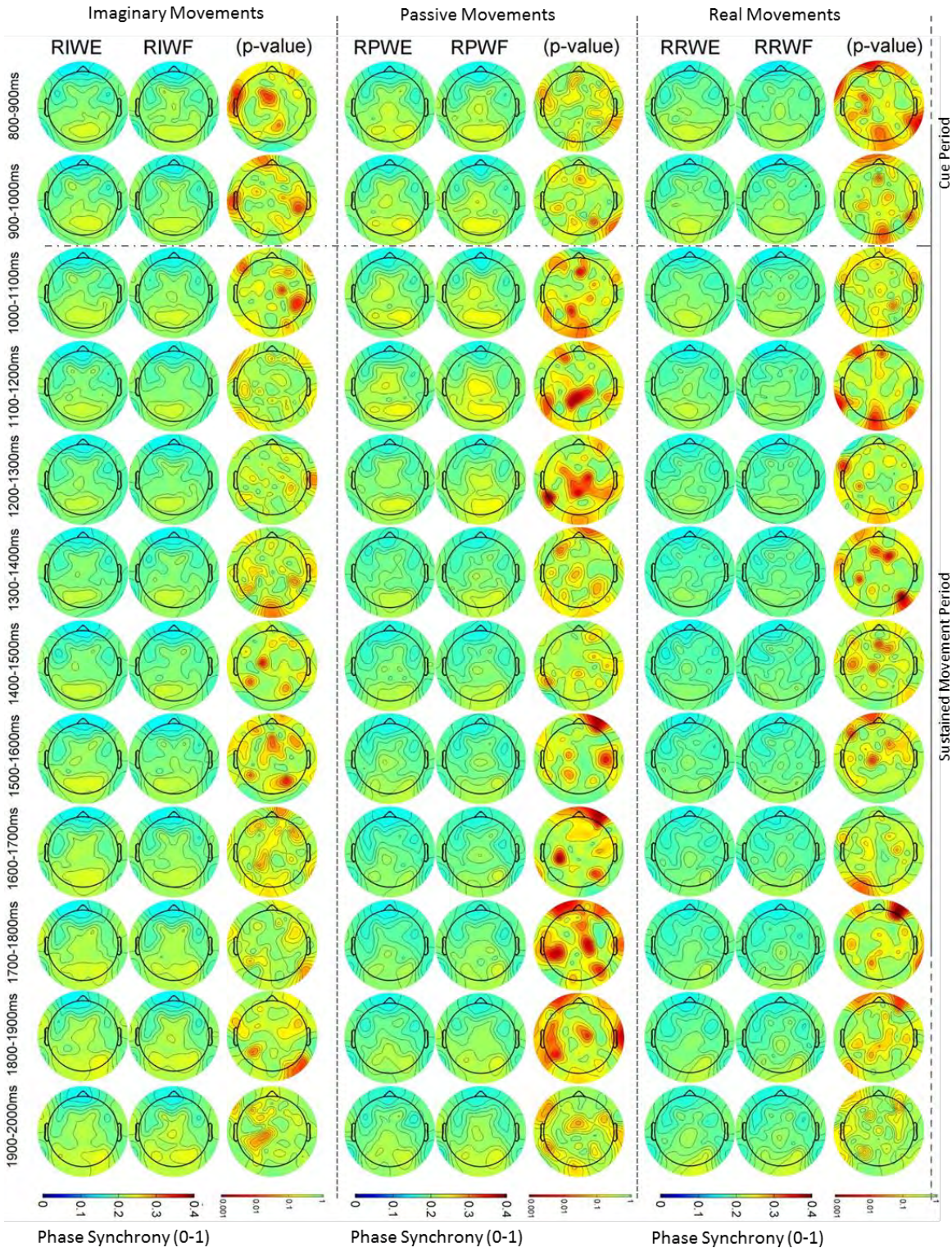

Figure E-8: Grand average PLV multivariate coefficient topographical plots of the mu range (8-13Hz), comparing wrist flexion and extension for imaginary, passive and real movements, in the 800ms to 2000ms trial region in 100ms average period windows. The horizontal dotted black line indicated the start movement location. The p-value-maps (colour bar; green & yellow $p>0.05$, red & orange $0.001<p<0.05$) illustrate the comparison between wrist flexion and extension for the different movement types.

E.2.1.1 Bi-phase Locking Value

The majority of current methods for calculating phase synchronization focus on a single frequency or frequency band. The effect of cross-frequency coupling has been studied using Bi-coherence, but this method is strongly dependent on the amplitudes of the independent signals. It has been shown that phase synchronization between distant cortical sites is important and can occur without local amplitude changes. Furthermore, Bi-phase locking value (bPLV) is independent of the signals amplitude, and therefore synchronization can be detected where there is no strong amplitude correlation, making bPLV more sensitive than bi-coherence measurements. Bi-phase locking value is an extension of the well-known phase-locking value (PLV) method and is sensitive to non-linear interaction, like multiplication and phase modulation signals. The ability for bPLV to detect non-linear synchronization between three different frequencies adds another dimension to cortical interactions. As a result of bPLV being insensitive to linear interaction it is able to clearly distinguish crosstalk effect from real interaction (F. Darvas et al., 2009), (Felix Darvas, Miller, Rao, & Jeffrey G. Ojemann, 2009).

The bPLV between three signals is defined as:

$$\boldsymbol{B_{xyz}(f_1, f_2, t)} = \left| \frac{1}{N} \sum_{i=1}^{N} e^{(j(\emptyset_X^i(f_1,t) + \emptyset_Y^i(f_2,t) - \emptyset_Y^i(f_1+f_2,t)))} \right|$$

The above equation represents the bPLV, is an extension of the simpler PLV equation, where bPLV is sensitive to the coupling of two independent frequencies, $\emptyset_X^i(f_1, t)$ and $\emptyset_Y^i(f_2, t)$ and a third frequency $\emptyset_Y^i(f_3, t)$ which is the sum of the first two frequencies (f1 + f2). bPLV is more sensitive than (bi) coherence because phase locking can be detected in situation where there is no strong amplitude correlation. It is important to note that bPLV cannot replace PLV due to the inability of detecting coupling between single frequency interactions (F. Darvas et al., 2009).

E.3 Grand Averaged EMG Results

The following section illustrated the recorded EMG results around the left and right hand wrist flexion and extension muscle groups (see section 4.1.3.2, refer to section 3.2.1), for motor imagined (see section E.3.1), passive (see section E.3.2) and real (see section E.3.3) movements.

E.3.1 Imaginary Movements

E.3.1.1 Left hand EMG

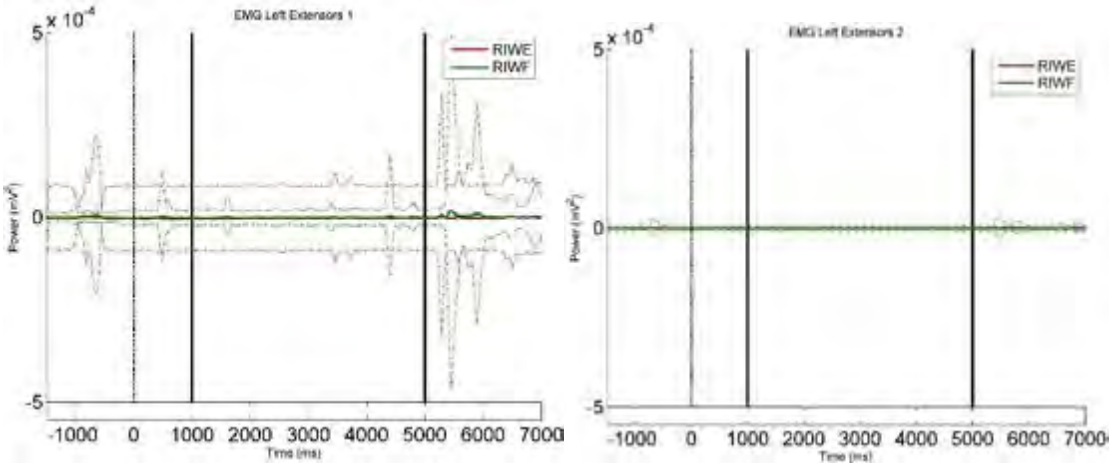

Figure E-9: The grand average EMG for imaginary wrist flexion (RIWF) and extension (RIWE) over the left hand extensor muscle groups. The standard deviation (SD) is illustrated for each movement (dotted line).

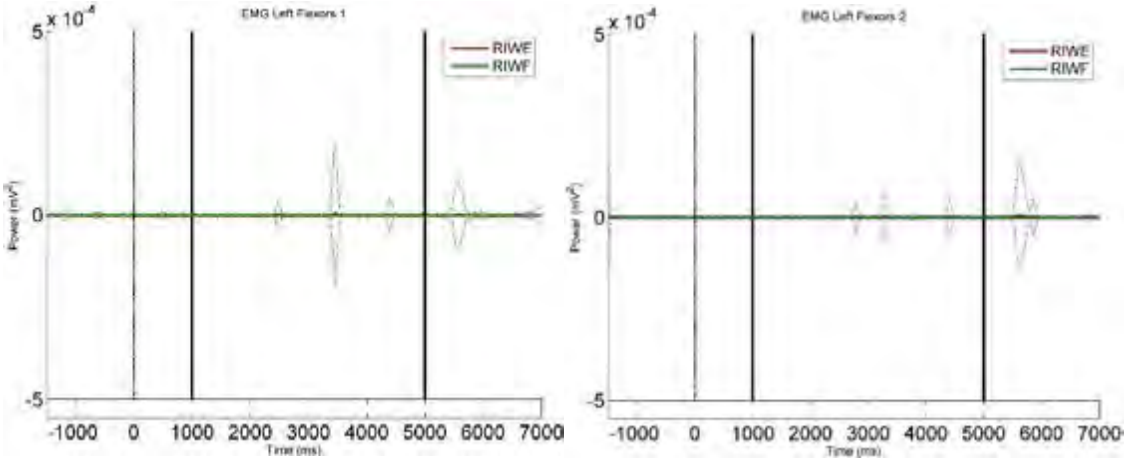

Figure E-10: The grand average EMG for imaginary wrist flexion (RIWF) and extension (RIWE) over the left hand flexors muscle groups. The standard deviation (SD) is illustrated for each movement (dotted line).

E.3.1.2 Right hand EMG

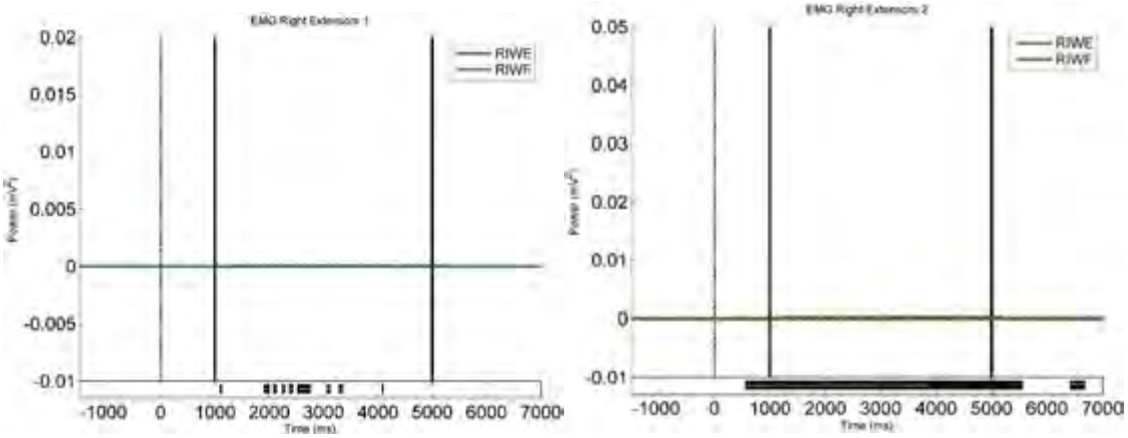

Figure E-11: The grand average EMG for imaginary wrist flexion (RIWF) and extension (RIWE) over the right extensor muscle groups. The standard deviation (SD) is illustrated for each movement (dotted line).

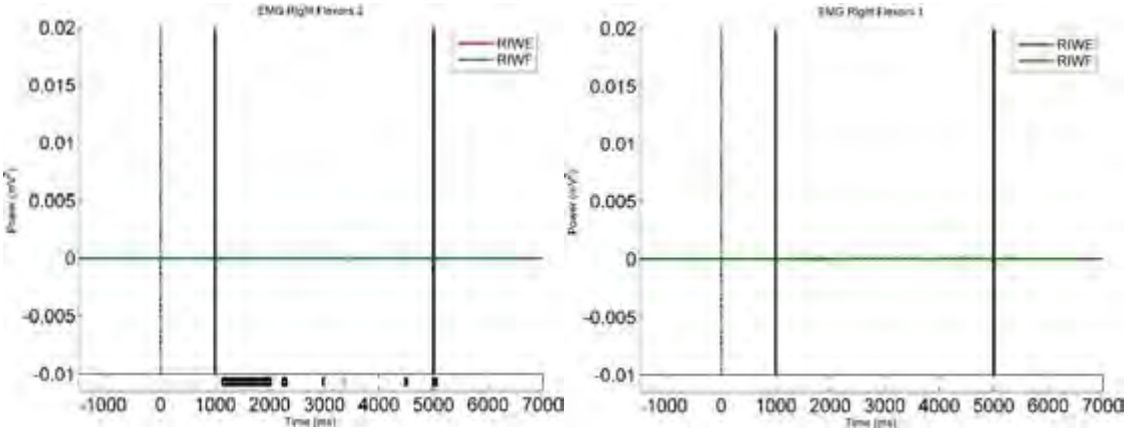

Figure E-12: The grand average EMG for imaginary wrist flexion (RIWF) and extension (RIWE) over the right flexors muscle groups. The standard deviation (SD) is illustrated for each movement (dotted line).

E.3.2 Passive Movements

E.3.2.1 Left hand EMG

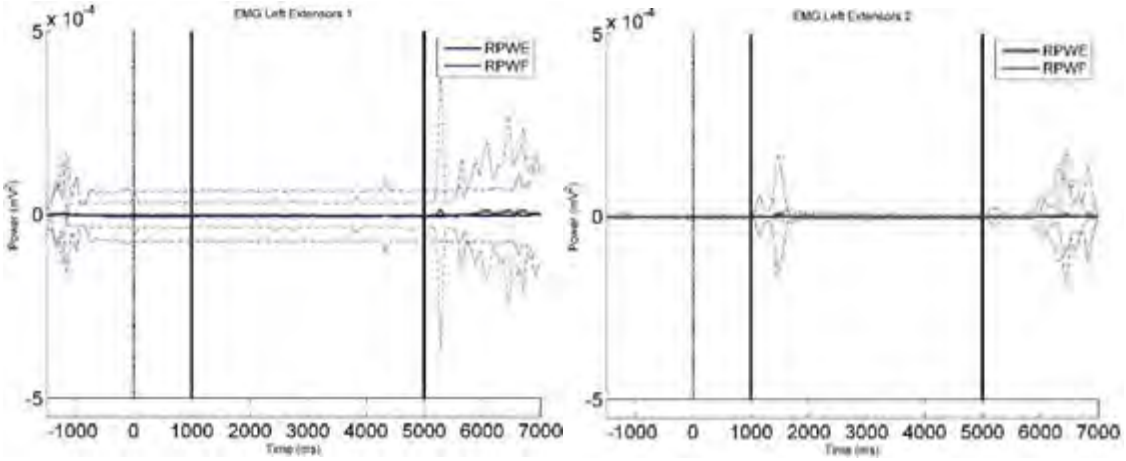

Figure E-13: The grand average EMG for passive wrist flexion (RPWF) and extension (RPWE) over the left extensor muscle groups. The standard deviation (SD) is illustrated for each movement (dotted line).

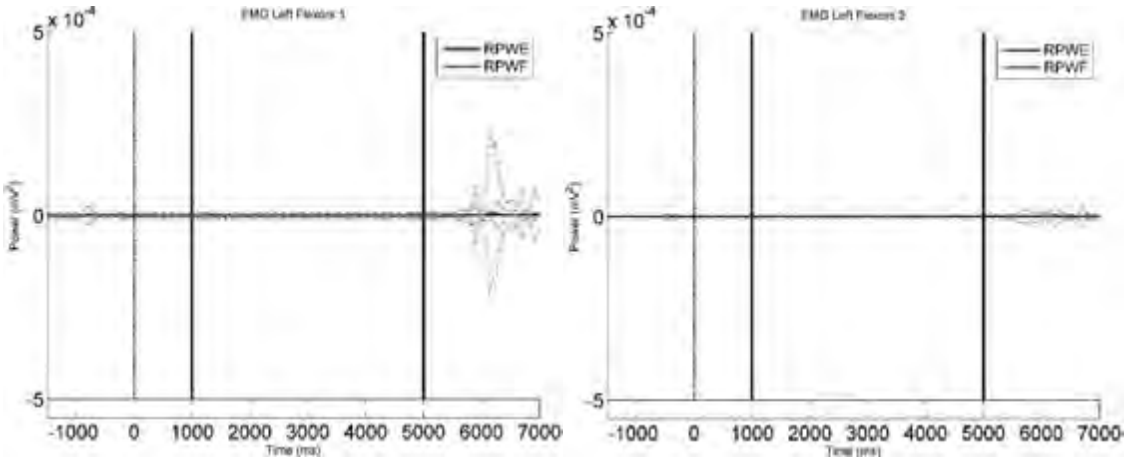

Figure E-14: The grand average EMG for passive wrist flexion (RPWF) and extension (RPWE) over the left flexor muscle groups. The standard deviation (SD) is illustrated for each movement (dotted line).

E.3.2.2 Right hand EMG

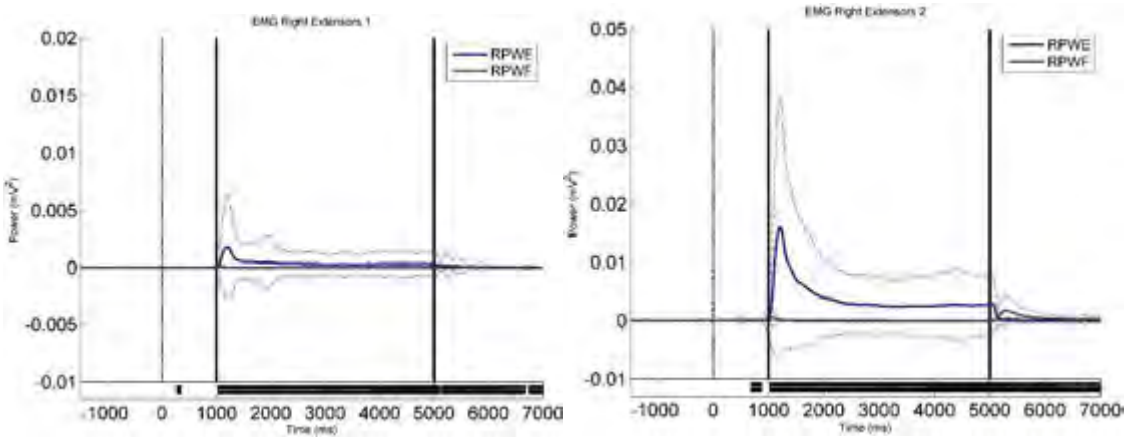

Figure E-15: The grand average EMG for passive wrist flexion (RPWF) and extension (RPWE) over the right extensor muscle groups. The standard deviation (SD) is illustrated for each movement (dotted line).

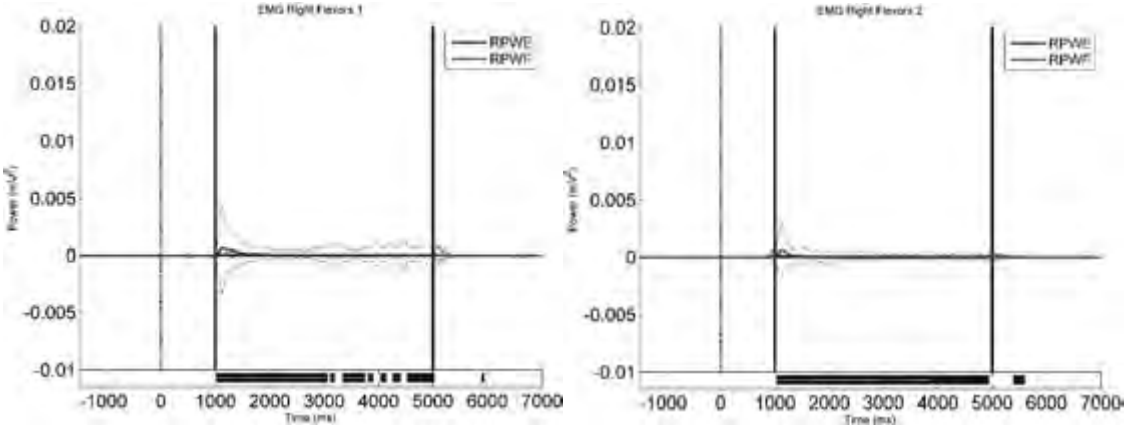

Figure E-16: The grand average EMG for passive wrist flexion (RPWF) and extension (RPWE) over the right flexors muscle groups. The standard deviation (SD) is illustrated for each movement (dotted line).

E.3.3 Real Movements

E.3.3.1 Left hand EMG

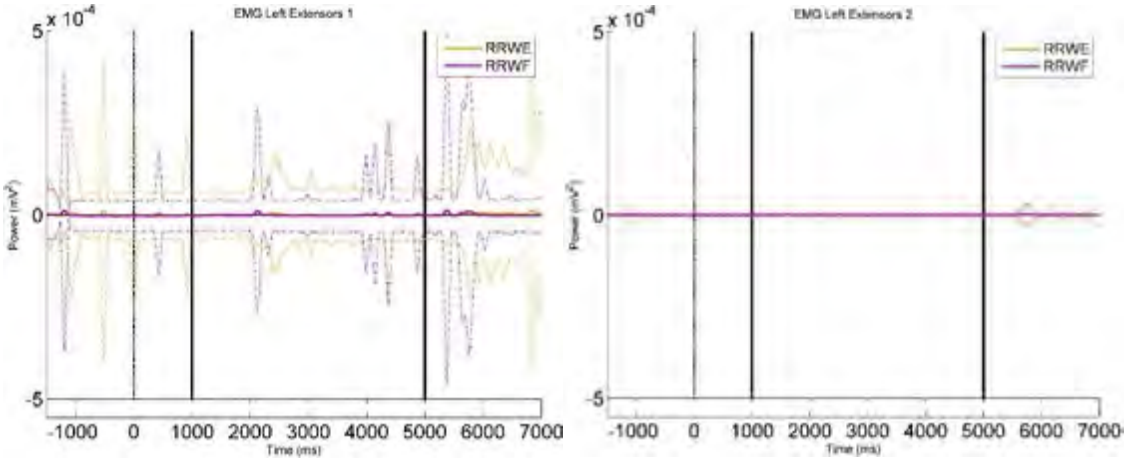

Figure E-17: The grand average EMG for real wrist flexion (RRWF) and extension (RRWE) over the left extensor muscle groups. The standard deviation (SD) is illustrated for each movement (dotted line).

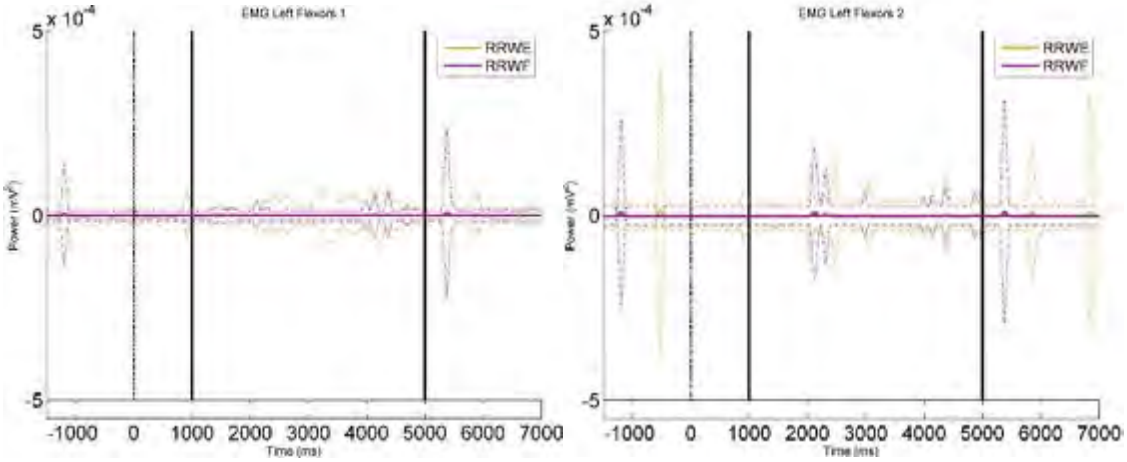

Figure E-18: The grand average EMG for real wrist flexion (RRWF) and extension (RRWE) over the left flexors muscle groups. The standard deviation (SD) is illustrated for each movement (dotted line).

E.3.3.2 Right hand EMG

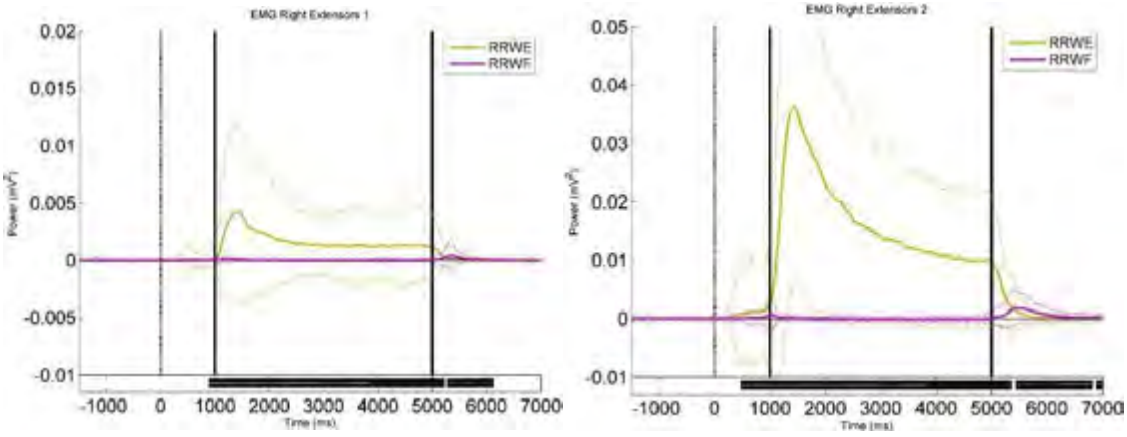

Figure E-19: The grand average EMG for real wrist flexion (RRWF) and extension (RRWE) over the right extensor muscle groups. The standard deviation (SD) is illustrated for each movement (dotted line).

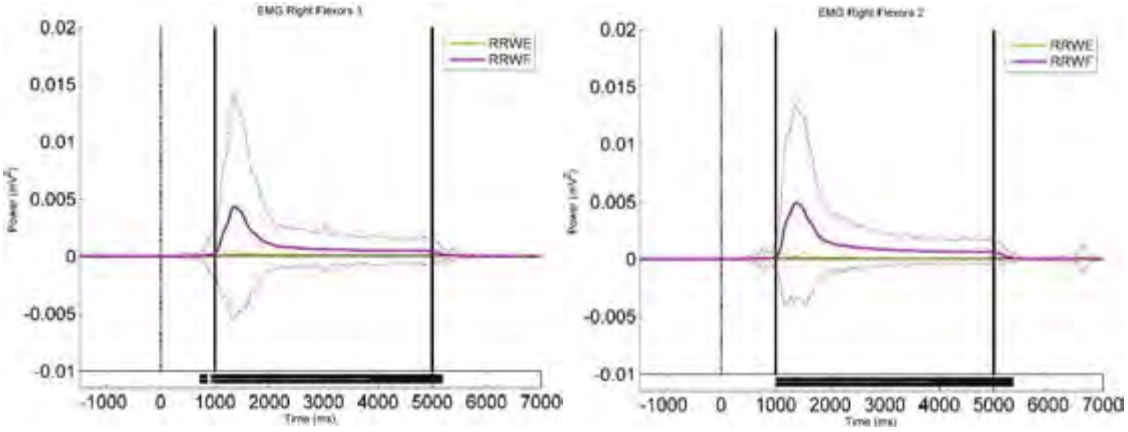

Figure E-20: The grand average EMG for real wrist flexion (RRWF) and extension (RRWE) over the right flexors muscle groups. The standard deviation (SD) is illustrated for each movement (dotted line).